CHAPTER III

THEORETICAL REVIEW

INTRODUCTION:

In recent years,exciting advances have been made in understanding the problem of how the disorder in amorphous semiconductor influence the band structure and hence the electrical properties.

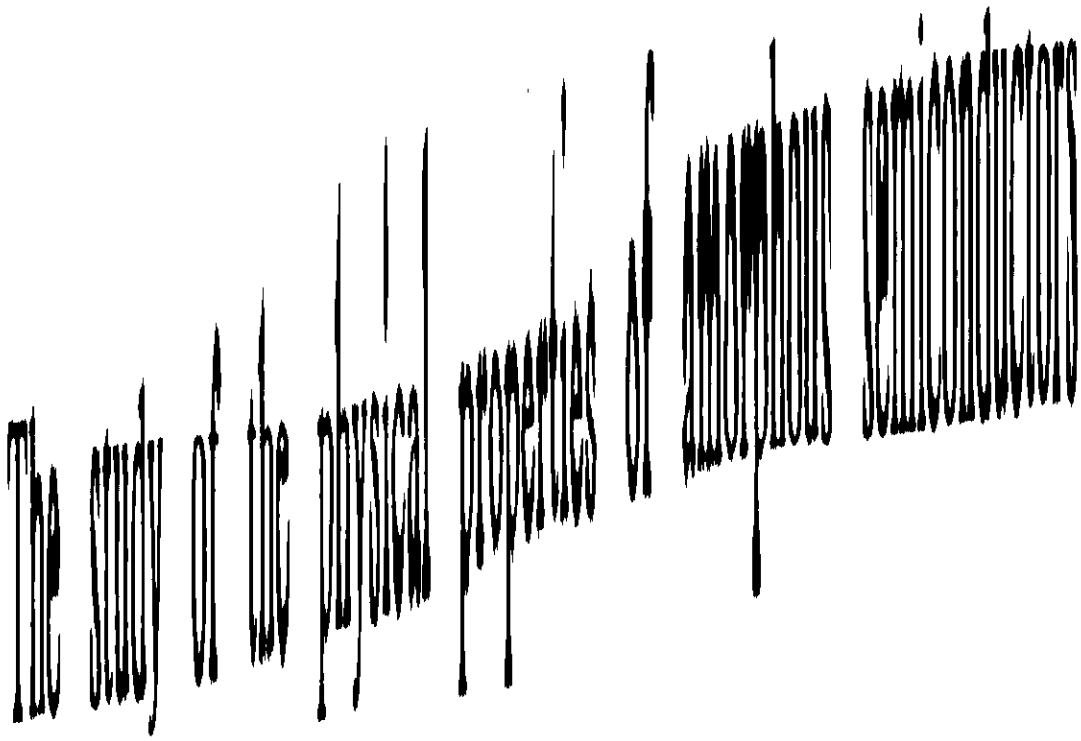

has become an active field in solid state physics over the last

INTRODUCTION:

In recent years,exciting advances have been made in understanding the problem of how the disorder in amorphous semiconductor influence the band structure and hence the electrical properties.

The study of the physical properties of amorphous semiconductors has become an active field in solid state physics over the last decade. In particular ,the nature of electronic transport in these material has attracted much attention during recent years. The interest arose from two sides. In 1968 Ovshinsky[12] reported the discovery of non destructive fast electrical switching in thin films of multicomponent chalcogenide glasses. This discovery immediately initiated long discussion about the physical interpretation of the effects.

From a fundamental point of view,the noncrystalline material is of considerable intrinsic interest. For many years the crystalline solid has been studied and a high degree of understanding of its various physical properties has been attained.

The crystalline state is characterized by a regular periodicity in the atom or ion positions over long distances. The salient features of crystalline semiconductors,e.g,the exsistance of sharp edges at the

valence and conduction bands leading to a well define forbidden energy gap, are direct consequence of the short and long- range order. This band structure determine the electrical properties that are commonly measured, such as the electrical conductivity and the Hall coefficient. In order to account for the translation disorder, accompanied by a possible compositional disorder in multicomponent system modification have been proposed for the band structure of the amorphous solid. These are the well-known Cohen-Fritzsche-Ovshinsky (CFO)[13],and Davis-Mott[14] models. Introducing the basic idea of the presence of localized states at the extremities, these models have been widly used to interpret experimental data in the field of electrical and optical properties.

3.1.BAND MODELS:

Experimental data of electrical transport properties can only be properly interpreted if a model for the electronic structure is available. Since the pioneering work of Bloch it is known that the electronic structure of the crystal shows universal characteristics.

For semiconductor,the main features of the density of states N(E) of crystalline solids are the sharp structure in the valence and conduction bands, and abrupt termination at the valence band maximum and the conduction band minimum. The sharp edges in the density of states produces a well -defined forbidden energy gap. Within the band the states are extended, which means that the wave functions occupy the entire volume.

Several models were proposed for the band structure of amorphous semiconductors, which have the same extent that they all used the band tails. Opinions vary ,however, as to the extent of this tailing.

3.1.1. THE SIMPLEST BAND MODELS:-

Economou[15] and other presented a band structure model for the amorphous semiconductors. This is shown in Fig(3.1). They suggested that the band structure consists of localized states (shaded area) above E_v,and a conduction band C.B with a tail of localized states below E_C. They proposed that the states from E_v to E_c are localized and extended outside it.

Anderson [16]proposed that the electrons in the localized states can not diffuse at O^0 k, but at a definite temperature, they presumably can contribute to the conductivity by assisted hopping only.

The localized states can be found, according to Mott[17] , when a dangling bond formed, then a filled state is pulled out from the valence band and an unoccupied state is formed in the conduction band. These produce localized states in the forbidden gap, a donor near the gap center and above it acceptor one, exists only when the donor is occupied.

fig.3.1.The simplest model for amorphous semiconductors.The localized states appear as a tail of the valence band and the conduction band leaving well defined mobility gap.

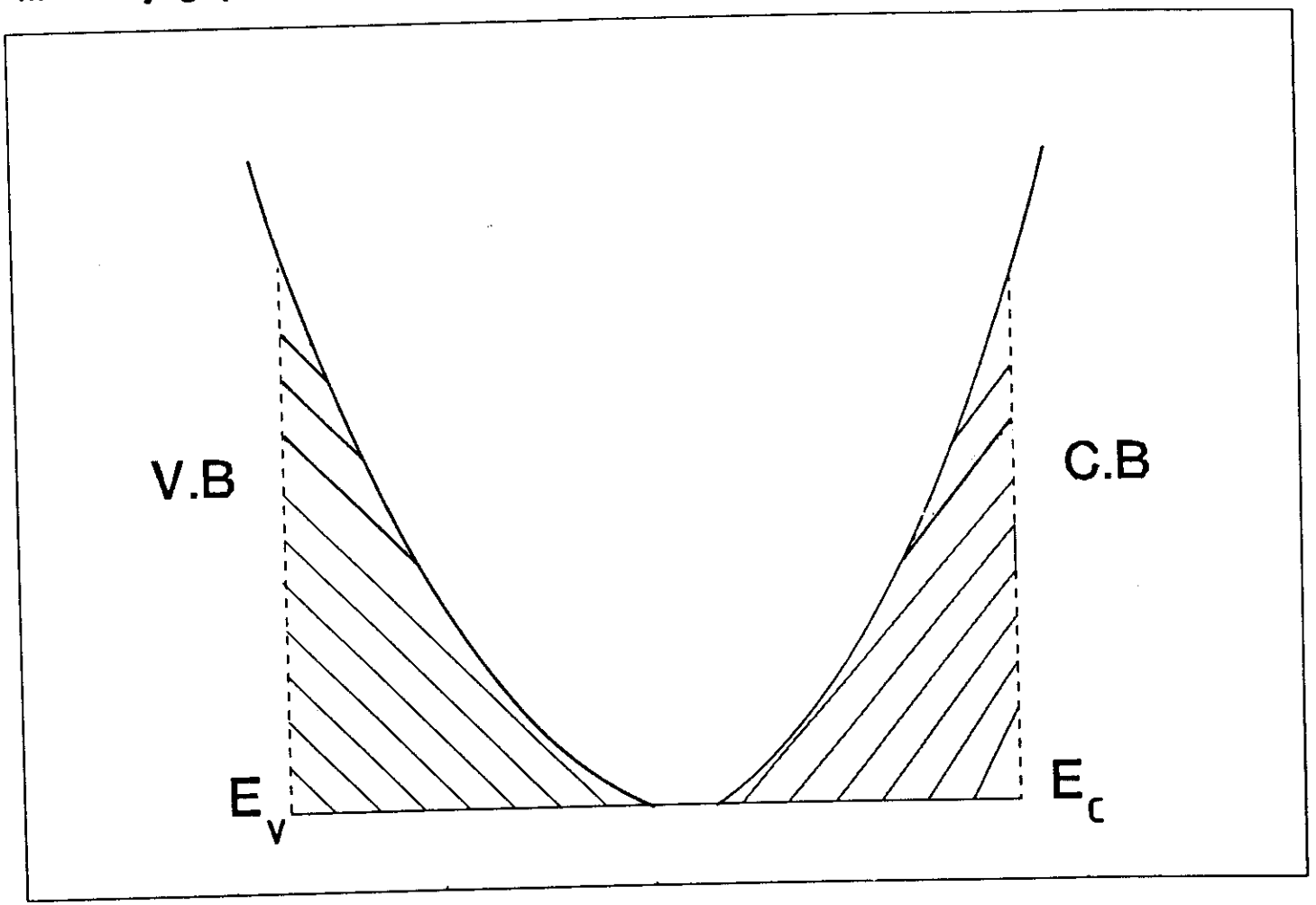

3.1.2. Mott-CFO model:

This model is based on the concept of an ideal covalent random network structure. It was perfect especially proposed for the multicomponent chalcogenide glasses. The model suggests that the valence and conduction band are separated by a gap. Transitional and compositional disorder are assumed to cause fluctuation of the potential of sufficient magnitude that they give rise to localized states to extend from the valence and conduction bands into the gap. The number and energy spread of localized states are increased with the degree of randomness and strength of scattering. It is important to assumed that the valence band tail states are neutral when they are occupied and the conduction band tail states are neutral when they are empty. This locates the Fermi energy somewhere near the gap center.

The deviation from ideal covalent random network,due to the presence of vacancies, dangling bonds, and chain ends, contributes the states to be localized in certain energy range. This give rise to nonmonotonicity of the density of the localized state curve. Mott[18] found that the character of the wave function changes at the critical energies E_c and E_v. These energies separated the extended and localized states.At temperature $T = 0^0$ K , the electron and hole mobilities drop sharply from low mobility band to thermally activated tunneling between localized states.

The so called mobility edges E_c and E_v according to Cohen[19] define a mobility gap (E_c-E_v) which contain localized states only as

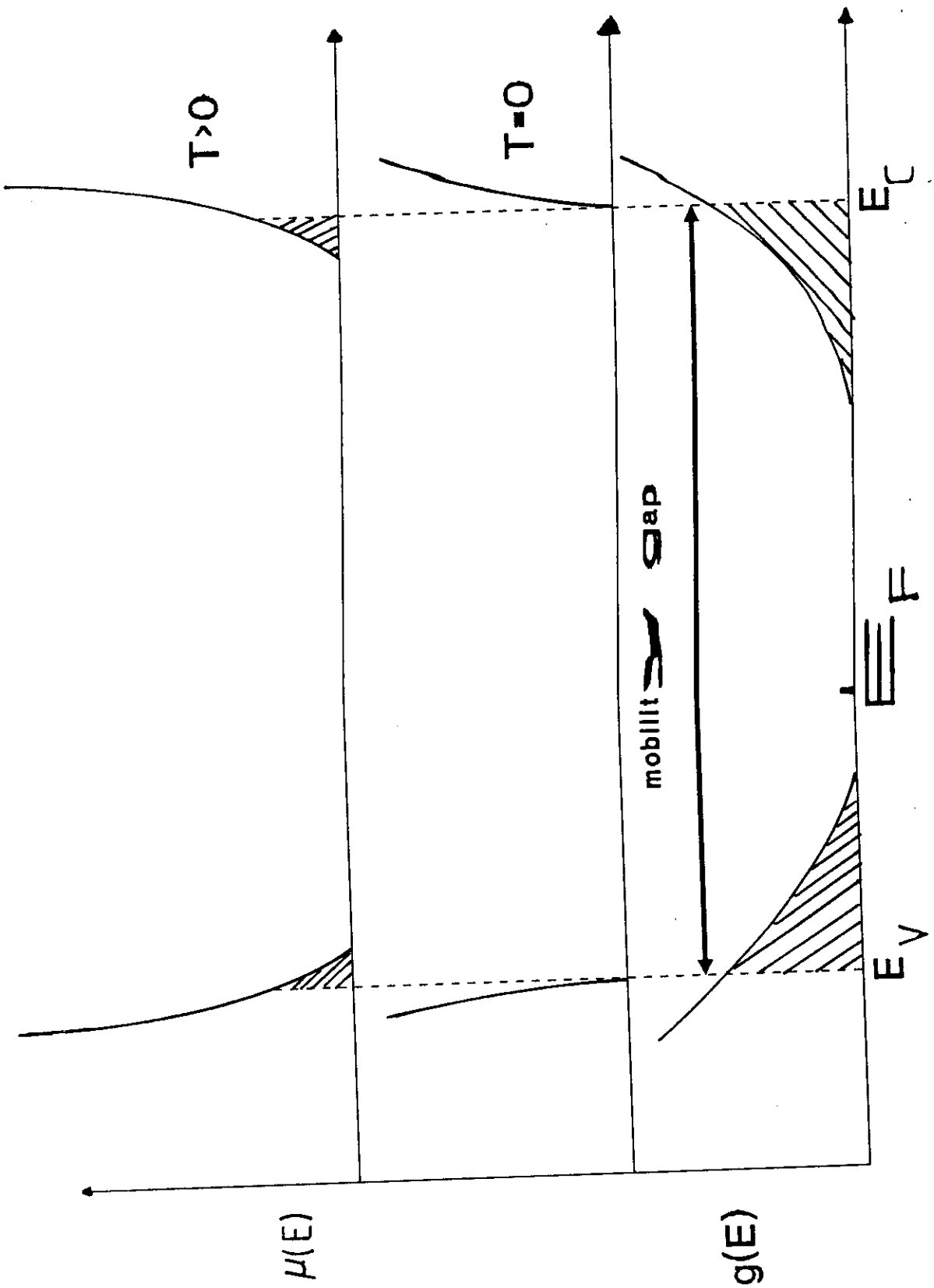

Fig.(3.2):Sketch of the Mott-CFO model for Covalent semiconductor having three dimentional network structure. The critical energies E_c,E_v define the mobility gap. For T=0 ,the mobility μ(E)may finite in the gap because of thermally assisted tunneling E_f equal Fermi

temperature ranges.

At low temperatures the conduction can occur thermally by thermally assisted tunneling between states at the Fermi level. At moderate temperatures, charge carriers excited into the localized states of the band tails. The charge carriers in these localized states transport only by hopping. At high temperatures the charge carriers are excited across the mobility edges into the extended states. The mobility in the extended states is much higher than in the localized states.

3.1.3.DAVIS -MOTT MODEL[20]

They proposed that the mobility edges of electrons and holes lie at E_c and E_v respectively. A strong distinction is found between the localized states and others.

The first type was originated from the lack of long range- order and extended to E_A and E_B only in the mobility gap,as shown in fig.(3.3). Thus the range, between E_C and E_A, and between E_B and E_V determine the position of the localized states as shown in fig(3.3).

The other type of states are called the defect states ,which generates from the defects in the structure. These states form longer hypothetical tails but of insufficient density to pin the Fermi level, therefore they proposed a band of compensated level near the gap

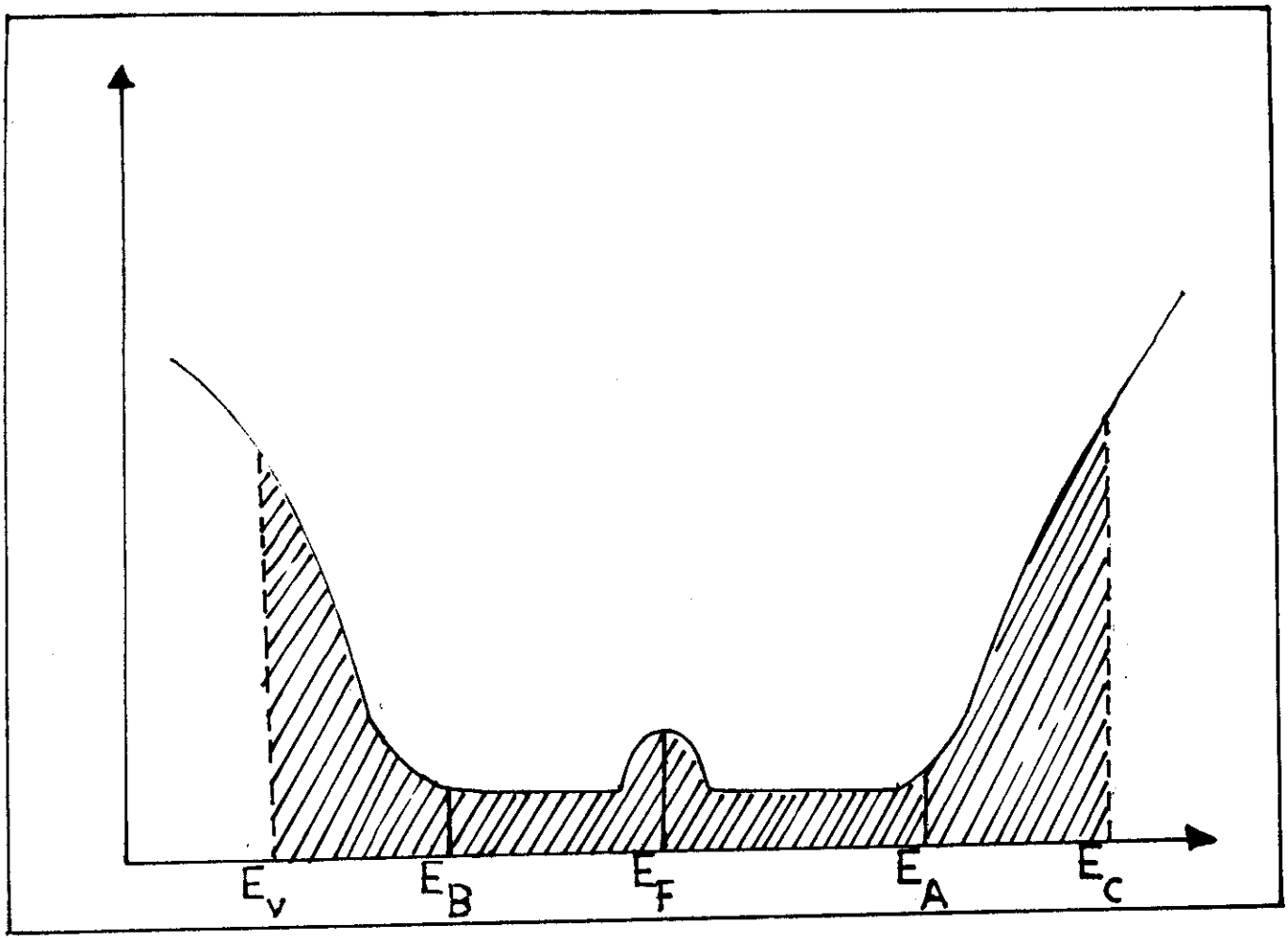

Fig. (3·3): The density of states suggested by Davis and Mott. $(E_c - E_v)$ is the mbility gap. $(E_c - E_A)$ and $(E_B - E_v)$ contain localized states originating from the lake of longe range order. Thermally assisted hopping (tunneling) may be take place in these ranges.

center in order to pin the Fermi level. So that the semiconductor is extrinsic rather than intrinsic. According to Mott[21] the center band may split into two bands, a donor and acceptor one.

3.1.4.MARSHALL-OWEN MODEL:[22]

In this model the position of the Fermi level is determined by means of donors and acceptors in the upper and lower halves of the mobility gap respectively. The concentration of donors and acceptors adjust themselves by self compensation to be nearly equal, so that the Fermi level remain near the gap center. At low temperature it moves to one of the impurity bands because self compensation is not likely to be complete. This model is based on the observation that the high field drift mobility in "$As_2 Se_3$" is of the " Pool - Frenkel "form presumably because of the field stimulated emission of carriers form charged trapping centers(acceptors) as shown in fig(3.4).

3.1.5.KAF MODEL:

This model is an ultimated model proposed by Kastner[23]. It is presented for the structure and properties of active centers in lone-pair semiconductors. It was based on the knowledge of the chemical bonds in chalcogenide crystals and glasses and their variation in the glassy state. The most important variation will be of course in the bond angle even if the short-range order is preserved glass. Kastner et al.[24] have started their model by identifying the

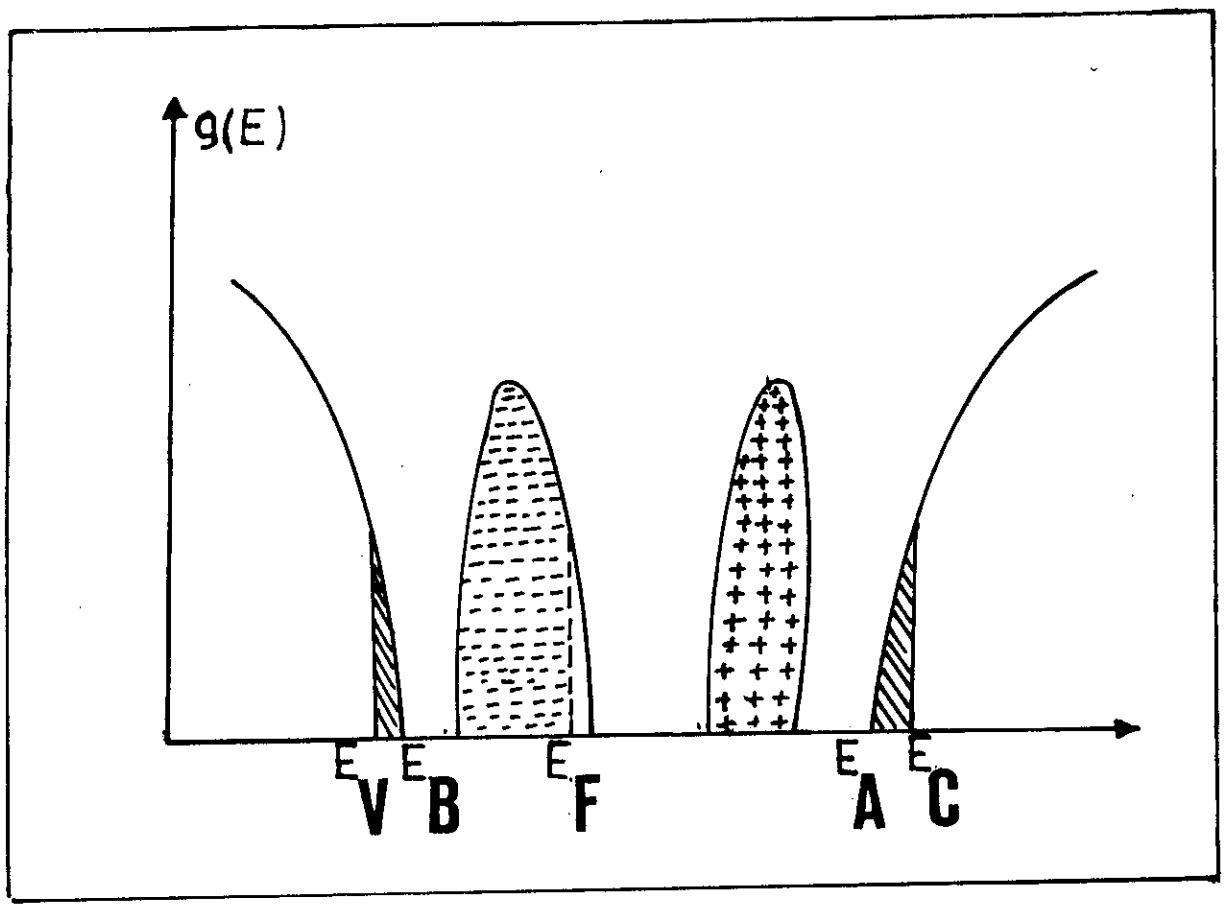

Fig. (3.4): Density of states g(E) suggested by Marshall and Owen (1971) for As_2Se_3-E_c, E_v, E_B, E_A have the same meaning of Davis and Mott model. A band of Localized acceptor and donor state lie below and above the gap center. In this case the acceptor are a compensated by the donors. As the temp. increase, E_p move toward the gap center.

normal bands and their lower energy states. Then they looked for chemically likely variations and determine their energy of formation.The highest are ignored, the lowered are looked at, and considered as giving states in the gap. Level bands and bonds are shown in fig(3.5) due to Kastner[25].

3.2.D.C. ELECTRICAL CONDUCTIVITY OF AMORPHOUS SEMICONDUCTORS:-

The D.C conductivity of amorphous semiconductor may be expressed by the equation:[26]

$$\sigma = \Sigma \int dE_n \; n_b(E) \; e \; \mu_b(E) \; F_b(E) \qquad (3.1)$$

Where b: The band index

n(E): The density of states.

$\mu_b(E)$: The average mobility for all carriers of energy E.

$F_b(E)$: The probability of occupation for a state of energy ,E, by electrons for b=c and holes for b=v.

In the crystalline state, the cut-off of $n_b(E)$ leads to the well defined activation energy observed in σ ,while in the disordered case there is no sharp cut-off of $n_b(E)$ as can be shown in fig(3.2).

On applying of the notation of Davis and Mott[27]one distinguish three types of contribution to the conductivity:

3.2.1. **Band conduction of electrons** above E_c or holes below E_v written for electrons this yields:

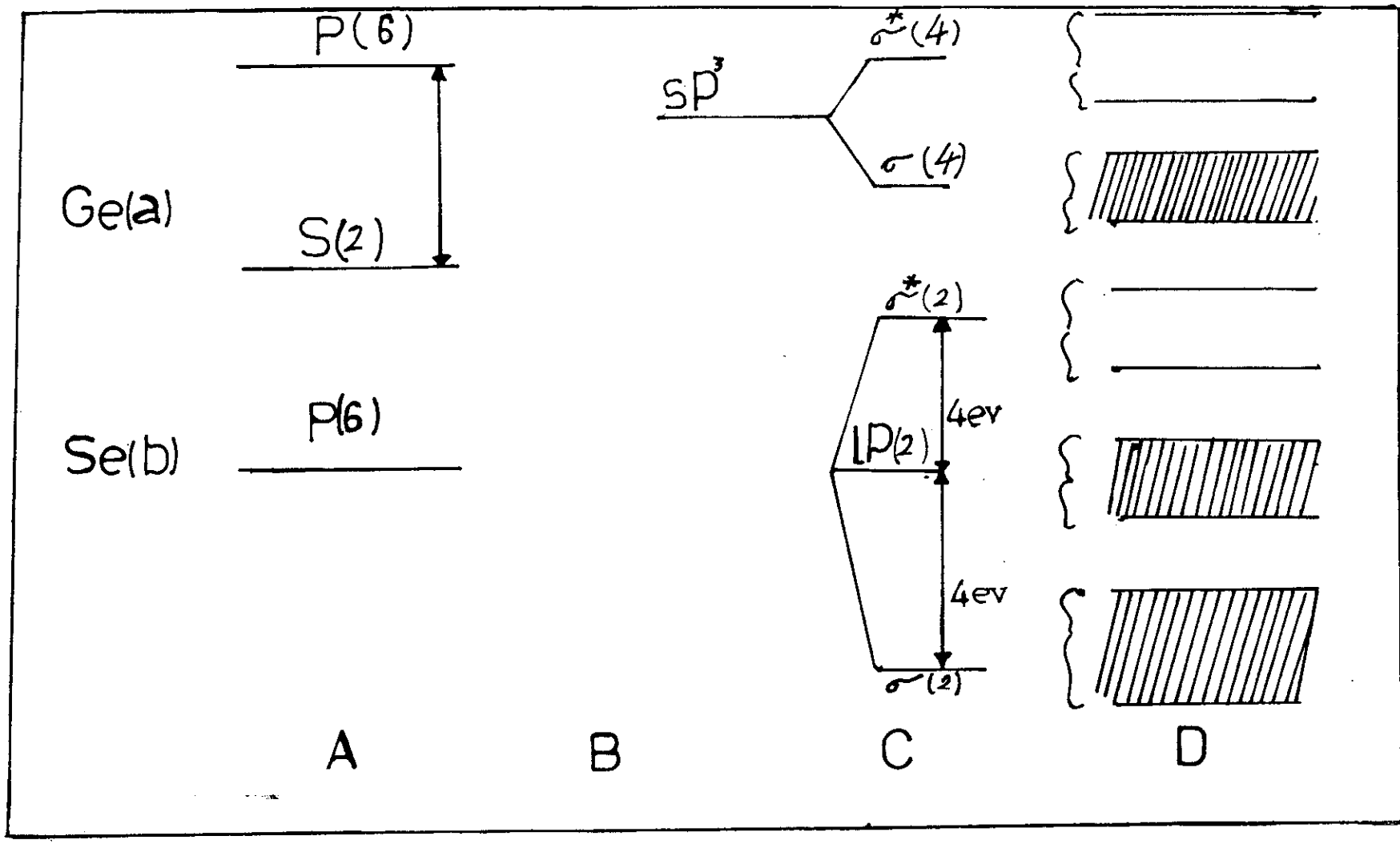

Fig. (3.5): Bonding in (a) Ge and (b) Se.
(A) Atomic states, (B) hybridized states,
(C) molecular states, (D) broadening of
states into bands in the solid.

$$\sigma = \sigma_o \exp -(E_c - E_f)/KT \qquad (3.2)$$

The separation of E_f from the mobility edge will change with temperature. Assuming a linear temperature dependence in the temperature range of interest ,then:

$$E_c - E_f = \Delta E - \gamma T$$

Then equation (3.2) becomes:

$$\sigma = C \exp (-\Delta E/KT) \qquad (3.3)$$

where,

$$C = eg(E_c)\ KT\mu_c \exp(\gamma /K)$$

In non-crystalline solids it appears that γ ,which corresponds to mean free path ,is less than the interatomic spacing. In this case Cohen[28]suggested that the charge carriers transport proceed by means of diffusion or Brawnian motion. The conductivity does not follow simple exponential law, when ΔE depends on T as a result of temperature dependent shift of E_f.

3.2.2.THERMAL ASSISTED TUNNELING in the localized gap states near the mobility edges ,near E_A and E_B in fig(3.3),or in the donor or acceptor bands of fig(3.4). The largest tunnel contribution arises from jumps to unoccupied levels of nearest neighbour centers. The tunneling process involves emission or absorption of a phonon. Hence this thermally assisted tunneling involves a hopping energy ΔW_t in addition

to the activation energy ($E-E_f$)needed to raise the electron to the appropriate localized states at E. Thus the conductivity will be in the form

$$\sigma = \sigma_1 \exp - (E-E_f+\Delta W_1)/KT \qquad (3.4)$$

The tunnel probability and density of states g(E) decreases whereas F(E) increases as the energy moves towards the gap center, thus the maximum tunneling contribution shifts towards E_f as the temperature is lowered.

3.2.3. **Tunneling conduction near E_f:-**

This process should be of the form:

$$\sigma = \sigma_2 \exp(-\Delta W_2 /KT) \qquad (3.5)$$

Where ΔW_2 is the hopping energy.

As the temperature is lowered the number and the energy of phonons available for absorption decreases,so that tunneling is restricted to seek centers which are not nearest neighbours but which instead lie energetically closer and within the range KT.

The manner in which the position of the Fermi level affects the conductivity of a semiconductor can be derived theoretically[29]. It is clear that the number of the electrons in the conduction band and holes in the valence band gives semiconductors of the conductive

properties of an intrinsic semiconductor.

$$\sigma_{tot.} = \sigma_h + \sigma_e \qquad (3.6)$$

Using the Fermi statistics it can be shown that the concentration of electrons in the conduction band is:

$$n_e = \text{const.} \cdot T^{3/2} \exp\{ -(E_g - E_f) / KT \} \qquad (3.7)$$

Where:

E_g: The energy gap.

E_f:The Fermi level of the given semiconductor.

K : The Boltzmann constant and

T : The absolute temperature.

From equation (3.6),however the conductivity is given by

$$\sigma = n\, e\mu_e + pe\mu_h \qquad (3.8)$$

Which for an intrinsic semiconductor reduces to :

$$\sigma_i = n_i e(\mu_e + \mu_h) \qquad (3.9)$$

if the free electron and hole concentration are equal.

In a simple terms the mobilities would be expected to vary with

temperature as ,

$$\mu = \text{const} \cdot T^{3/2} \qquad (3.10)$$

Substituting this expression and equation(3.7) into equation(3.9) gives the following expression for the conductivity of an intrinsic semiconductor,where of course $E_f = 1/2\ E_g$:

$$\sigma_i = \sigma_0 \exp (- E_g /2KT) \qquad (3.11)$$

Where σ_0 is a constant.

For extrinsic semiconductors the excitation of carriers from the impurity level must also be allowed for and equation (3.6)apply in general. If the impurity level excitation energy is E_i then a similar equation to equation(3.11)can be written namely :

$$\sigma_E = \sigma_{0E} \exp (-E_i /KT) \qquad (3.12)$$

Where σ_{0E} is a constant and σ_E is the contribution to the conduction of the material due to the presence of the impurities. In general, the conductivity of a semiconductor is made up of two terms which,because of different magnitude of E_g and E_i ,dominate in different temperature regions. At low temperatures the extrinsic term(equation 3.12) is most important while the intrinsic term(equation 3.11)dominate at high temperatures. The total conductivity is :

$$\sigma_t = \sigma_0 \exp(-E_g/2KT) + \sigma_{oE} \exp(-E_i/KT) \qquad (3.13)$$

The form of this equation provides a method of measuring both E_g and E_i for,as suggested above,one or other term can be neglected, depending on temperature. Thus if the electrical conductivity is measured as a function of temperature and if Ln σ is plotted against 1/T a graph of the form shown in figure(3.6.A) is obtained.The graph consists of two straight line regions, the slope of which yield E_i and E_g for the low and high temperature ranges respectively. The intercepts of the two regions give the constants σ_0 and σ_{oE}.

In practice a graph of the form shown in fig.(3.6.B)is obtained where there is a region in which the conductivity decreases as the temperature increases. This occurs in the intermediate temperature range(0-60°C) where the impurities are all ionized but the electrons being excited across the forbidden gap are few in number, so that the carrier concentrations remains almost constant as the temperature rises.Therefore the variation of the conductivity with temperature is determined by the temperature variation of the mobility which as we saw above was of the form ; $T^{-3/2}$.It has been shown that the conductivity of a semiconductor can be increased by heating or by adding appropriate impurities to increase the carrier concentrations.

By adding a minute amount of suitable impurities to the melt during the growth of the semiconductor crystal it is possible to increase the

Fig.(3.6).Variation of conductivity with temperature for an extrinsic S.C for(A)ideal case(B)amorphous realistic case.

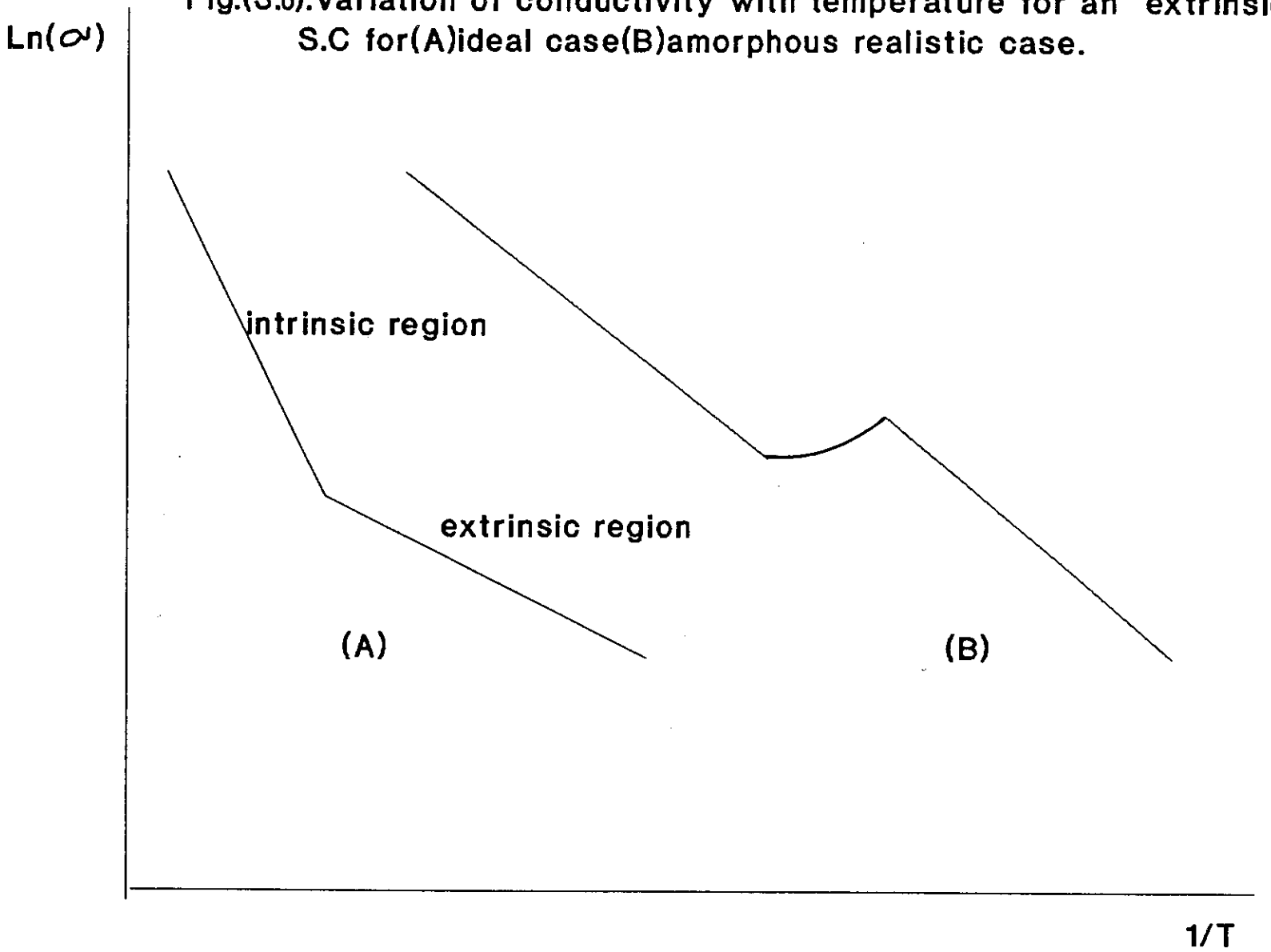

conductivity. For silicon(and germanium) two types of impurities are used. These are from , group III and V of the periodic table, respectively i.e.trivalent elements such as Boron and Indium and pentavalent elements such as Arsenic and phosphorus.

3.3.CHALCOGENIDE GLASSES:-[30]

Chalcogenide glasses comprise one of the major categories of amorphous semiconductors. The D.C conductivity of this materials obey the Arrhenius type equation[31]:-

$$\sigma = \sigma_o \exp(- E/KT) \qquad (3.14)$$

Chalcogenide glasses have well defined optical absorption edges which usually be fitted to the equation :

$$\alpha h\upsilon = B(h\upsilon - E_g)^n \quad (3.15) \qquad (3.15)$$

Where B is a constant, E_g is the optical energy gap and n=2. Seebeck coefficient (S) for chalcogenide glasses is in the order of millivolts per degree and it decreases with temperature according to the relation:

$$S=(k/e)\{(E_s/KT) + A \} \qquad (3.16)$$

Where A is constant. The energy E_s is not necessarily the same as E_σ or $(E_g/2)$. With few exceptions the chlacogenide glasses have positive Seebeck coefficients indicating that the holes dominate in the transport

processes.

The hole mobility is always at least an order of magnitude greater than the electromobility but in both cases, over a wide range of temperature the mobility is activated i.e[32]:

$$\mu = \mu_o \exp(-E_\mu/KT) \qquad (3.17)$$

3.3.1 ELECTRONIC BAND STRUCTURE AND TRANSPORT:

Several research groups have been devoted considerable efforts to experiments which probe the density of states near the mobility edges and within the mobility gap. Mobility measurements by the time of flight method are particularly important but it must be augmented by others and a particular model of the band structure can be regarded as satisfactory only if there is reasonable consistency with several different experiments.

In addition to transient time mobility measurements relevant information is also obtained from, for example, optical absorption, D.C conductivity over a range of field and temperatures, steady state and transient photoconductvity , thermoconductivity , thermoelectric power,field effect measurements and A.C conductivity. The results are shown in fig.(3.7)

There is still controversy about the precise mechanism for electronic transport but there is no doubt that where measurements

Thus although one can envisage the origin of the localized defect states in general, it is much more difficult to provide a theoretical basis.

Mott et al.[33], have proposed the first theoretical model, it assumes that a dangling bond, which contains one unpaired electron when neutral, may be occupied by zero, one or two electrons.

The three states are labelled D^+ , D° ,and D^- respectively and it is further assumed that there is a sufficiently strong lattice distribution, that the reaction:-

$$2\ D^\circ \text{ -----> } D^+ + D^-$$

is exothermic.

The lattice distortion is an important feature of the model and in the chalcogenide glasses it is suggested that they arise from a strong attraction between a D^+ state and occupied lone-pair orbitals, a bond with the (empty) D^+ and hence a large electronic energy is released (exothermic) because the lone-pair electrons are transformed into deeper bonding states.

The D^+ complex with an extra electron forms a shallow donor. The D^- states with its two electrons can not form a covalent band and instead appear as a valence band like lone - pair with characteristics of shallow acceptor level.

In the ground state of the system all the states are therefore either positively or negatively charged and neutral (singly occupied) D^{o} states occur only by excitation. Hence the model accounts for the absence of paramagnetism and of E.S.R, for the absence of optical absorption just below the band gap energy and for the lack of $Log(\sigma)$ $\&(1/T)^{1/4}$ behaviour.

It is also generally consistent with photoconductivity and transport data on most chalcogenide glass.

Moreover,the D^{+} and D^{-} states are present in equal numbers and the situation is analogous to perfectly compensated semiconductors. Thus the model also predicted that the Fermi level is pinned near the middel of the gap, in agreement with the widely observed intrinsic nature of conduction in chalcogenide glasses. It has been well known since the earliest work on chalcogenide glasses that while they are relatively insensitive to composition, small additions of some metals such as Ag,Cu,Tl,and, Mn . cause a large increase in conductivity and coupled with a decrease in activation energy.

Mott[34] has extended the model of defect states to explain these affects, by assuming that in the glass net-work the metallic impurity is charged (through either a deficient or an excess valency) and tend to neutralize the D^{-} center of opposite sign. The effect of the metal is, therefore, to remove the compensation and hence to un-pin the

Fermi level from its position near the center of the mobility gap causing an increase in conductivity and a decrease in activation energy.

3.4. A.C CONDUCTIVITY

3.4.1. THEORY OF A.C CONDUCTIVITY :-

In many amorphous semiconductors and insulators[35] the A.C conductivity invariably has the form:

$$\sigma(\omega) = A\ \omega^{S} \qquad (3.18)$$

Where :

A: constant depends on temperature and

S: it is generally less than or equal to unity.

Many different theories[36,37] for the A.C conduction in amorphous semiconductors have been proposed to account for the frequency and temperature dependence of $\sigma(\omega)$ and S. It is commonly assumed that the pair approximation holds, namely, the dielectric loss occurs because the carrier motion is considered to be localized within a pair of sites.

In essence, two distinct processes have been proposed for the relaxation mechanism,namely the quantum mechanical tunneling through the barrier separating two equilibrium positions and classical hopping of carriers over the barrier or some contribution or variant of the two, and it is assumed generally that electrons (or polarons)or atoms are the carriers responsible. In the following, models have been proposed to interpret the A.C conductivity data of the glassy semiconductors.

3.4.2.QUANTUM MECHANICAL TUNNELING MODEL:

Several authors[38-42] have evaluated, within the pair approximation, the A.C conductivity for single electron motion undergoing the Quantum Mechanical Tunneling(Q.M.T)model and obtained the following expression for $\sigma(\omega)$:

$$\sigma(\omega) = Ce^2 K_B T [N(E_f)]^2 \alpha^{-1} \omega R^4 \omega \qquad (3.19)$$

Where

C : a numerical constant which varies slightly according to different authors.

$N(E_f)$: The density of states at the Fermi level (assumed to be constant).

α : The special decay parameter for the localized wave function.

The frequency exponent S in this model is given by:

$$S = 1-\{4/Ln(1/\omega\tau_o)\} \qquad (3.20)$$

Thus for the Q.M.T. model, the A.C conductivity is linear in the dependence on temperature(equation 3.19) and the frequency exponent S is temperature independent but frequency dependent(equation 3.20). For a typical example, if the characteristic relaxation time $^{(43)}\tau = 10^{-13}$ sec, $\omega = 10^4 s^{-1}$ then S = 0.81 from equation(3.20).

A temperature dependent frequency exponent can be obtained within the framework of Q.M.T.model by assuming that the carrier form a non overlapping small polarons. In this case, however, the frequency exponent S increases with increase in temperature. The simple Q.M.T. model also predicts that S should change appreciably with increasing frequency.

Nevertheless eqn.(3.19) suggests temperature dependence of the A.C conductivity in the form:

$$\sigma(\omega) \backsimeq T^n \qquad (3.21)$$

With n=1

3.4.3.OVERLAPPING LARGE POLARON TUNNELING (O.L.P.T) MODEL:-

Long[44]proposed a mechanism for polaron tunneling model, where large polaron wells of two sites overlap, thereby reducing the polaron hopping energy[45].i e.

$$W_H = W_{H_o}(1-r_p / R) \qquad (3.22)$$

Where:

W_H : The polaron hopping energy

r_p : The polaron radius

R : The intersite separation.

W_{H_o} is given by : $W_{H_o} = e^2 / 4 \varepsilon_p r_p$ (3.23)

Where ε_p is the effective dielectric constant.

The A.C conductivity for this model has been deduced as

$$\sigma(\omega) = \pi^4 e^2/12 \ (K_B T)^2 \{N(E)\}^2 \{\omega R^4_\omega / (2\alpha K_B T + (W_{Ho} r_p / R^2_\omega)\} \quad (3.24)$$

Where R_ω is the intersite hopping separation length at frequency ω.

The frequency exponent S in the O.L.P.T model can be evaluated from:

$$S = 1 - \frac{\{ 8\alpha R_\omega + (6\beta W_{H_o} r_p / R_\omega) \}}{(2\alpha R_\omega + \beta W_{H_o} r_p / R_\omega)^2} \quad (3.25)$$

Where $\beta = 1 / K_B T$

Thus the O.L.P.T model predicts that S should be both temperature and frequency dependent (eqn.3.25)and that S decreases from unity with increasing temperature. For large value of r_p, S continues to decrease with increasing of temperature eventually tending to the value of S predicted by the simple Q.M.T model, whereas for small value of r_p ,S exhibits a minimum at a certain temperature and subsequently increases in similar fashion to the case of the small polaron Q.M.T.

The O.L.P.T. model also predicts the frequency dependence of S(eqn.3.25). The O.L.P.T. model predicts(eqn.3.24) a considerably stronger temperature dependence of the A .C conductivity in the temperature regime where the frequency exponent S is a decreasing

function of temperature.

The functional form of the temperature dependence of $\sigma(\omega)$predicted by equation(3.24) is complicated and can not be simply expressed as :

$$\sigma(\omega) = T^n \qquad (3.26)$$

Where n, constant over a wide temperature range.

3.4.4.CORRELATED BARRIER HOPPING (C.B.H) MODEL:-

A model for the A.C conduction which correlates the relaxation variable W with the interstice separation R has been developed initially by Pike[46] for single electron hopping and extended by Elliott[47] for the two electrons hopping simultaneously. For neighbouring sites at a separation R , the Coulomb wells overlap, resulting in lowering of the effective barrier from W_h to a value W.

The A.C conductivity in the model termed correlated barrier hopping (C.H.B) model, in the narrow band limit, is given by:

$$\sigma(\omega)=(\pi^3/24)\ N^2\ \varepsilon\ \varepsilon_0\ \omega\ R_\omega^6 \qquad (3.27)$$

Where N is the concentration of pair sites.

The frequency exponent S for this model is evaluated as:

$$S = 1 - \frac{6K_B T}{W_H + K_B T \, \mathrm{Ln}(\omega \tau_o)} \qquad (3.28)$$

Thus , in the C.B.H model , a temperature dependent frequency exponent S is predicted ,with S increasing towards unity as T-----> O K , in a marked contrast to the Q.M.T or simple hopping over barrier model.

Many investigators have been studied the A.C conductivity [48-64] as a function of frequency and temperature for the amorphous semiconductors. Generally it was found that as the frequency and temperature increase the A.C conductivity increases.

3.5.DIELECTRIC PROPERTIES OF GLASSES:

Dielectric properties are of especial importance when used as capacitive element or as insulation. The dielectric constant, dielectric loss factor and dielectric strength usually determines the suitability of a particular glass. Variation of dielectric properties with frequency, field strength, and other circuit variable influence the performance of glass. Environmental effects such as temperature, humidity and radiation also influence the performance of glass in dielectric applications. Glass as an insulating material has some definite advantage over plastics which are major competitors.

3.5.1.THEORY :

Dielectric properties comprise the non-long-range conducting electrical characteristics of glass. Dielectric response result from the short range motion of charge carriers under the influence of applied electric field. The motion of the charge leads to the storage of electrical energy and the capacitance of the dielectric.

3.5.2.POLARIZATION IN GLASS:-

There are four primary mechanisms of polarization in glass. Each mechanism involves a short range motion of charge and contribution to the total polarization of the material. The polarization mechanisms

include[64]:-

1-electronic polarization (p_e).

2-atomic polarization (p_a).

3-orientational polarization (p_o).

4-interfacial polarization (p_i).

A schematic of the mechanism of operation of each of these major types of polarization as well as two especial cases is given in Fig.(3.8).

Electronic polarization is due to the shift of the valence electron cloud of the ions within the material with respect to the positive nuclei. This mechanism of polarization occurs at a very high frequency(10^5.Hz).

At frequencies in the ranges (10^{12} -10^{13} Hz), atomic or ionic polarization occurs. Atomic polarization is the displacement of positive and negative ions in a material with respect to each other. In the sub-infrared range of frequencies, orientation polarization contributes to the dielectric properties of glass. Orientational polarization , also referred to as dipolar polarization, involves the perturbation of the thermal motion of ionic or molecular dipoles, producing a net dipolar orientational in the direction of the applied field.

The last polarization mechanism, interfacial or space charge polarization , occurs when mobile charge carriers are impeded by a physical barrier that inhibits charge migration.

Fig.(3.9). Vector diagram of charging,loss and total currents in a glass dielectric .

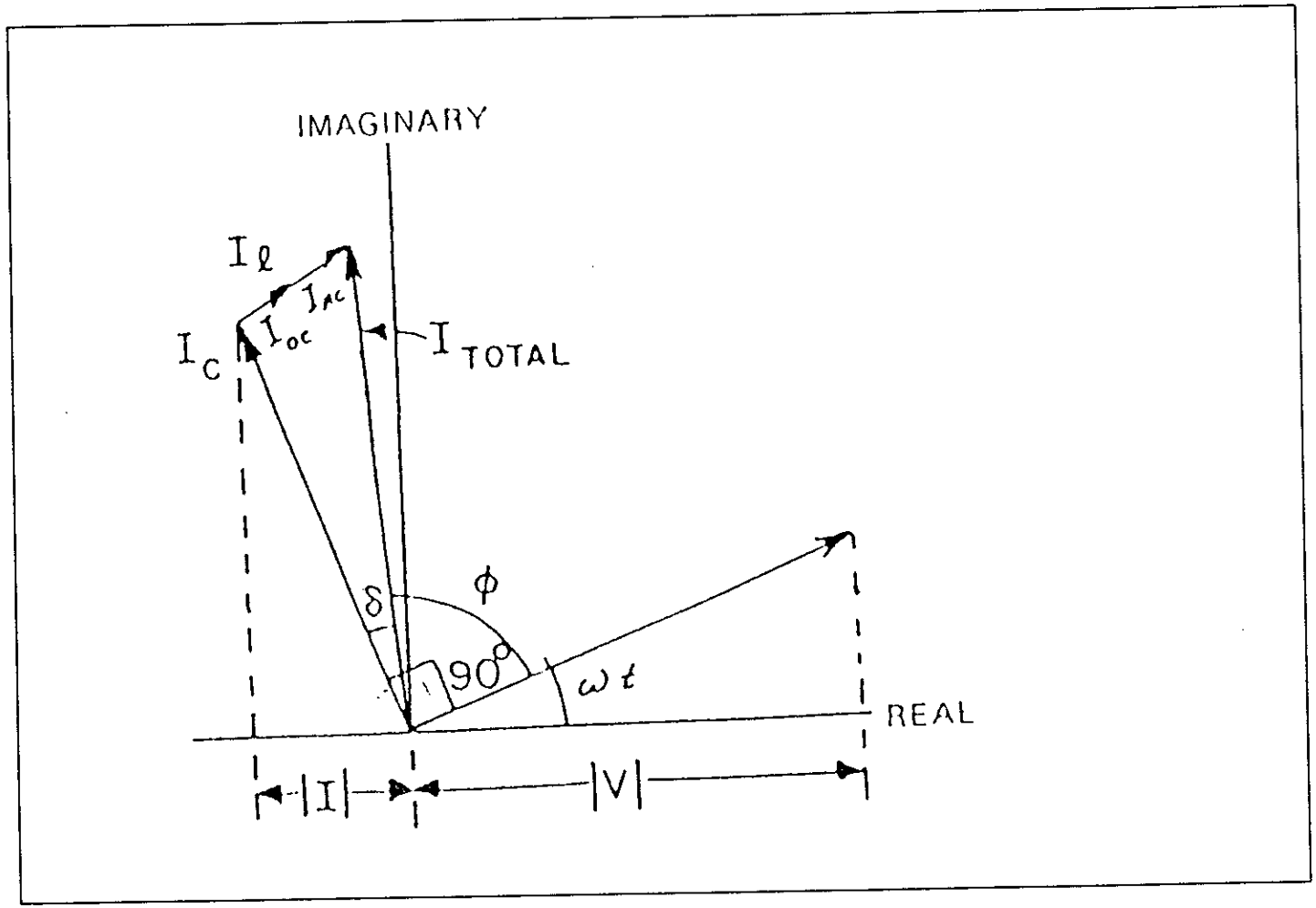

3.5.3.DIELECTRIC LOSS IN GLASS:-

If a sinusoidal potential $V = V_0 \exp (i\omega t)$ is applied to the dielectric, the charge density must vary with time, which consistent a charging current[65]:

$$I_c = dQ/dt = c\ dv/dt = i\omega c\, v = \omega c v_0 \exp [i(\omega t + \pi/2)] \qquad (3.29)$$

The charging current in an ideal dielectric leads the applied voltage by $\pi/2$. This relation can be illustrated vectorially in fig.(3.9)[66].In addition to the charging current associated with storage of electric charge by the dipoles, a loss current must also be considered for real dielectrics. The loss current arises from two sources:

a-The long range migration of charges,dc Ohmic conduction, and
b-The dissipation of energy associated with rotation or oscillation of dipoles.

The latter contribution to the dielectric loss is a consequence of the charged particles having a specific mass and therefore, an inertial resistance in their movement. Electrical energy from the field is lost in the overcoming of this inertia during polarization.

The ac conduction from the inertial resistance and the dc conduction

both are in phase with the applied voltage and a loss current can be written as :

$$I_\ell = (\sigma_{dc} + \sigma_{ac}) V \qquad (3.30)$$

The total current for a real material is thus:

$$\vec{I}_T = \vec{I}_c + \vec{I}_\ell = (i\omega c + \sigma_{dc} + \sigma_{ac}) V \qquad (3.31)$$

The total current in a real dielectric is a complex quantity which leads the voltage by an angle (90 -δ) where δ is called the loss angle.

An alternative way of expressing the concept of a real dielectric possessing both charging and loss processes is the use of a complex permitivity to describe the material:

$$\varepsilon^* = \varepsilon' - i\varepsilon'' \qquad (3.32)$$

The total current in the dielectric material can now be expressed as :

$$I_T = i\omega K' C_o V + \omega K'' \cdot C_o V \qquad (3.33)$$

Where:

$$K^* = \varepsilon^*/\varepsilon_o = K' - iK''$$

The first term on the R.H.S in eqn(3.33) describes the charge

storage in the dielectric and K' (or $\grave{\varepsilon}$) is called the charging constant or the dielectric constant. The second term represents dielectric losses and ε'' and K'' represent the dielectric loss factor and the relative dielectric loss factor respectively.

3.5.4.THE DIELECTRIC LOSS TANGENT($\tan \delta$):

$$\tan (\delta) = \varepsilon''/ \varepsilon' = K''/ K' \qquad (3.34)$$

This form represents the relative expenditure of energy to obtain a given amount of charge storage. The product $\varepsilon \tan (\delta)$ is sometimes called the total loss factor. To minimize the dielectric losses in the insulator it is necessary to have small dielectric constant and a very small loss angle. The frequency dependent relationships of the dielectric constant, dielectric loss and the loss tangent are given by:

$$K' = K_{00} + \frac{K_s - K_{00}}{1+\omega^2 \tau^2} \qquad -- (3.35)$$

$$K'' = \{K_s - K_{00}\} \{\omega\tau / (1+ \omega^2\tau^2) \} \text{---(3.36)}$$

$$\tan(\delta) = \frac{K''}{K'} = \frac{(K_s - K_{00})\omega\tau}{K_s + K_{00} \omega^2\tau^2} \qquad \text{-----(3.37)}$$

Where K_S & K_∞ are the static and infinite dielectric constant.

These equations are known as the Debye[67] equations and they yield the graphical relationships shown in fig(3.10).

It is found that the ionic conduction of glasses is always accompanied by dielectric relaxation. Such dielectric relaxation arising from ionic motion is also called conductivity relaxation. In resent years, conductivity relaxation has been studied while the fast ionic conduction of glasses is investigated because the study of conductivity relaxation of ion conductive glass is not only essential for understanding the mechanism of the ionic conduction but also beneficial to their application as dielectrics[68].

There are different ionic motions in glass which are responsible for the presence of the dielectric properties. The first is the rotation of ions around their negative sites. The second is short distance transport. The ions hop out of sites with low free energy barriers and tend to pile up at sites with high free energy barriers in the electric field direction in the dc low frequency electric field or oscillate between the sites with high free barriers in an ac electric field. Both the first and the second mechanisms make a contribution to the dielectric constant of glasses.

The third ionic motion is that the ions with higher energy can

Fig.(3.10).Frequency variation of dielectric parameters due to Debye relaxation process.

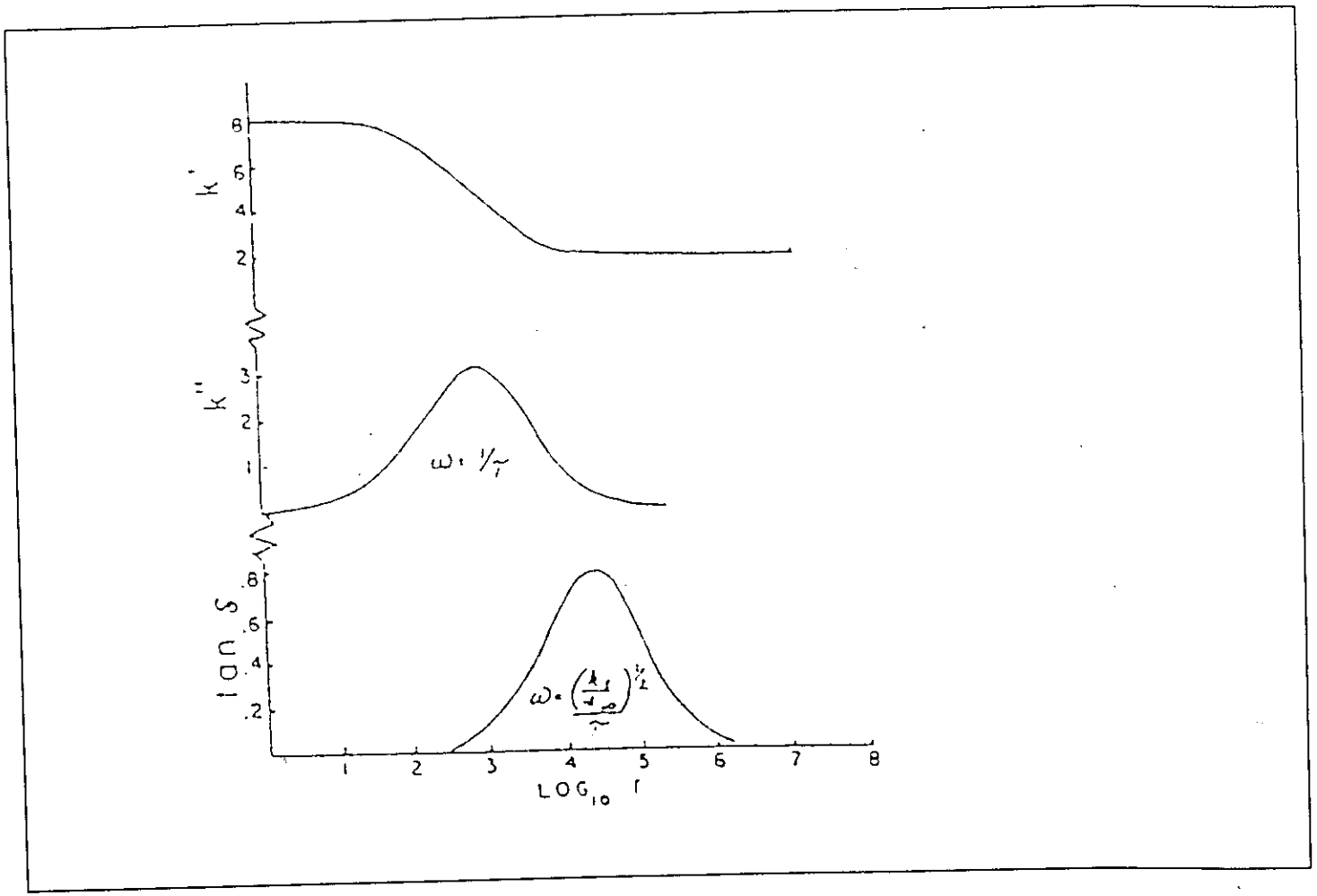

penetrate the glass i.e. conduct electricity and cause the dielectric loss ε''.

The dielectric loss is similar to that expected by Debye dielectric process characterized by relaxation time τ such that the dielectric loss ε'' is proportional to a term :

$$\omega\tau \ /(\ 1+\omega^2\tau^2)$$

In this case a peak should occur in the dielectric loss when $\omega\tau=1$ and τ usually decreases with temperature according to the relation[69]:

$$\tau = \tau_o \quad \exp\ (\ E_{rel.} / KT\ ) \qquad (3.38)$$

Where $E_{rel.}$ is the activation energy of relaxation.

3.5.5.THE EFFECT OF FREQUENCY AND TEMPERATURE ON THE DIELECTRIC LOSS :

At high temperature for a given frequency a peak is observed in the dielectric loss, which shifts to higher temperature when the frequency of measurement is increased[70]. The dielectric loss – frequency dependence obeys the relation[71]:-

$$\tan\ (\ \delta\ ) = A\ \omega^s \qquad (3.39)$$

Where A is constant.

The loss peak and dispersion curve shift to higher frequency as the temperature dependence is increased. If the peak shape is remain the same as the temperature is changed, the shift of the peak maximum gives a measure of the temperature dependence of the loss. For glasses, the frequency at which the loss is a maximum increases exponentially with temperature following the relation[72]:

$$f_m = A \exp (-Q / RT) \qquad (3.40)$$

Where

Q: is the activation energy ,

R: is the gas constant , and

A: is independent of temperature.

The A.C conductivity and the dielectric constant properties of glasses are caused by the delayed response of carrier hopping motion in an applied field[73] F.

In an alternating field, the frequency dependent(or a.c conductivity) is then given by[74]:

$$\sigma(\omega) = \frac{(\varepsilon_s - \varepsilon_\infty) \omega^2 \tau}{1 + \omega^2 \tau^2} \qquad (3.41)$$

Where:

$$\varepsilon_s - \varepsilon_\infty = \frac{4\pi N e^2 R^2}{3KT} \exp(-w/KT) \qquad (3.42)$$

In this equation:

N : The number of pairs per unite volume

$\varepsilon_s, \varepsilon_\infty$: The static and high frequency dielectric constant respectively and τ is the relaxation time characterizing the delayed response.

The relaxation time in equation(3.41)is given by :

$$\tau = (\upsilon_{ph})^{-1} \exp(2\alpha R) \qquad (3.43)$$

for phonon- assisted quantum mechanical tunnelling and by

$$\tau = (\upsilon_{ph})^{-1} \exp(W/KT) \qquad (3.44)$$

for thermal activation over a barrier of height W, with (υ_{ph}) corresponding to a lattice vibrational frequency.

Equations (3.41) and (3.42) have been extensively applied to the dielectric relaxation processes caused by ionic processes in glasses. Electronic migration may also invlove thermal - activation over an energy barrier, however, and classical models of this sort have been

introduced for Debye - like dielectric processes due to electrons[75].

Frequently, of course, one would expect electronic hopping to occur by tunneling with eqn.(4.43) the more appropriate for the relaxation time.

On the other hand, there are situations, particularly at low temperature, where the atoms or ions may hop by QMT[76]. Consequently ,electronic and ionic effects often make very similar contribution to dielectric polarization phenomena and they may, indeed, be closely intermoven.

In an amorphous semiconductor for which the density of states of fig.(3.7)are appropriate, hopping at the Fermi-level,or in states in the tail near E_c and E_v ,or in the levels of discrete localized states in between, could give rise to an ac conductivity and dielectric polarization.The former would not require thermal excitation of carriers and would at the most be only weakly temperature dependent. The latter two cases would require the thermal generation of carriers and hence the associated a.c conductivity should have a substitutional activation energy. In all three cases,however, the hopping sites would be randomly distributed(especially) and spread over a range of energies, causing a spread in the associated relaxation times.

The temperature dependence of the A.C conductivity in the amorphous material is given by [77]:

$$\sigma_{ac}(\omega) = \frac{n \pi^2 \varepsilon_1 \varepsilon_0 N N_p \omega R_\omega^6}{6} \exp\left(\frac{e^2}{4\pi \varepsilon_1 \varepsilon_0 K T_g R_\omega}\right) \quad (3.45)$$

Where:

N: The total density of charged defect states.

N_p: The number of pairs contributing to A.C conduction.

T_g: The glass transition temperature.

ε_1: The real dielectric constant.

ε_0: The permitivity of free space.

K: The Boltzmann constant.

3.6 . CRYSTALLIZATION :-

Impeding or controlling crystallization, both are of utmost importance for any application of glasses, and crystallization studies are of interest:

-In understanding glass formation and assessing the thermal stability of glasses.

-In elucidating the fundamentals of nucleation and growth processes during crystallization.

-In learning to produce particular novel and useful microstructures by controlling crystallization unobtainable by other means.

Resent experimental and theoretical studies on the crystallization of glasses should be helpful in predicting crystallization rates in new compositions and also in defining the limiting times and temperatures to which a glass piece can be subjected.

For many years ago it was believed that the physical properties of glasses can not be modified by adding small amount of doping elements into them. However recently appreciable changes in some physical properties of many glasses have been observed when small amount of doping elements have been introduced in these glasses[78,79].

The crystallization of amorphous materials can be induced by changing various parameters (e.g. temperatures optical radiation, electric field, pressure, impurities,.....etc) and a number of experiments have been carried out to study these effect[80-83].

3.6.1- GLASS FORMATION

What is can be glasses ?In principle any substance can be made into a glass by cooling it from the liquid state fast enough to prevent crystallization. The final temperature must be slow that the molecules move too slowly to arrange to the more stable crystalline form. Turnbull[84] concludes that there is no rigorous proof that the most stable state of a substance at low temperature is crystalline rather than glassy, but that with the exception of Helium it is found experimentally that the most stable forms of pure substances are crystalline. It is recognized that glasses can be formed using a variety of techniques, including cooling from the liquid state, condensation from the vapour (using vacuum evaporation, reactive or non-reactive sputtering, vapour phase hydrolysis decomposition of metal organics or plasma reaction) pressure quenching solution hydrolysis, anodization, gel formation , bombardment of crystals by high energy particles and possible shook wave method as well.

3.6.2.MODELS OF GLASS FORMATION[85]

"STRUCTURAL AND THERMODYNAMIC VIEWS ".

The problem of glass formation has been considered from many points of view. In all cases it is recognized that the formation of glasses require cooling to a sufficiently low temperature- below the glass transition without occurrence of detectable crystallization. In some cases, it is suggested that certain structural features or properties of the materials will result in glasses being formed. This lead to categorizing materials as glass formers or non-glass formers, where in other cases it is suggested that the critical factor in glass formation is the rate of cooling relative to the kinetics of crystallization. This direct attention to other characteristics of the materials, and suggest that nearly all liquids will form glasses if cooled very rapidly and crystallize if cooled very slowly.

The various models which have been advanced to discribe glass formation can then be grouped into three categories, depending on factors which are viewed as a decisive in determining the likelihood of materials being formed as glasses. These groups are[86]:

1-structural.

2-Thermodynamic and

3-kinetic

3.6.3- THERMODYNAMIC OF CRYSTALLIZATION

The driving force during the crystallization process is the difference in free energy between the glass and the appropriate crystalline phase(S).

The difference in the free energy (δG) can be calculated from the observed enthalpy of fusion δH_f and undercooling δT, an approximation for δG is given by the following equation:

$$\delta G = \frac{\delta H_f}{T_f} \cdot \delta T \cdot \frac{2T}{(T_f + T)} \qquad (3.47)$$

The driving force is such that most metallic glasses can crystallize by two or more different reactions.

Which crystallization reaction does occur depends not only on its thermodynamic driving force, but on its kinetics. In most cases the equilibrium phase do not form directly from the glass, but crystallization proceeds by the formation of metastable phase.

3.6.4-PHASE TRANSITION "GLASS MELTING PHASE ----> CRYSTALLINE PHASE

It is well known that ,from the thermodynamic point of view, the metastable condition of glass differs from the stable condition of

crystal by its higher free energy. The transition " vitreous -----> crystalline "takes place via two kinds of reactions : " nucleation and crystal growth."The first one is an endothermal process, while the latter is an exothermal process.

Tammann[87] established that both processes are based on different rate controlling mechanisms. Consequently, the resulting separate treatment of the two problems can be taken for granted.The continued subdivision of the phase transition " glass melting ------> crystalline phase " into homogeneous and heterogeneous nucleation is undertaken for reasons of conveniency in the sense of thermodynamic supposition. This is where we speak of heterogeneous nucleation when nucleation proceeds energetically more than without them.

It has been generally accepted,[88] that the amorphous-crystalline transformation of elemental Se takes place through two different temperature-dependent processes: the nucleation of fine crystalline centers and growth of these nuclei:

3.6.4.1.NUCLEATION

Nucleation phenomena can be investigated only indirectly ,e.g. by analyzing the microstructure after amount of crystallization by extrapolating growth reaction to shorter time[89].
In classic nucleation theory the steady state homogeneous nucleation rate I_{st} is given by:

$$I_{st} = I_o \exp\left(\frac{-L\,\Delta G_c}{RT}\right) \exp\left(\frac{Q_n}{RT}\right) \quad \ldots\ldots (3.48)$$

Where

I_o : a constant factor

L : the Loschmidt number

Q_n : the activation energy for the transfer of atoms across the liquid /nucleus interface, and

ΔG_c : the free energy required to form a nucleus of critical size. For heterogeneous nucleation at a limited number of nucleation sites the activation energy ΔG_c is reduced due to the gain in surface energy thus leading to a significant higher nucleation rate I_{st}.

The nucleation can be internal or surface,homogeneous or heterogeneous, and transient or in steady state. In the brief survey below, homogeneous nucleation is considered first then, heterogeneous nucleation, and finally surface nucleation. Various types of kinetic behaviour for internal nucleation occurring isothermally are shown in fig.(3.11)[90].

Fig.(3.11).Schmatic variation of the no. of nuclei with time in an isothermal anneal for the following types of nucleation:

a)steady state nucleation(homogenous) b) transient homogenous

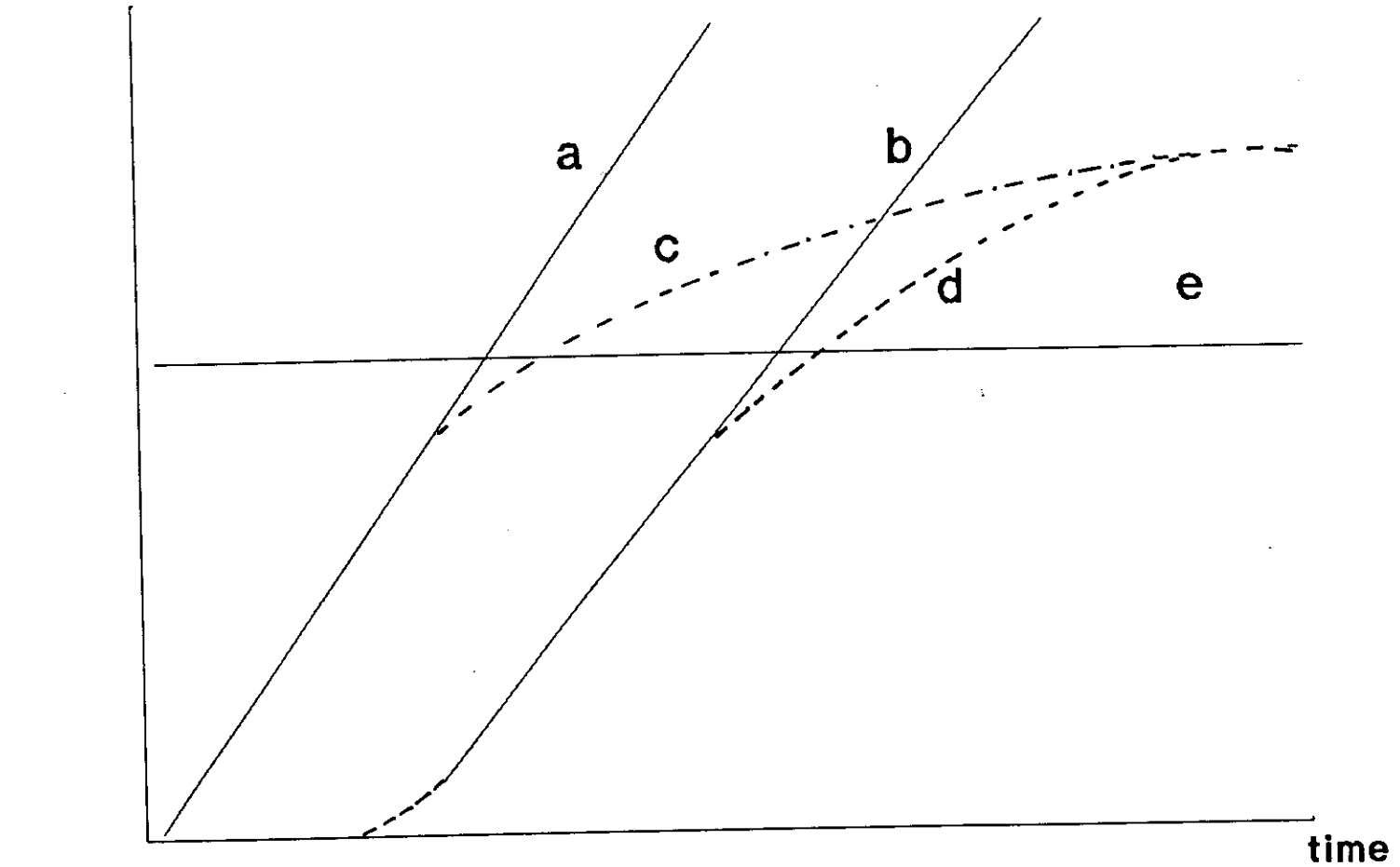

c)steady state hetrogenous d) transient hetrogenous

e) equnched in -active nuclei.

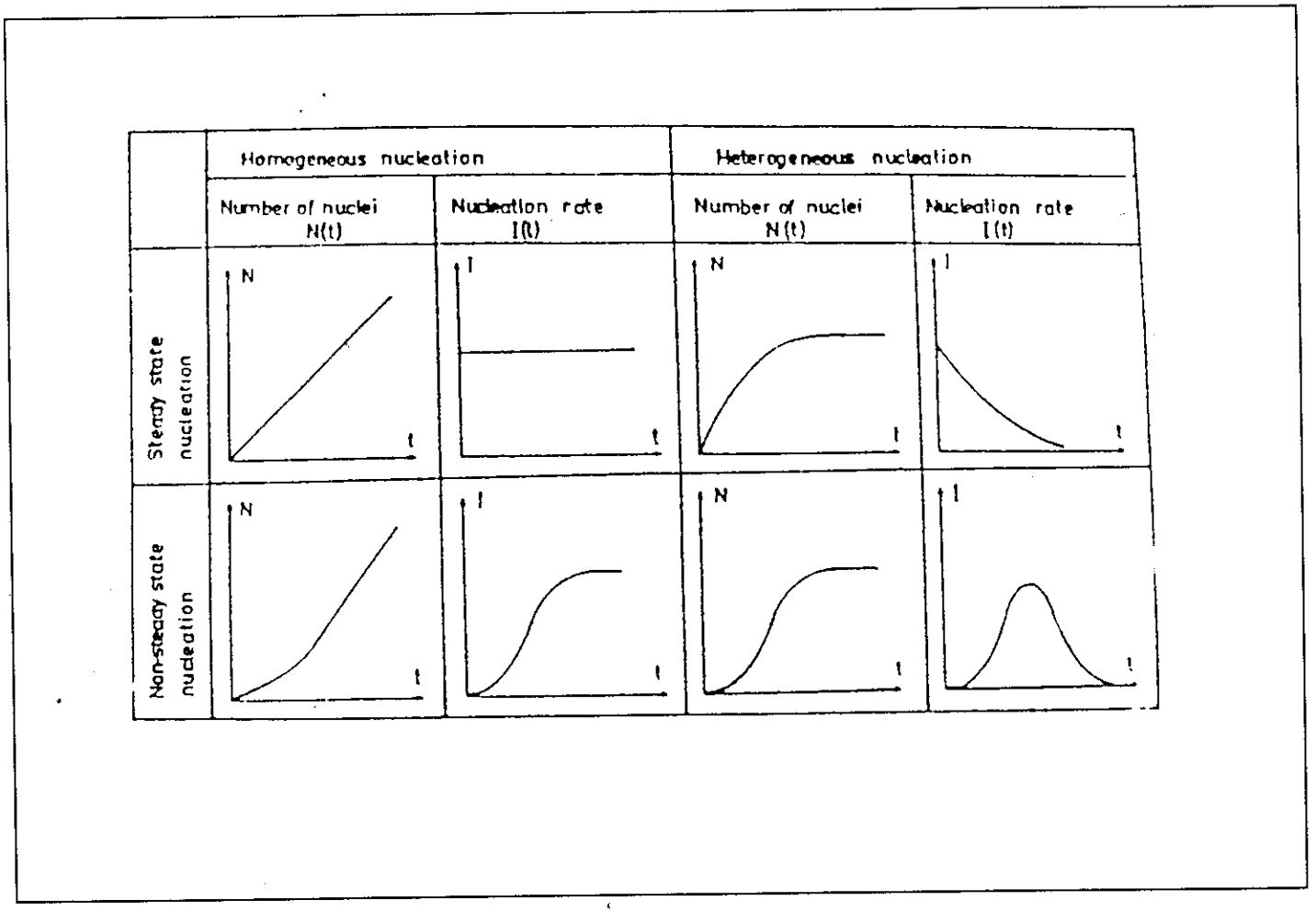
Homogeneous nucleation
Heterogeneous nucleation
Number of nuclei N(t)
Nucleation rate I(t)
Number of nuclei N(t)
Nucleation rate I(t)
Steady state nucleation
Non-steady state nucleation
N
I
t

Fig.(3.12).

3.6.4.3- HETEROGENEOUS NUCLEATION:-

The classical theoretical rule for heterogeneous nucleation can be attributed to the statement that nucleation work on an active foreign substance,e.g, the walls of containers, impurities, nucleating agents,etc is always lower than in the previously described case of non-initiated nucleation,i.e homogeneous nucleation[93].

The heterogeneous nucleation rate was given by the equation :

$$I^{het} = I_o^{het} \, Exp(-\tau^{het}/t) \qquad (3.50)$$

at the initial stage of the steady state nucleation .Where:

I^{het} :non-steady state nucleation rate ,

I_o^{het}: steady state nucleation rate and

τ : the induction period.

The number of nuclei depending upon time and the nucleation rate, are schematically represented in fig.(3.12).

3.6.4.4.SURFACE NUCLEATION :-

Surface nucleation of glasses is important because there may be less resistance to surface than internal crystallization, and because it may affect not only on surface-sensitive properties but also, e.g,magnetic properties through the generation of stresses[94].

The stress energy due to the volume change during crystallization

may be reduced at the surface by a reduction in the thickness of crystalline phase. The oxygen content at the surface may stabilize the number of crystalline phase, thus increasing the driving force for crystallization.

The surface crystallization of glass can lead to serious problems in glass manufacture because of the resultant changes in glass properties such as viscosity and coefficient of thermal expansion. The glass technologists have always been careful to avoid surface crystallization by not holding their glasses at temperatures where crystals grows rapidly in them.

3.6.5.CRYSTAL GROWTH:-

Crystal growth may be primary ,eutectic or polymorphic and has been observed to be always thermally activated. Growth rates have been calculated from crystal diameter distribution after appropriate annealing times. Depending on the crystallization mode we can distinguish between parabolic and linear growth.(95)

3.6.5.1.Parabolic growth

Primary crystallization is generally assumed to be controlled by volume diffusion. If we assume that the diffusion rate,D, is independent on concentration, the radius, r,of a spherical particle will be proportional with the square root of time shown below:

$$r = \alpha\sqrt{Dt} \qquad (3.51)$$

and the growth rate U_p will be given by :

$$U_p = 1/2 \ \alpha^2 D \ r^{-1} \qquad (3.52)$$

Where:

α: is a dimensionless parameter.

3.6.5.2.Linear growth:

Linear growth, i.e constant growth rate, has been found to occur in crystalline reaction which do not involve any compositional change or in a cooperative transformation into two phase involving long - range diffusion in such a way that the mean composition of the crystallized region is equal to that of the glassy matrix.

Once a stable nucleus has formed, it grows during isothermal annealing at large undercooling with a rate U_1 given by:

$$U_1 = U_o \exp \{-Q_g / RT \} \qquad (3.53)$$

Where $Q_g$is the activation energy for growth. The pre-exponentional $U_o$equals to :

$$U_o = \delta \cdot \upsilon \qquad (3.54)$$

Where :

υ : is a characteristic frequency in the order of the Debye -frequency

δ : the distance across the crystallization front.

3.6.6- CRYSTALLIZATION KINETICS

It has bee generally accepted[96] that the amorphous-crystalline transformation takes place through two different temperature-dependent processes, nucleation of fine crystalline centers and growth of these nuclei.

Avrami's equation [97,98] relating the fraction of the crystalline volume(α) grown from the amorphous phase to the time of annealing as :

$$1-\alpha = \theta = \exp\ (-Kt^{n}) \qquad (3.55)$$

This has been successfully applied to study the crystallization kinetics of amorphous semiconductors. The amount of material left uncrystallized at time (t) was calculated by the empirical relation[99]:

$$\theta_t = (H_\infty - H_t)/(H_\infty - H_0) \qquad (3.56)$$

Where :

H_0,H_∞ :are the physical property at the beginning and end of the process respectively.

H_t :the physical property at time " t " between these limits.

The untransformed supercooled liquid volume is assumed to be equivalent to the amorphous part.

The parameter(n)of equation (3.55) characterizing the nucleation mechanism and the dimension of the crystal growth [100] has been calculated using equation[101]:

$$Ln\ (\ -Ln\ \theta_t\ )\ =\ Ln(\ K\ )\ +\ n\ Ln\ (\ t\ ) \qquad (3.57)$$

According to equation (3.57) the plot of $Ln(-Ln\theta_t)$ versus Ln(t) leads to a straight line of slope n. The value of crystallization constant, which depends on temperature, and the definition of the crystallization rate " K ", for each value of, θ, could be determined by the equation:

$$K\ =\ Ln\ (\ \theta^{-1}\ )\ /\ t^n \qquad (3.58)$$

According to (Becker)[102] the energy of activation necessary for the formation of crystalline grain,E,depends on the activation energy of the transfer of particles to nucleus, q, and on the energy of nucleation,ΔF. The theoretical dependence of K on T is given by the equation :

$$K\ =\ K_0\ exp\ (\ -\Delta F-q\ )\ /RT\ =\ K_0 exp\ (-E\ /\ RT\ ) \qquad (3.59)$$

Where R is the universal gas constant.

The radius " r " of the spherulite crystalline domain as a function of time at different temperatures is given by the relation[103]:-

$$r^2 = 2K\ (t - t_n) \qquad (3.60)$$

Where :

t_n : the nucleation (induction) time.

The growth of the crystalline phase in the old amorphous phase is a diffusion process. The diffusion coefficient ,D, of such a process is given by the relation[104]:

$$D = 4.5\ K \qquad (3.61)$$

4.1.THE PHYSICAL PROPERTIES OF THE SYSTEM $Se_{90}Ge_{10-X}In_X$ IN THE GLASSY STATE:-

To study the physical properties of sample owing to the system, $Se_{90}Ge_{10-x}In_x$ where X =2, 4 and 6, the proper temperature ranges have to be specified to avoid the possible phase transformation .

Accordingly, the DTA thermograms for each sample were recorded at the same heating rate (10 degree/min.)and the same constant mass (0.04 gm) as in fig.(4.1). The temperature range between the obtained glass transition temperature (T_g), and the crystallization temperature (T_c) for each sample has been detected in addition to the melting point(T_m) and tabulated in table(4.1).

To ensure that the samples are in a glassy state, X-ray spectrums were recorded.The results are shown in fig.(4.2)

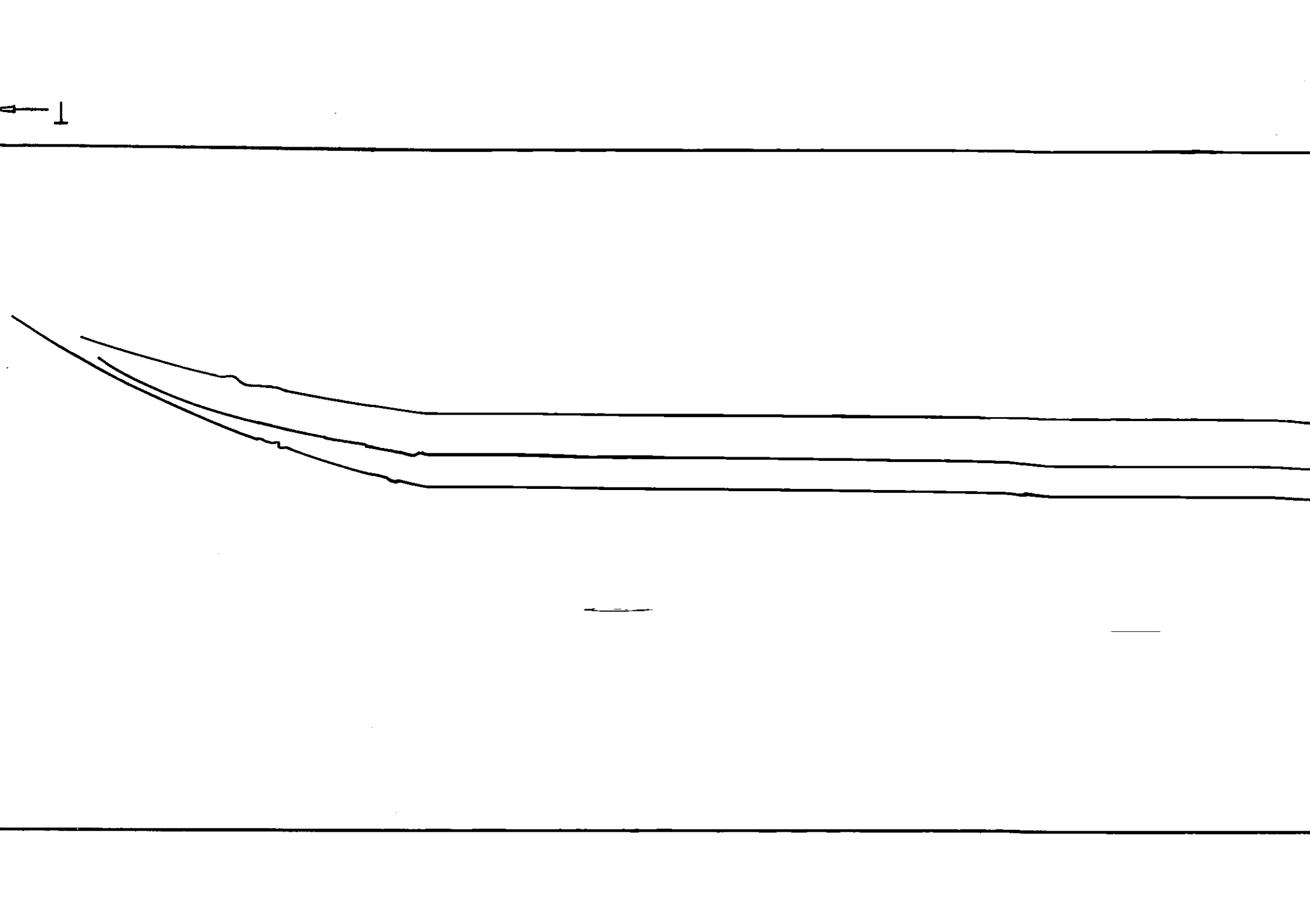

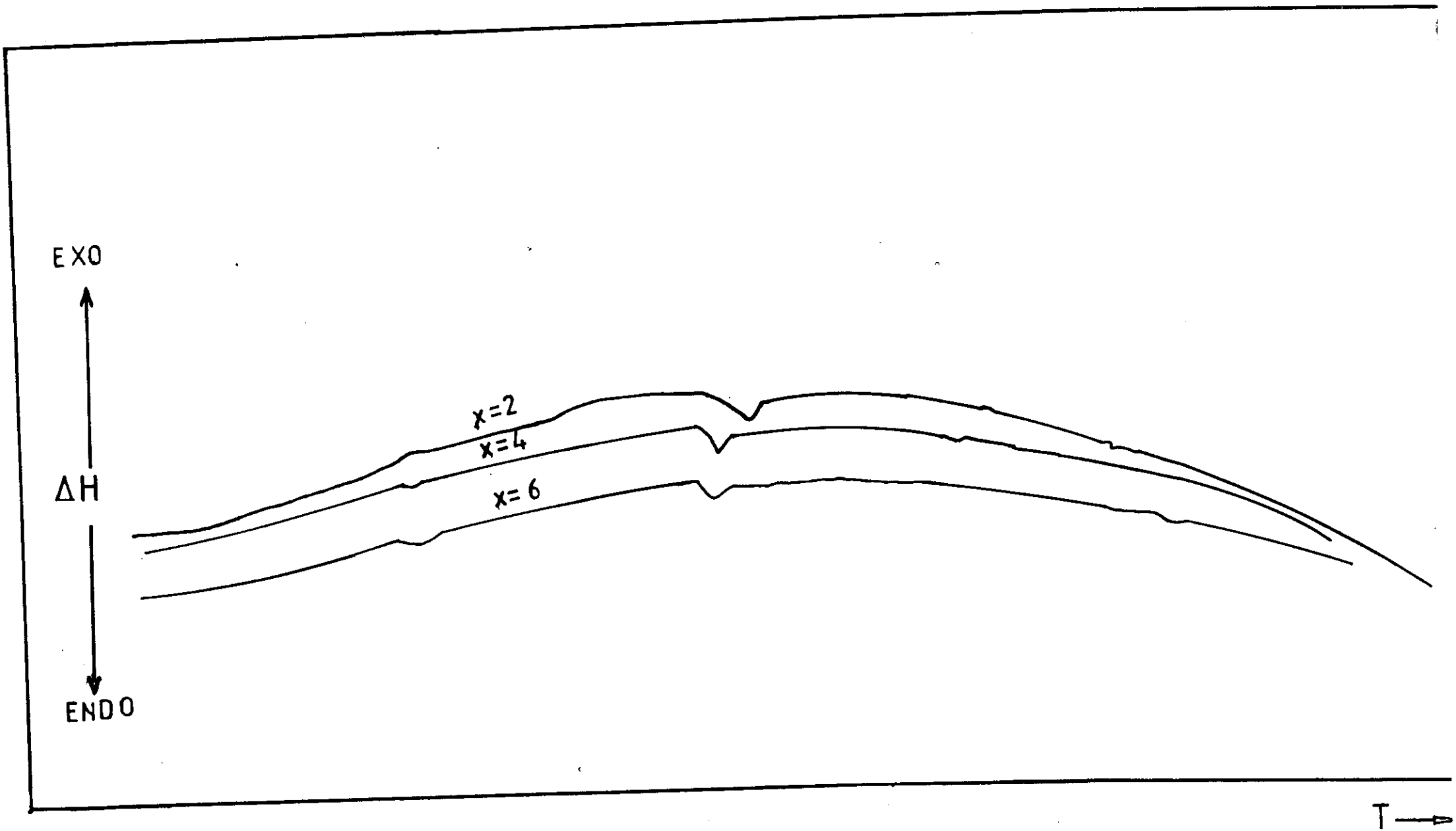

Fig.(4.1):DTA thermograms for the system $Se_{90}Ge_{10-x}In_x$(X=2,4 and 6) in the glassy state.

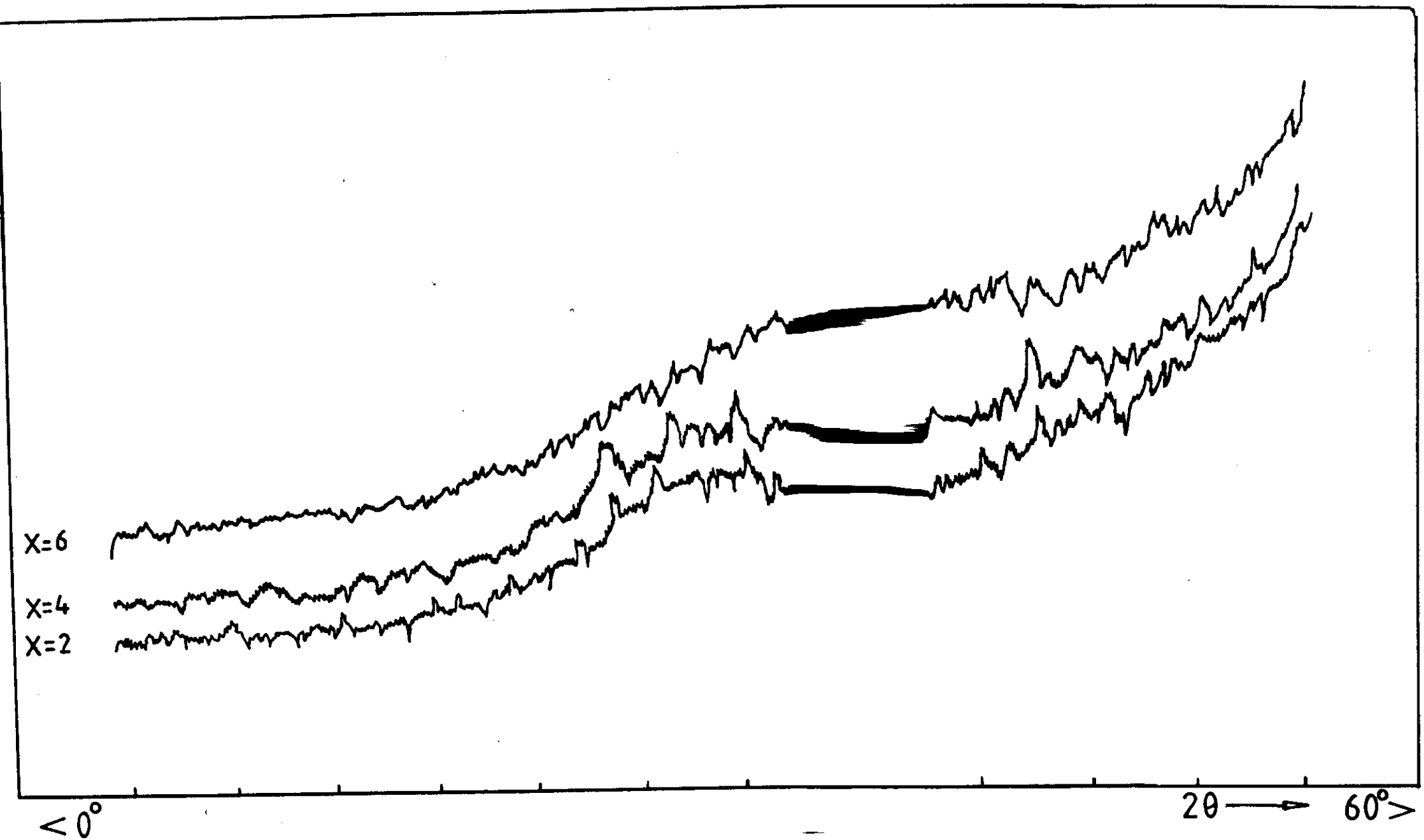

Fig.(4.2):X-ray diffraction Pattern for the system $Se_{90}Ge_{10-x}In_x$(X=2, ▬ and 6)in the glassy state.

Sample composition (X at. %)	T^0_g(C)	T^0_c(C)	T^0_m(C)
2	115	170	210
4	80	160	208
6	78	155	205

Table(4.1):The effect of composition on glass transition temperature (T_g), crystallization temperature (T_c), and the melting point(T_m) of the system $Se_{90}Ge_{10-x}In_x$.

4.1.1.THE TEMPERATURE DEPENDENCE OF THE A.C CONDUCTIVITY:

The temperature dependence of A.C conductivity of the virgin in the glassy system $Se_{90}\ Ge_{10-x}\ In_x$, where X= 2, 4 and 6 at different constant values of frequency has been recorded as shown in figures (4.3,4.4,4.5). It is clear that the A.C conductivity increases as the temperature increases . This may be attributed to the hopping of the electrons at low temperature, while at high temperature it may be due to thermal excitation. The slopes of the obtained curves seem to decrease as the frequency increases.

Fig(4.6)shows the composition dependence of the A.C conductivity at constant temperature (45° C) and different constant values of frequency.

These curves show that the A.C conductivity increases by increasing the Indium content. The rate of increasing σ_{ac} is not constant but it decreases as the Indium content increases.This behaviour may be explained as:

The glasses under study contain Selenium as a major constituent and therefore it expected to exhibit the characteristic features of lone pair (Lp) vitreous semiconductors[24]. The conduction bands in these substances arises from the usual anti-bonding bond but the valence

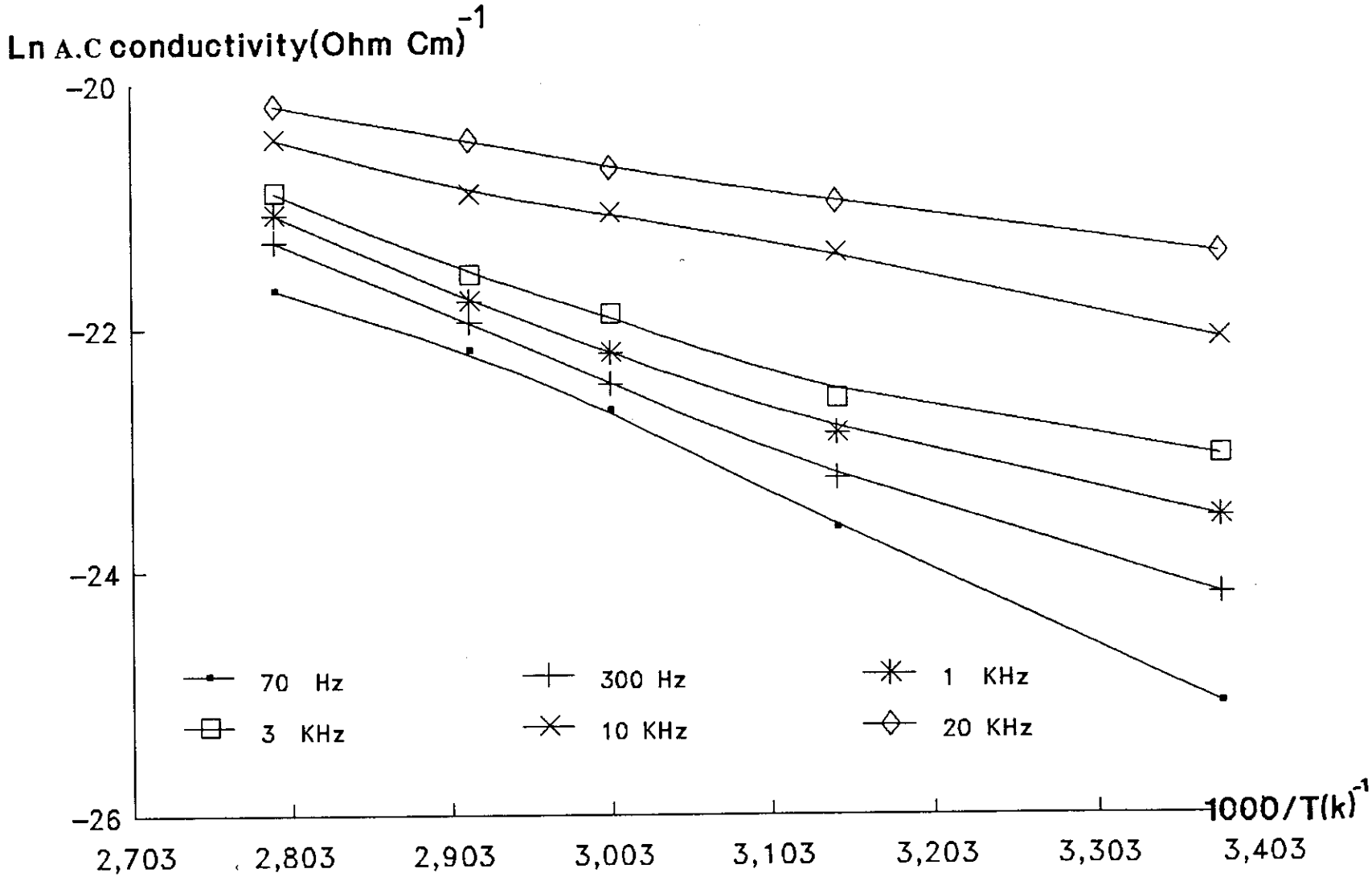

fig.4.3:The temperature dependence of the ac conductivity at different constant frequencies for $Se_{90}Ge_8In_2$ in the glassy state.

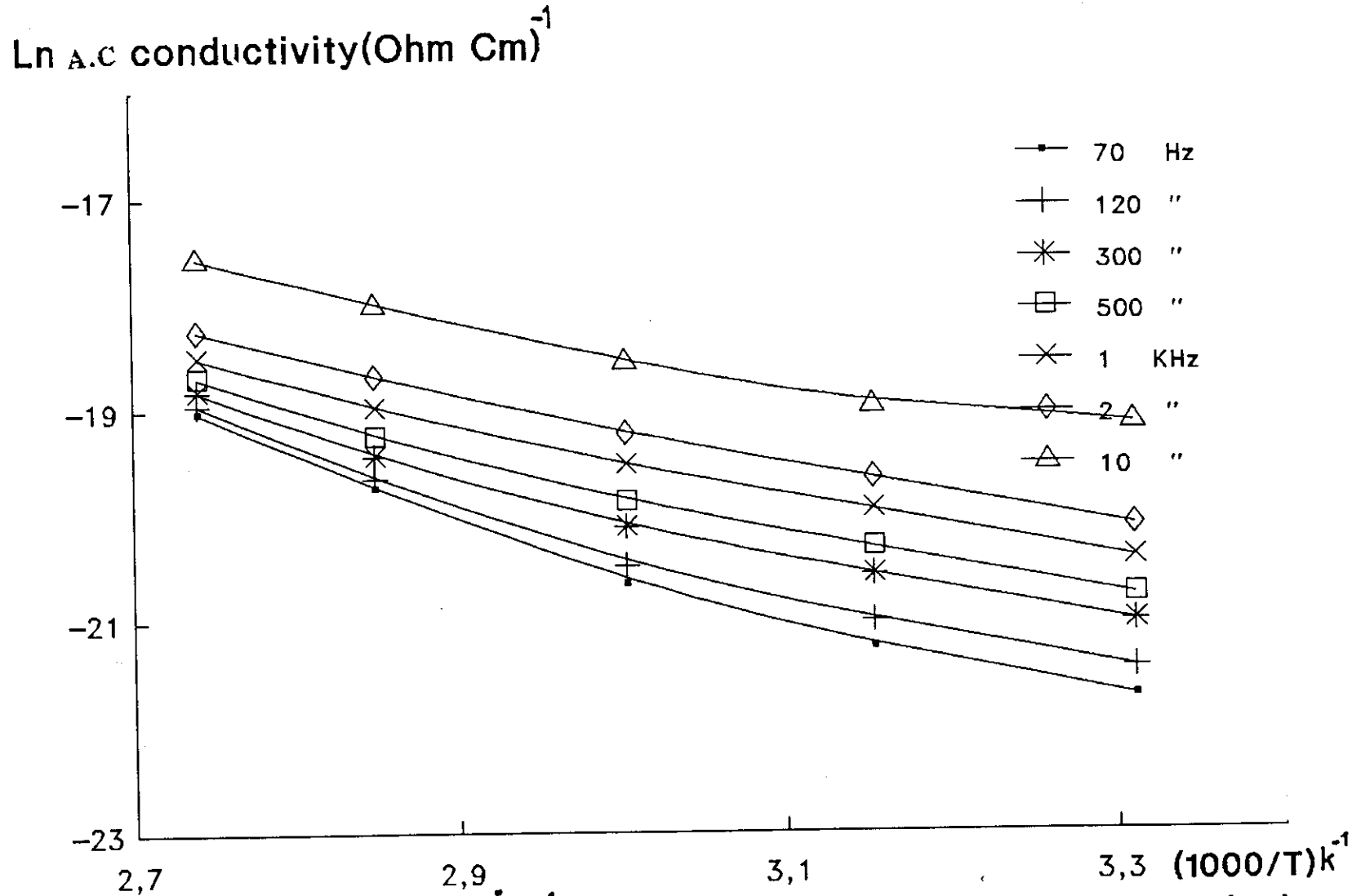

Fig.4.4:Shows the variation of σ_{ac} as a function of temperatures at constant frequencies for $Se_{90}Ge_6In_4$ in the glassy state.

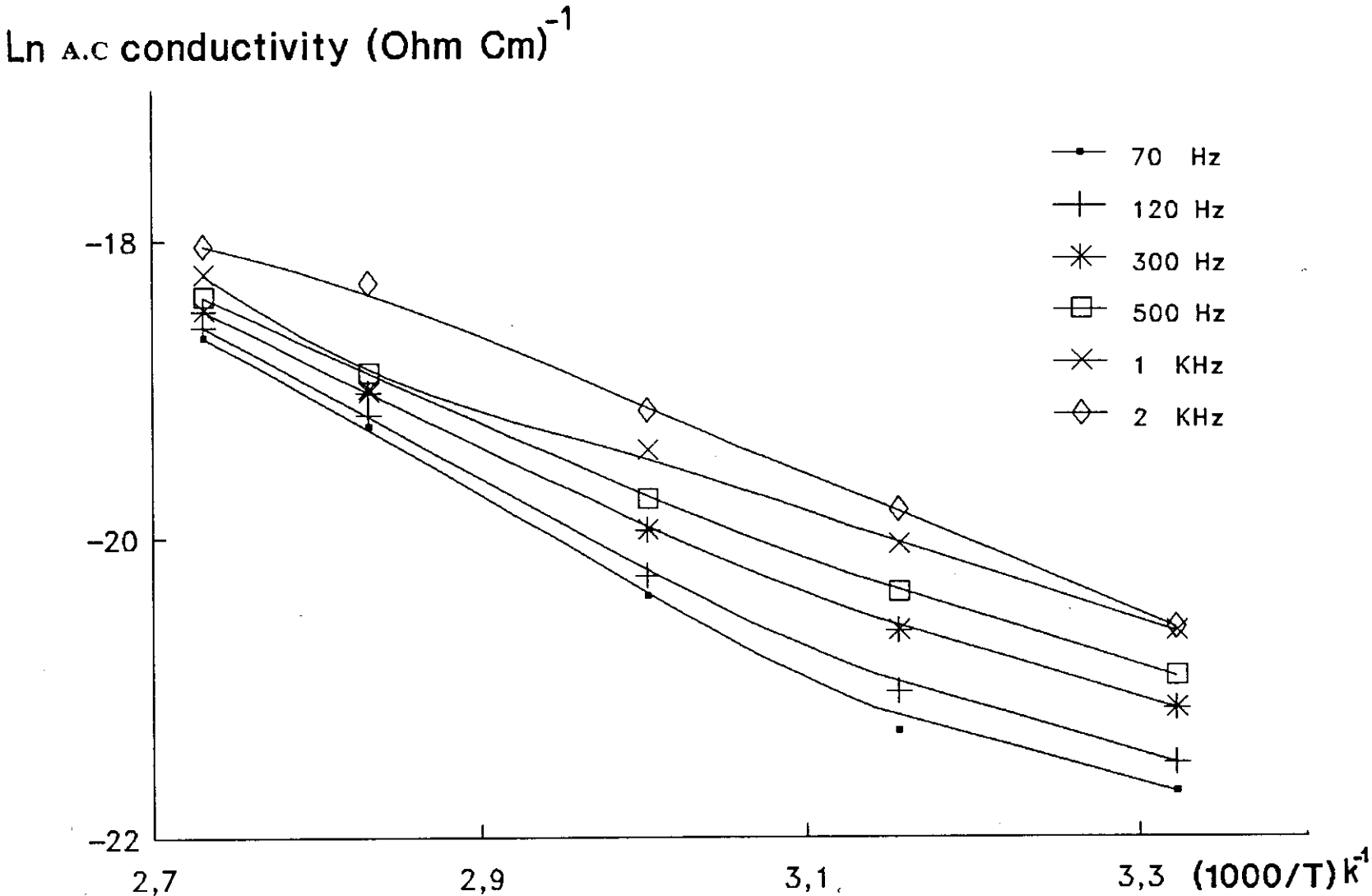

Fig.4.5:Shows the variation of "σ_{ac}" as a function of temperature at constant frequencies for $Se_{90}Ge_4In_6$ in the glassy state.

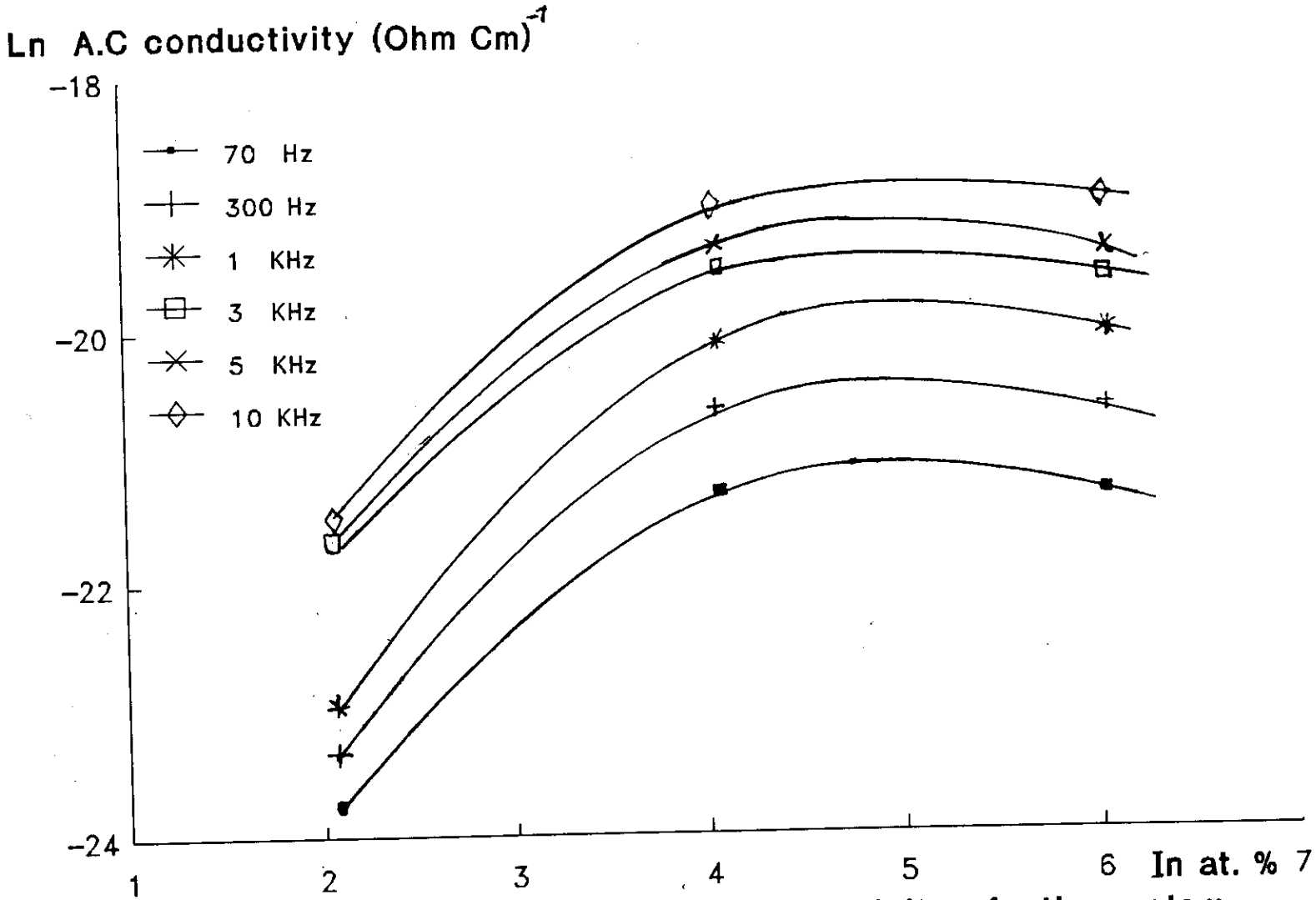

Fig4.6:The effect of composition on the ac conductivity of the system $Se_{90}Ge_{10-x}In_x$ at different constant frequencies in glassy state.

band is Lp band of the group VI elements. The density of states of the top of the Lp valence band tails into the gap because of the local energy fluctuations. The Lp electrons next to electroposotive atoms will have higher energies than those near electronegative atoms. In amorphous semiconductor the band edges are broadened ,mainly by the lake of long range order. Therefore the presence of electropositive atoms (Ge,In) dangling bonds and the lake of long range order in the sample (Se_{90} Ge_8 In_2)results in the band tailing into the gap and contribute to the A.C conductivity. As the Indium concentration in the system increases ,more strong bonds(Se-Ge) are replaced by other weaker ones(Se-In)[24]. This may lead to the observed increase in the conductivity of Se_{90} Ge_6 In_4 by relatively high rate. As the more electropositive atoms (Ge) in the system decreases ,this result in the Lp electrons of the sample Se_{90} Ge_4 In_6 decreases. This lead in turn to decrease the rate by which σ_{ac} increases as the Indium increases.

4.1.2.THE FREQUENCY DEPENDENCE OF A.C CONDUCTIVITY :

The A.C conductivity as a function of frequency for the glassy system Se_{90} Ge_{10-x} In_x (X= 2, 4 and 6) at different isotherms were recorded in figures(4.7,4.8,4.9).

These curves show,for each sample ,that σ_{ac} increases. The slope of the obtained curves decreases as the temperature increases. This behaviour fit well to the well known equation:

$$\sigma_{ac} = A\ \omega^{S} \qquad (4.1)$$

Where A,S are constants and ω is the angular frequency.

The values of S in equation (4.1)have been calculated from the curves of figures(4.7,4.8,4.9). The temperature dependence of S for each composition of Se_{90} Ge_{10-x} In_x (X= 2 , 4 and 6)was redrawn in fig.(4.10). These curves show that S decreases as the temperature increases.

Analysis of the results of A.C conductivity in the light of the various theoretical models shows that the correlated barrier hopping (CBH)model proposed by Elliot[47]is the most appropriate for explaining the frequency and temperature dependence of the A.C

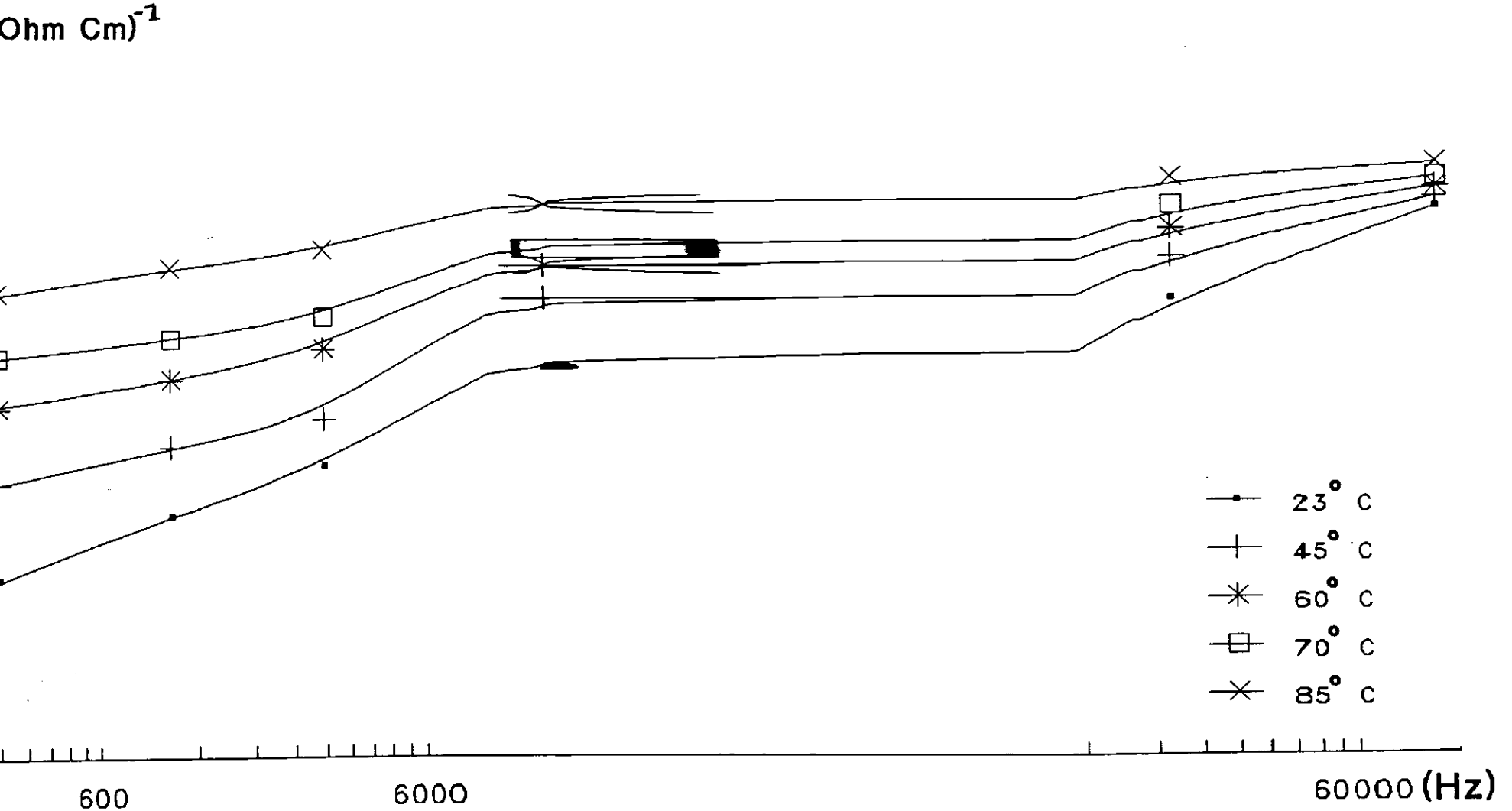

ation of σ_{ac} with frequency at nstant temperatures for
e glassy state.

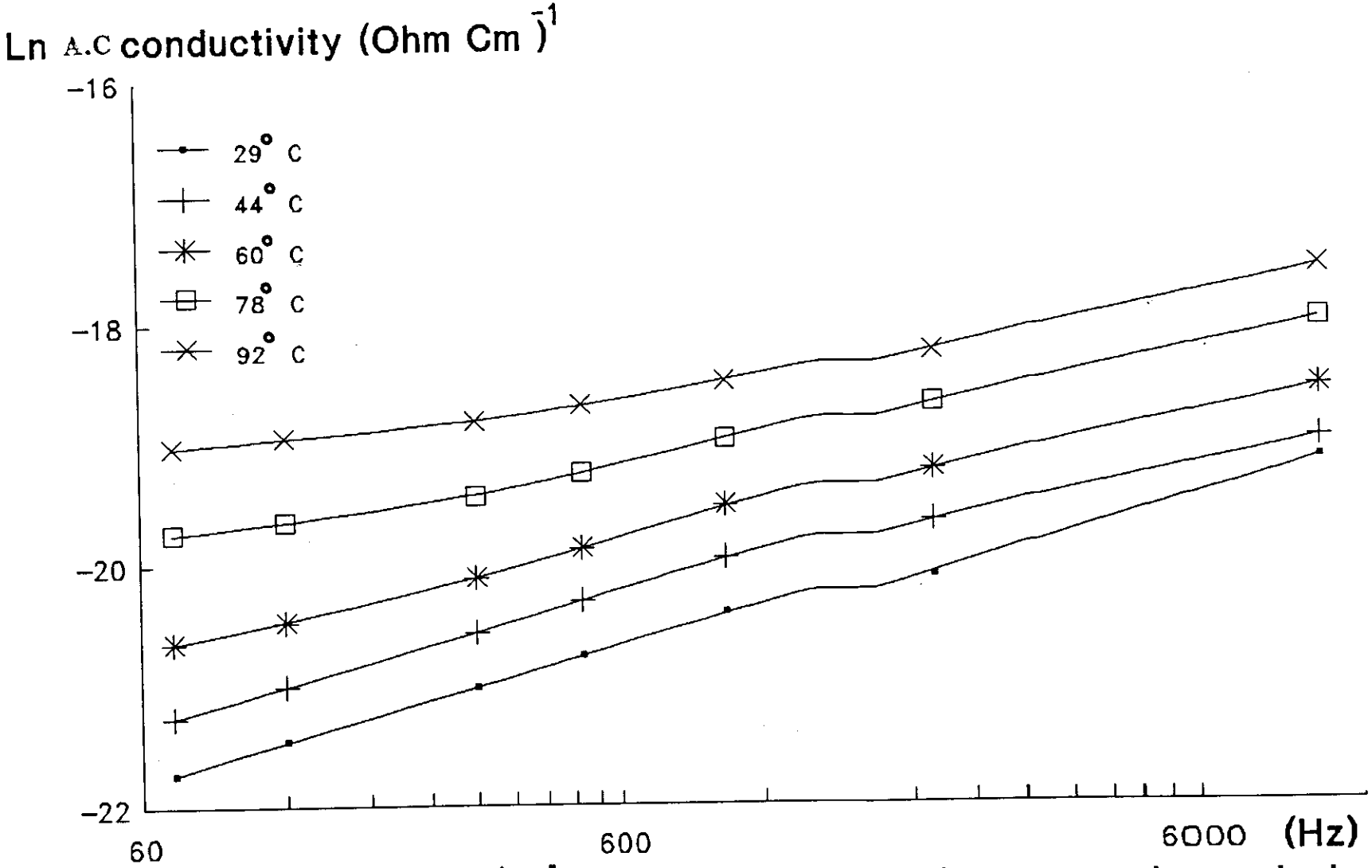

Fig. 4.8: Shows the variation of σ_{ac} as a function of frequency at constant temperatures for $Se_{90}Ge_6In_4$ in the glassy state.

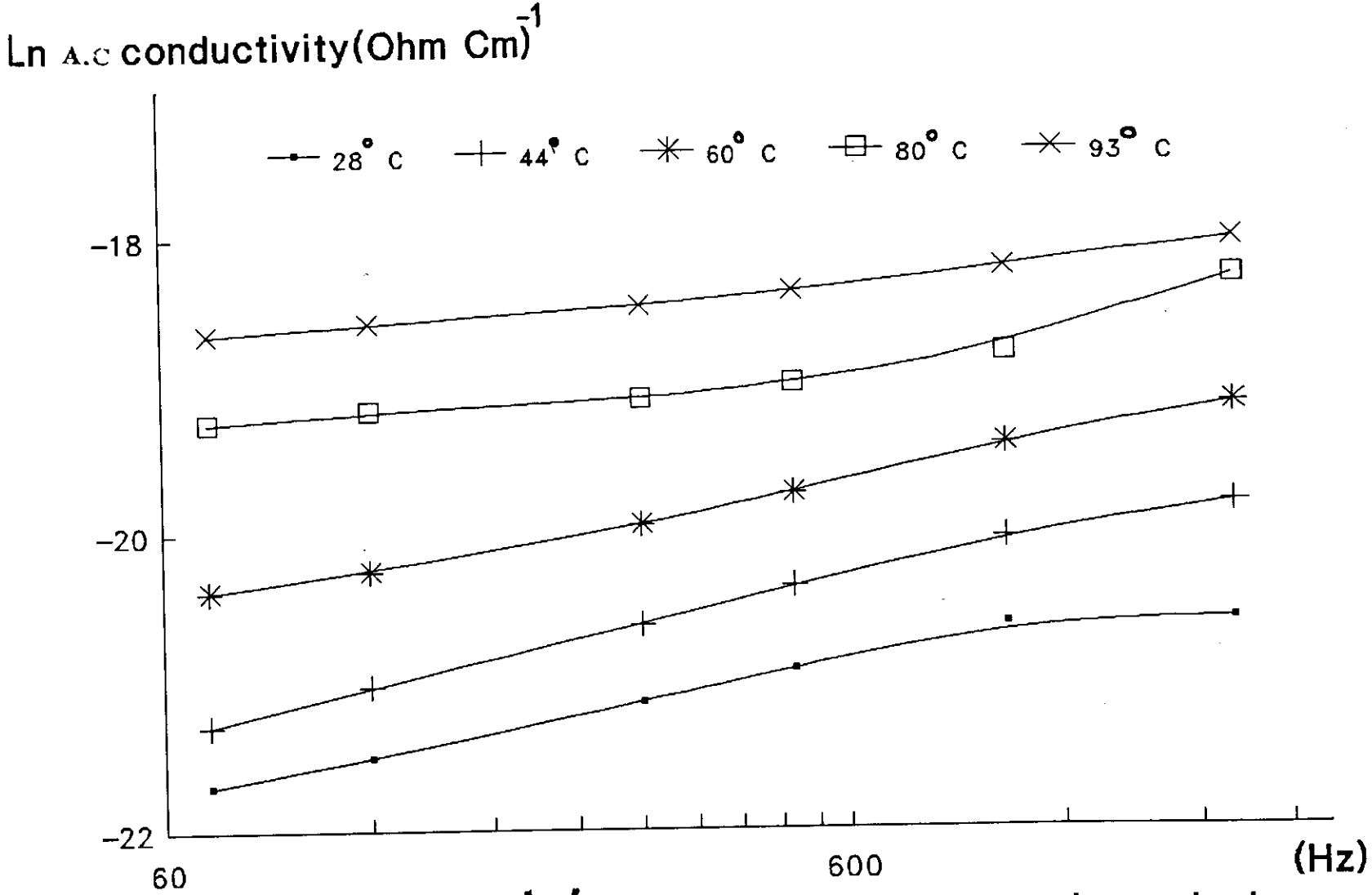

Fig.4.9:Shows the variation of "σ_{ac}" as a function of frequecy at constant temperatures for $Se_{90}Ge_4In_6$ in the glassy state.

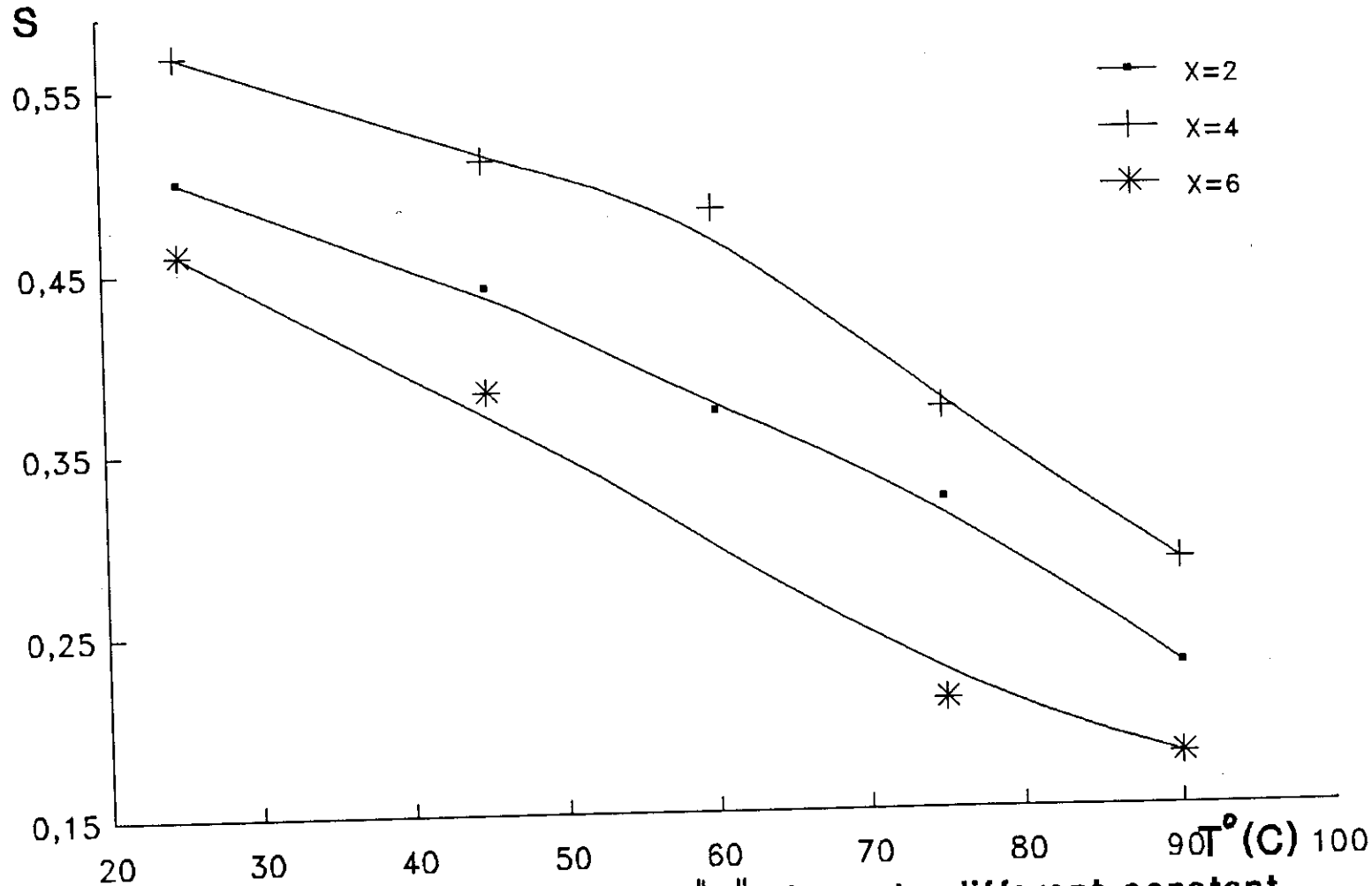

Fig.4.10: The effect of temperature on the "S" values at different constant composition of the system $Se_{90}Ge_{10-X}In_X$ in the glassy state.

conductivity and its frequency exponent.The CBH model predicts that σ (ω) should have negative temperature dependence of the frequency exponent S which agree with our results. The frequency dependence of conductivity, which rises almost linearly with frequency ,may be due to the hopping of electrons between pairs of localized states at the Fermi level. The A.C conductivity have been found to obey ω^S law and the S values are found to agree with the theoretical predictions for phonon activated conduction mechanism which indicate that the conduction process in this sample is thermally activated process. According to the Quantum Mechanical Tunneling model (QMT) proposed by Pollak and Geballe [105], the exponent S is almost equal to 0.8 and increases slightly by increasing temperature.

Therefore the QMT model is not applicable to the chalcogenide glass. The CBH model is thus introduced to explain the frequency dependence of conductivity. Shimakawa[106] suggested that D° states are produced by thermal excitation of D^+ and/or D^- states and that single-polaron hopping contributes to the A.C conductivity at high temperature.

4.1.3. *THE* FREQUENCY DEPENDENCE OF THE DIELECTRIC CONSTANT :

The frequency dependence of the dielectric constant(ε) was studied at constant different isotherms for the glassy system Se_{90} $Ge_{10-x}In_x$ where X=2, 4 and 6. The results are presented in figures(4.11,4.12,4.13). These curves show that the highest value of ε starts to decreases by high rate and then by low rate as the frequency increases to reach constant value. This may be attributed to that at low and moderate frequency ,the dielectric constant (ε) is due to contribution of each electronic,ionic,orientational, and interfical polarizability, while at high frequency the dielectric constant is only due to the electronic polarizability.

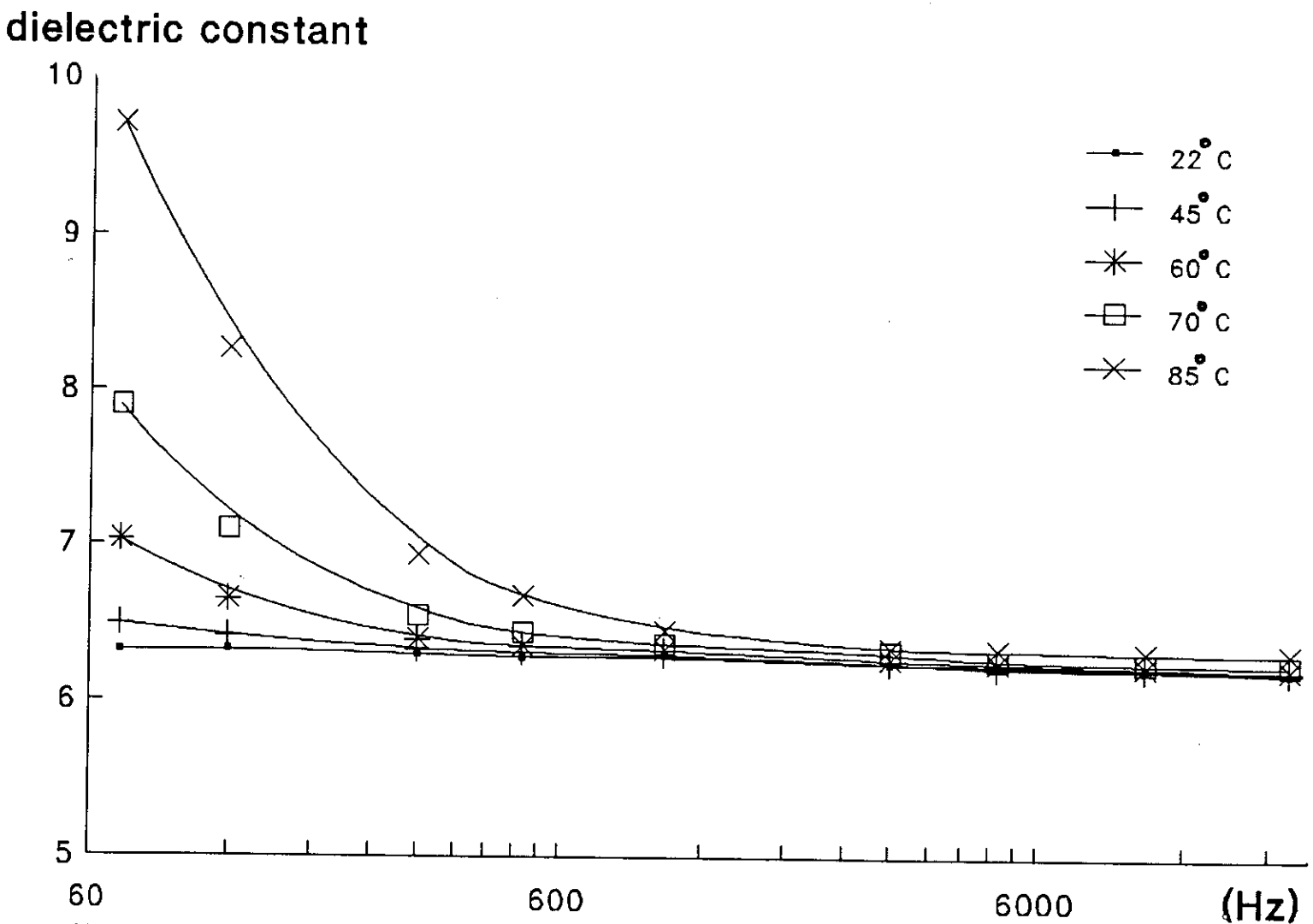

Fig.4.11: Shows the variation of the dielectric constant as a function of frequency at constant temperatures for the sample $Se_{90}Ge_8In_2$ in glassy state.

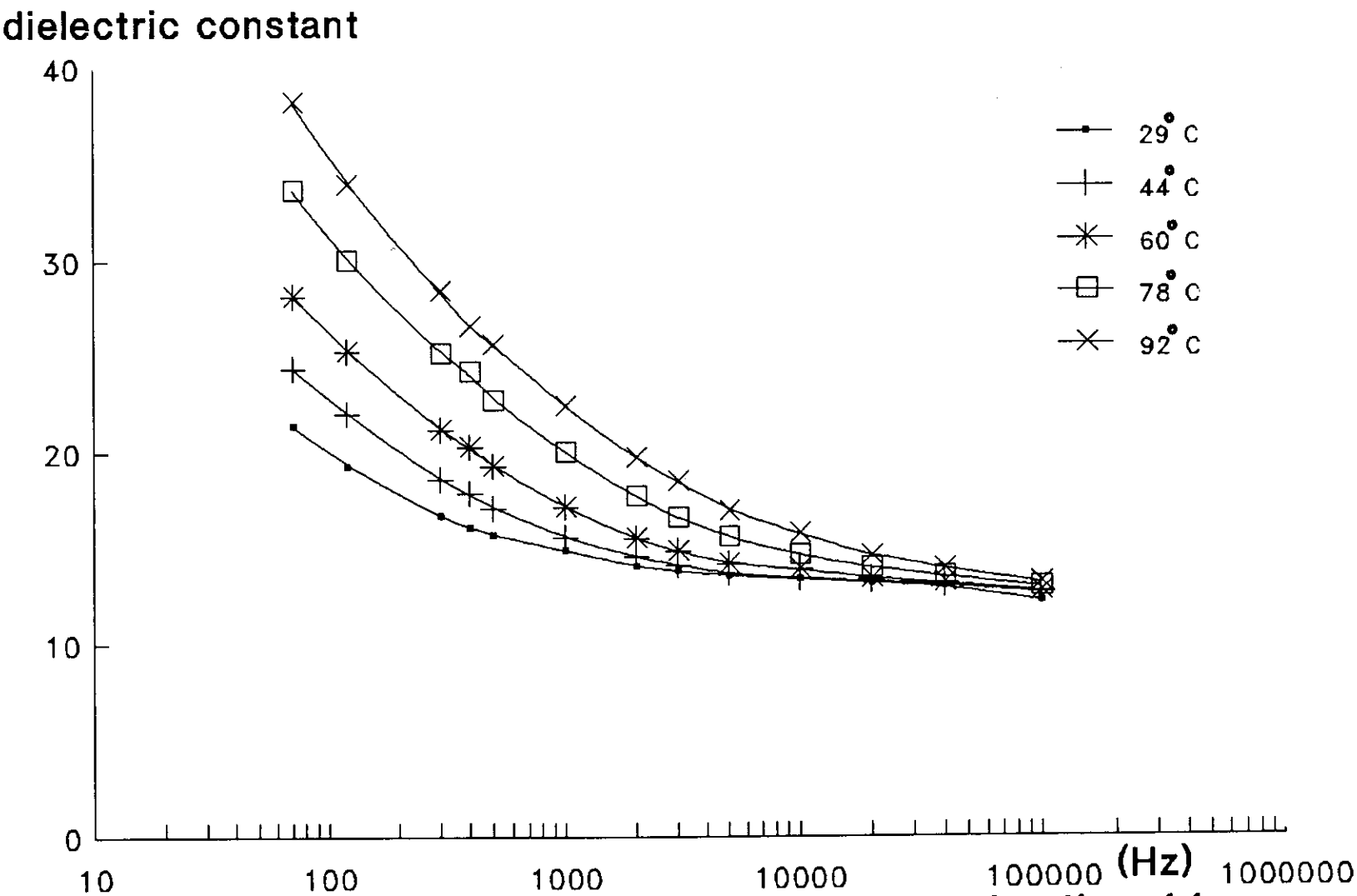

Fig.4.12 :shows the variation of the dielectric constant as a function of frequency at constant temperatures for the sample $Se_{90}Ge_6In_4$ in glassy state.

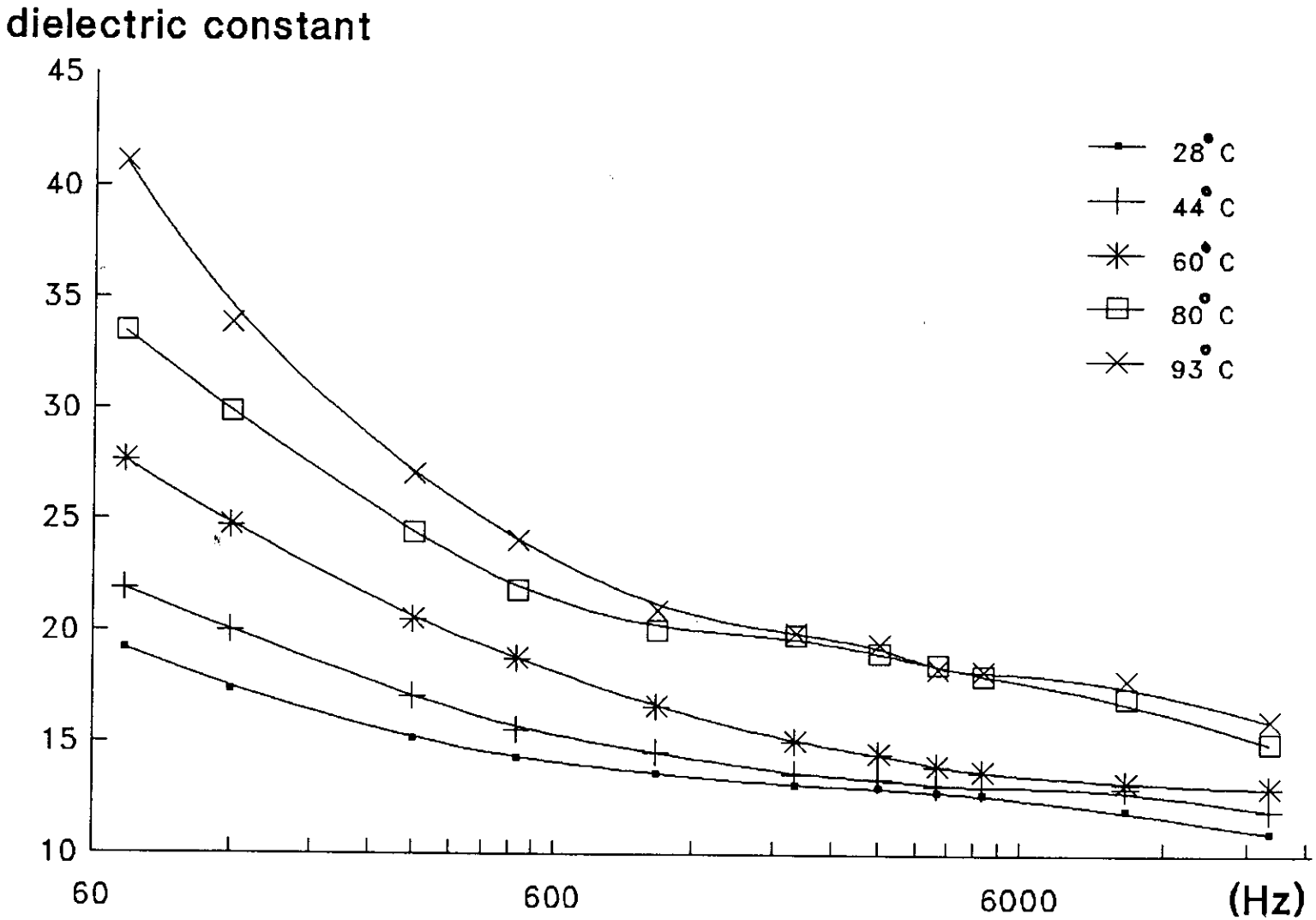

Fig.4.13:Shows the variation of the dielectric constant as a function of frequency at constant temperatures for the sample $Se_{90}Ge_4In_6$ in glassy state.

4.1.4.THE TEMPERATURE DEPENDENCE OF THE DIELECTRIC CONSTANT :

Figs.(4.14,4.15,4.16)show the temperature dependence of the dielectric constant ε at different constant frequencies for the virgin glassy system Se_{90} Ge_{10-x} In_x where x = 2, 4 and 6. These curves show that the dielectric constant increases as temperature increases. In the low temperature range these curves increase with low rate, while at high temperature range the rate of increasing becomes more pronounced. This behaviour can be explained on such that at high temperature ranges,multicomponents contribute to the polarization of the sample while at low temperatures this contribution was only due to the space charge.

Fig(4.17)shows the composition dependence of ε at different constant frequency. It is clear that ε increases as Indium increases. This may be attributed to the Indium activity at low concentration which may be decreases as the surrounding atoms of Indium becomes Indium atoms also.

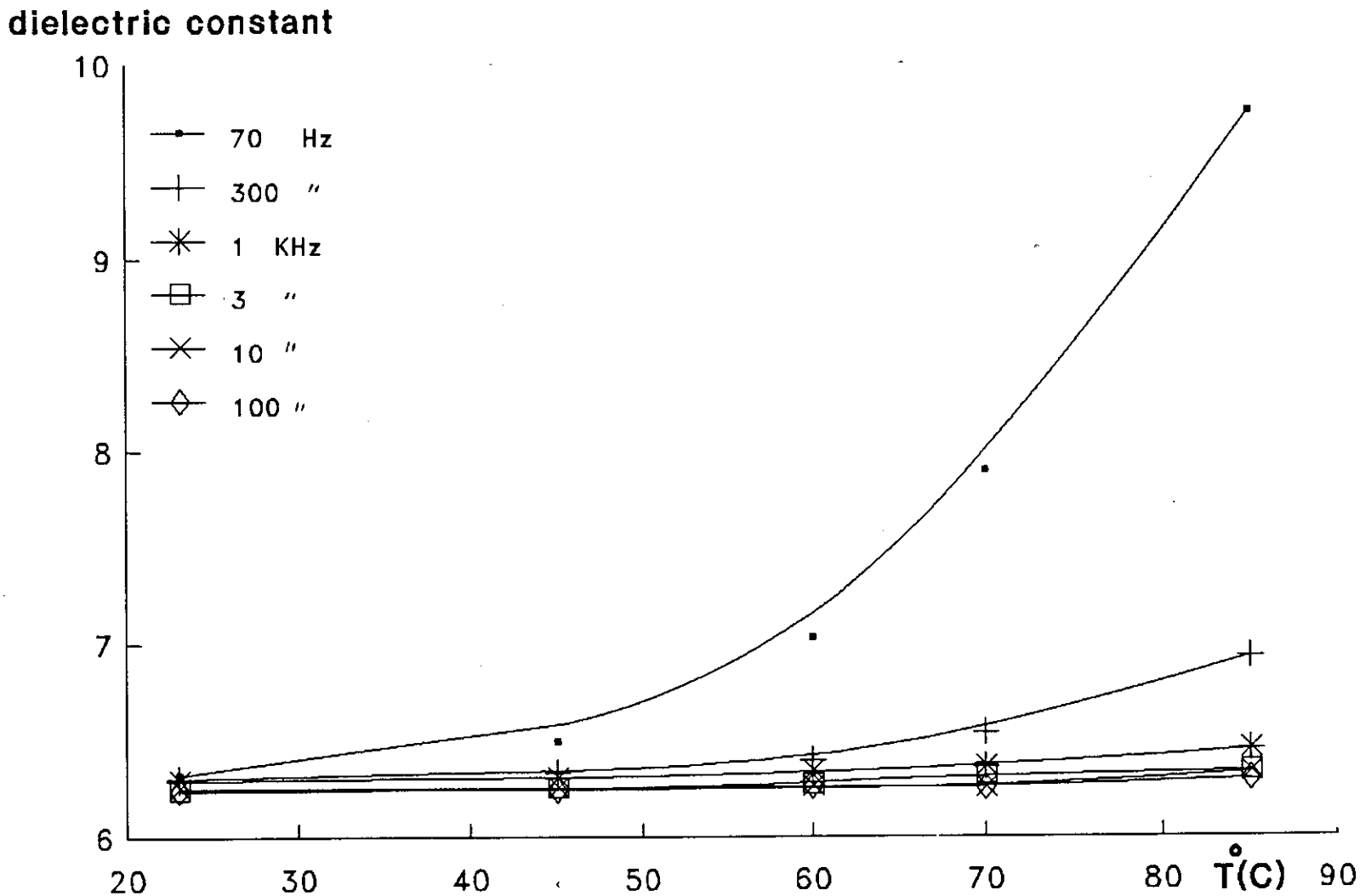

Fig.4.14: The temperature dependence of the dielectric constant at different constant frequencies for the sample $Se_{90}Ge_8In_2$ in the glassy state.

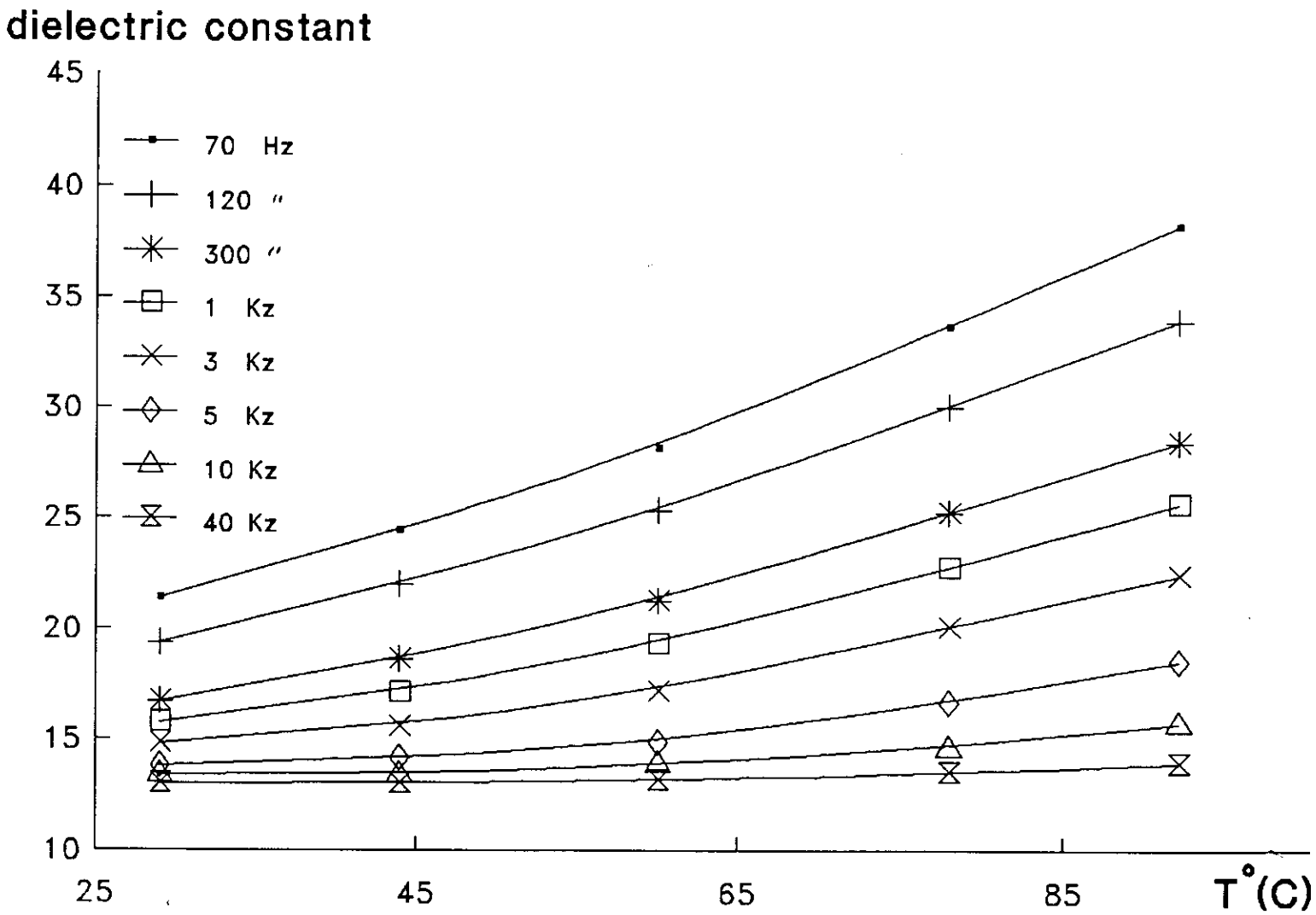

Fig.4.15:Shows the variation of the dielectric constant as a function of temp -erature at constant frequencies for the sample $Se_{90}Ge_6In_4$ in glassy state.

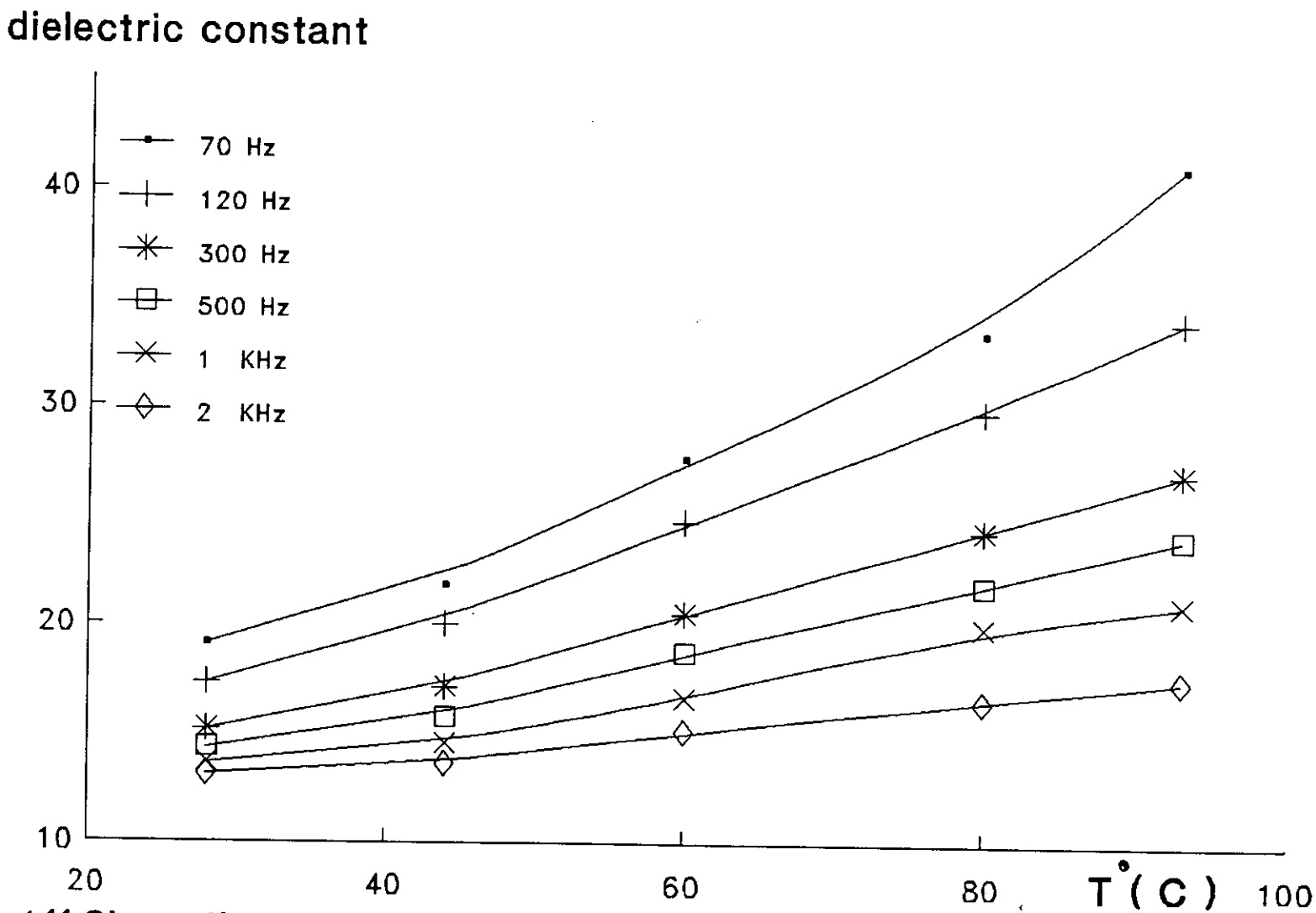

Fig.4.16:Shows the variation of the dielectric constant as a function of temperature at different constant frequencies for the sample $Se_{90}Ge_4In_6$ in glassy state.

4.1.5.THE TEMPERATURE DEPENDENCE OF THE DIELECTRIC LOSS TANGENT

Figs.(4.18,4.19,4.20) show the temperature dependence of the dielectric loss tangent (tan δ) at different values of frequency for $Se_{90}Ge_{10-x}In_x$ where x=2,4 and 6. From these figures it is clear that as the temperature increases the dielectric loss tangent increases. This may explained as :

Stevels[107] divided the relaxation phenomena into three parts, conduction losses,dipole relaxation losses and deformational losses.

The losses that are attributed to conduction presumably involve the migration of ions over large distances.This motion is the same as that occurring under direct-current conditions. The ions jump over the highest barriers in the network. As the ions move, they give some of their energy to the lattice as heat and the amount lost per cycle is proportional to (σ/ω).The conduction loss increases with temperature since $(1/\sigma)$decreases.

At low temperature,conduction loss, deformation loss and vibration loss bound the minimum. At high temperatures conduction loss, dipole loss, and vibration loss all contribute to the dielectric loss.

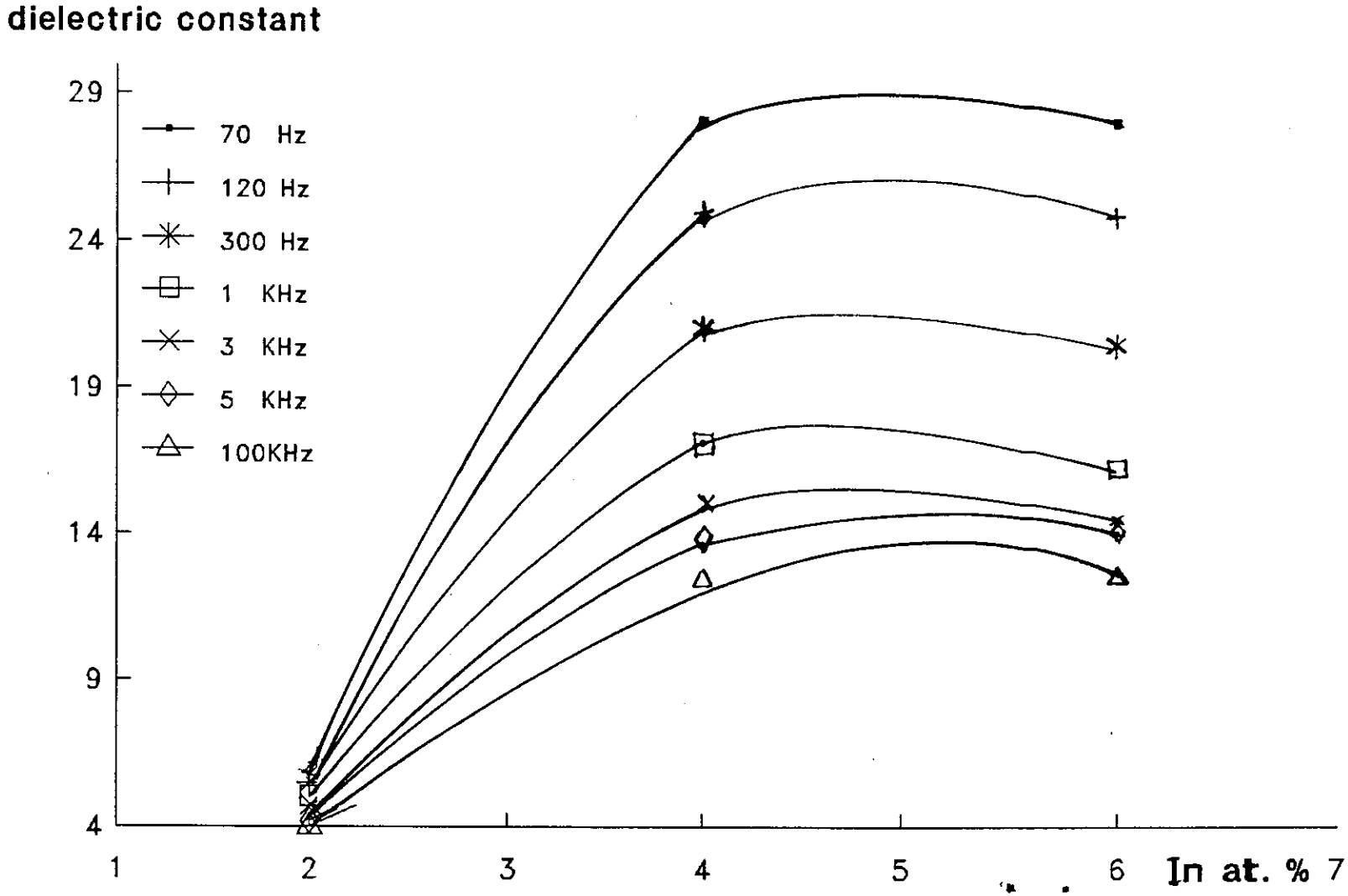

Fig.4.17: The effect of composition on the dielectric constant ε of the system $Se_{90}Ge_{10-x}In_x$ at different constant frequencies in the glassy state .

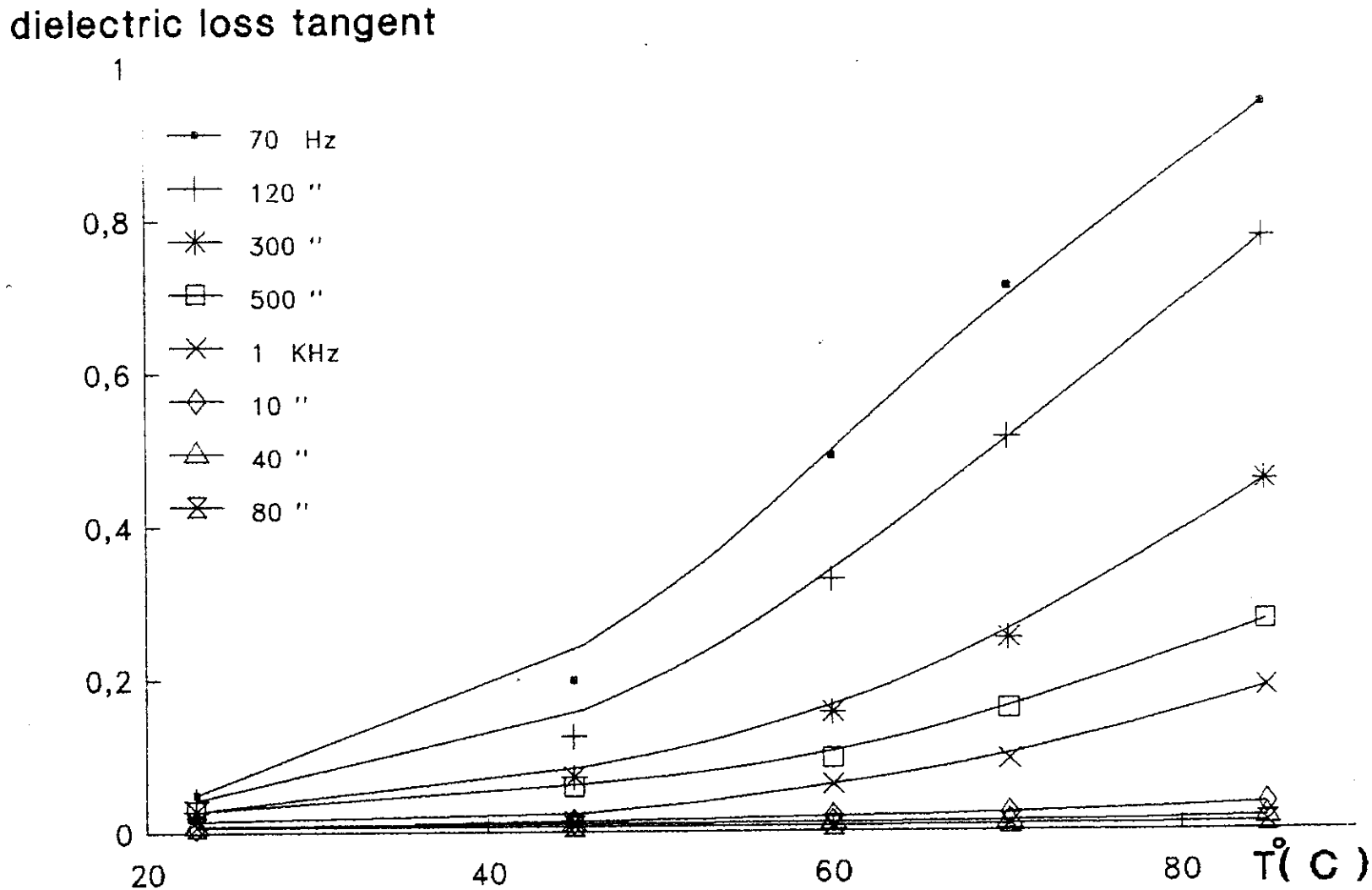

Fig.4.18 Shows the variation of the tan(δ) as a function of temperature at constant frequencies for $Se_{90}Ge_8In_2$ in glassy state.

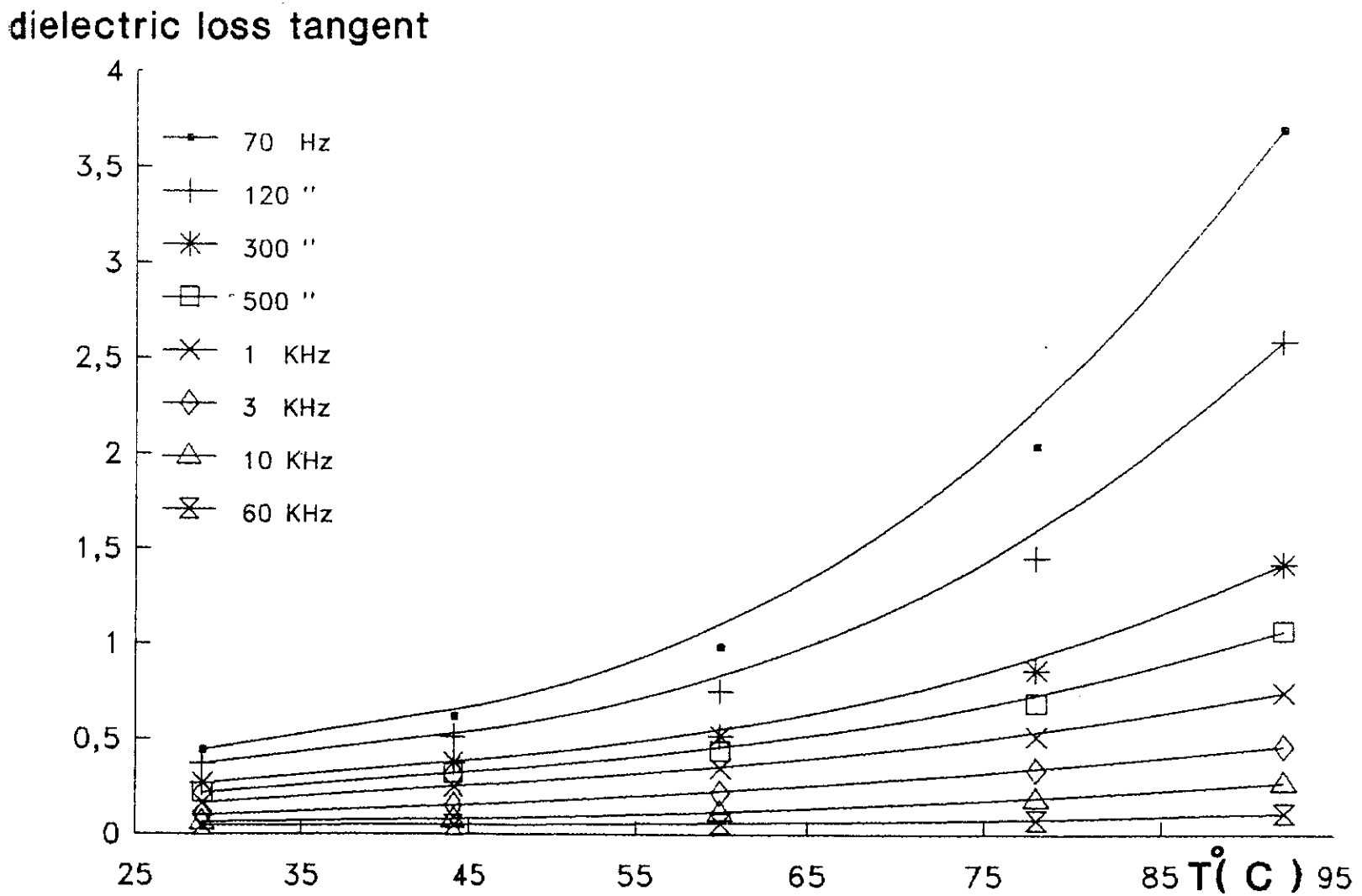

Fig.4.9: Shows the variation of tan(δ) as a function of temperature at constant frequencies for $Se_{90}Ge_6In_4$ in glassy state.

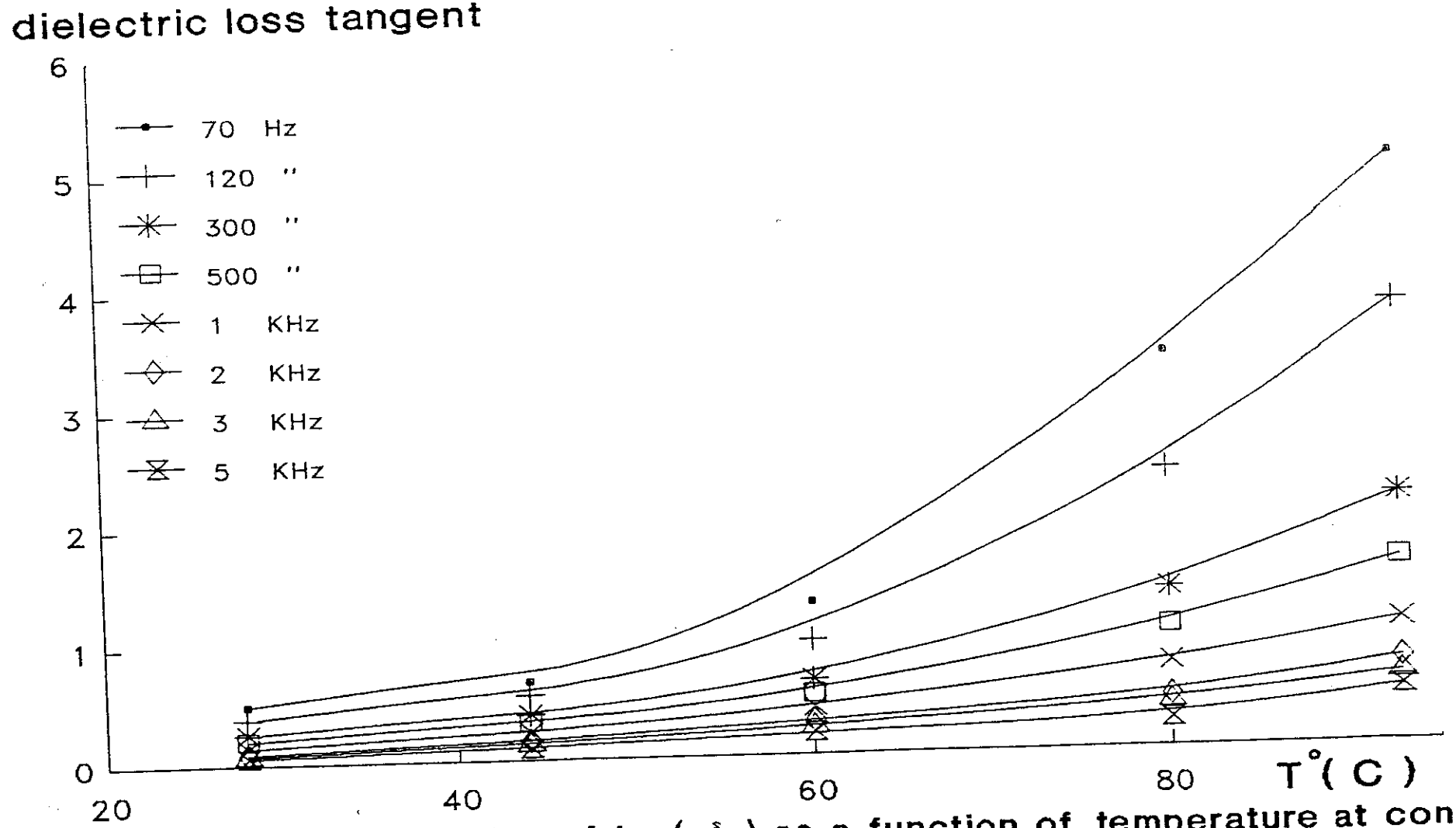

Fig4.20:Shows the variation of tan(δ) as a function of temperature at cons
ant frequencies for $Se_{90}Ge_4In_6$ in glassy state.

4.1.6.THE FREQUENCY DEPENDENCE OF THE DIELECTRIC LOSS TANGENT:

The frequency dependence of the dielectric loss(tan δ) was studied for $Se_{90}Ge_{10-x}In_x$ where X=2,4 and 6 as in figures(4.21,4.22,4.23). It is clear that the dielectric loss tangent decreases as the frequency increases.

The mentioned three relaxation type losses are all considered to be consequences of ion displacement. They differ in kind of ion motion taking place.

The dipole relaxation losses are though to be motion over short distances. This ions move through a few interstices but finally arrive at a barrier too high for it to overcome. This fixing of the ions to the downhill sides of their large inter-connected cavities create a polarization and takes time for this ion drift to be completed. The extra energy needed for these motions come from the electric field and is associated by thermal vibrations in a statistical way. For very low frequencies the loss factor is maximum. At This frequency the ions are pushed back and forth, just about as far as they can go either way,loosing the most energy from the electric field each cycle,since peak fields are needed to complete the motion. At much lower frequencies,the ions have adequate time to move and do so at lower fields and hence absorb little energy. At higher frequencies the field alternates so rapidly that the ions can not follow,and the loss is again quite low.

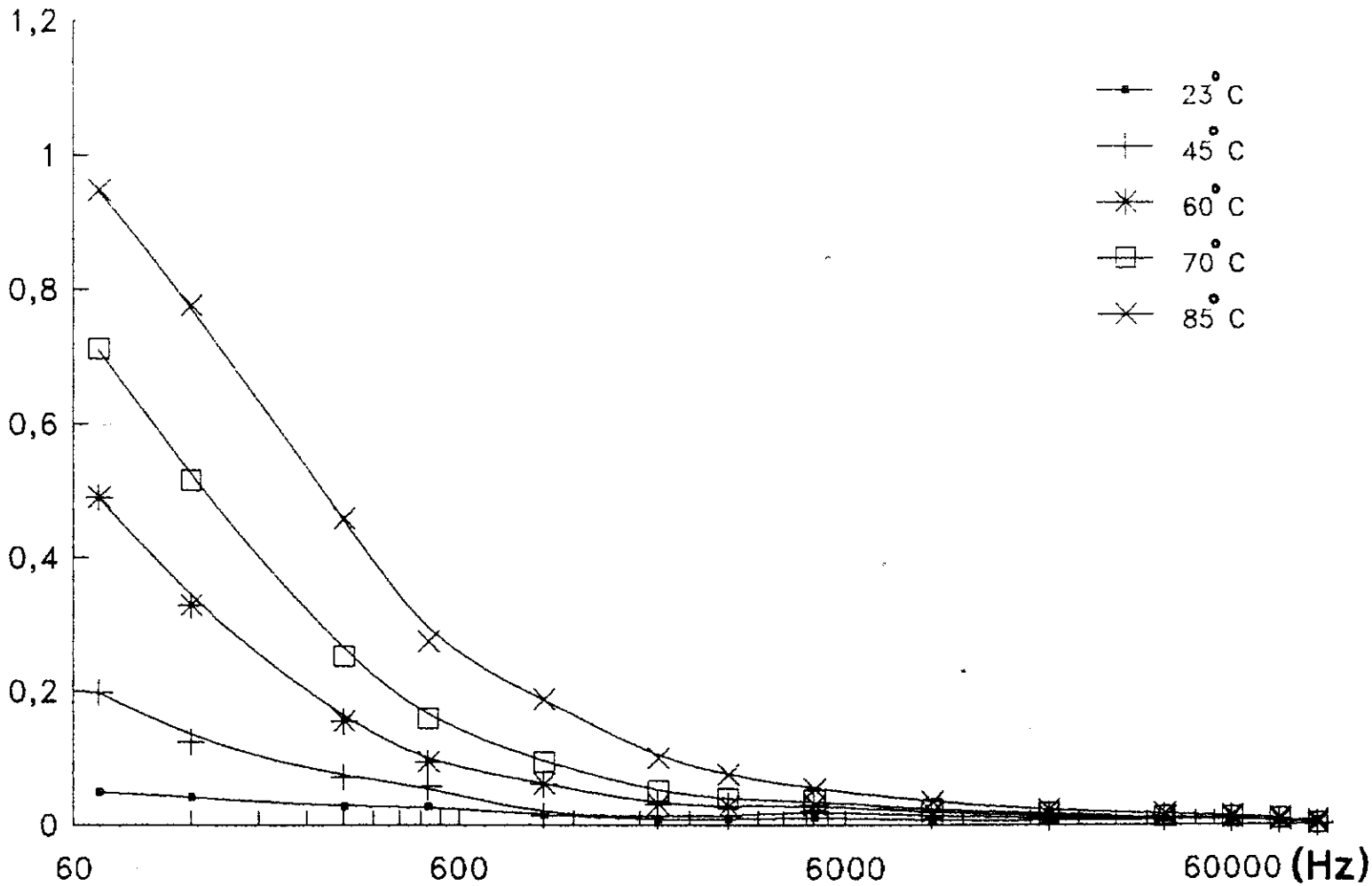

Fig.4.21:Shows the variation of tan (δ) as a function of frequency at constant temperatures for the $Se_{90}Ge_8In_2$ in glassy state.

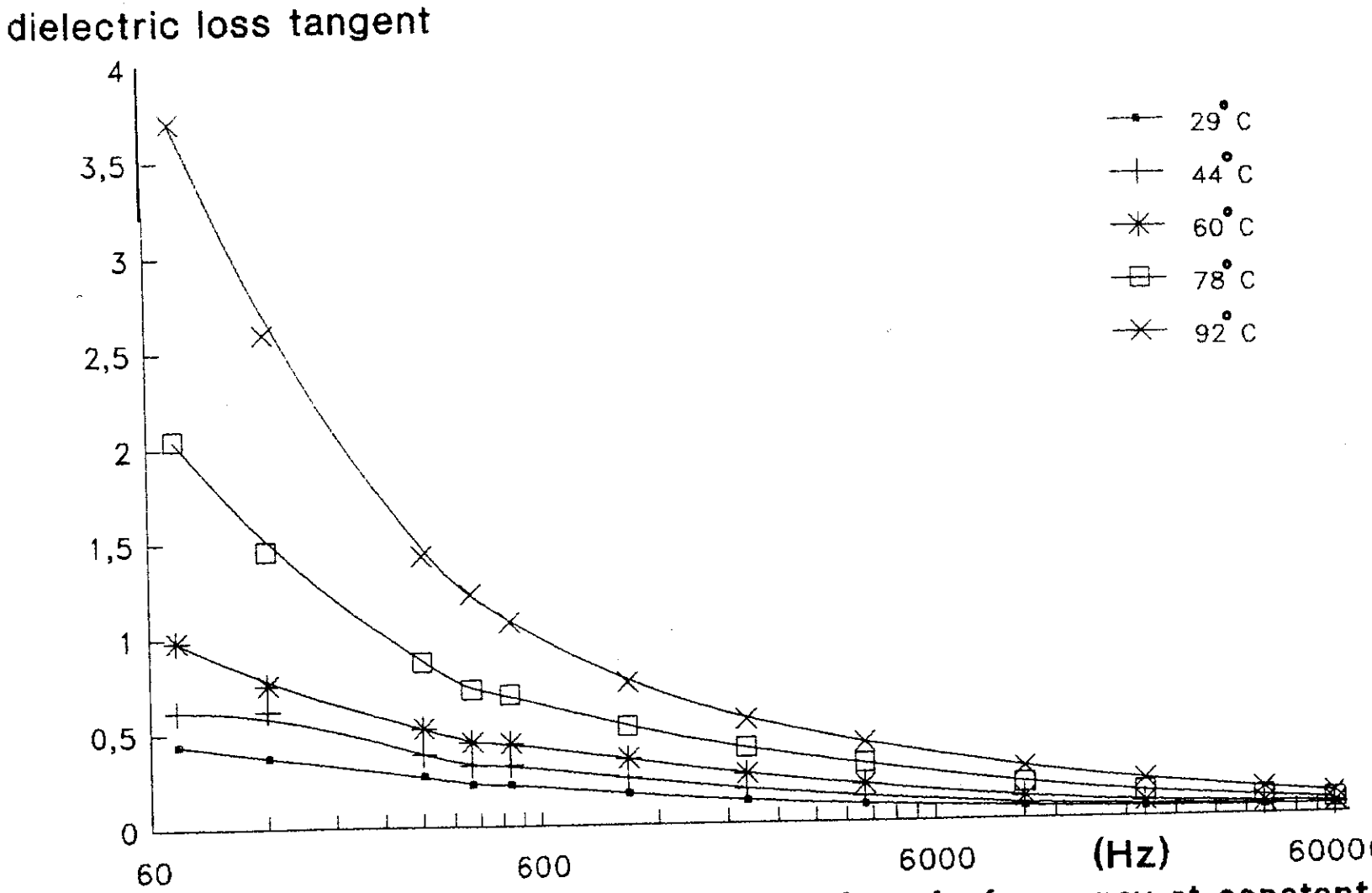

Fig 4.22 Shows the variation of tan(δ)as a function of frequency at constant temperatures for $Se_{90}Ge_6In_4$ in glassy state.

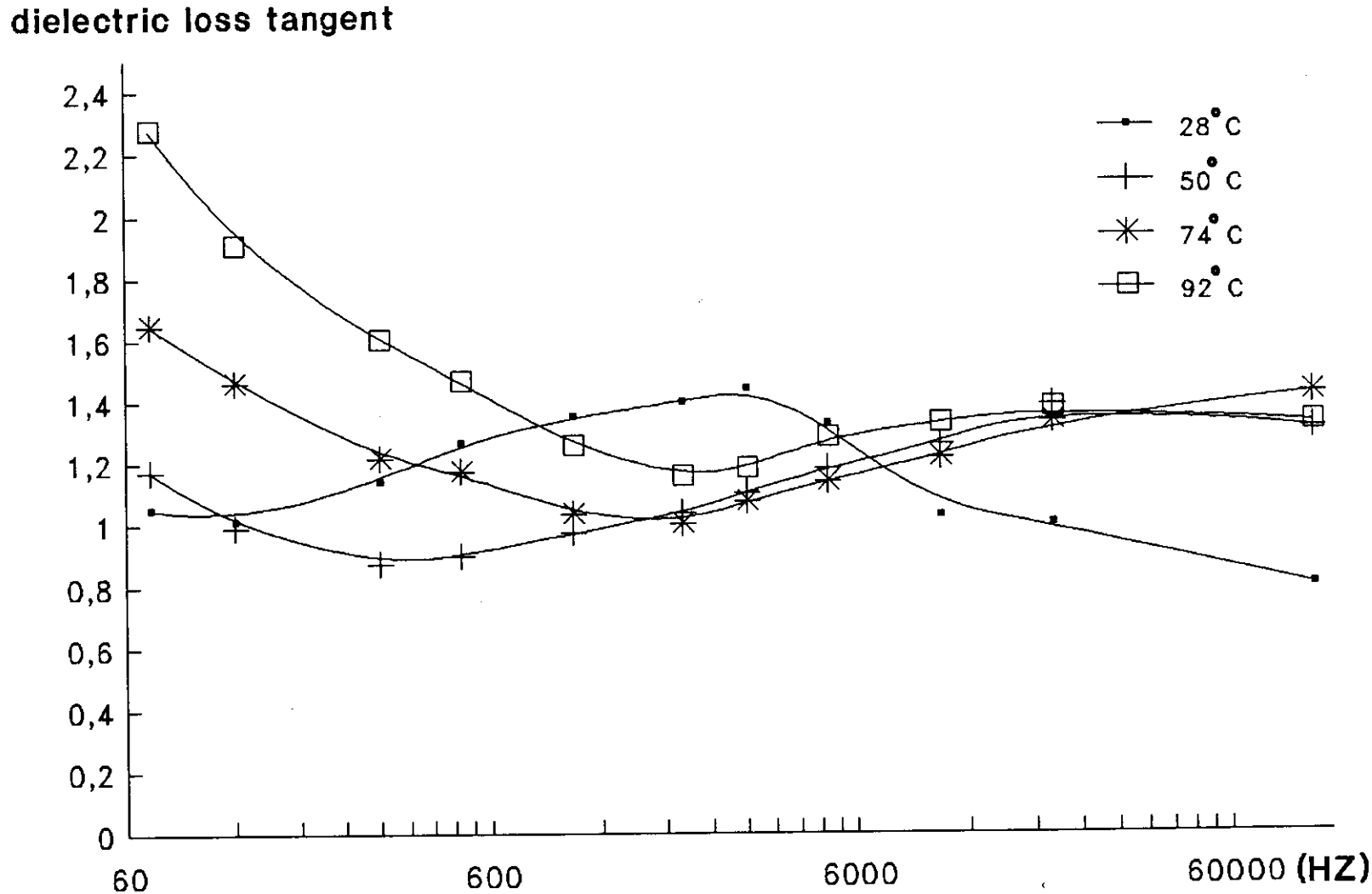

Fig.4-23: The frequency dependence of the dielectroic loss tangent at different constant temperatures for $Se_{90}Ge_4In_6$ in the glassy state.

Deformation loss is a term used to describe even more limited motions of atoms of the glass. Usually the network atoms are considered as causing the loss rather than the more mobile modifier ions. The vibration loss occurs at frequencies approaching infrared frequencies. All the atoms in a glass can vibrate around their equilibrium positions at frequencies determined by their mass and by restoring forces in their potential well. Whenever the applied electric field alternates at a frequency near that of one of the constituent atoms,they are excited to a high resonant amplitudes, accompanied by high dielectric losses.

In summary the four kinds of losses in glass result in the following behaviour :

Conduction loss occur at low frequencies starting from direct current up to about 100 C/s. Dipole relaxation occurs at low frequencies. Deformation loss can appear at low temperatures in the Kilocycle-Megacycle region but at high temperatures it moves up to higher frequency. Vibration loss occur at frequencies 10^{10} C/S upwards. Conduction losses increase as the temperature rise,since the resistance falls. Both dipole and deformation losses shift to higher frequencies as the temperature rises and vibration losses shift down in frequency somewhat as temperature rises. Changes in any direction in frequency and temperature will cause an increase in $\tan(\delta)$.

It can be concluded that the increasing in dielectric loss tangent at low temperature may be attributed to that the relaxation loss is

the main contributor and appeared to be very much greater than the conduction loss. As the temperature increases, the relaxation loss is reduced and the conduction loss increases more and more rapidly.

The frequency dependence of the dielectric loss tangent can be attributed to that the migration of ions in glass is the main source of the dielectric loss at low frequency. Accordingly,the dielectric loss at low and moderate frequency characterized by high values due to the contribution of ion jump and conduction loss of ion migration loss,in addition to the electron polarization loss while at high frequency values the ion vibrations may be the only source of dielectric loss.

4.2.STRUCTURE AND PHYSICAL PROPERTIES OF $Se_{90}Ge_{10-x}In_x$ IN THE CRYSTALLINE STATE :-

Sample of the system $Se_{90}Ge_{10-x}In_x$,where X=2,4 and 6,were divided into four parts. Each part has been subjected to thermal heating at one of the crystallization temperatures 120,130,140 and 150 ^{o}C for periods of time enough to transfer it completely from amorphous state to crystalline state. The mentioned crystallization temperatures were selected to be suitable for the different values of,x,according to DTA curves in the temperature range between T_g and T_c,fig(4.1). In addition to this, this selection also verify the intermediate rate of phase transformation to give chance to pick-up all of the possible phase transformation in step wise. These parts of each sample were prepared to be suitable for the following studies in the crystalline state:-

1-The A.C.conductivity as a function of temperature and frequency.

2-The D.C conductivity as a function of temperature.

3-The dielectric constant ε as a function of temperature.

4-The dielectric constant ε as a function of frequency.

5-The dielectric loss tangent tan(δ) as a function of temperature.

6-The dielectric loss tangent as a function of frequency.

4.2.1.X-RAY STRUCTURE STUDIES OF $Se_{90}Ge_{10-x}In_x$ THE CRYSTALLINE STATE:-

Fig(4.24) shows the X-ray diffraction pattern of the samples owing to the system $Se_{90}Ge_{10-x}In_x$,where X=2,4 and 6. These samples were annealed at 120 °C for a long period to ensure disorder-order transformation. The analysis of the recorded curves show that,the formed crystalline phases were the same in all samples. The intensity of the detected peaks increases or decreases. This may be attributed to the change of the crystalline phases from minor to majors depending on the value of Indium replacing Germanium.

The effect of the crystallization temperature on the detected crystalline phase was investigated by annealing three parts of the sample $Se_{90}Ge_8In_2$ at 120,130 and 150 °C respectively.

Fig(4.25) shows that, the same crystalline phases were detected and the peak intensity increases as the crystallizaton temperature increases.

The detected crystalline phases were tabulated in table(4.2)and (4.3). These tables show that the main crystalline phases are Hex. Se,Hex. InSe,tet. or cubic Ge and/or orth. Ge-Se.

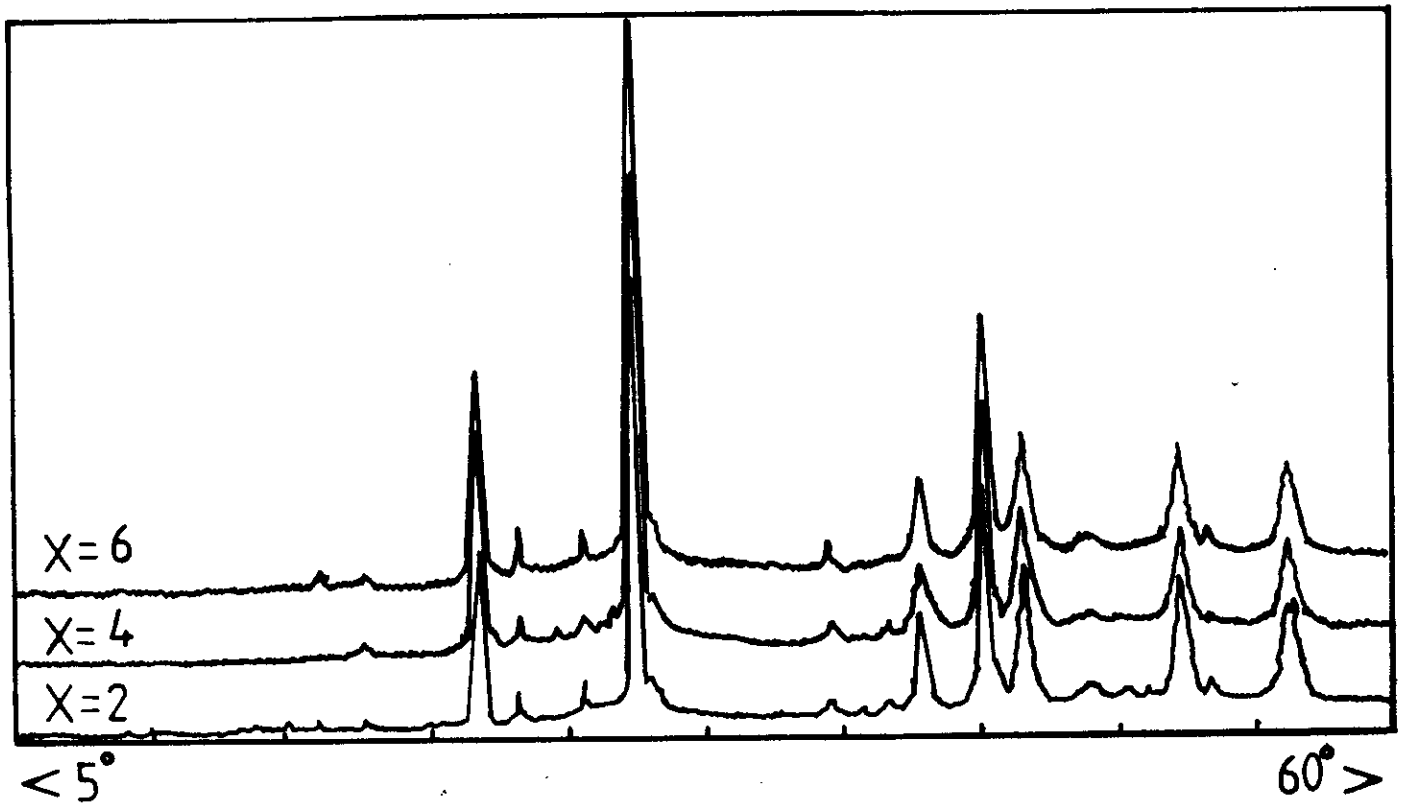

Fig.(4.24):X-ray diffraction pattern of $Se_{90}Ge_{10-x}In_x$(x=2,4 and 6)in the crystalline state after annealing at 120° C.

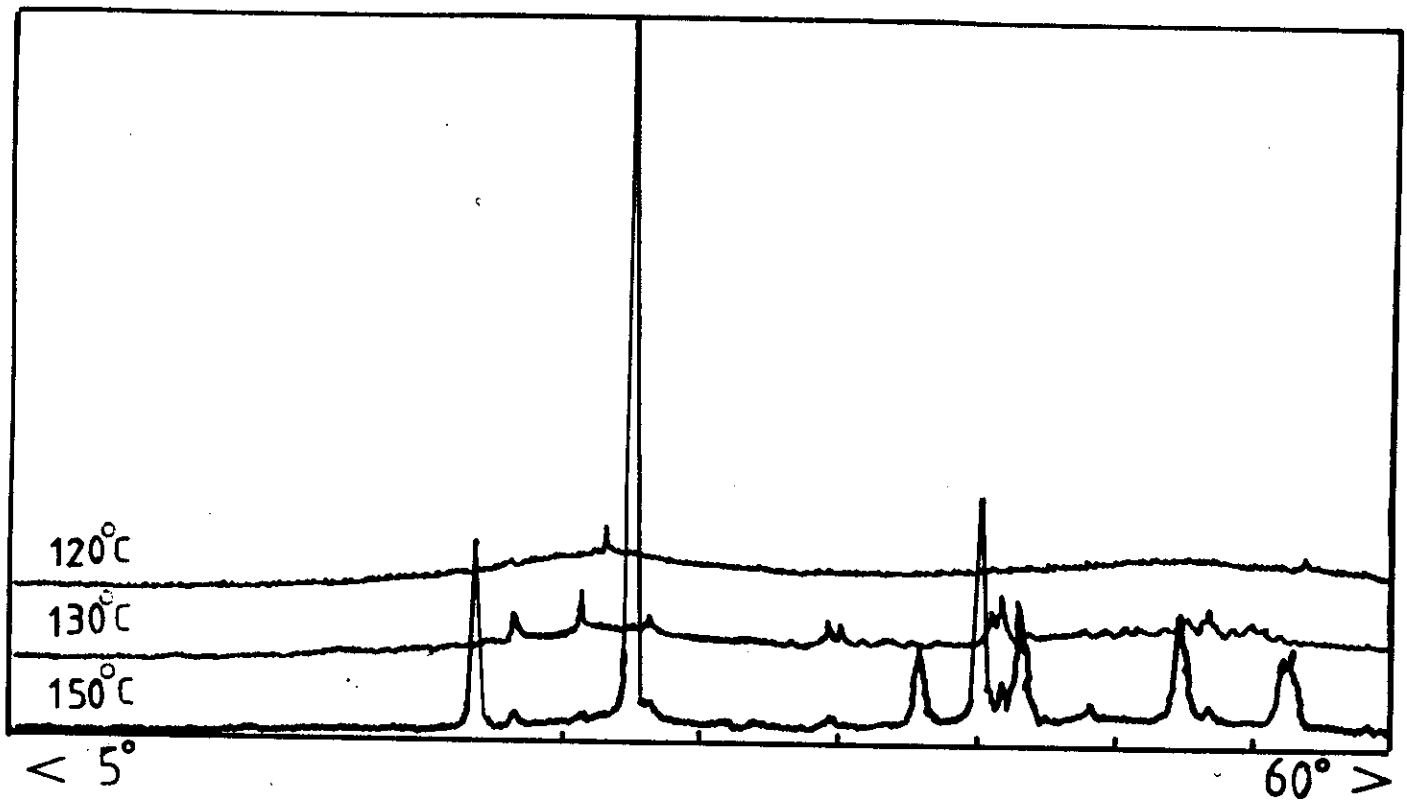

Fig.(4.25):X-ray diffraction pattern of the sample $Se_{90}Ge_8In_2$ in the crystalline state at 120, 130, 150° C.

Experimental					A S T M cards				
		I/I_o						cryst.	cryst.
2θ	$d(A^o)$	x=2	x=4	x=6	$d(A^o)$	I/I_o	hkl	system.	phase
20,3	4,37	25	35	48	4,34	9	211	Hex	Se
22	4,03	6	12	29	4,16	100	400	Hex	SeIn
24,8	3,58	7	16	28	3,59	16	111	Tet(B.c)	Ge
27	3,299	100	100	100	3,266	100	111	Cubic	Ge
35,5	2,526	5	15	26	2,471	21	002	Tet	In
39,5	2,27	16	23	35	2,298	36	110	Tet	In
42	2,14	37	42	56	2,184	16	110	Hex	Se-Se
44	2,05	23	30	40	2,072	35	102	Hex	Se-Se
47	1,93	7	17	25	1,95	20	711	Hex	SeIn
51	1,78	21	27	39	1,791	30	222	Tet	Ge
55,5	1,65	18	25	31	1,65	10	003	Hex	Se-Se

Table(4.2)

Experimenal				A S T M cards				
T^{O} (C)	2θ	$d(A^{O})$	(I/I_{o})	$d(A^{O})$	(I/I_{o})	hkl	cryst. form	cryst. phase
	29,7	3,005	100	3,00	100	101	Hex	Se
120	41,28	2,185	39,7	2,184	16	110	Hex	Se-Se
	24,99	3,56	53,1	3,57	22	121	Hex	Se
	28,64	3,11	80,8	3,14	20	420	Hex	InSe
	30,49	2,92	59,4	2,99	35	102	Tet	Ge
130	37,49	2,39	71,4	2,38	40	700	Hex	InSe
	38,15	2,35	40,6	2,35	20	101	Tet	Ge
	45,04	2,01	50	2,00	100	002	Hex	InSe
	56,79	1,61	77,7	1,62	20	432	Hex	InSe
	23,38	3,801	32,5	3,78	55	100	Hex	Se
	27,26	3,268	21,7	3,266	100	111	Cubic	Ge
	27,82	3,203	29,1	3,208	20	400	Hex	Se
	29,65	3,01	78,9	3,01	40	012	Tet	Ge
	37,45	2,399	19,6	2,395	7	123	Hex	Se
150	38,13	2,35	17.3	2,38	40	601	Hex	InSe
	41,14	2,19	21,7	2,189	40	200	Orth	GeSe
	43,6	2,07	25,3	2,08	20	800	Hex	InSe
	45,14	2,006	32,5	2	100	002	Hex	InSe
	45,81	1,97	30	1,97	60	114	Orth	GeSe
	47,22	1,92	22,8	1,9	10	301	Tet(B.C)	Ge
	50,09	1,81	18,4	1,8	40	402	Hex	InSe
	56,78	1,62	27,4	1,63	20	432	Hex	InSe

Table(4·3)

4.2.2.THE EFFECT OF TEMPERATURE ON A.C CONDUCTIVITY OF $Se_{90}Ge_{10-x}In_x$ IN THE CRYSTALLINE STATE:-

Figs.(4.26-4.29)show the temperature dependence of the A.C conductivity of $Se_{90}Ge_8In_2$ in the crystalline state during the temperature range (27 -100 ^{o}C) at different constant values of frequency. These records were traced for the given sample,after complete crystallization at the crystallization temperature 120,130,140 and 150 ^{o}C. These curves show that as the temperature increases ,the A.C conductivity increases.

This experiment was repeated for the two samples $Se_{90}Ge_6In_4$ and $Se_{90}Ge_4In_6$ at the same crystallization temperature, and the results are illustrated in figures(4.30-4.33) and (4.34-4.37).

The increase of crystallization temperature leads to the increase of the A.C.conductivity. This may be due to the increase of the conduction path cross-section area as a results of the increase of the surface area of adjacent crystalline phase, as well as the decrease of the potential barriers between them. This may be confirm the observation that the X-ray peaks intensity increases as crystallization temperature increases.

In the same time the D.C conductivity was recorded for these two samples after complete crystallization at the same crystallization

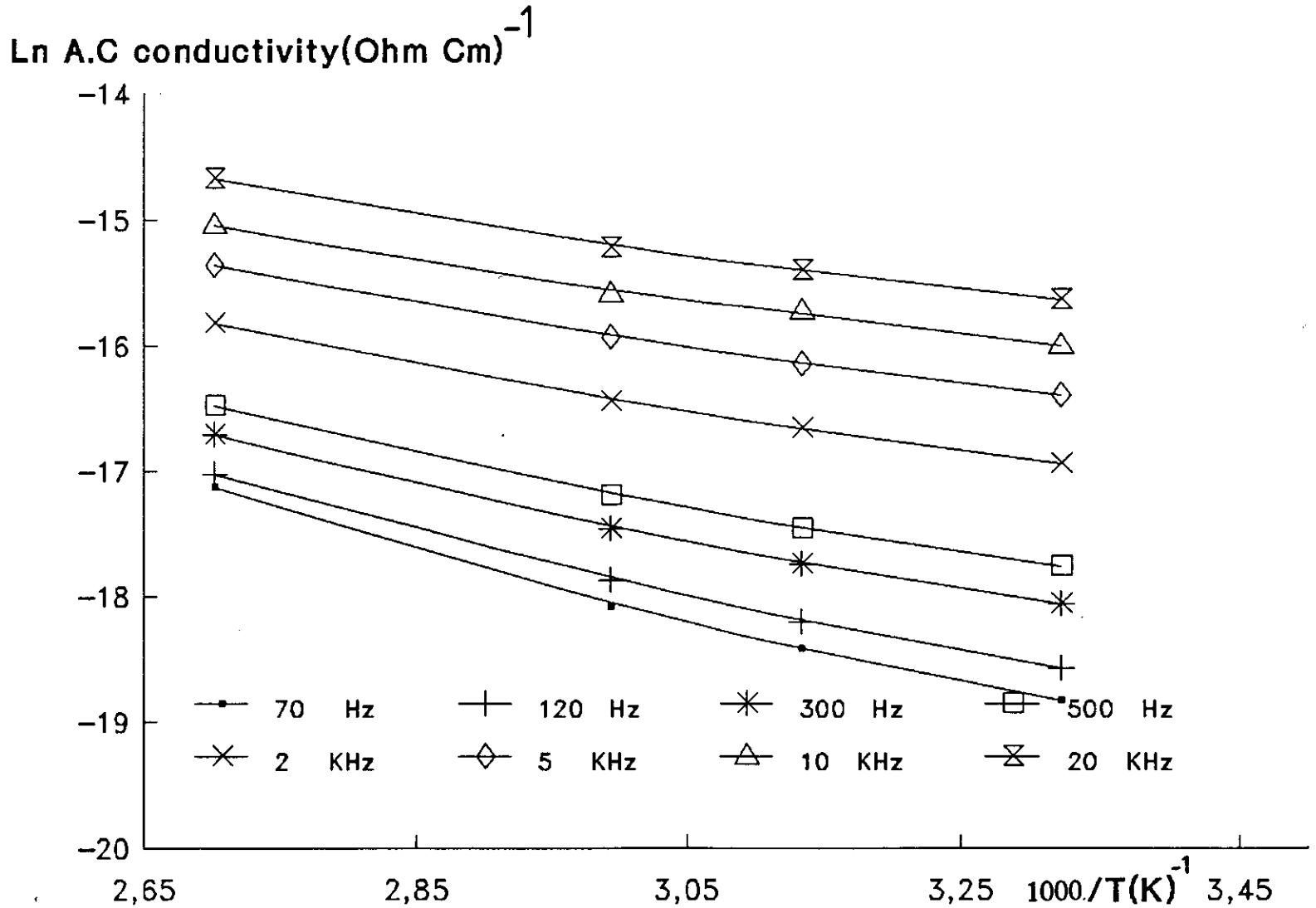

Fig.4.26: The temperature dependence of σ_{ac} at different constant frequencies for the sample $Se_{90}Ge_8In_2$ in the crystalline state at 120°C.

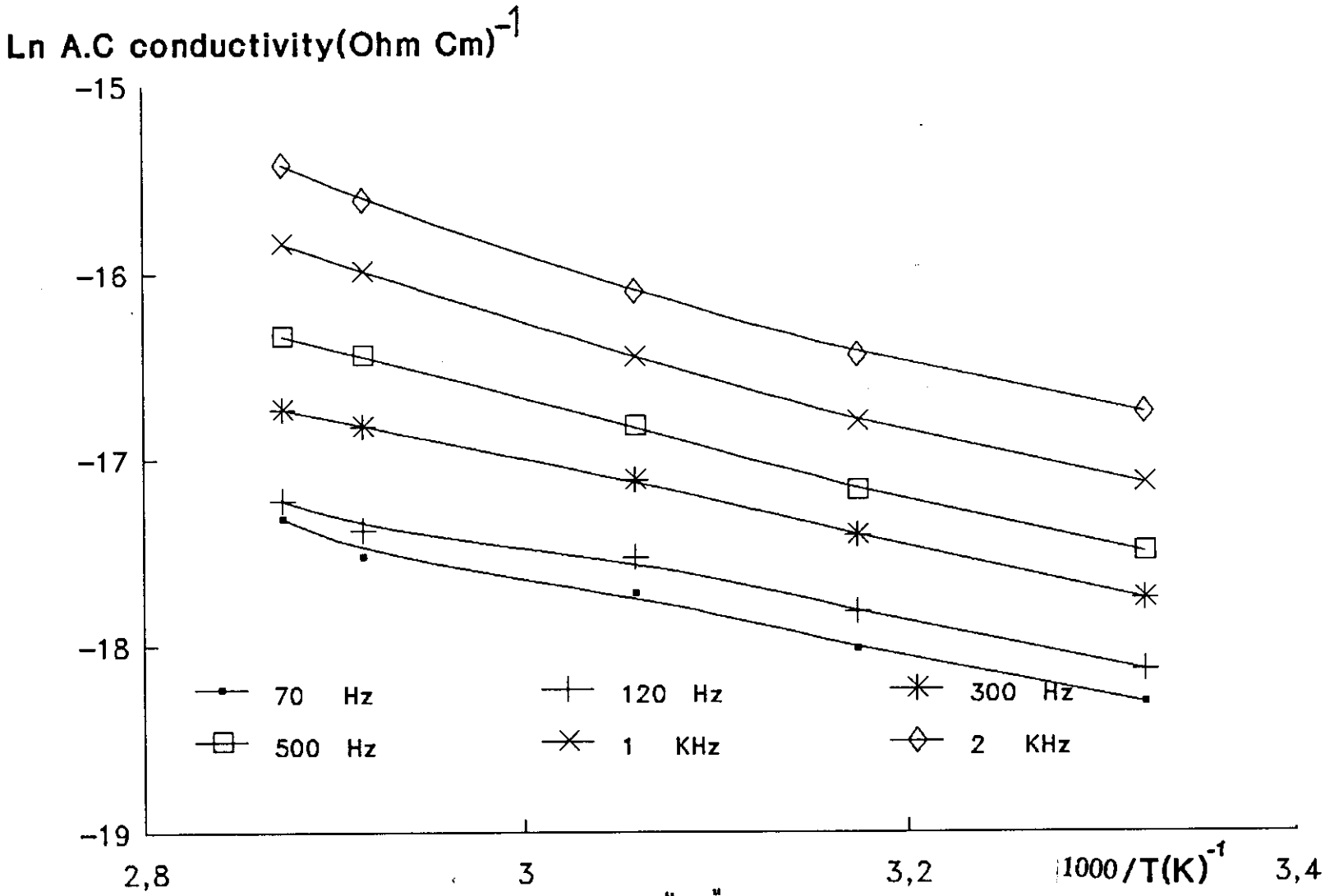

Fig.4.27: The temperature dependence of "σ_{ac}" at different constant frequencies for the sample $Se_{90}Ge_8In_2$ in the crystalline state at 130°C.

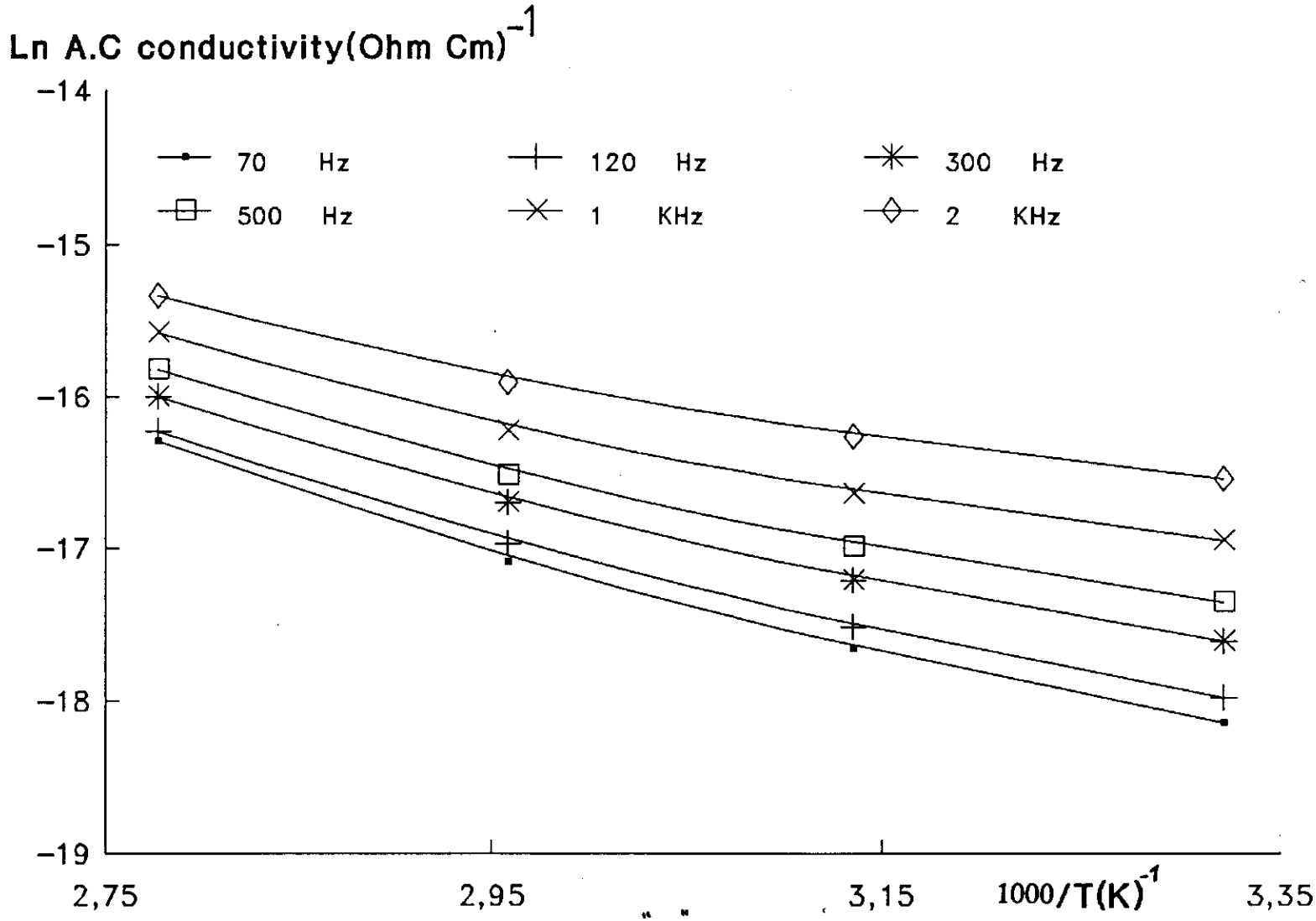

Fig.4.28: The temperature dependence of "σ_{ac}" at different constant frequencies for the sample $Se_{90}Ge_8In_2$ in the crystalline state at 140°C.

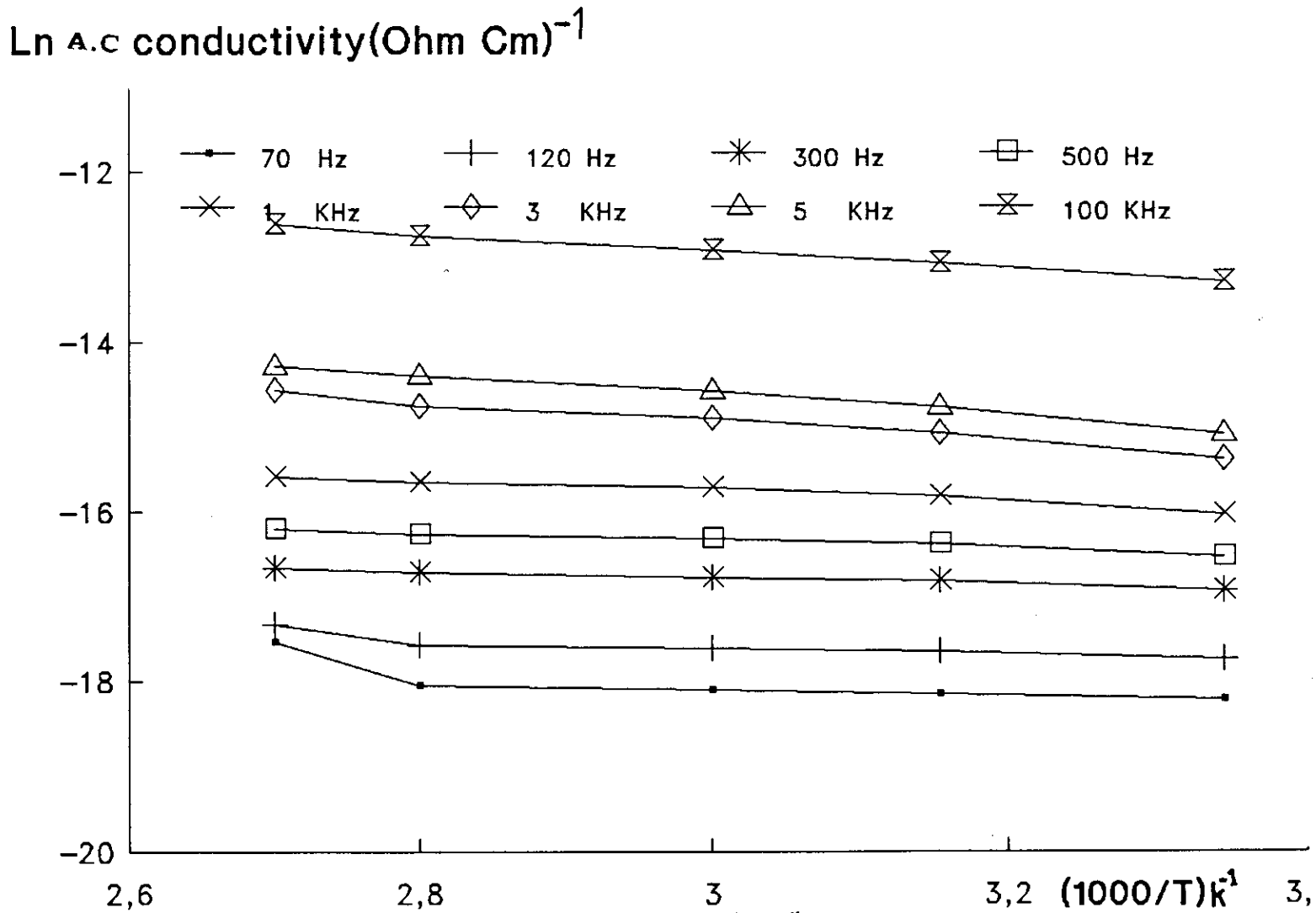

Fig.4.29:shows temperature dependence of "σ_{ac}" at various constant frequencies for the sample $Se_{90}Ge_8In_2$ in the crystallin state at 150°C

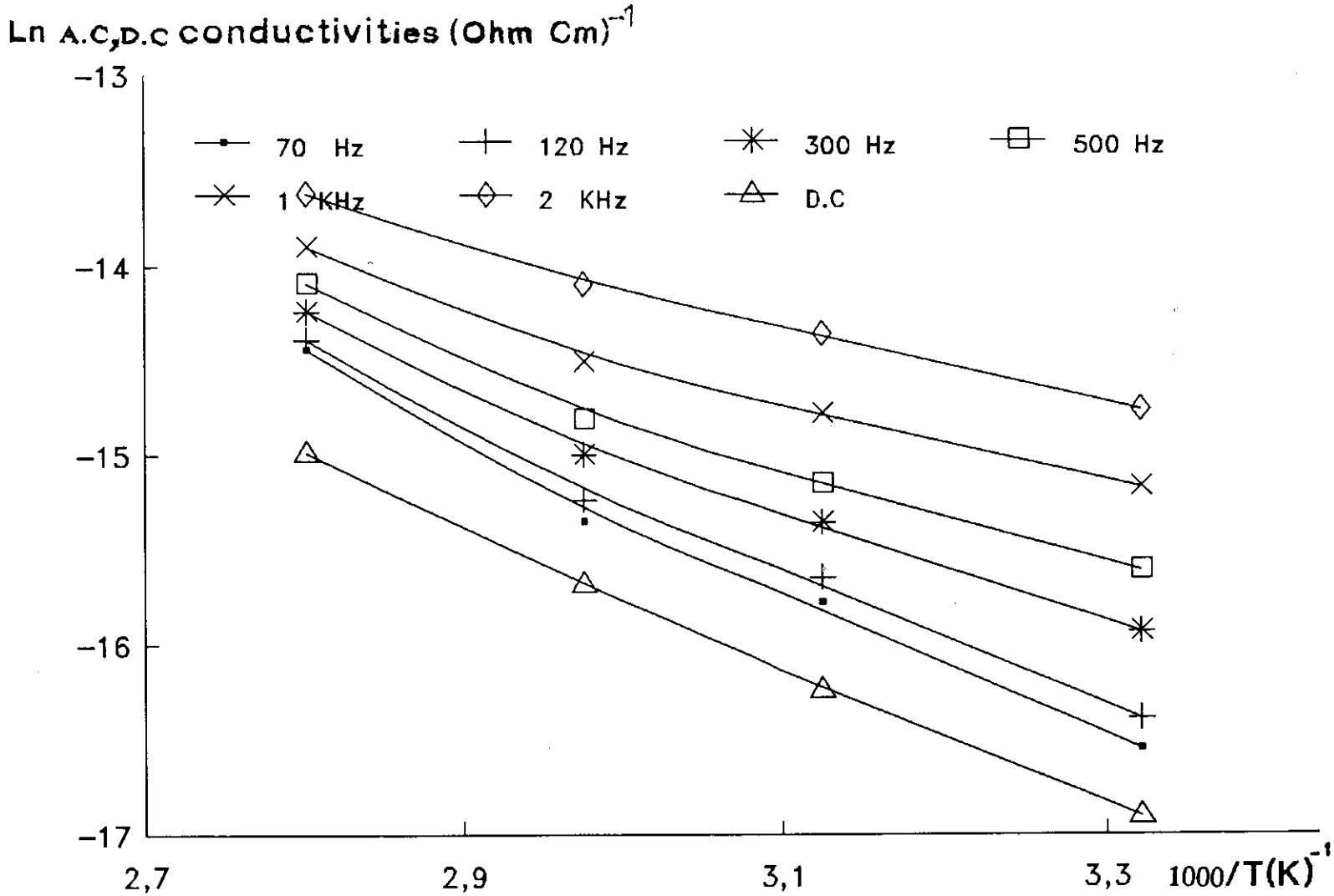

Fig.4.30: The temperature dependence of σ at various constant frequencies of the sample $Se_{90}Ge_6In_4$ in the crystalline state at 120°C.

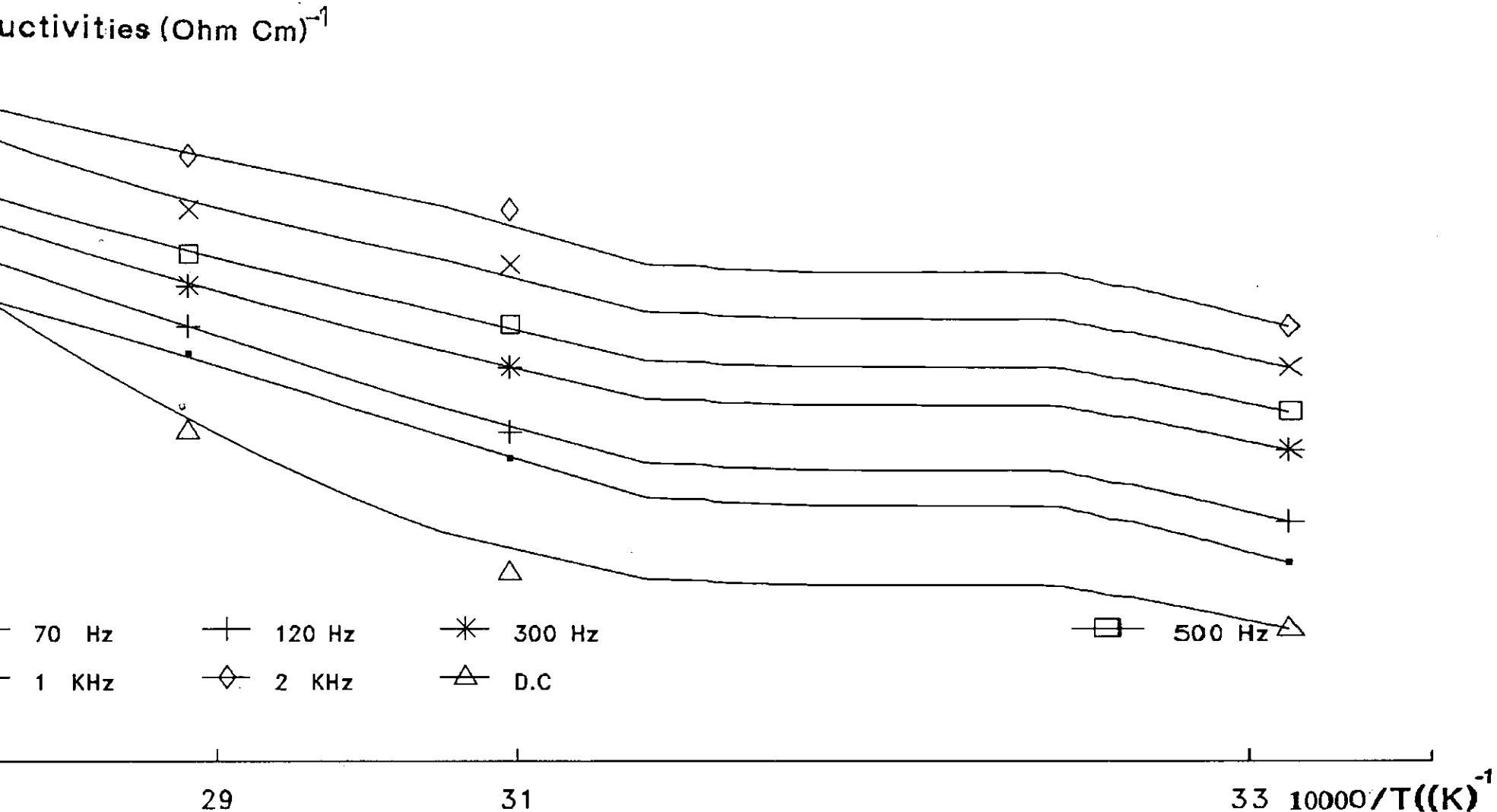

mperature dependence of "σ" at different [illegible] nstant frequencies for ample $Se_{90}Ge_6In_4$ in the crystalline state at [illegible] 0°C.

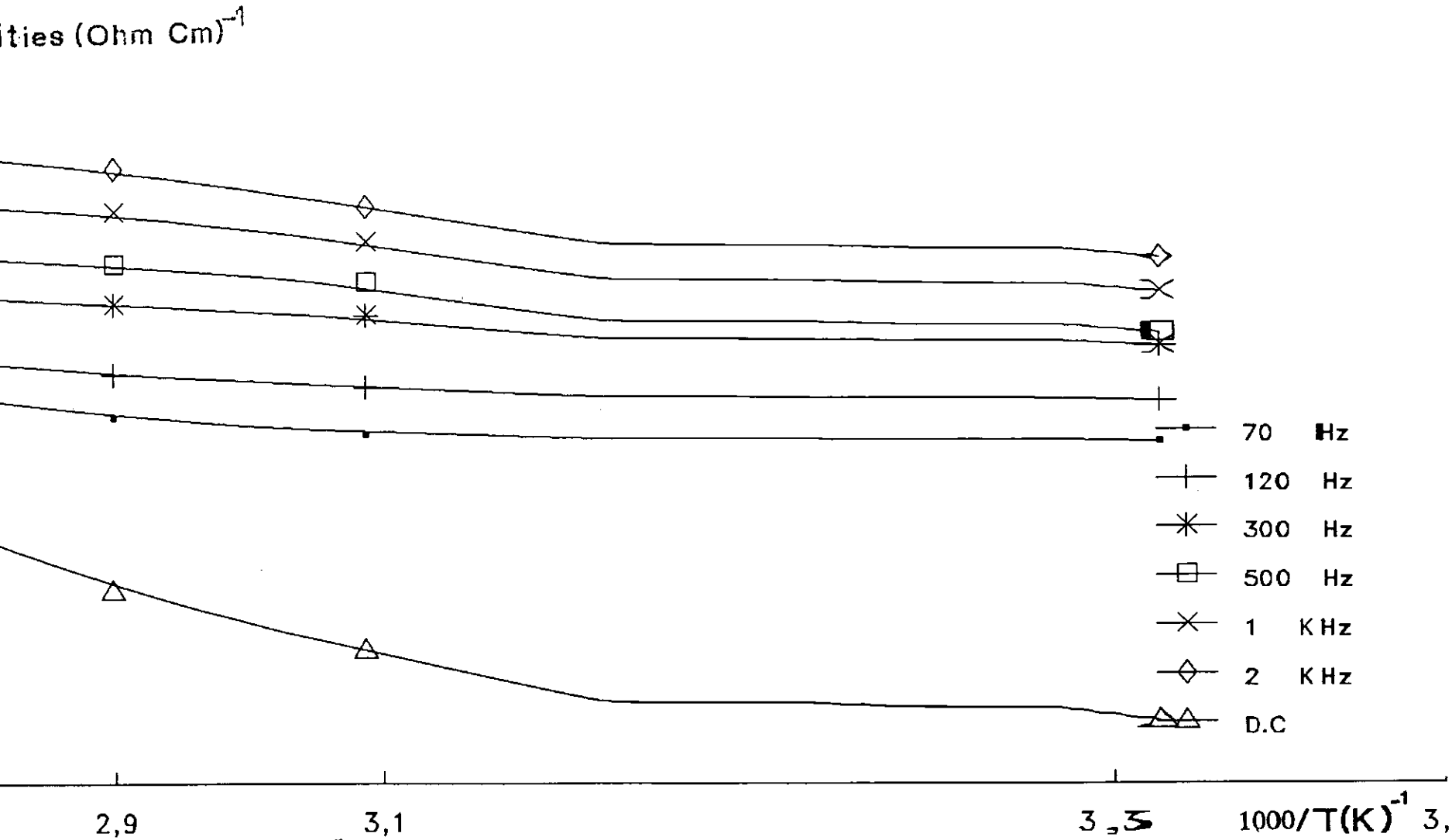

rature dependence of "σ" at different c [redacted] stant frequencies
ple $Se_{90}Ge_6In_4$ in the crystalline state at [redacted] 40°C.

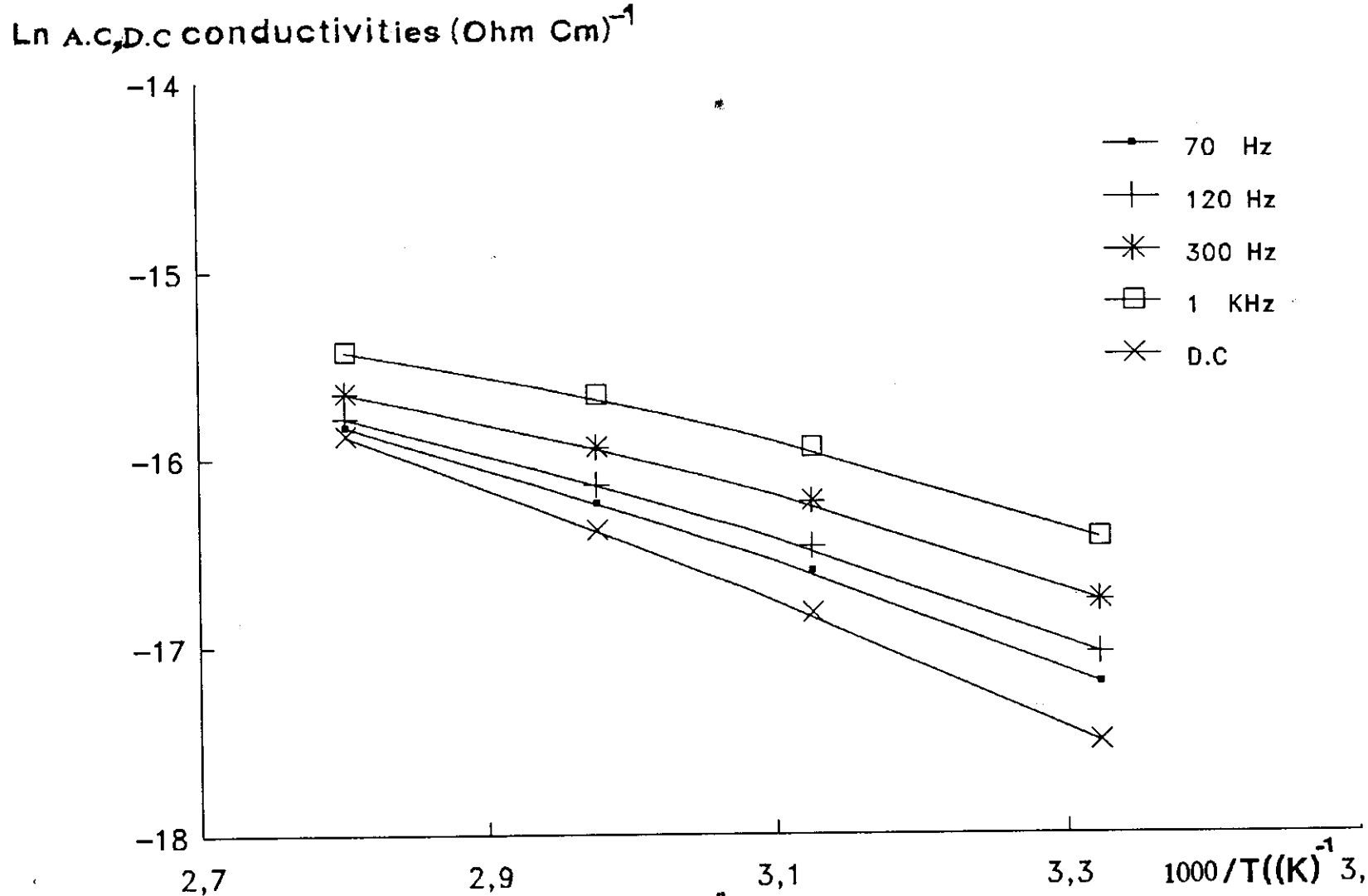

Fig.4.33 The temperature dependence of σ'' at different constant frequencies for the sample $Se_{90}Ge_6In_4$ in the crystalline state at 150°C.

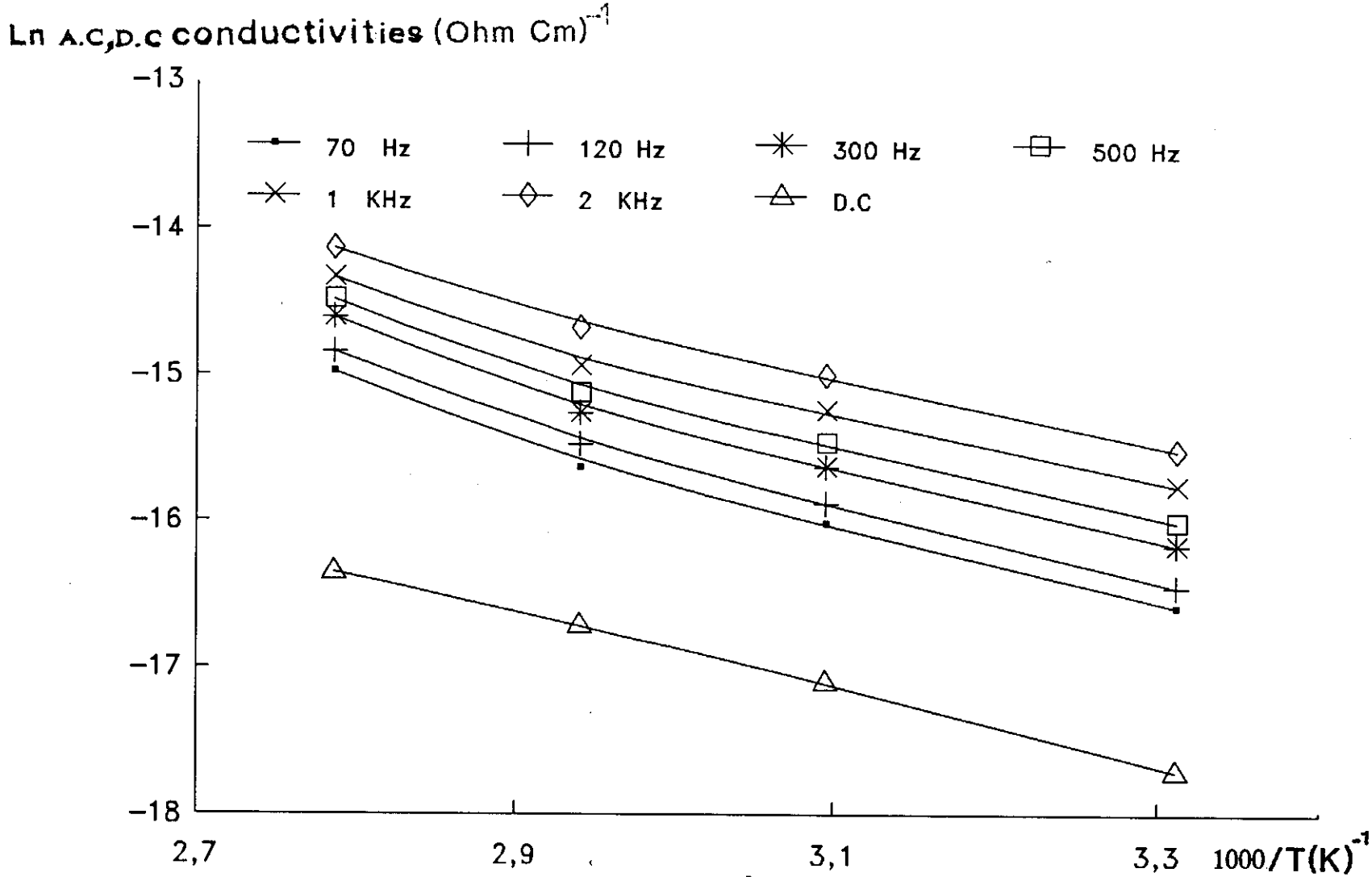

Fig.4.34: The temperature dependence of σ at different constant frequencies for the sample $Se_{90}Ge_4In_6$ in the crystalline state at 120°C.

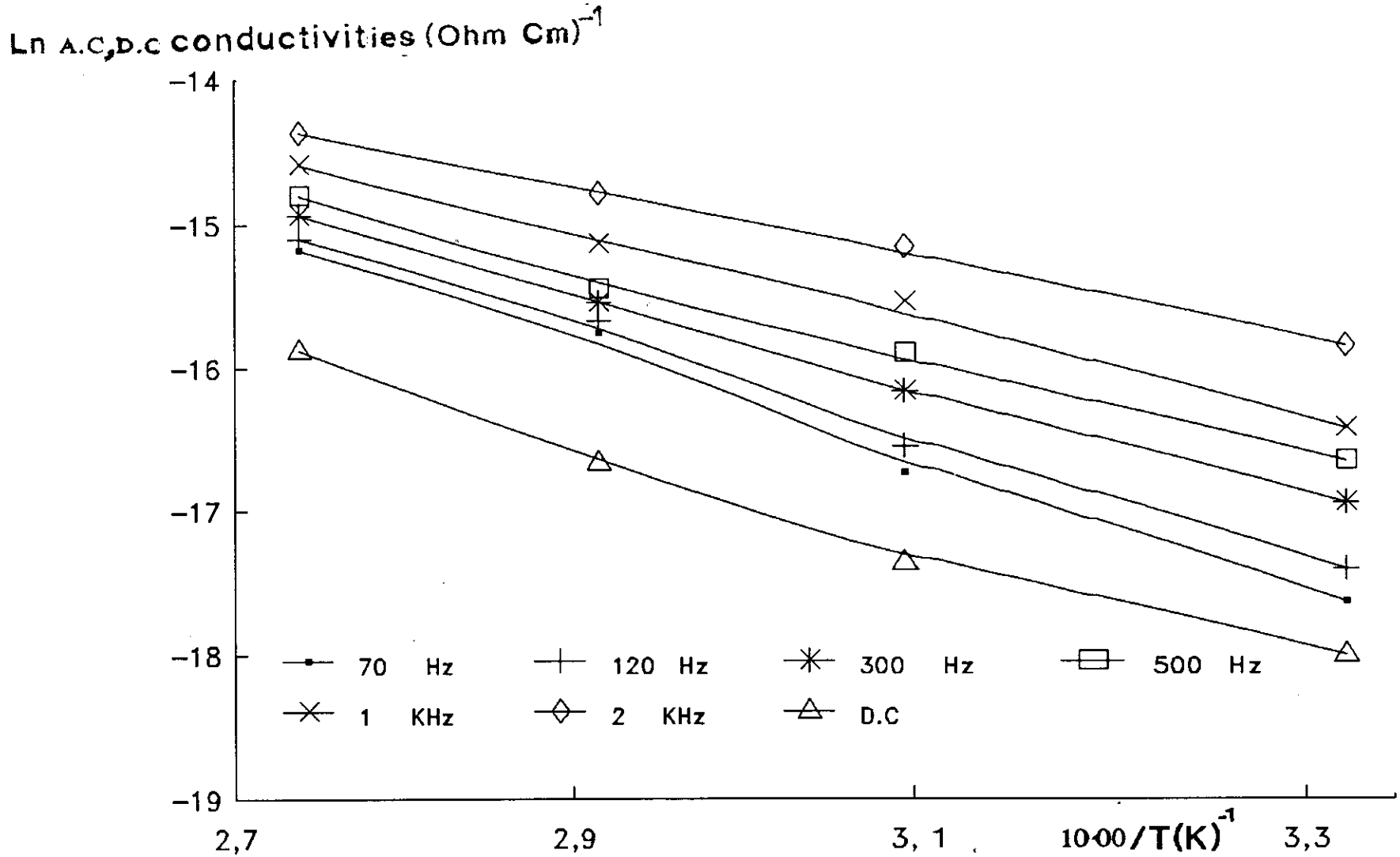

Fig.4.35: The temperature dependence of "σ" at different constant frequencies for the sample $Se_{90}Ge_4In_6$ in the crystalline state at 130°C.

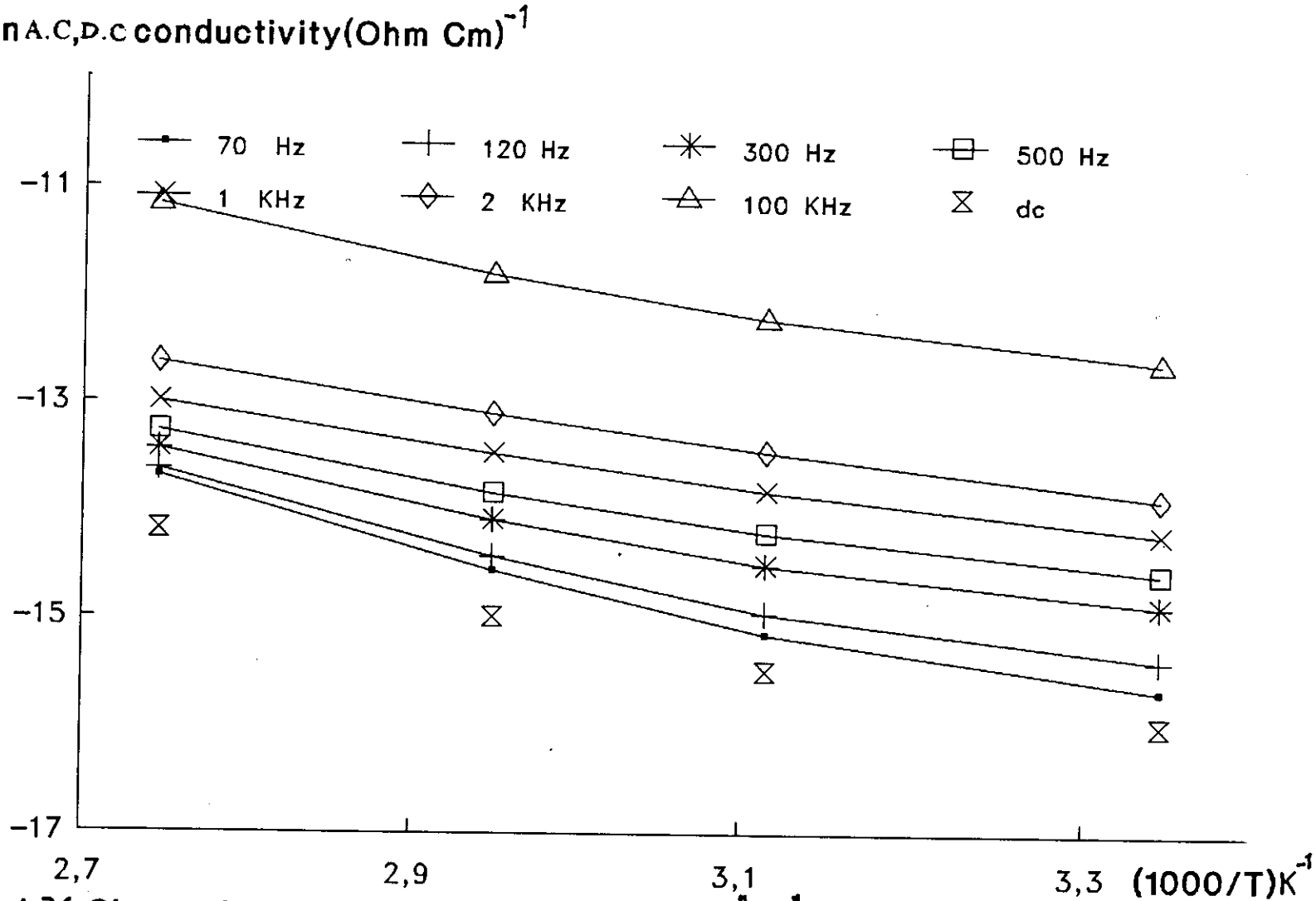

Fig.4.36:Shows the temperature dependence of σ at various constant frequencies for the sample $Se_{90}Ge_4In_6$ in the crystalline state at 140°C.

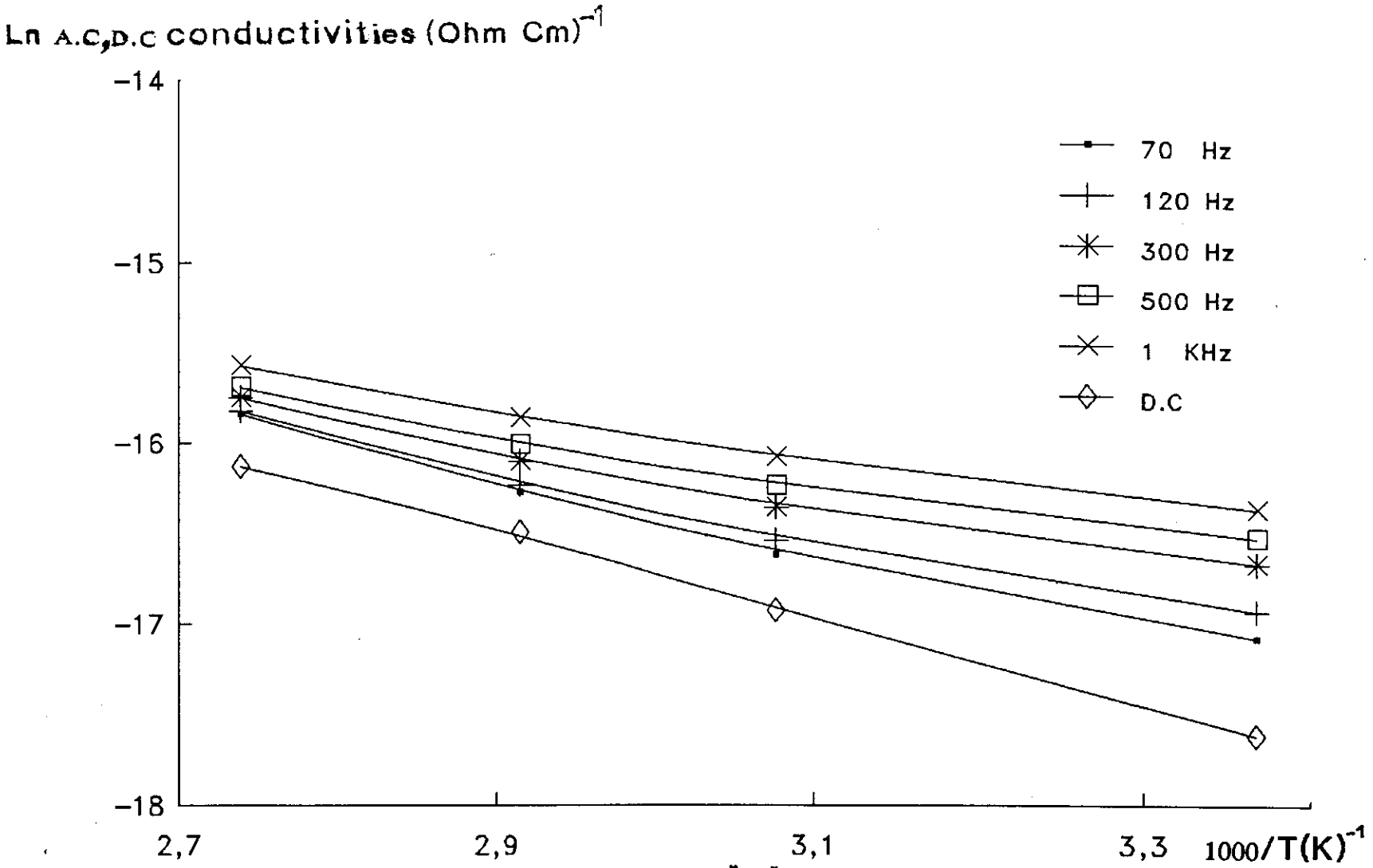

Fig.4.37: The temperature dependence of the σ at different constant frequencies for the sample $Se_{90}Ge_4In_6$ in the crystalline state at 150°C.

temperatures. The results were recorded on figs.(4.30-4.37).Generally the D.C conductivity of each Sample of the system Se_{90} Ge_{10-x} In_x increases as the temperature increases. The increases of the crystallization temperature increases the value of D.C.conductivity. This confirm the point of view that the increase of crystallization temperature leads to the increase of the cross sectional area of the conduction path.

The activation energy (ΔE) of the D.C conductivity has been derived and tabulated in table(4.4). It is clear from this table(4.4) that (ΔE) decreases as crystallization temperature increases. This may be due to the decrease of the potential barrier between adjacent crystallites.

The increase of the Indium content leads to the decrease of the activation energy (ΔE). This may be due to the effect of gradual reducing of the network resistance as Indium atoms increases.

On the light of the previous result the conduction mechanism in the system $Se_{90}Ge_{10-x}In_x$ in the crystalline state may becomes clear as:

The decrease in activation energy due to the addition of Indium may modify the energy band diagram of GeSe by creating new charged centers in the mobility gap. It may results in the unpinning of the Fermi energy level which in the undopped chalcogenides is located midway between the deep line levels of the C_3^+ and C_1^- charged centers. The Fermi level may shift towards the valence band since the charge carriers are holes as reported by M.Zope et al.[108]. The shift in the Fermi level with the increase of Indium can be explained with the

help of charged centers as follow:

In order to understand the nature of the defect states,Kastner et al[23]. proposed that in amorphous semiconductors,the lowest energy defect states are positively charged threefold coordinated C^{+}_{3} and negatively charged one fold coordinated C^{-}_{1} chalcogen atoms. These contents are present in equal concentrations. A high density of such inherent defect is observed in many amorphous semiconductors as proposed by Kastner et al.[23] to explain the switching mechanism in thin film. According to them the C^{-}_{1} center captures a hole [$C^{-}_{1} + e^{+}$ ------> C^{0}_{1} -----> C^{o}_{3}] and the C^{+}_{3} center captures an electron [$C^{+}_{3} + e^{-}$ -----> C^{0}_{3}]. The second process is faster than the first, since it does not involve a local band rearrangement and thus has no activation barrier. This effect further enhance the p-type nature of the state. Neutral C^{0}_{3}centers are formed when the C^{+}_{3}center capture an electron or the C^{-}_{1} center capture a hole. Here C^{0}_{1} centers are unstable with respect to the C^{0}_{1} ------> C^{0}_{3}transition and 2 C^{0}_{3} --------> $C^{-1} + C^{+}_{3}$is also energetically favoured. For Se_{90} Ge_{10}, the Fermi level is approximately pinned at the center of the mobility gap since the charged defect center C^{+}_{3} and C^{-}_{1} are equal in concentration as shown in fig.(4.38)[108]. When, M, concentration increases in the system Se_{90} Ge_{10}{M=Tl,In} a structural changes in the host network SeGe which leads to a readjustment in the local environment. This might disturb the balance of characteristic charged defects(C^{-}_{1} & C^{+}_{3}) in a chalcogenide semiconductor which can change the electronic conduction. In such a situation the distribution and density of localized states are modified and even some new trap

states can appear in the gap of the semiconductor.

So it is asssumed that the Fermi level is shifed on increasing of Indium owing to the change of the energy spectrum of the states in the mobility gap. Indium is supposed to form states different from the valence states of elements interacting with chalcogenide according to the (8-N) rule.

The formation of tetrahedrally coordinated atoms of Tl similar to In in the SeGe system as reported by Kosek et al.[109] may be written as :

$$In^{0}_{3} + C^{0}_{2} \text{ -------> } In^{-}_{4} C^{+}_{3}$$

This reaction produces pairs of charged centers are linked together by a donor-acceptor binding and Coulombic attraction. Evidently the C^{+}_{3} center is characterized by another energy such as the C^{0}_{3} center which is, according to Kastner,Adler and Fritzsch, formed by the reaction :

$$2\ C^{0}_{3} \longrightarrow C^{-}_{1} + C^{+}_{3}$$

This difference results from:

(1) The difference in energy of the C-C bond and Tl-C bond (in our case In-C bond) and

(2) The additional Coulombic interaction between In^{-}_{4} or Tl^{-}_{4} and C^{+}_{3} that can not be neglected.

Fritzsch[110],and M.Zope et al.[108] supposed that the equilibrium

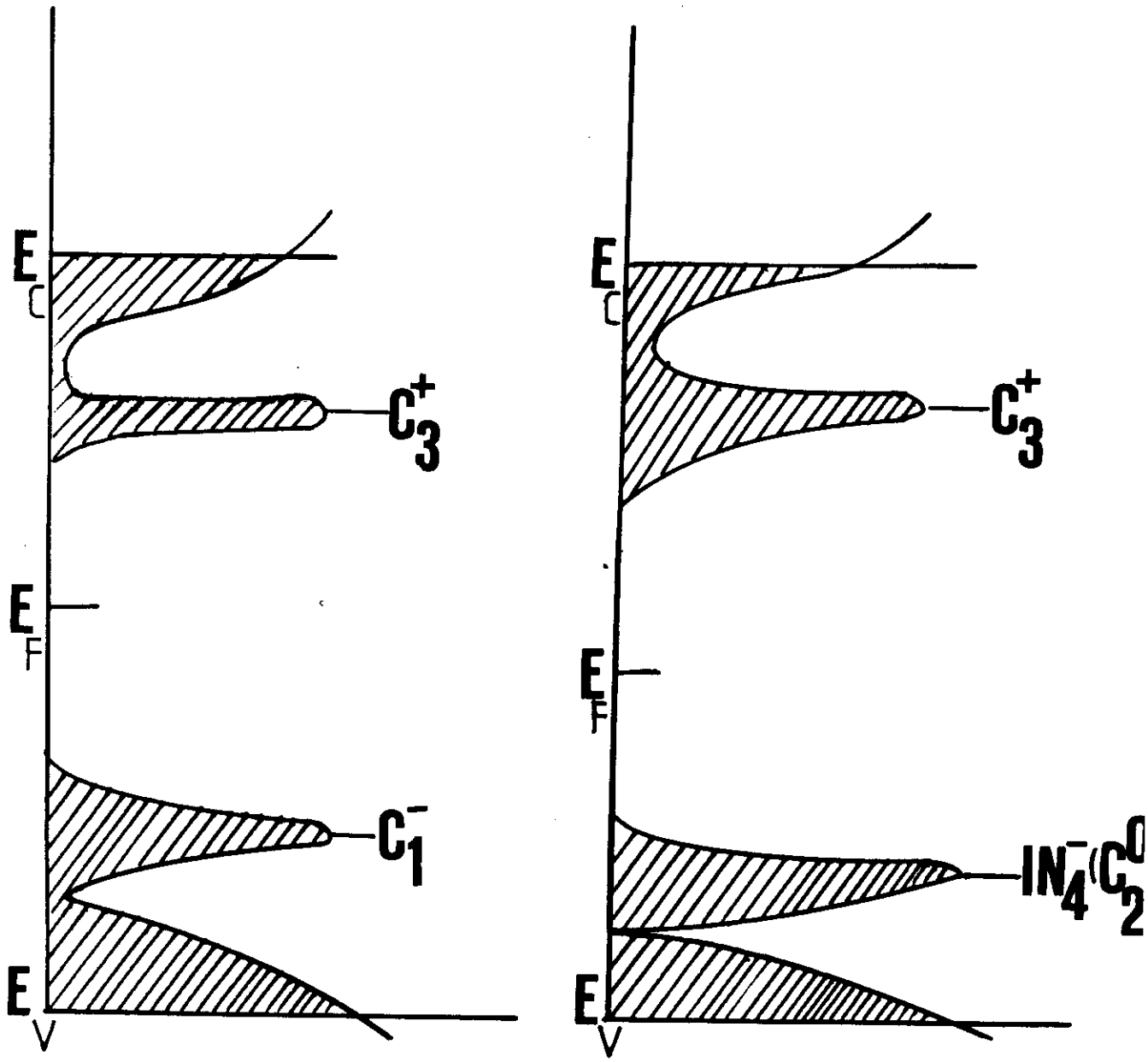

Fig.(4.38):(a):Energy band diagram of Ge-Se with C^{-}_{1} and C^{+}_{3} centers.
(b):Energy band diagram of Ge-Se-In with C^{+}_{3} and $In_4(C^{o}_{2})_3$centers.

constant

$$2\,C_2^0 \longleftrightarrow C_1^- + C_3^+$$

does not depend on the concentration of additives i.e the product $[C_1^-][C_3^+]$is determined by the nature of chalcogen and the temperature at which the equilibrium is frozen in. Then on addition of Tl or In the formation of C_3^+ centers must cause a decrease in concentration of C_1^- centers ,instead of which $Tl_4^-(C_2^0)[In_4^-$ (C_2^0) in our case]are formed.

Finally it can be concluded that ,as the percentage of In increases in the sample,the density of charged centers $In_4^-(C_2^0)_3$increases, the Fermi level will shift towards the valence band,since carriers are holes[108]. A band diagram for Se-Ge-In is shown in fig.(4.38b). The increasing of In can not neglect the formation of In-C bonds and the decreasing in concentration of other bonds in the glass. This may result in a perturbation in the system which will broaden the valence and conduction band edges in the mobility gap.

4.2.3.THE EFFECT OF FREQUENCY ON THE A.C CONDUCTIVITY OF $Se_{90}Ge_{10-x}In_x$ IN THE CRYSTALLINE STATE :-

The frequency dependence of the A.C conductivity was recorded for the sample $Se_{90}Ge_8In_2$ at different isotherms. This experiment was carried out on four parts of this sample crystallized at 120,130,140 and 150 ^{o}C separately,figs.(4.39-4.42). These curves show that, the A.C conductivity increases as the frequency increases.

This experiment was repeated for the two samples $Se_{90}Ge_6In_4$ and $Se_{90}Ge_4In_6$ using parts crystallized at the same crystallization temperatures. Figs.(4.43-4.50) show that the same behaviour was confirmed.

The exponent ,S,in the relation :

$$\sigma_{ac} = A\omega^{S}$$

was derived as a function of temperature for the three compositions(X=2, 4 and 6) and tabulated in tables (4.5,4.6,4.7).

It is clear that ,S, decreases as the temperature increases.These results are in agreement with the correlated barrier hopping (CBH)model proposed by Elliott[111]. In this model,correlated barrier hopping of bipolarons (i.e two electrons hopping between charged defect states D^{+} and D^{-})has been proposed to explain the frequency

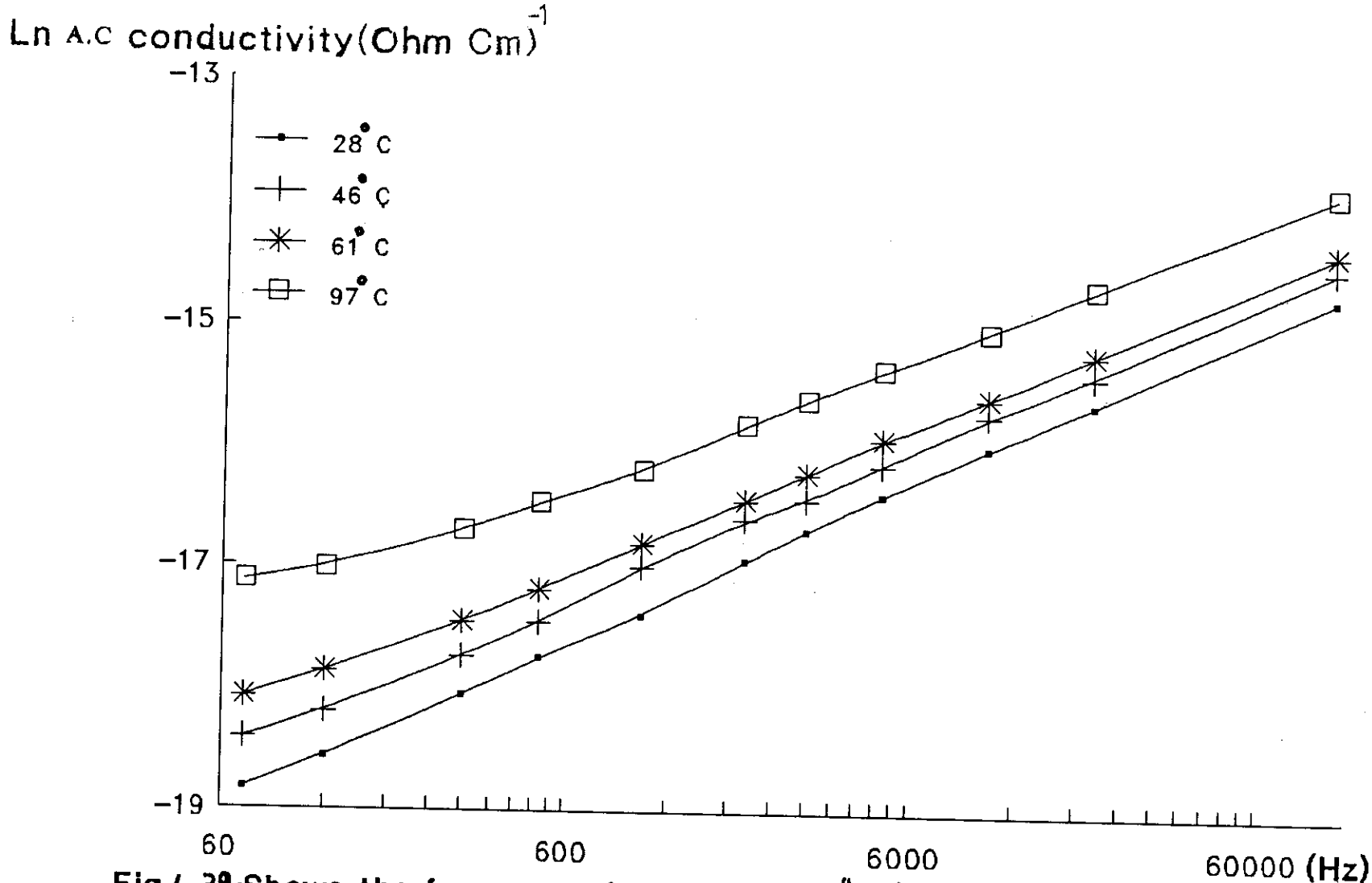

Fig.4.39:Shows the frequency dependence of "σ_{ac}" at constant various temperatures for the sample $Se_{90}Ge_8In_2$ in the crystalline state at 120° C.

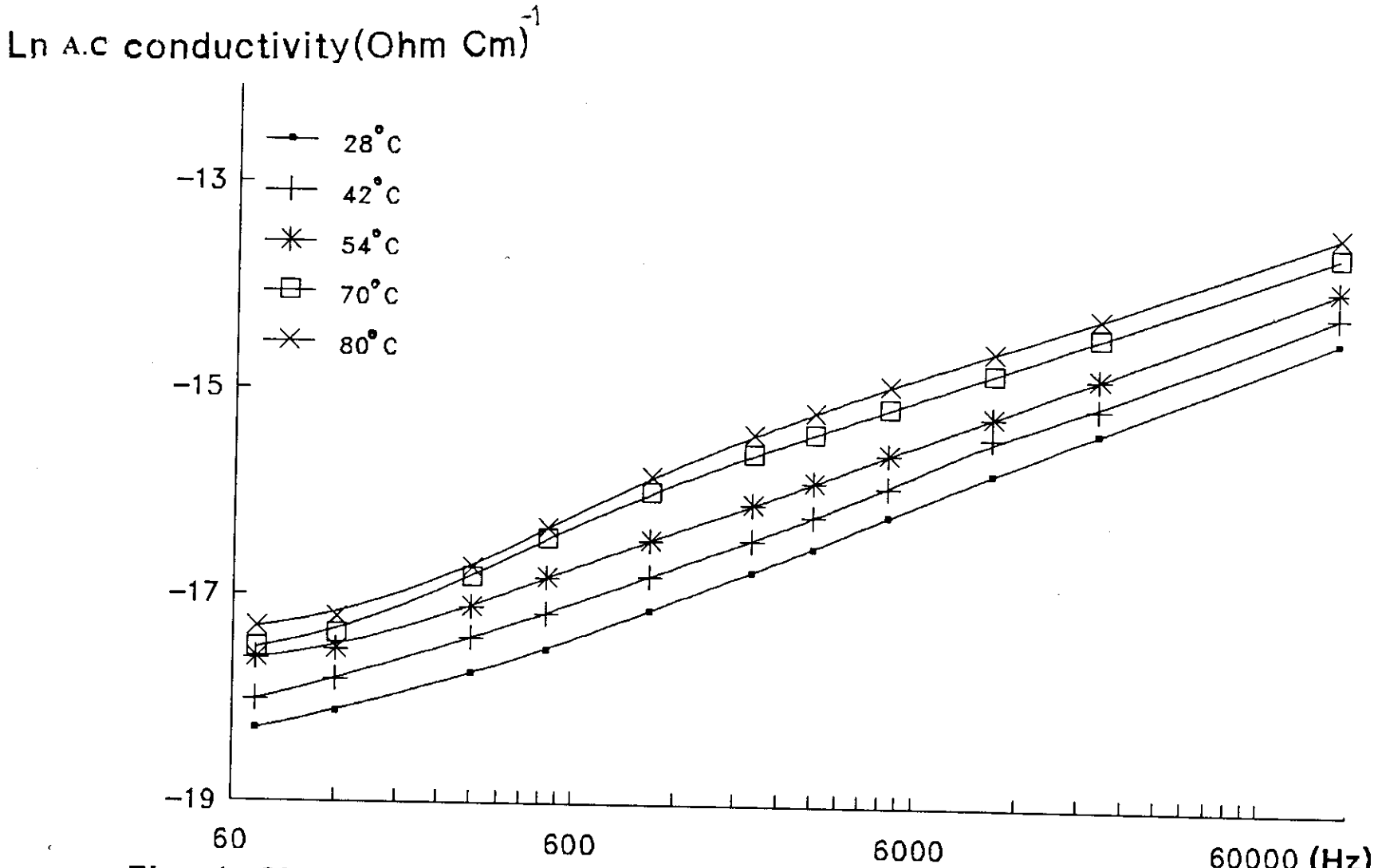

Fig.4.40:Shows the frequencey dependence of "σ_{ac}" at constant temperatures for the smple $Se_{90}Ge_8In_2$ in the crystalline state.at 130°C.

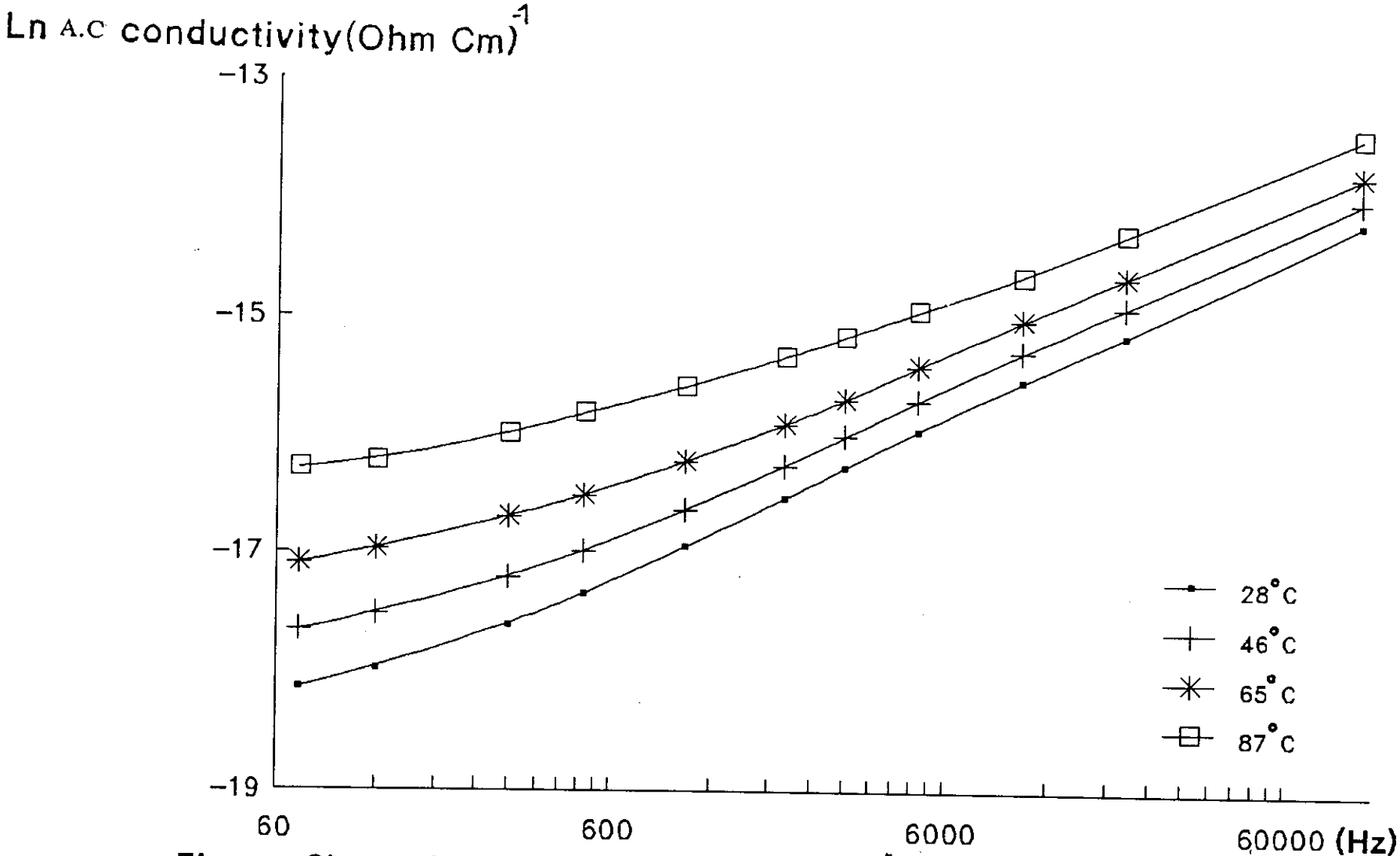

Fig.4.41:Shows the frequency dependence of "σ_{ac}" at constant temperatures for the sample $Se_{90}Ge_8In_2$ in the crystalline state at 140°C.

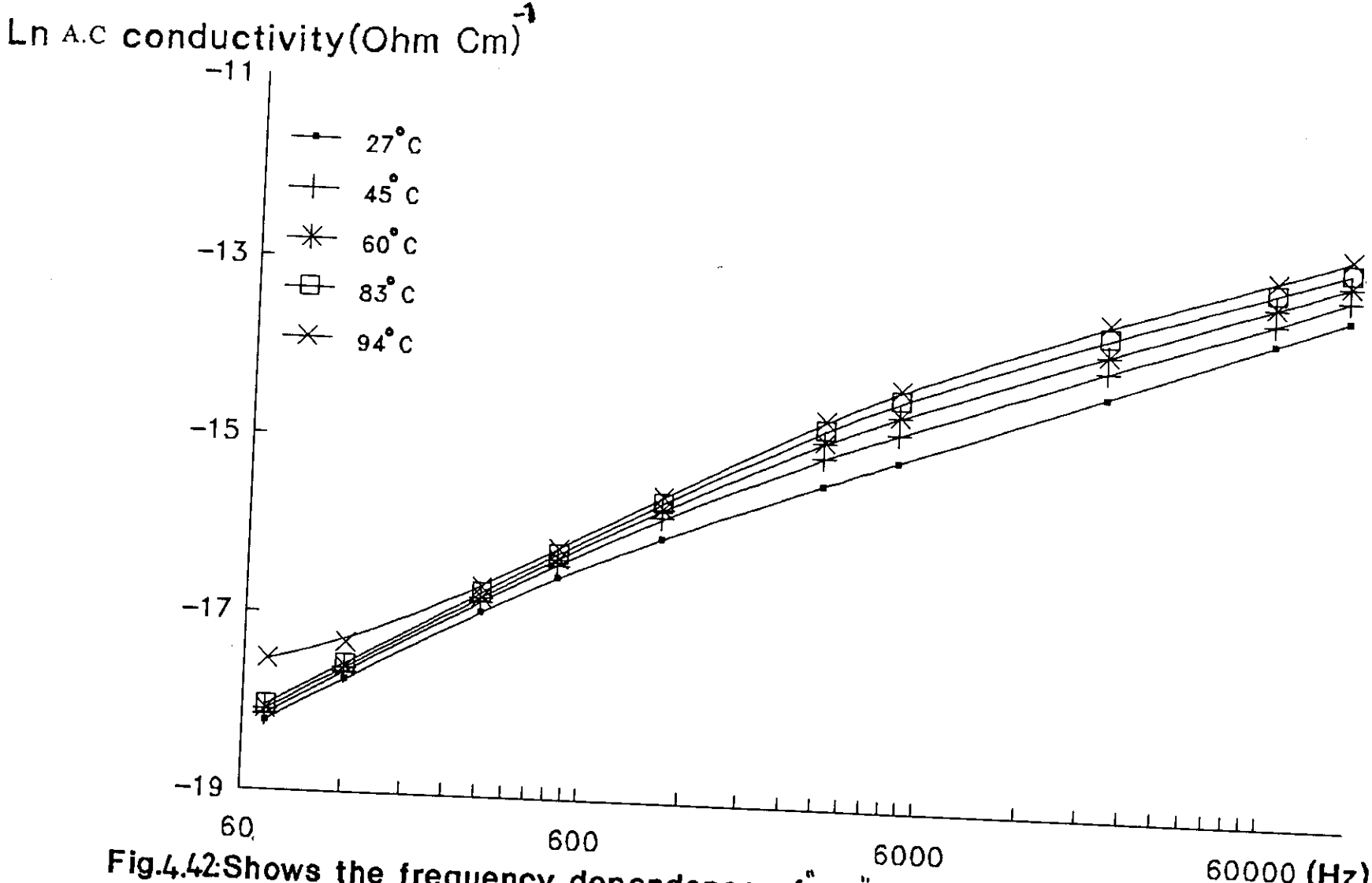

Fig.4.42:Shows the frequency dependence of "σ_{ac}" at different constant temperatures for the samnple $Se_{90}Ge_8In_2$ in the crystalline state at 150°C.

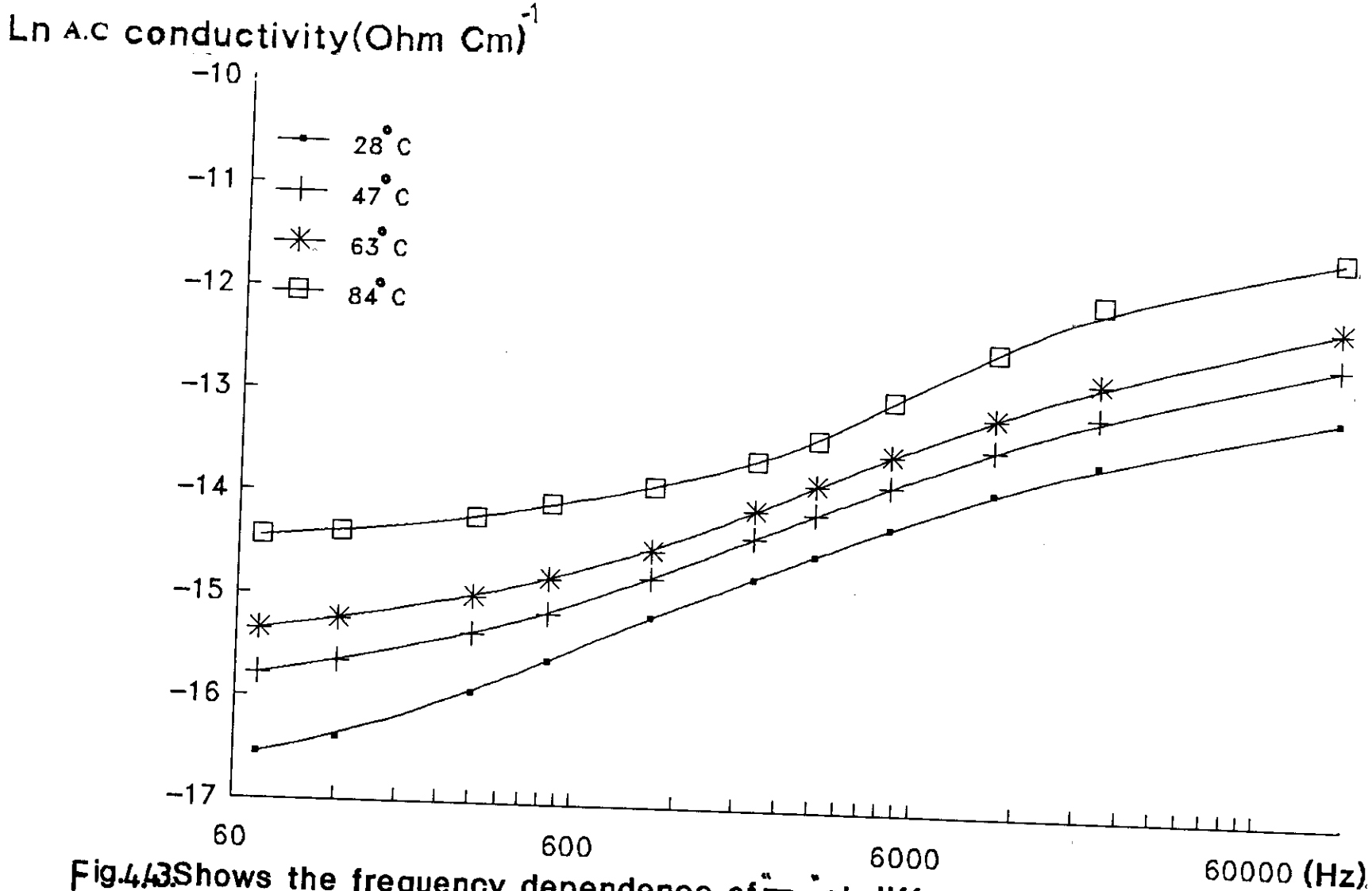

Fig.4.43 Shows the frequency dependence of σ_{ac} at different constant temperatures for the sample $Se_{90}Ge_6In_4$ in the crystalline state at 120°C.

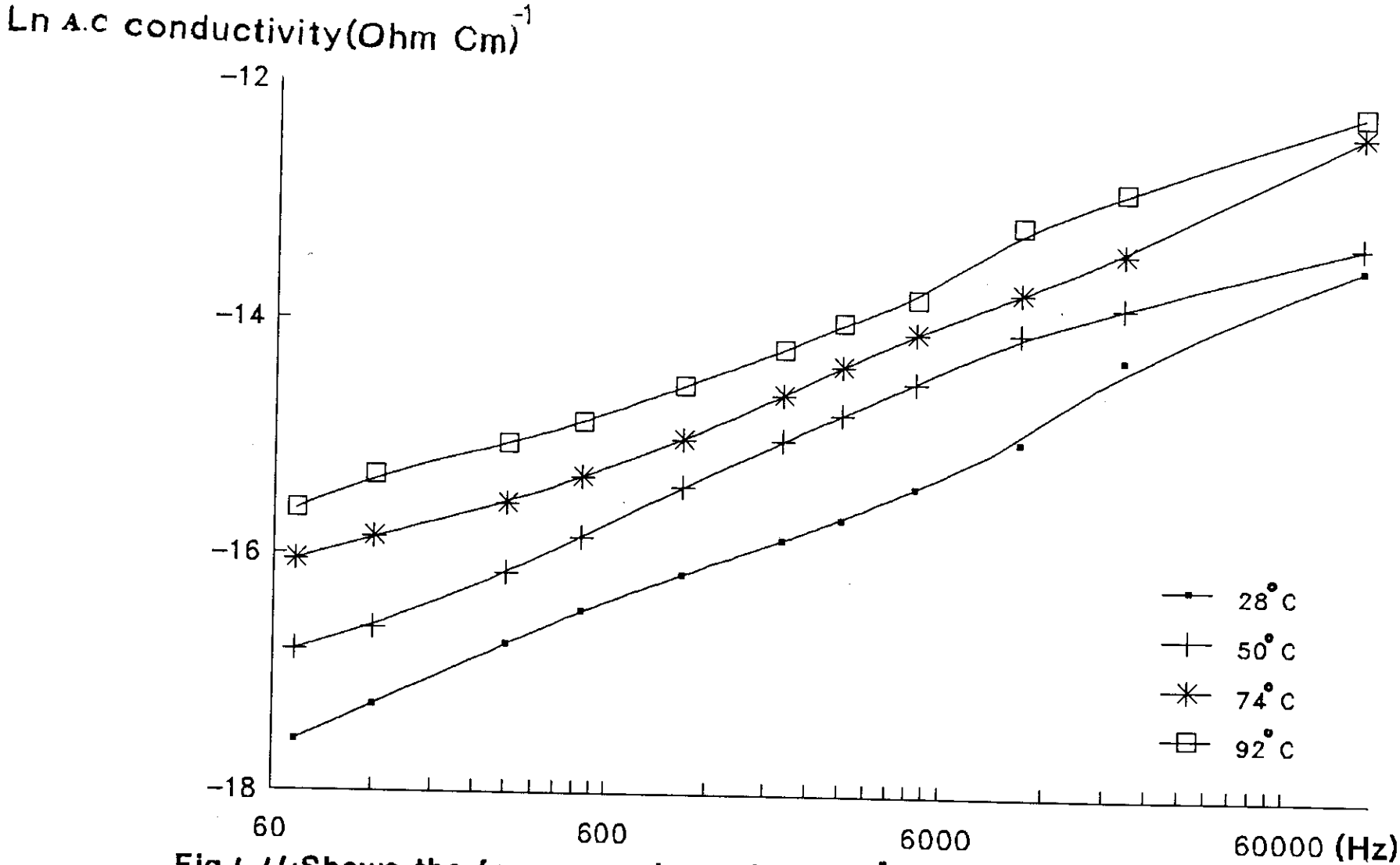

Fig.4.44:Shows the frequency dependence of σ_{ac} at different constant temperatures for the sample $Se_{90}Ge_6In_4$ in the crystalline state at 130° C.

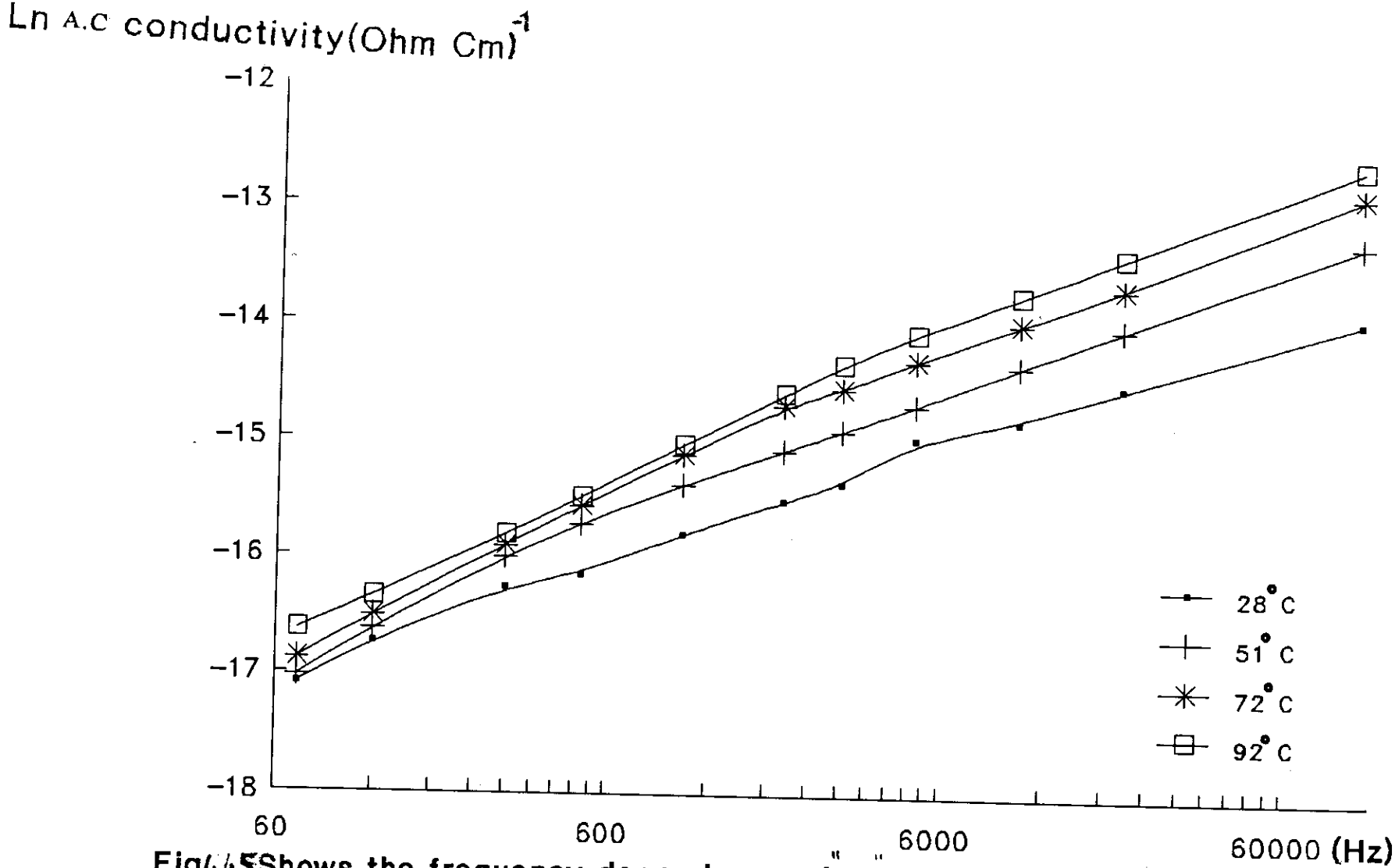

Fig 4.45 Shows the frequency dependence of "σ_{ac}" at different constant temperatures for the sample $Se_{90}Ge_6In_4$ in the crystalline state at 140°C.

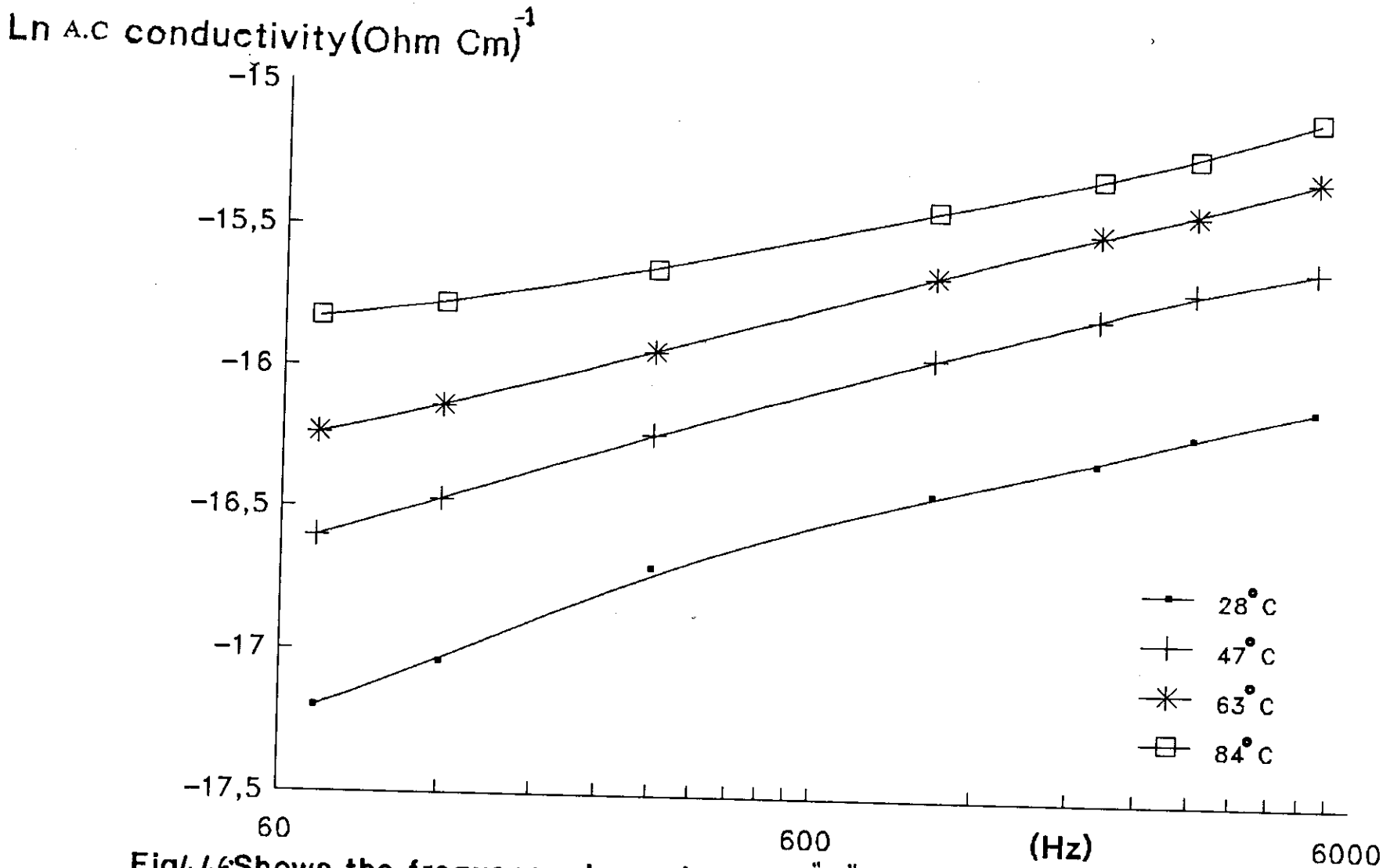

Fig 4.46 Shows the frequency dependence of "σ_{ac}" at different temperatures for the sample $Se_{90}Ge_6In_4$ in the crystalline state at 150°C.

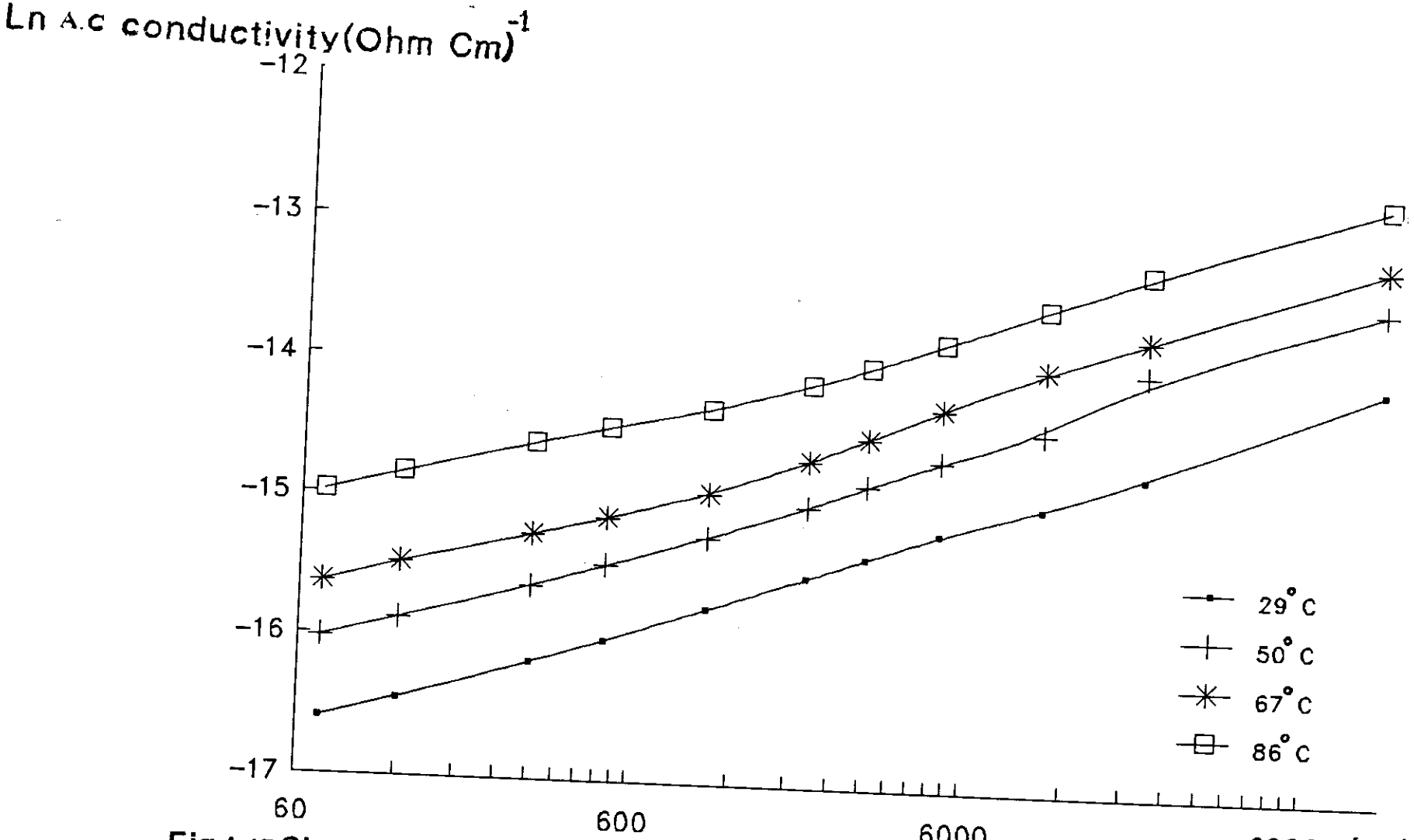

Fig.4.47:Shows the frequency dependence of σ_{ac} at constant temperatures for the sample $Se_{90}Ge_4In_6$ in the crystalline state. at 120°C.

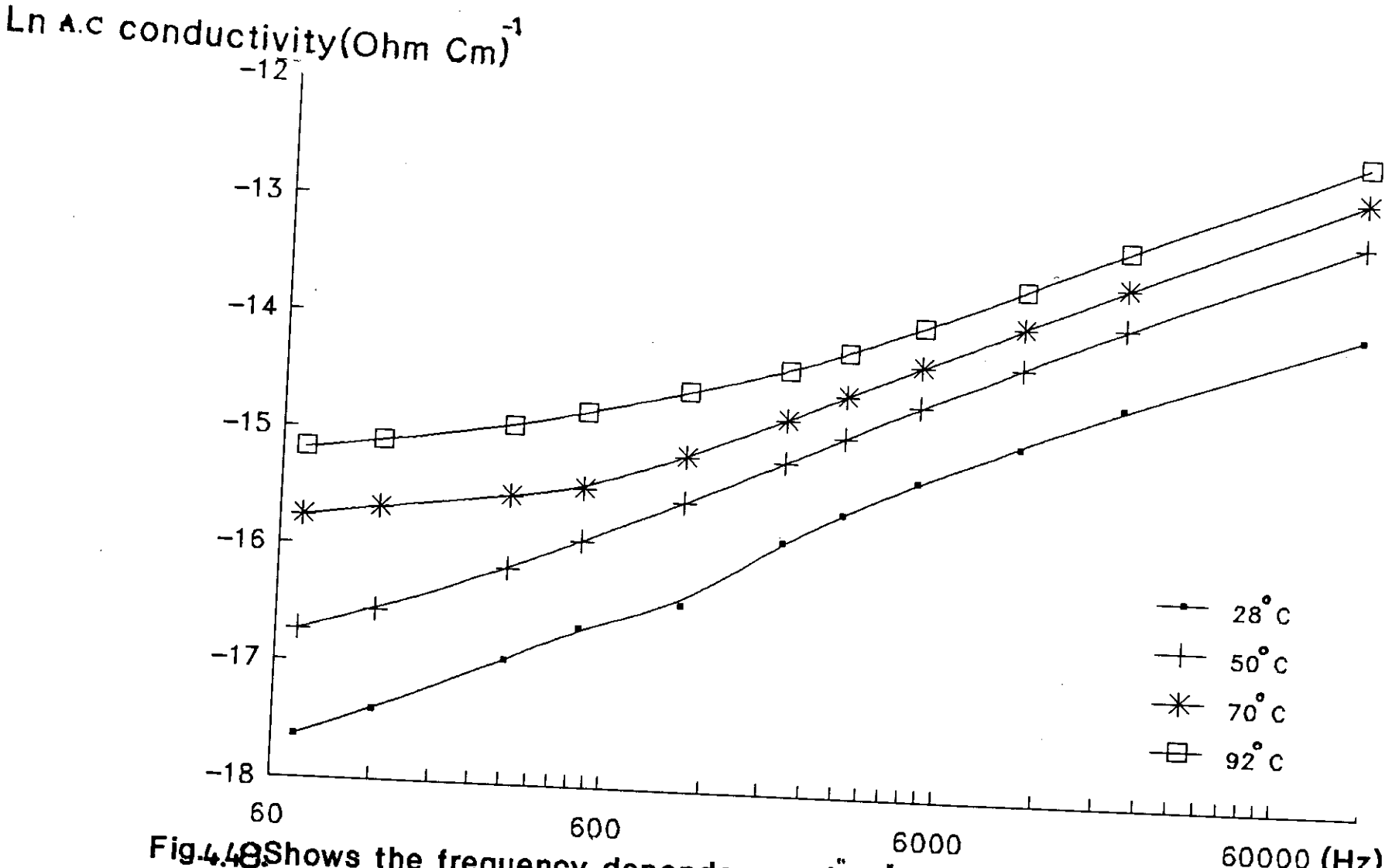

Fig.4.48. Shows the frequency dependence of σ_{ac} at various constant temperatures for the sample $Se_{90}Ge_4In_6$ in the crystalline state at 130°C.

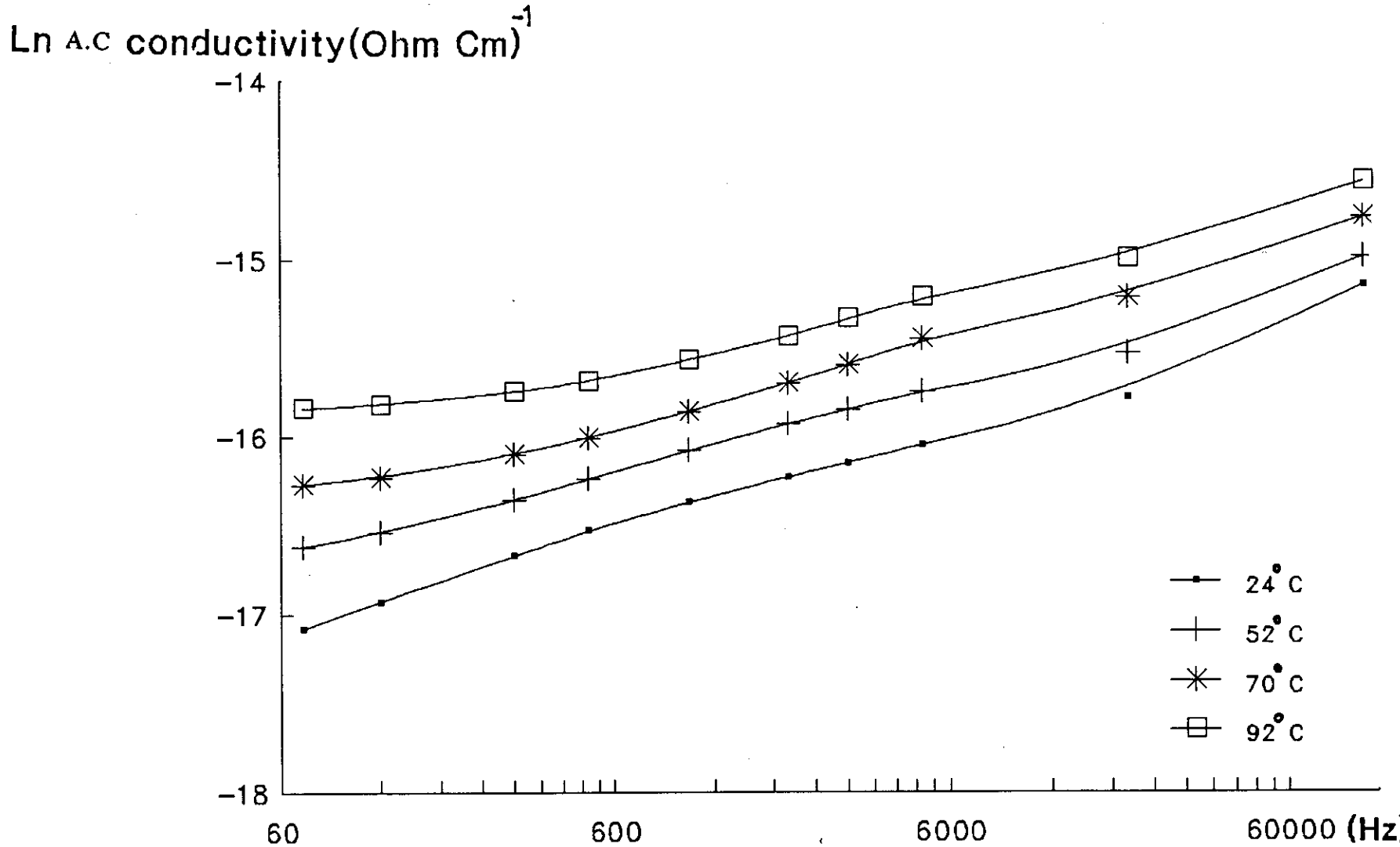

Fig.4.50 Shows the frequency dependence of "σ_{ac}" at various constant temperatures for the sample $Se_{90}Ge_4In_6$ in the crystalline state at 150°C.

dependence of A.C conductivity in the chalcogenide glasses.

Shimakawa[106] suggested that D^0 states are proposed by thermal excitation of D^+ and /or D^- states and that single-polaron hopping (i.e one electron hopping between D^0 and D^+ or D^-) contributes to A.C conduction at high temperatures.

Table(4.5) $Se_{90}Ge_8In_2$

crystallization temperature°(C)	T°(C)	S
120	28	0,568
	46	0,547
	61	0,523
	97	0,452
130	28	0,5485
	42	0,54
	54	0,521
	70	0,514
140	28	0,562
	46	0,5131
	65	0,462
	87	0,3927
150	28	0,5102
	45	0,5009
	61	0,443
	94	0,3703

Table(4.6) $Se_{90}Ge_6In_4$

crystallization temperature(^{O}C)	T^{O}(C)	S
120	28	0,485
	47	0,4106
	63	0,393
	84	0,29
130	28	0,56
	50	0,5172
	74	0,4723
	92	0,4723
140	28	0,4558
	51	0,5009
	72	0,5491
	92	0,5646
150	28	0,2598
	47	0,2309
	63	0,2205
	84	0,1702

Table(4.7): $Se_{90}Ge_4In_6$

Crystallization temperature(^{O}C)	T^{O}(C)	S
120	29	0,3456
	50	0,3239
	67	0,313
	86	0,3089
130	28	0,5309
	50	0,5094
	70	0,4272
	92	0,3745
140	27	0,4726
	49	0,4718
	75	0,4621
	90	0,447
150	24	0,2496
	52	0,2165
	70	0,1193
	92	0,085

4.2.4.THE EFFECT OF TEMPERATURE ON THE DIELECTRIC CONSTANT OF $Se_{90}Ge_{10-x}In_x$ IN THE CRYSTALLINE STATE:-

Figs.(4.51-4.54) show the temperature dependence of the dielectric constant of $Se_{90}Ge_8In_2$ in the crystalline state during the temperature range (27-100 ^{o}C)at different constant values of frequency.

These records were traced for the given sample at the crystallization temperature 120,130,140 and 150 ^{o}C after complete crystallization. From these results it is clear that the dielectric constant increases as the temperature increases. At low temperature the dielectric constant increases with slow rate and at high temperature range the rate of increment becomes higher.

This experiment was repeated for the two samples $Se_{90}Ge_6In_4$ and $Se_{90}Ge_4In_6$ at the same crystallization temperatures, figs.(4.55-4.58) and figs(4.59-4.62) respectively. The strong frequency dependence of the dielectric constant at high temperature can be understood on the basis of the presence of molecular dipoles in the glass. At low temperatures the dipoles remain frozen and at high temperatures they obey freedom of rotation.

The detected behaviour of the dielectric constant may be explained as:

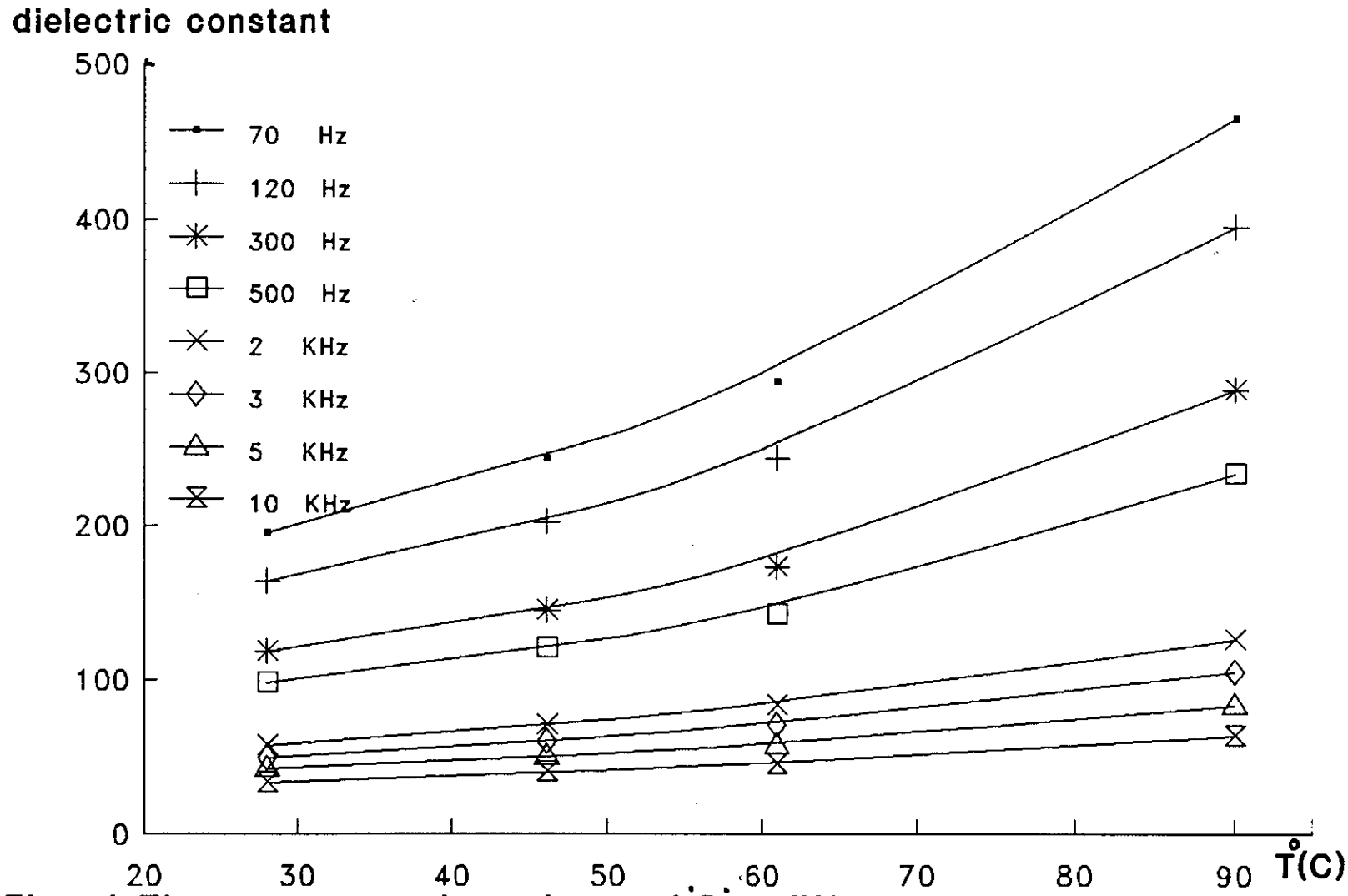

Fig.4.51: The temperature dependence of ε' at different constant frequency for the sample $Se_{90}Ge_8In_2$ in the crystalline state at 120°C.

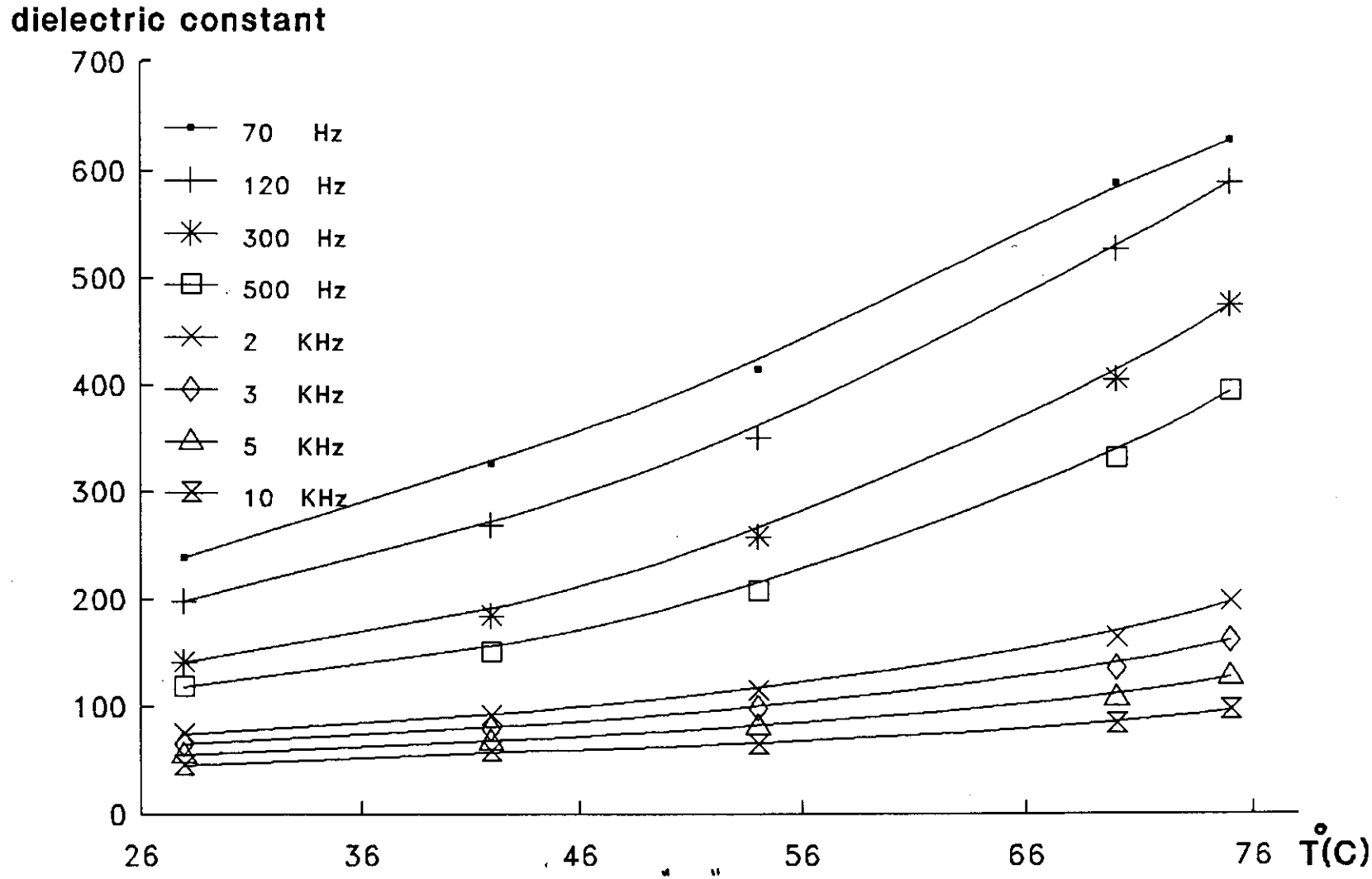

Fig.4.52:The temperature dependence of ε'' at different constant frequency for the sample $Se_{90}Ge_8In_2$ in the crystalline state at 130°C.

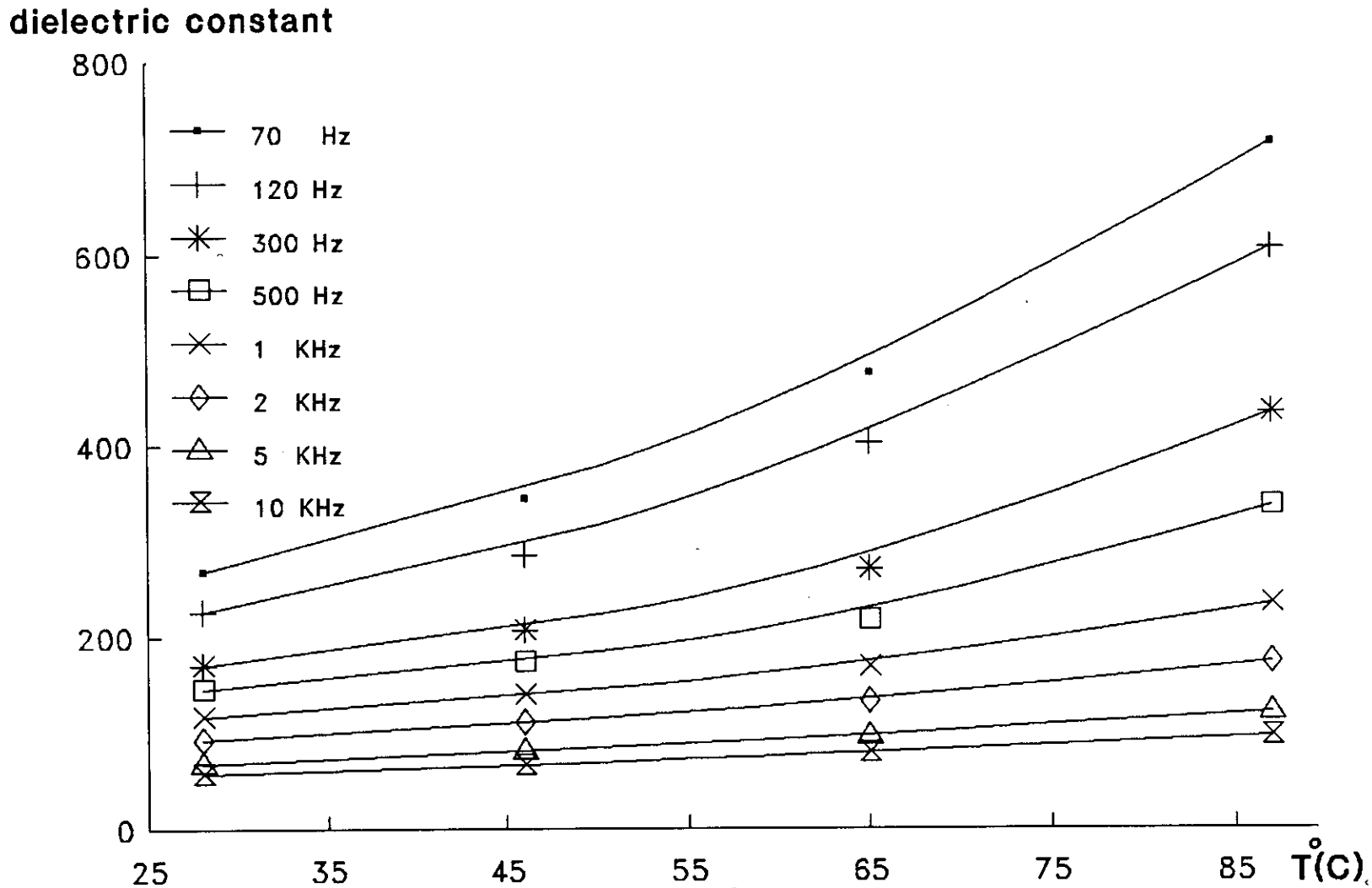

Fig4.53:The temperature dependence of ε' at different constant frequency for the sample $Se_{90}Ge_8In_2$ in the crystalline state at 140°C.

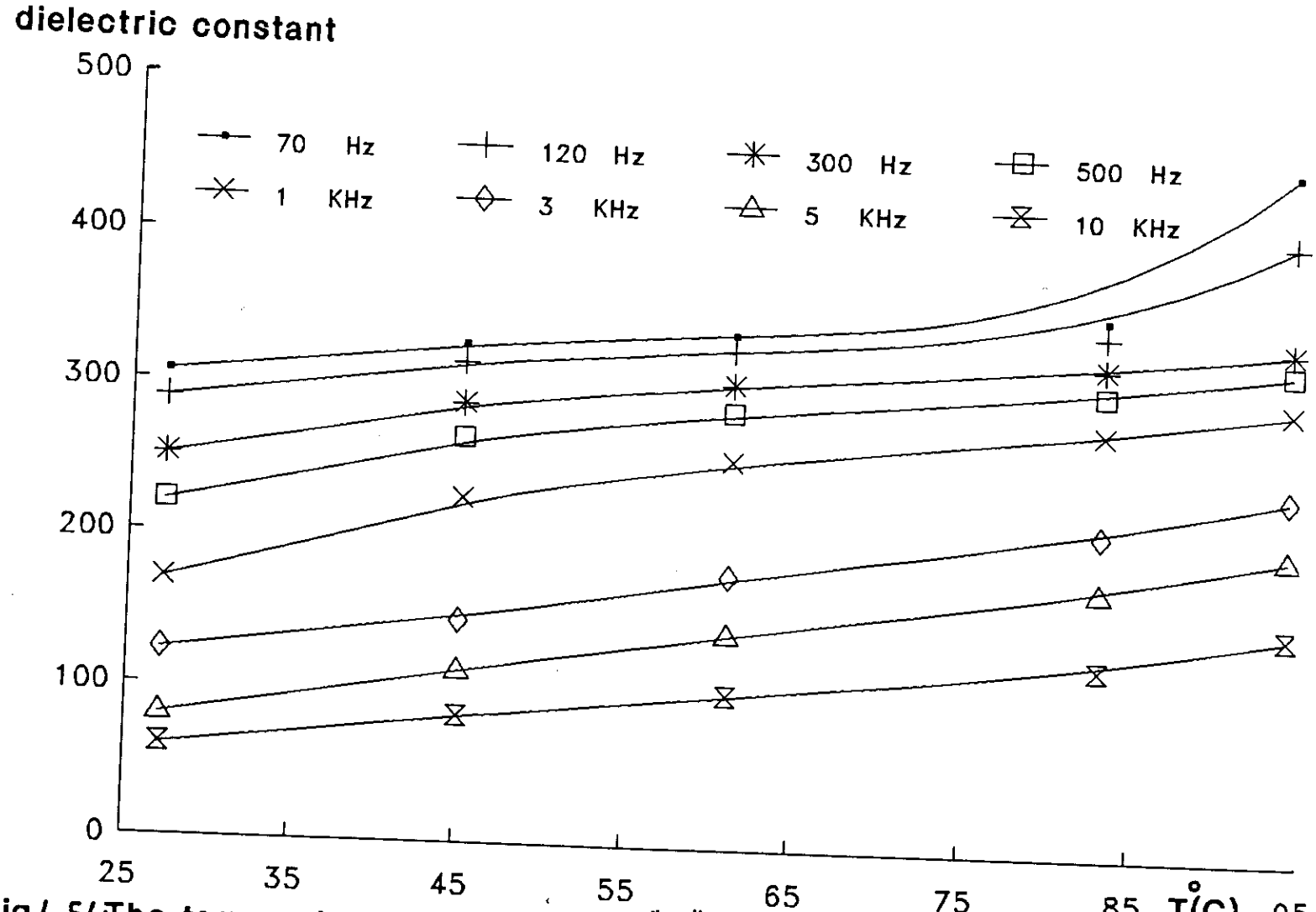

Fig.4.54:The temperature dependence of "ε" at different constant frequency for the sample $Se_{90}Ge_8In_2$ in the crystalline state at 150°C.

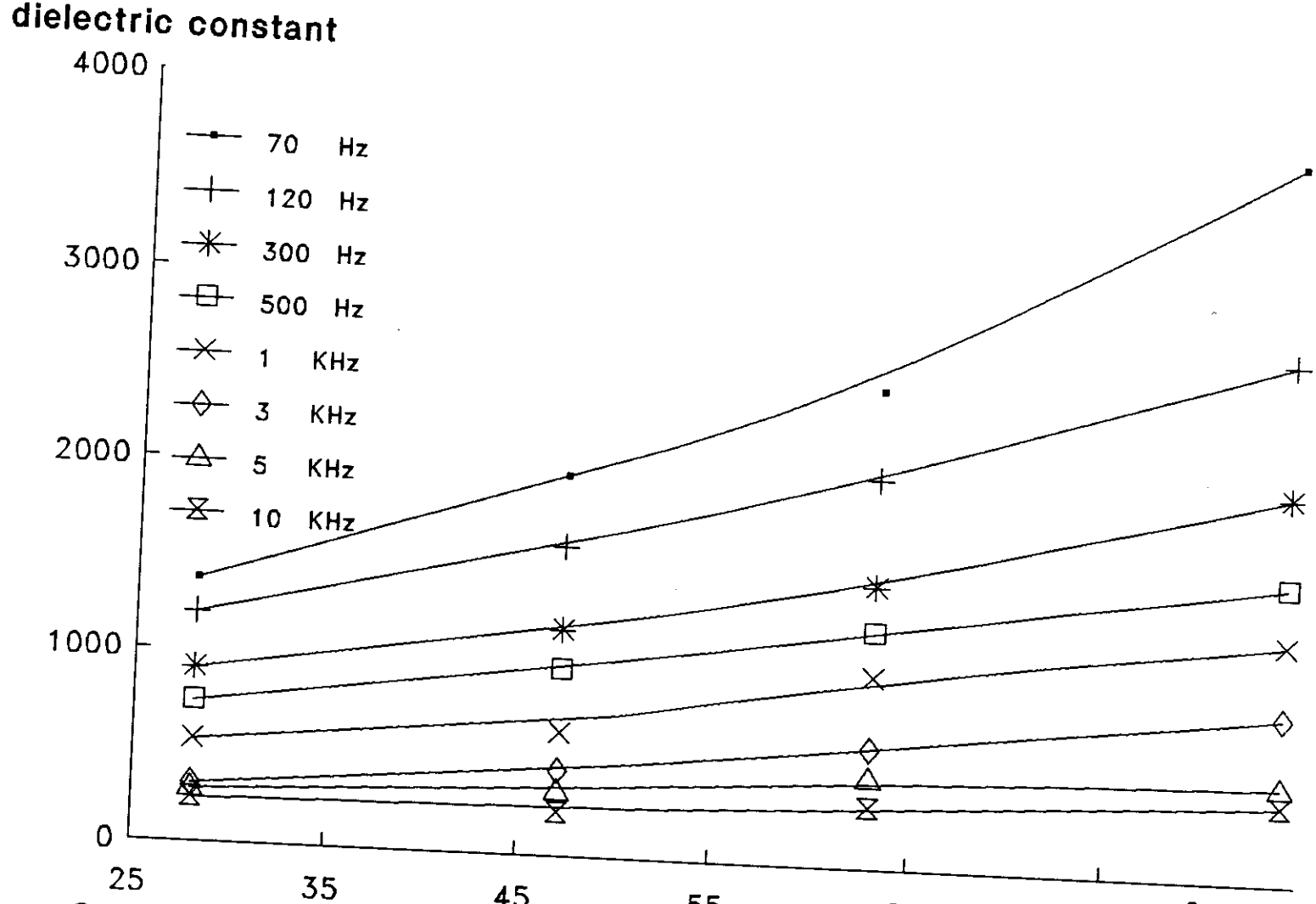

Fig.4.55: The temperature dependence of ε'' at different constant frequency for the sample $Se_{90}Ge_6In_4$ in the crystalline state at 120°C.

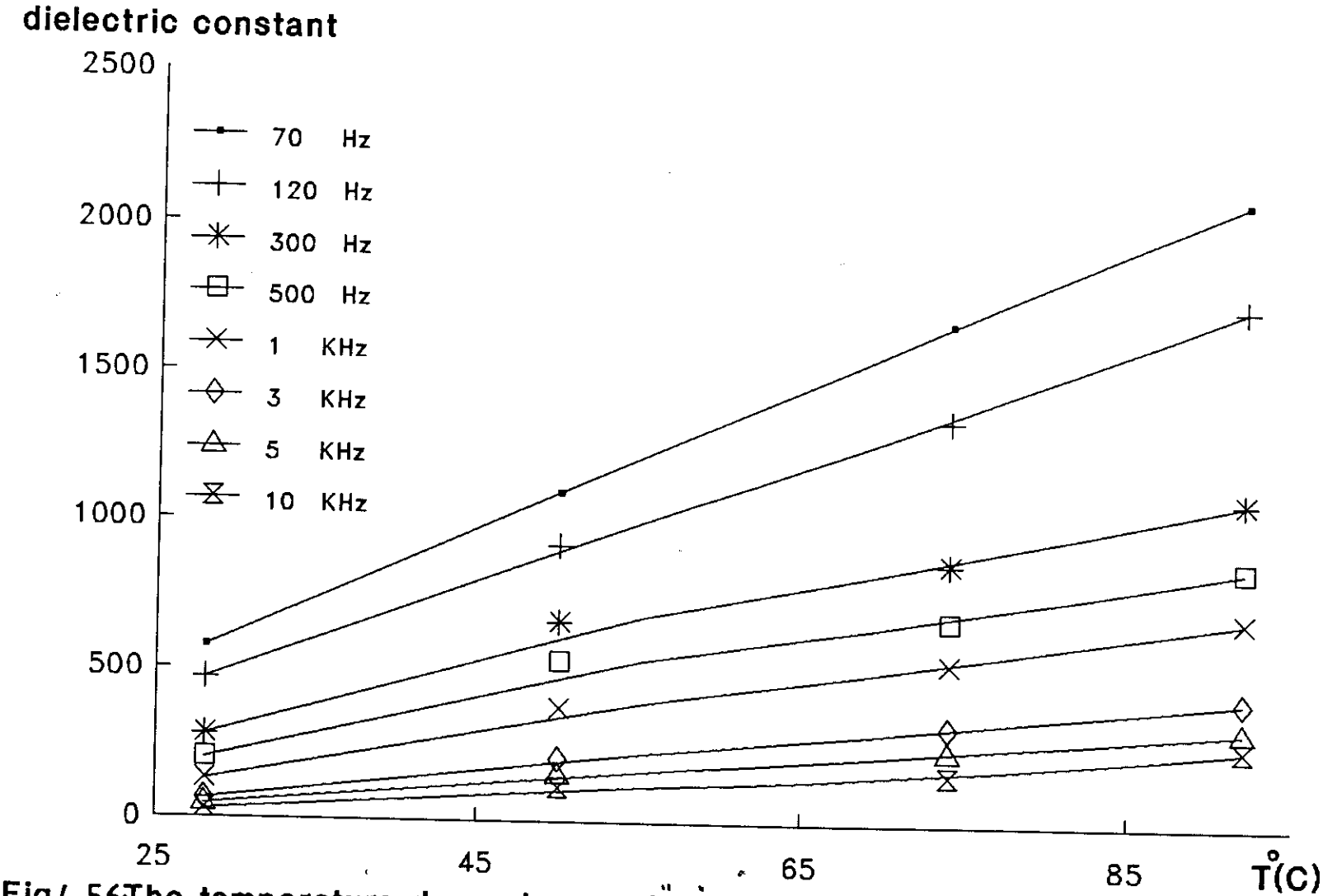

Fig.4.56:The temperature dependence of ε' at different constant frequency for the sample $Se_{90}Ge_6In_4$ in the crystalline state at 130°C.

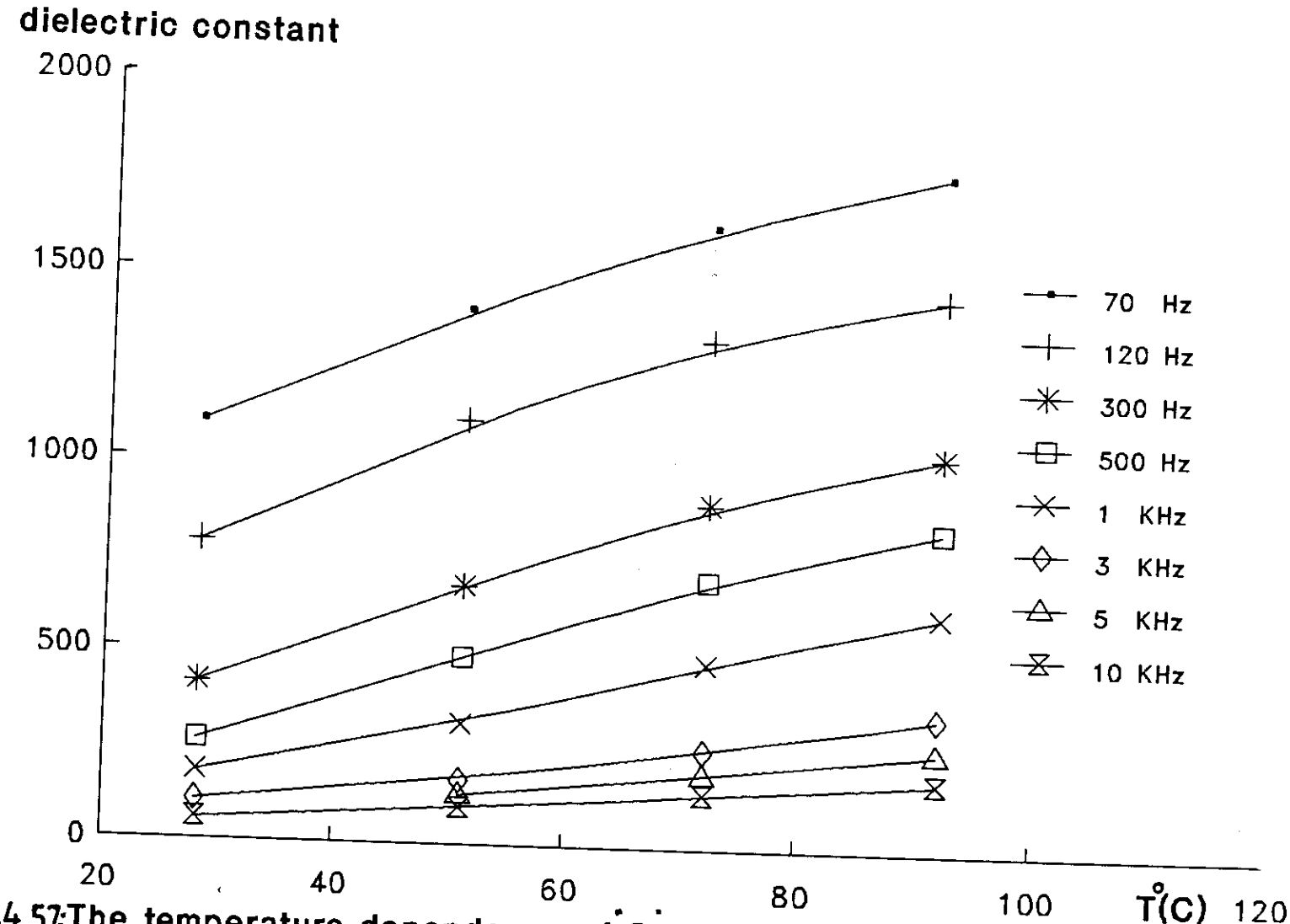

Fig.4.57:The temperature dependence of ε' at different constant frequency for the sample $Se_{90}Ge_6In_4$ in the crystalline state at 140°C.

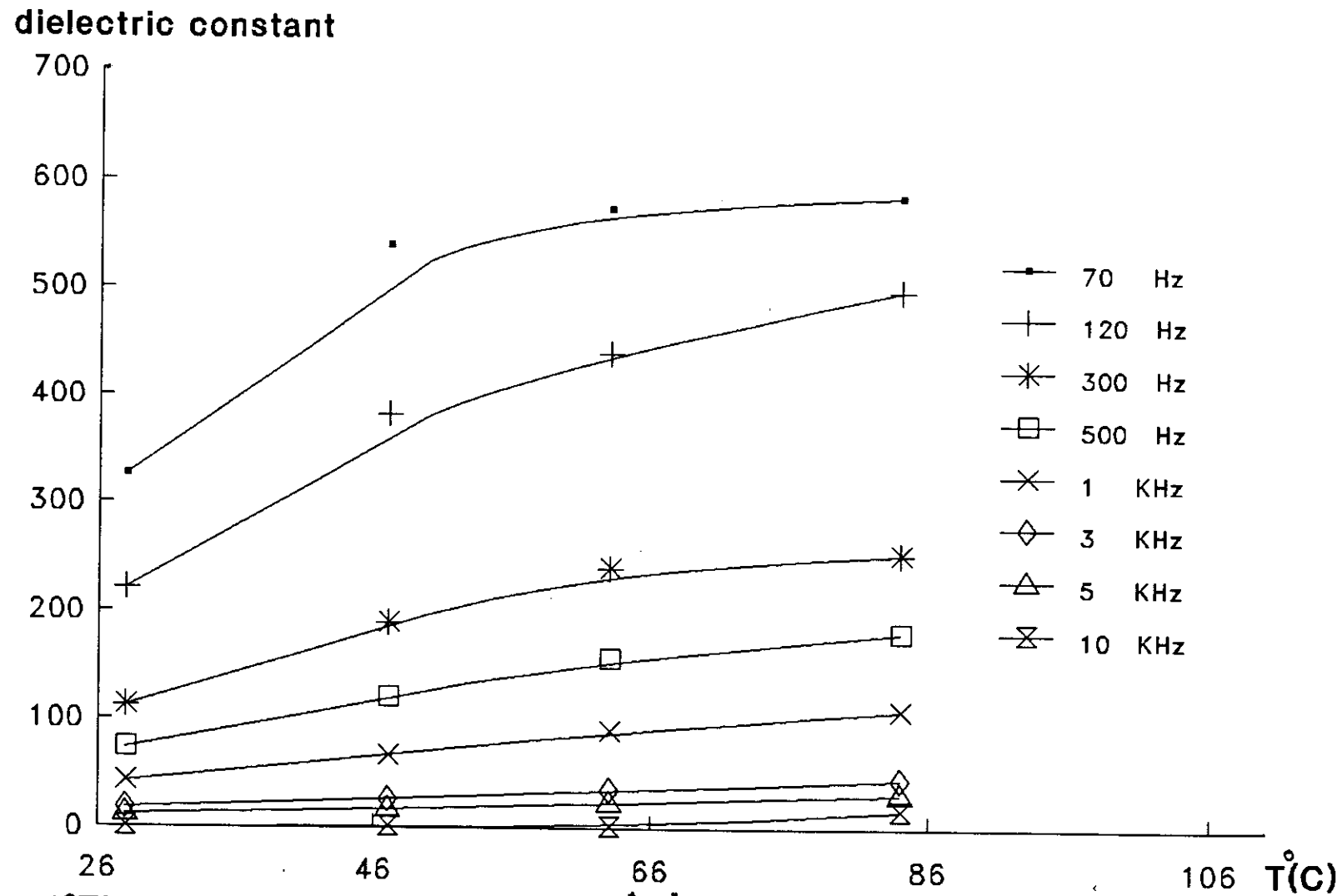

Fig.4.58:The temperature dependence of 'ε' at different constant frequency for the sample $Se_{90}Ge_6In_4$ in the crystalline state at 150°C.

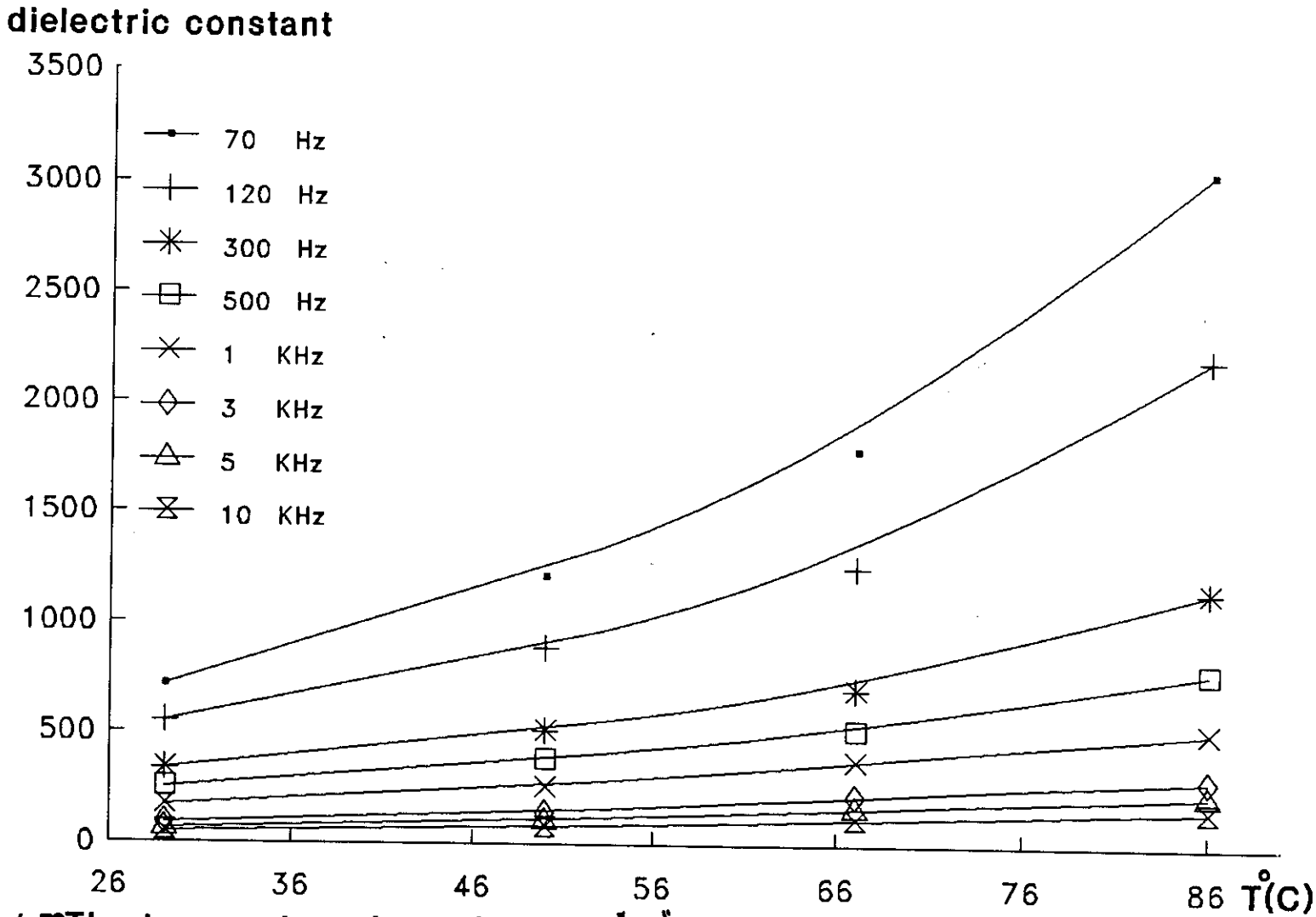

Fig.4.59: The temperature dependence of "ε" at different constant frequency for the sample $Se_{90}Ge_4In_6$ in the crystalline state at 120°C.

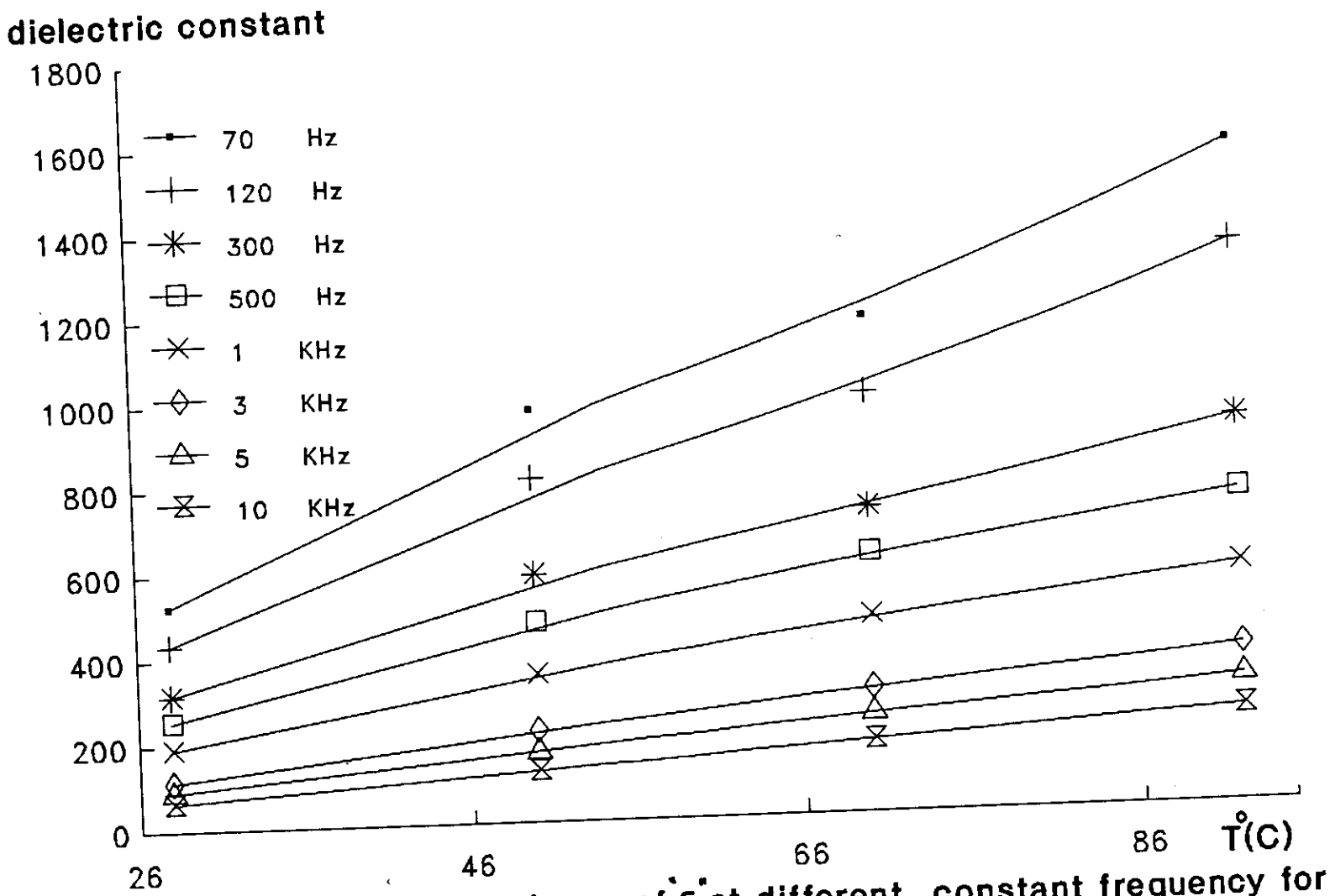

Fig.4.60: The temperature dependence of ε'' at different constant frequency for the sample $Se_{90}Ge_4In_6$ in the crystalline state at 130°C.

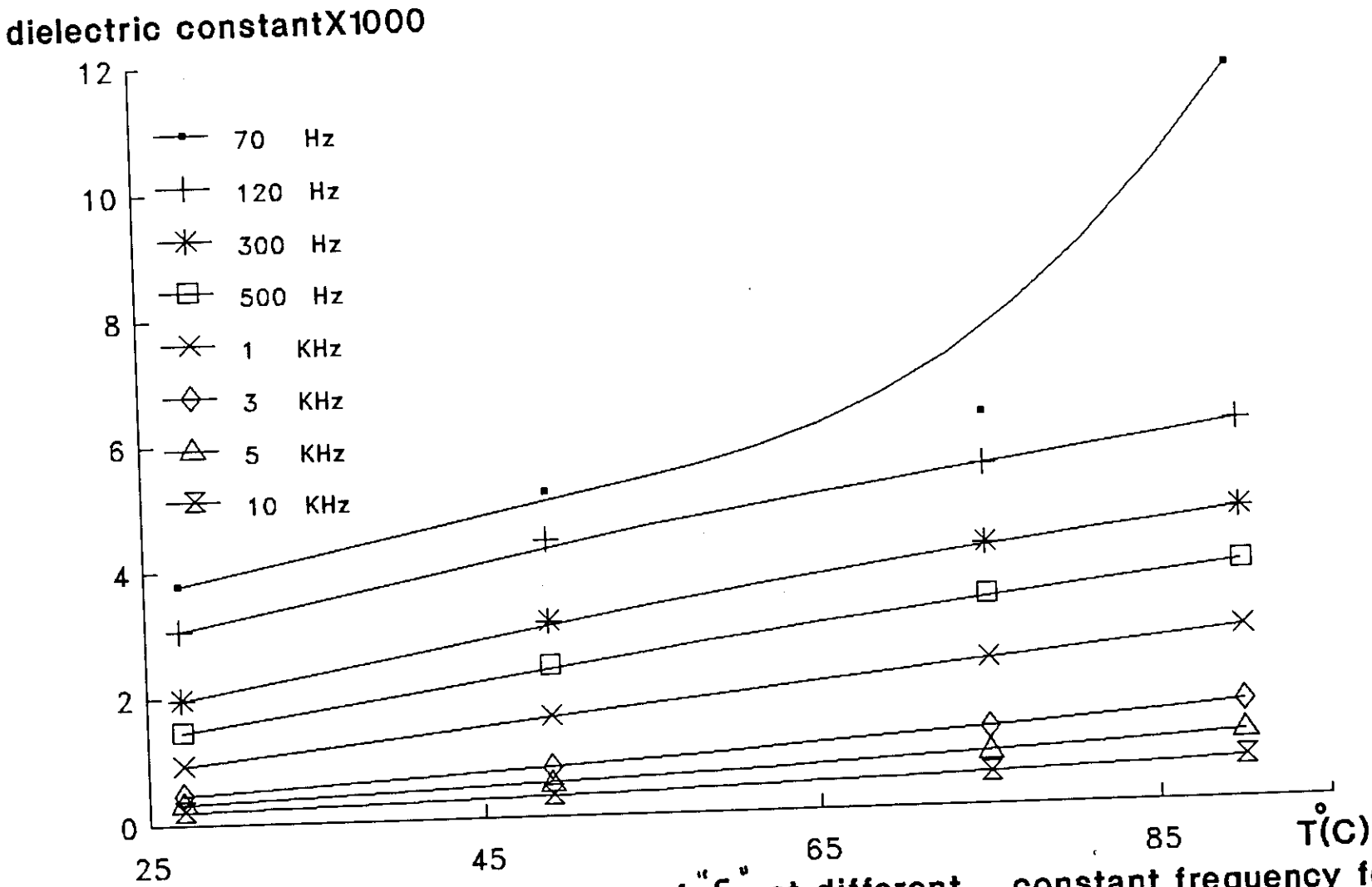

Fig.4.61:The temperature dependence of "ε" at different constant frequency for the sample $Se_{90}Ge_4In_6$ in the crystalline state at 140°C.

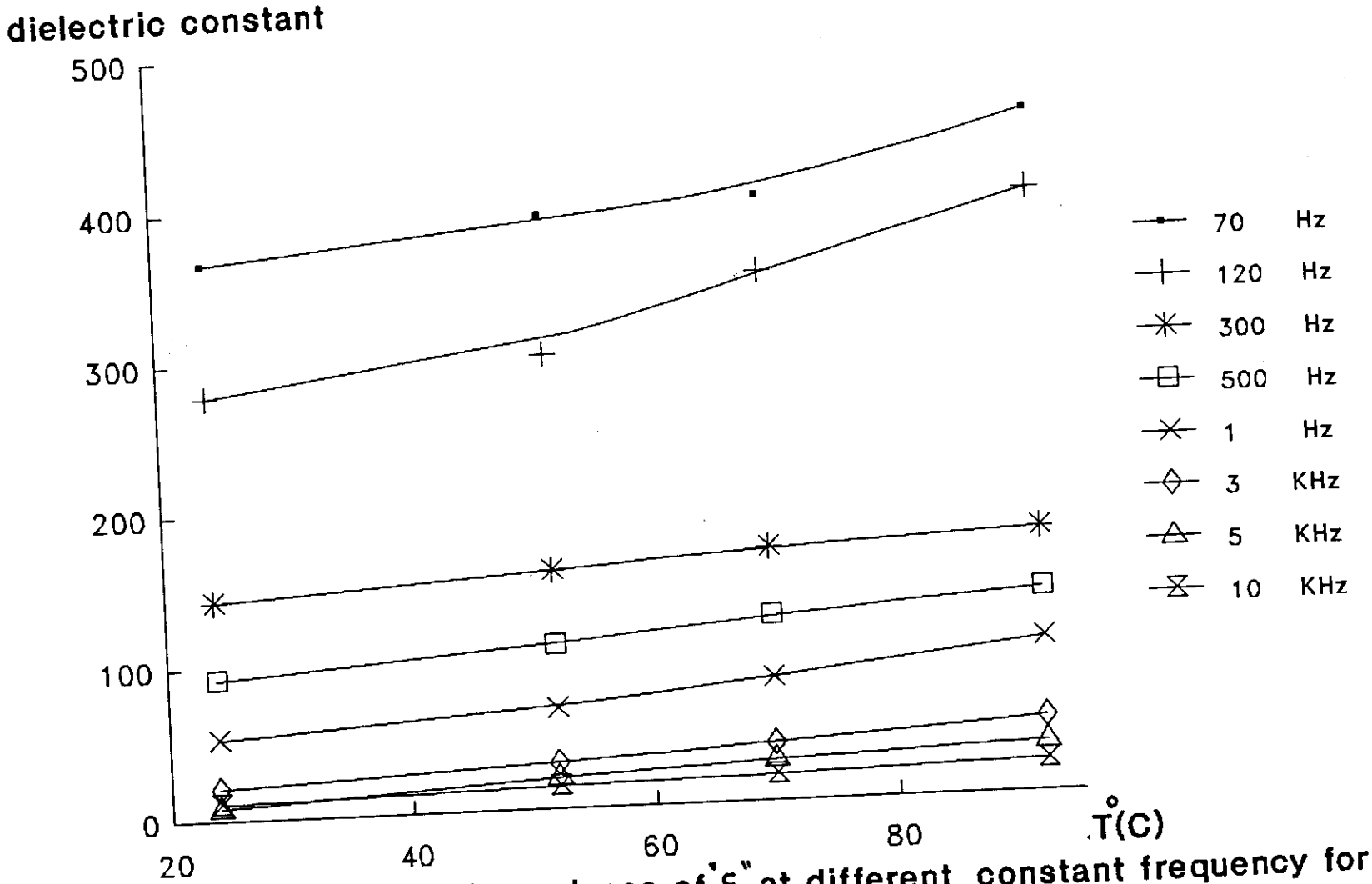

Fig.4.62:The temperature dependence of "ε" at different constant frequency for the sample $Se_{90}Ge_4In_6$ in the crystalline state at 150°C.

The total polarization in a solid can be regarded as made up of electronic, ionic and orientational contributions[112].

In chalcogenides there appear to be a fourth effect at low frequencies which might be called, migrational. Consequently this part of polarization is due to actual migration of an ion under the electric field. The ion may only move one interstice,or at low enough frequencies it may make many jumps. Since, for rising temperature the lattice relaxes,more thermal motion appears in the network and the ions can move more easily. Consequently, ε should increase with an increase in temperature. Also,a decrease in frequency should show an increase in ε since the migrational motions require relatively long times to be effective.

4.2.5.THE EFFECT OF FREQUENCY ON THE DIELECTRIC CONSTANT OF $Se_{90}Ge_{10-x}In_x$ IN THE CRYSTALLINE STATE:-

The results of the dielectric constant of four parts of the sample $Se_{90}Ge_8In_2$ as a function of frequency crystallized at 120,130,140 and 150^{0}C were illustrated in figs.(4.63-4.66). These records were traced at different constant values of frequency for each part.

These curves, show that as the frequency increases, the dielectric constant decreases. At low frequency the dielectric constant values were high and decreases firstly by high rate. The rate of decrement become slow as the frequency increases.

The same behaviour was recorded for the samples $Se_{90}Ge_6In_4$ and $Se_{90}Ge_4In_6$,figs.(4.67-4.74).This behaviour may be explained as :

The polarization of the materials depends on the ability of the fundamental particles to move to each other. At high frequencies the more massive molecular particles can not rotate rapidly enough to contribute to the polarization and remain ,on the average, at 90^o to the field direction. If the temperature is held constant and the frequency is increased, then the dielectric constant decreases towards ε_∞ as shown in figs.(4.63-4.74).

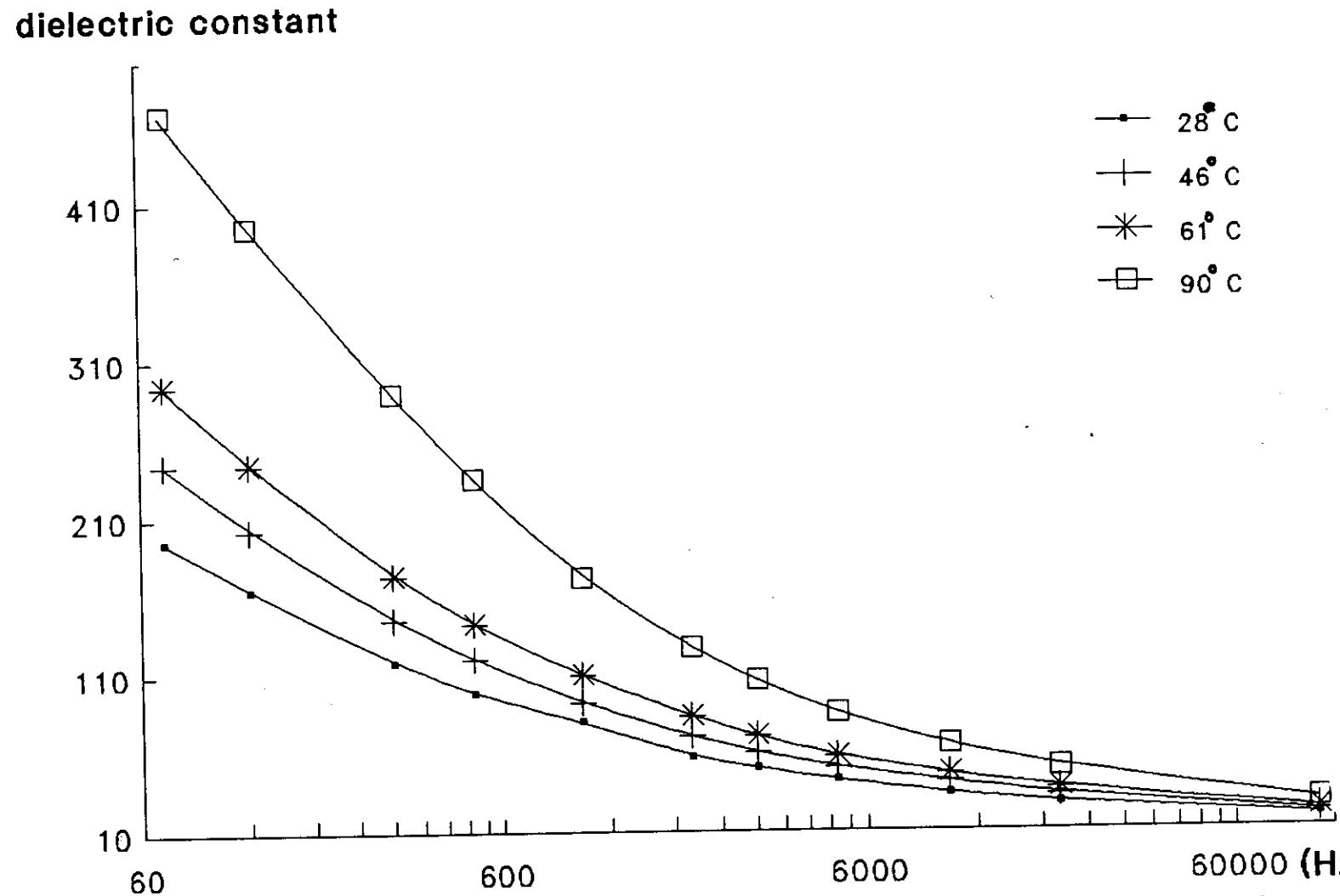

Fig.4.63:Shows the frequency dependence of the dielectric constant at various constant temperatures for the sample $Se_{90}Ge_8In_2$ in the crystalline state at 120°C.

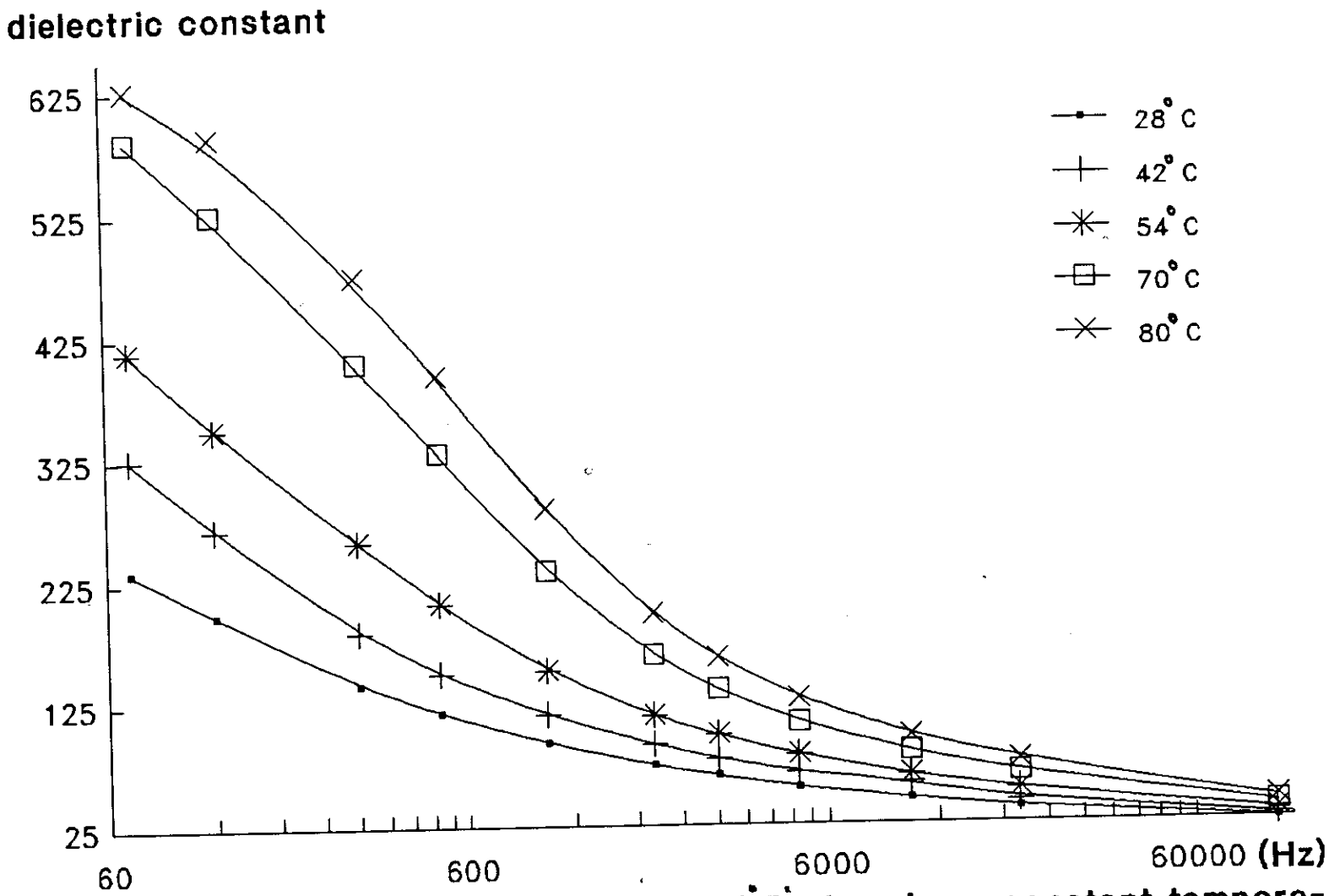

Fig.4.64:Shows the frequency dependence of ε' at various constant temperatures for the sample $Se_{90}Ge_8In_2$ in the crystalline state at 130°C.

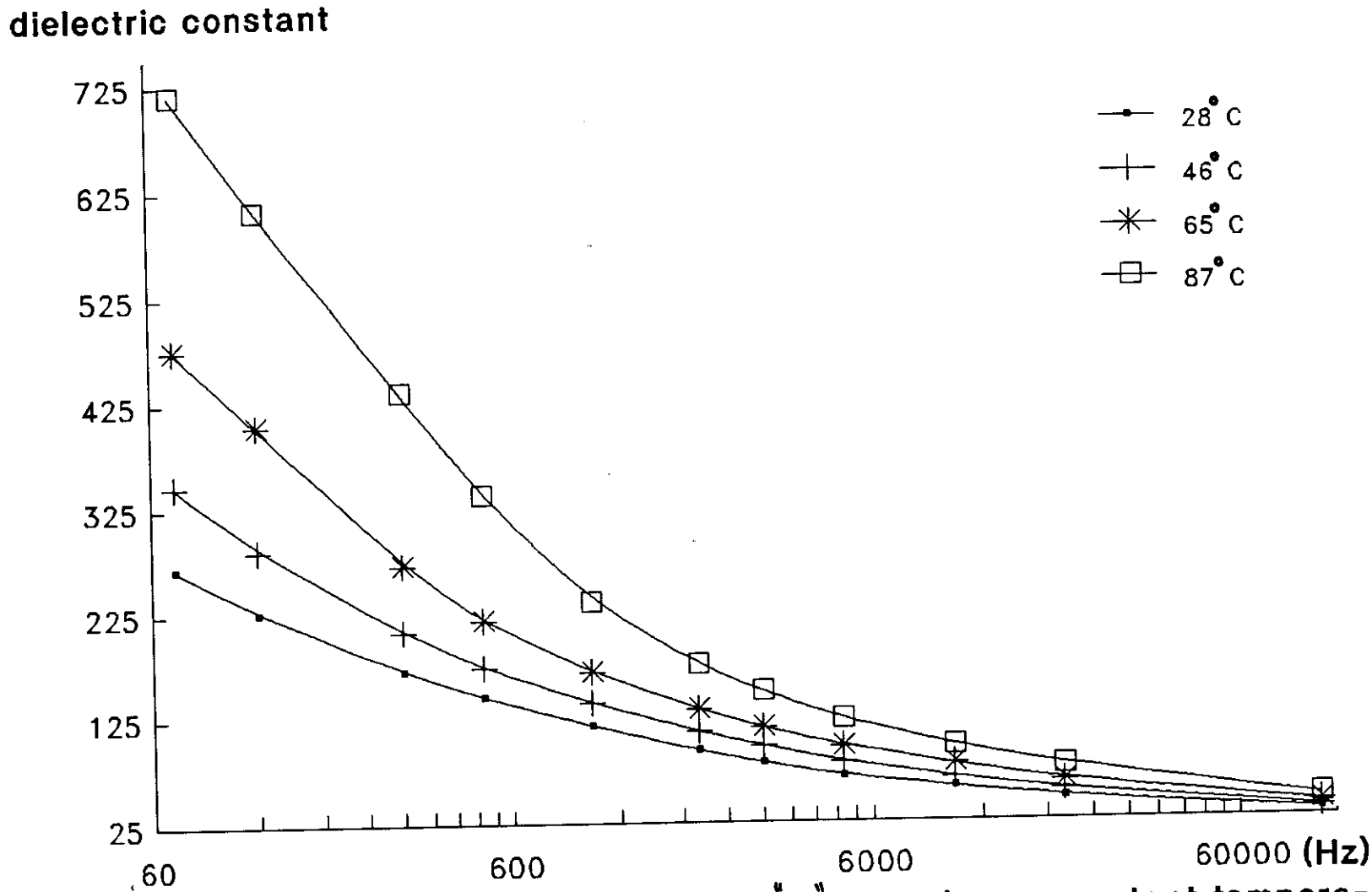

Fig.4.65: Shows the frequency dependence of "ε" at various constant temperatures for the sample $Se_{90}Ge_8In_2$ in the crystalline state at 140°C.

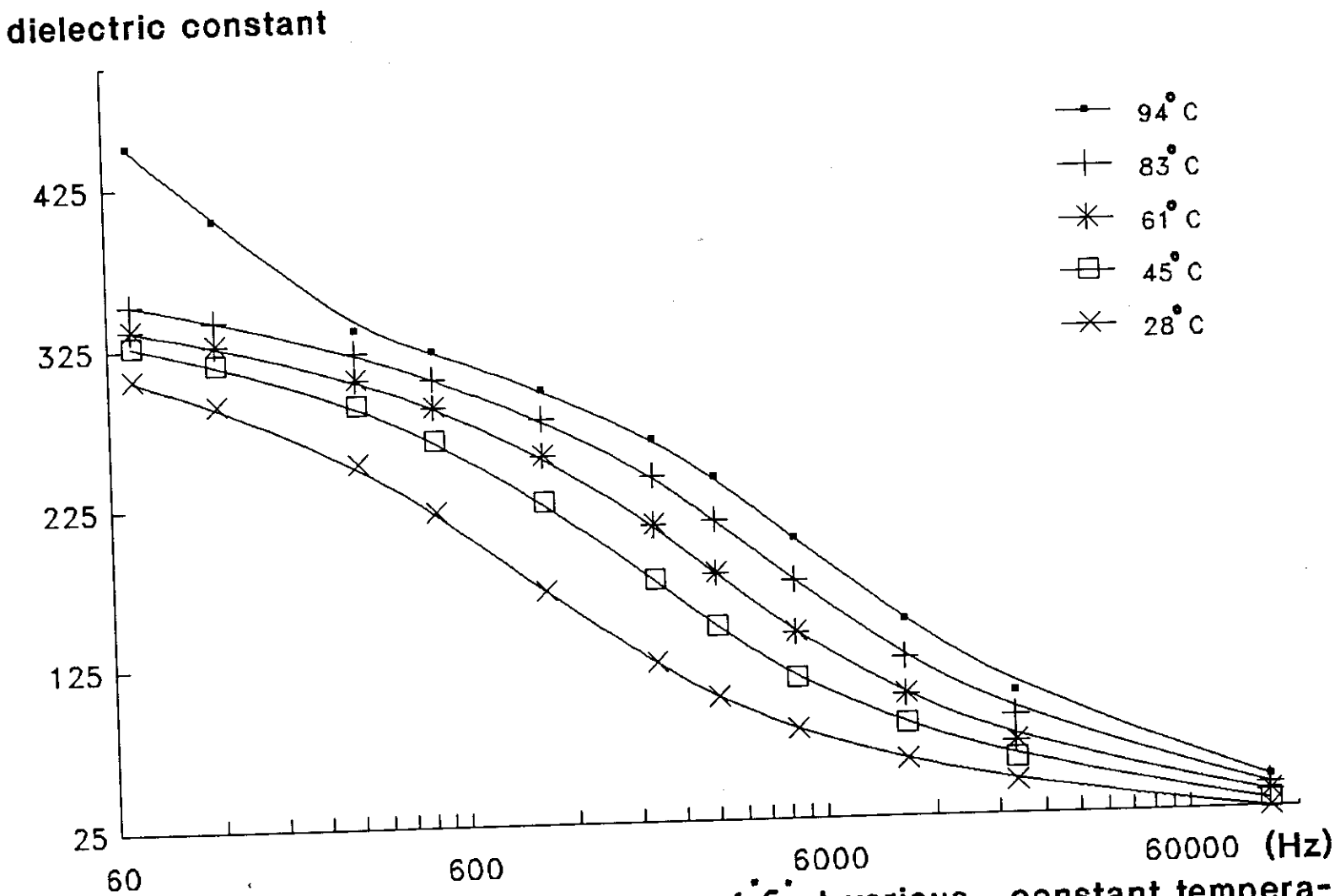

Fig 4.66 Shows the frequency dependence of ε' at various constant temperatures for the sample $Se_{90}Ge_8In_2$ in the crystalline state at 150° C.

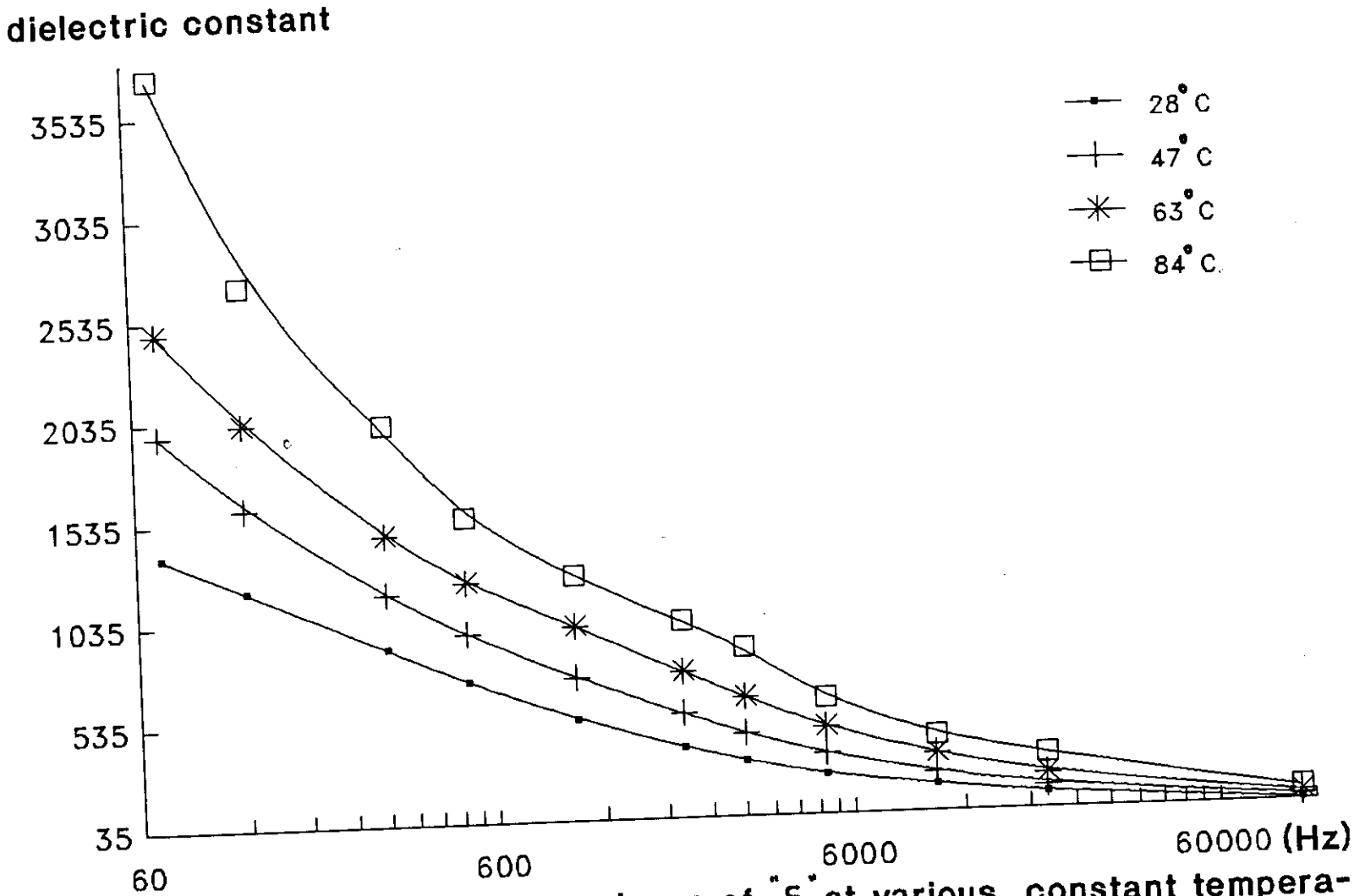

Fig.4.67:Shows the frequency dependence of "ε" at various constant temperatures for the sample $Se_{90}Ge_6In_4$ in the crystalline state at 120°C.

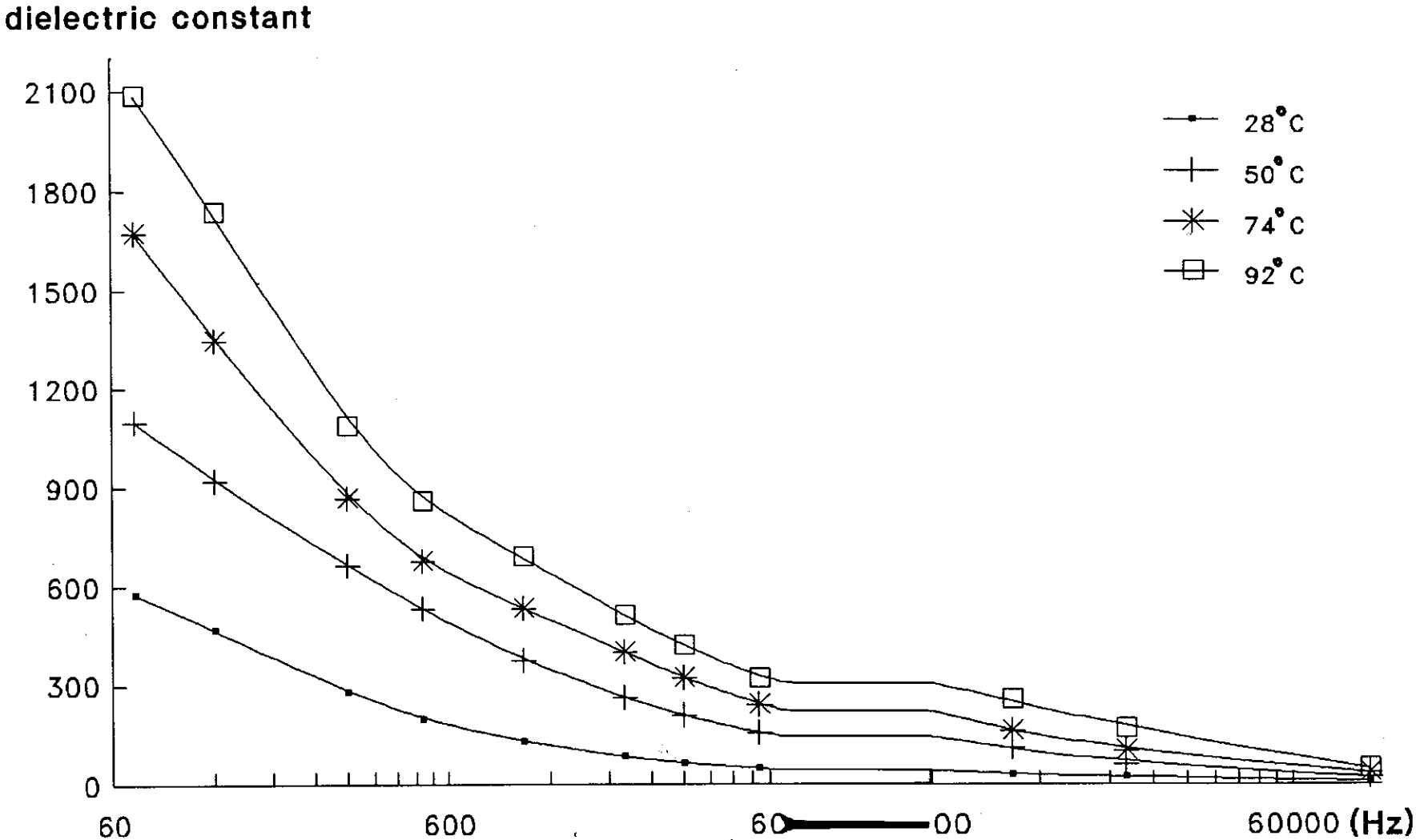

Fig.4.68. Shows the frequency dependence of "ε" at various constant temperatures for the sample $Se_{90}Ge_6In_4$ in the crystalline state at 130°C.

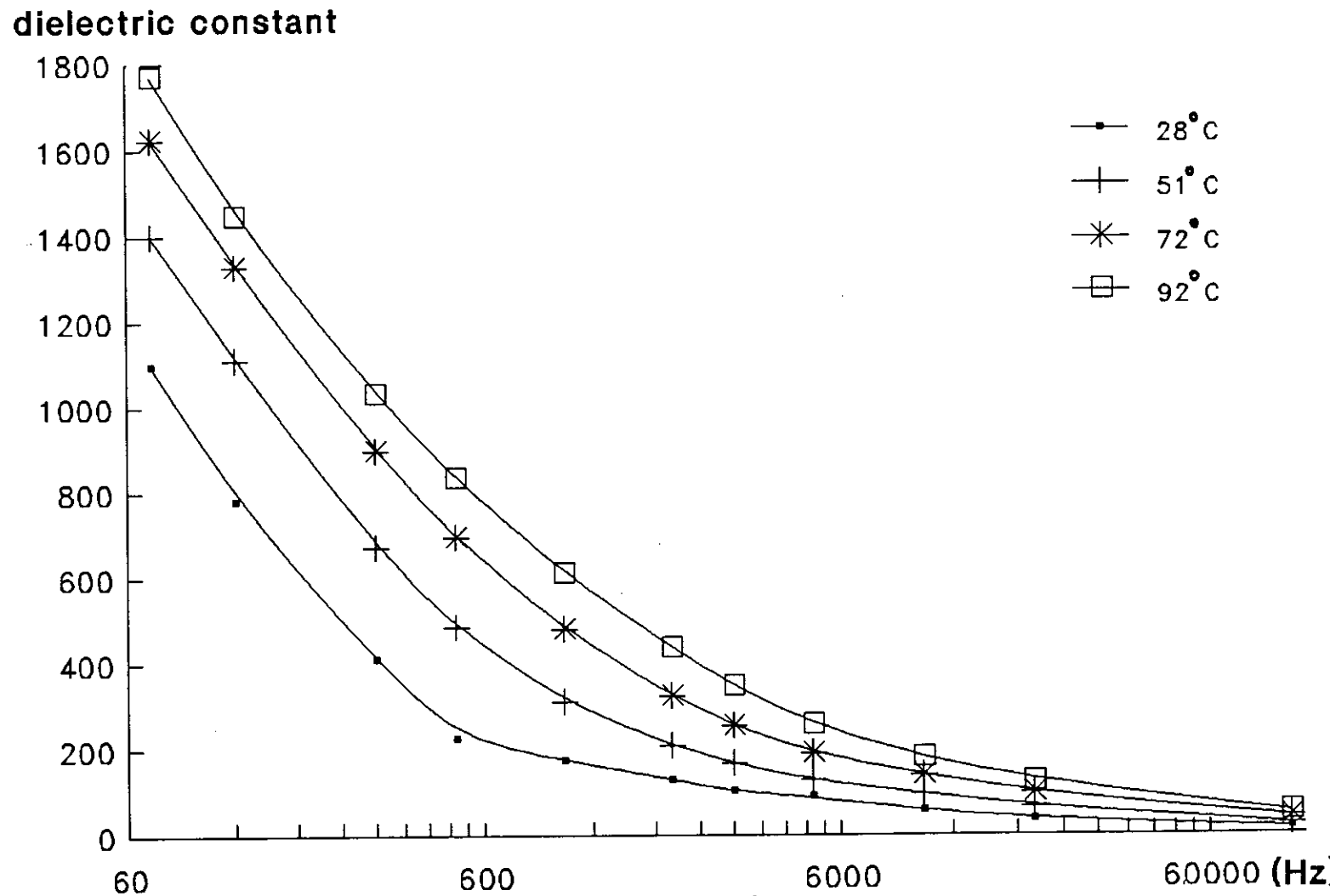

Fig.4.69:Shows the frequency dependence of ε'' at various constant temperatures for the sample $Se_{90}Ge_6In_4$ in the crystalline state at 140°C.

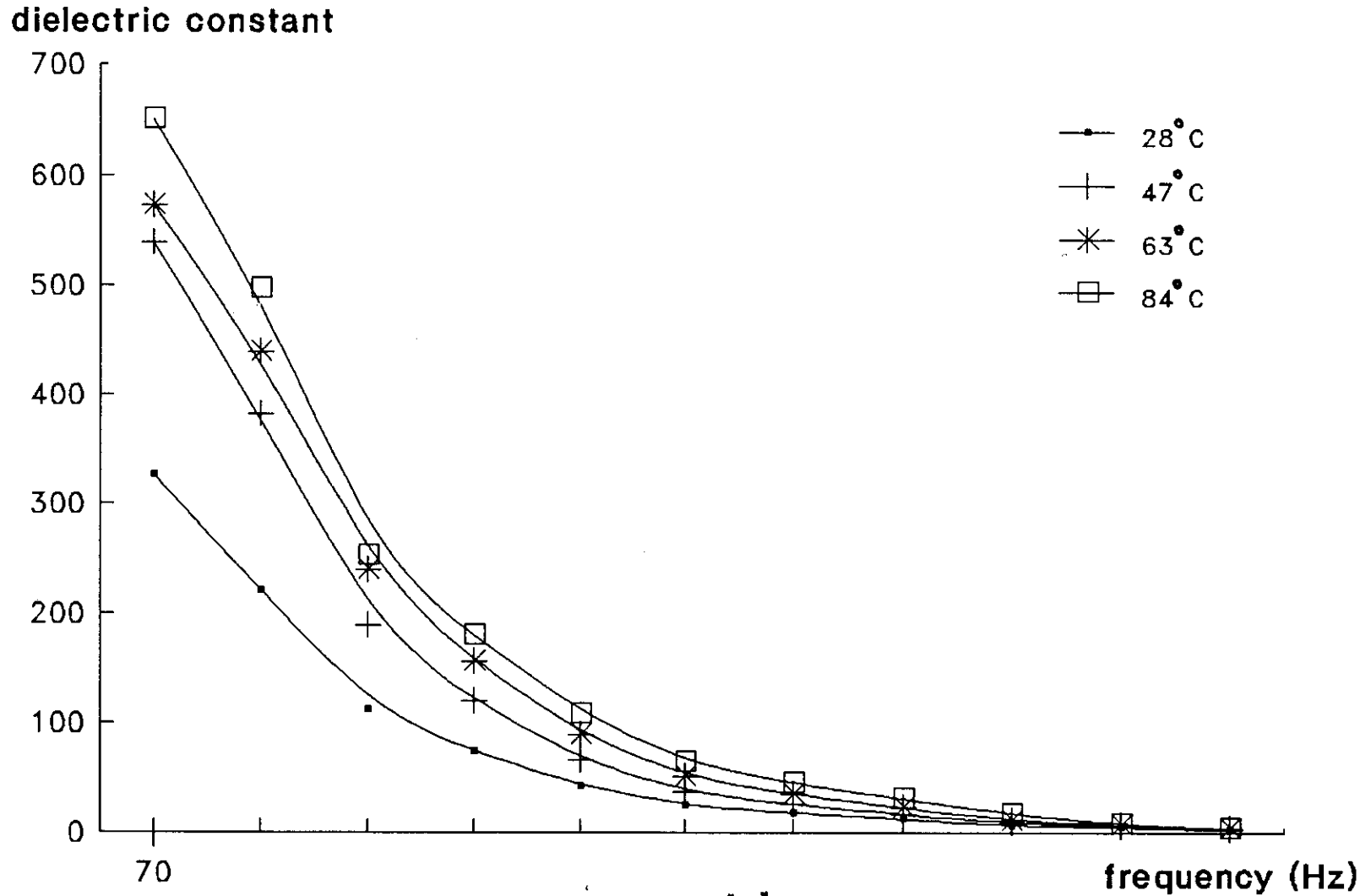

Fig.4.70:Shows the frequency dependence of "ε" at various constant temperatures for the sample $Se_{90}Ge_6In_4$ in the crystalline state.at 150°C.

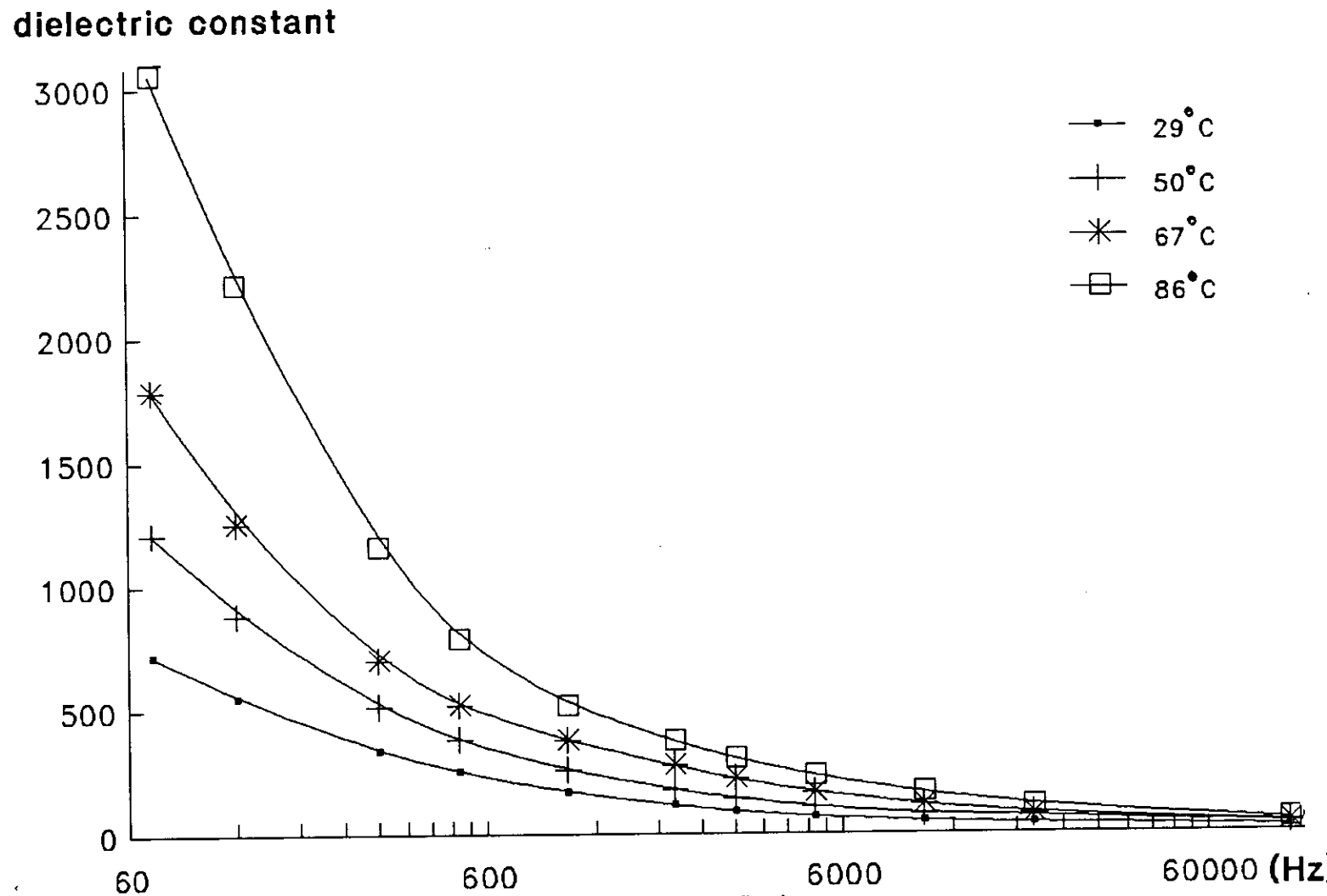

Fig.4.7 Shows the frequency dependence of "ε" at various constant temperatures for the sample $Se_{90}Ge_4In_6$ in the crystalline state at 120°C.

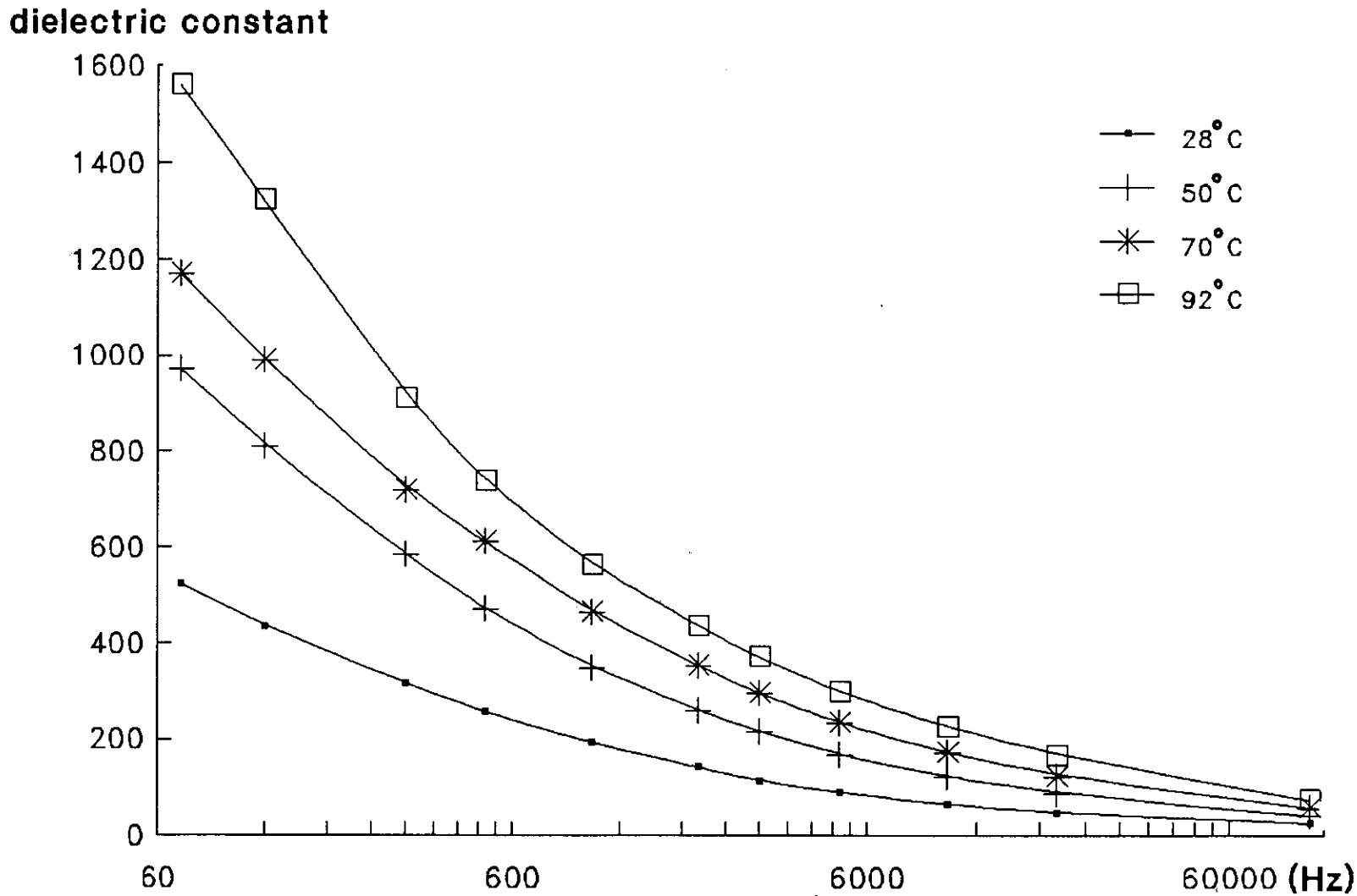

Fig.4.72:Shows the frequency dependence of "ε" at various constant temperatures for the sample $Se_{90}Ge_4In_6$ in the crystalline state at 130°C.

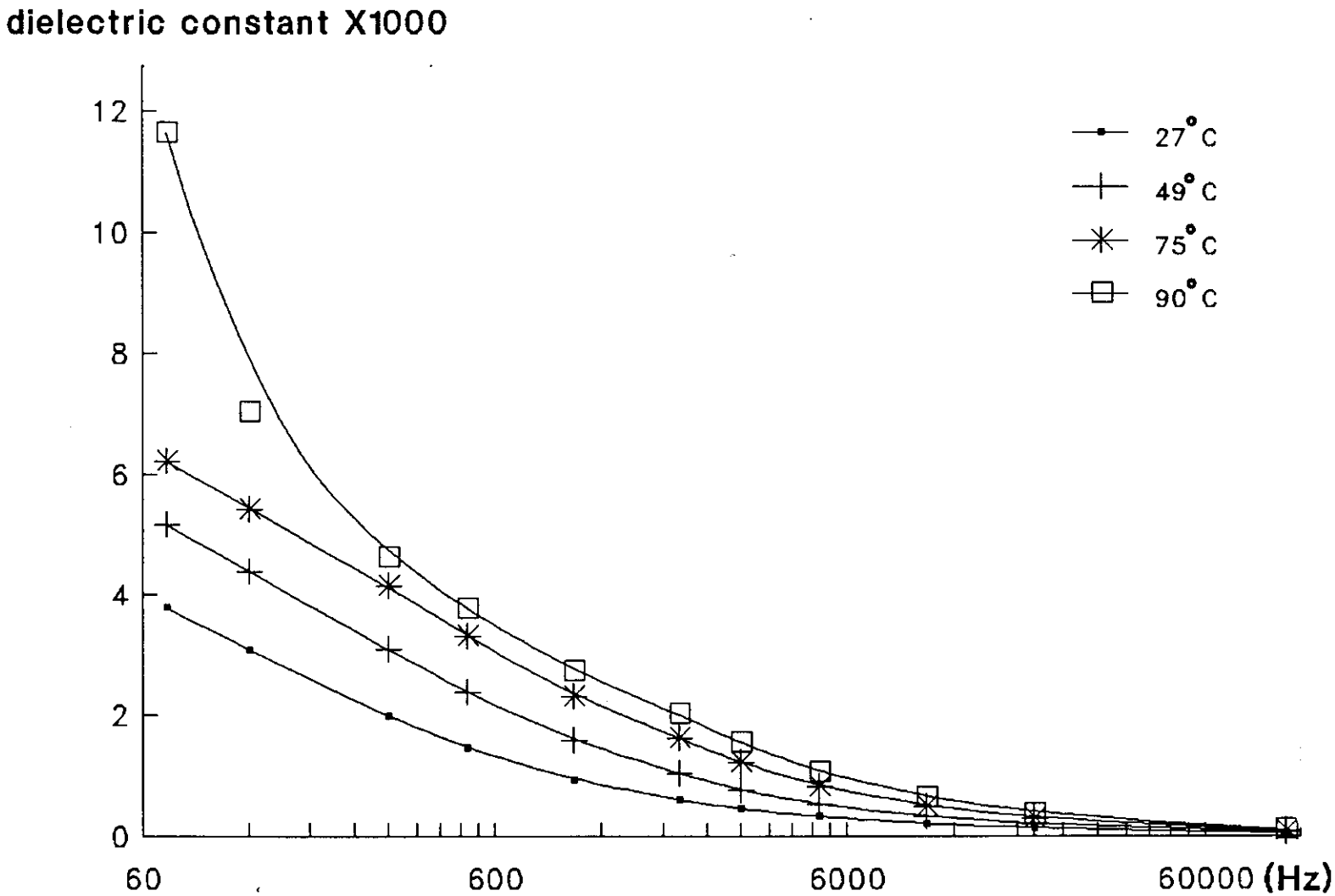

Fig.4.73 Shows the frequency dependence of "ε" at various constant temperatures for the sample $Se_{90} Ge_4 In_6$ in the crystalline state at 140°C.

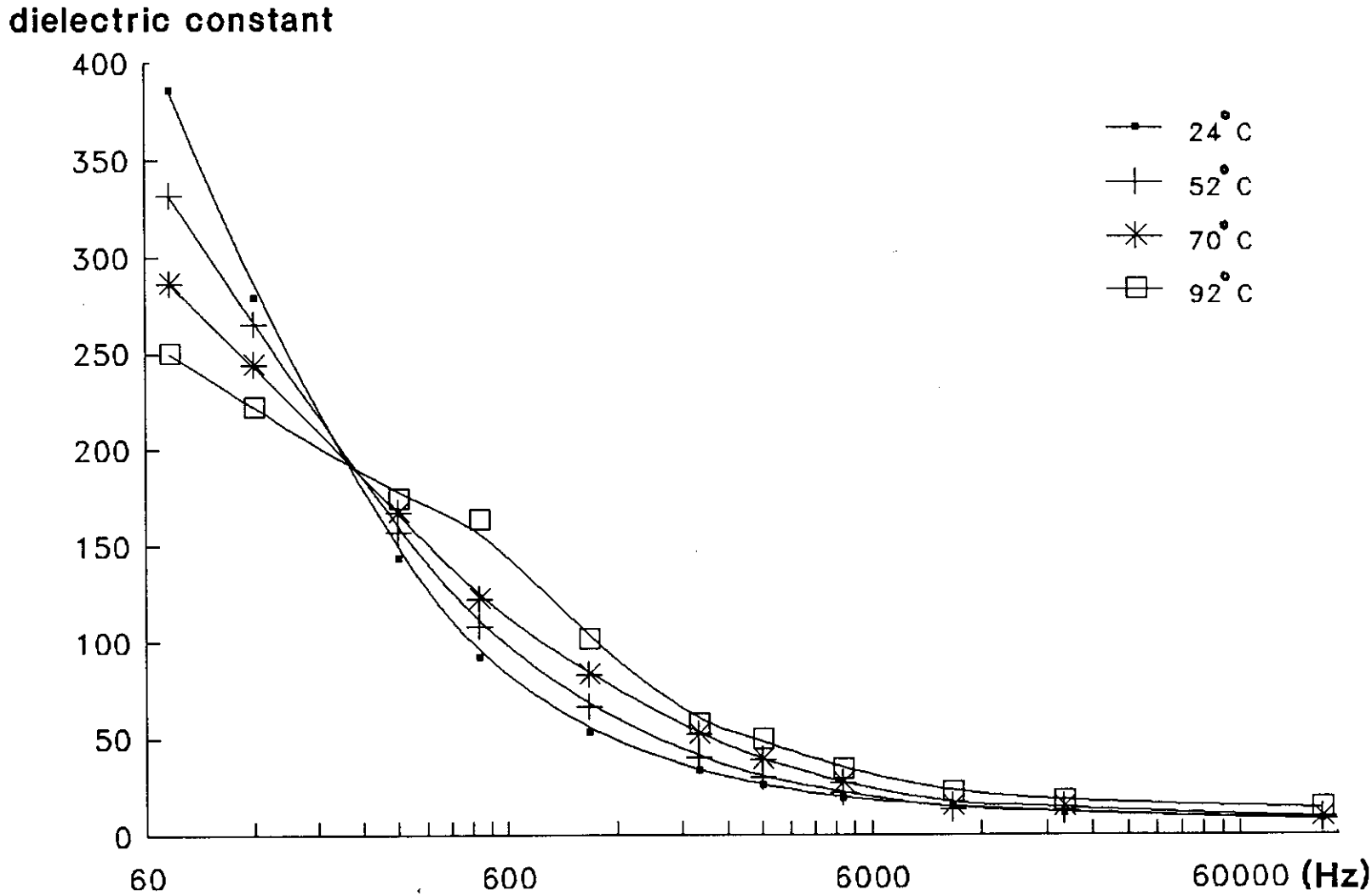

Fig.4.74 :Shows the frequency dependence of "ε" at various constant temperatures for the sample $Se_{90}Ge_4In_6$ in the crystalline state at 150° C.

4.2.6.THE EFFECT OF FREQUENCY ON THE DIELECTRIC LOSS TANGENT OF $Se_{90}Ge_{10-x}In_x$ IN THE CRYSTALLINE STATE :-

The dielectric loss tangent (tan δ)has been recorded as a function of frequency at different isotherms for the sample Se_{90} Ge_8 In_2.

The results have been recorded after complete crystallization on four parts of this sample at 120, 130, 140 and 150^{0}C , Figs.(4.75-4.78). From these figures it is clear that tan(δ)decreases as frequency increases. The rate of decrement at low frequency is faster than at high frequency . This experiment has been repeated for the two samples Se_{90} Ge_6 In $_4$ and Se_{90} Ge_4 In_6 after complete crystallization at the same crystallization temperatures. as shown in figs. (4.79-4.82)and (4.83-4.86) respectively.

The decrease in tan(δ) as the applied frequency increases may be attributed to that,at low frequency the conduction loss appears and leads to a migration and reordering of atoms over large distances. This motion require more energy to complete, which tends gradually to decrease as the frequency increases The applied field tend to supply the sample with the required energy. Anomalous behaviour to that mentioned above has been obtained as shown in figs.(4.76,78,85). This behaviour can be explained as follow:

The dielectric loss tangent undergoes dielectric loss minima

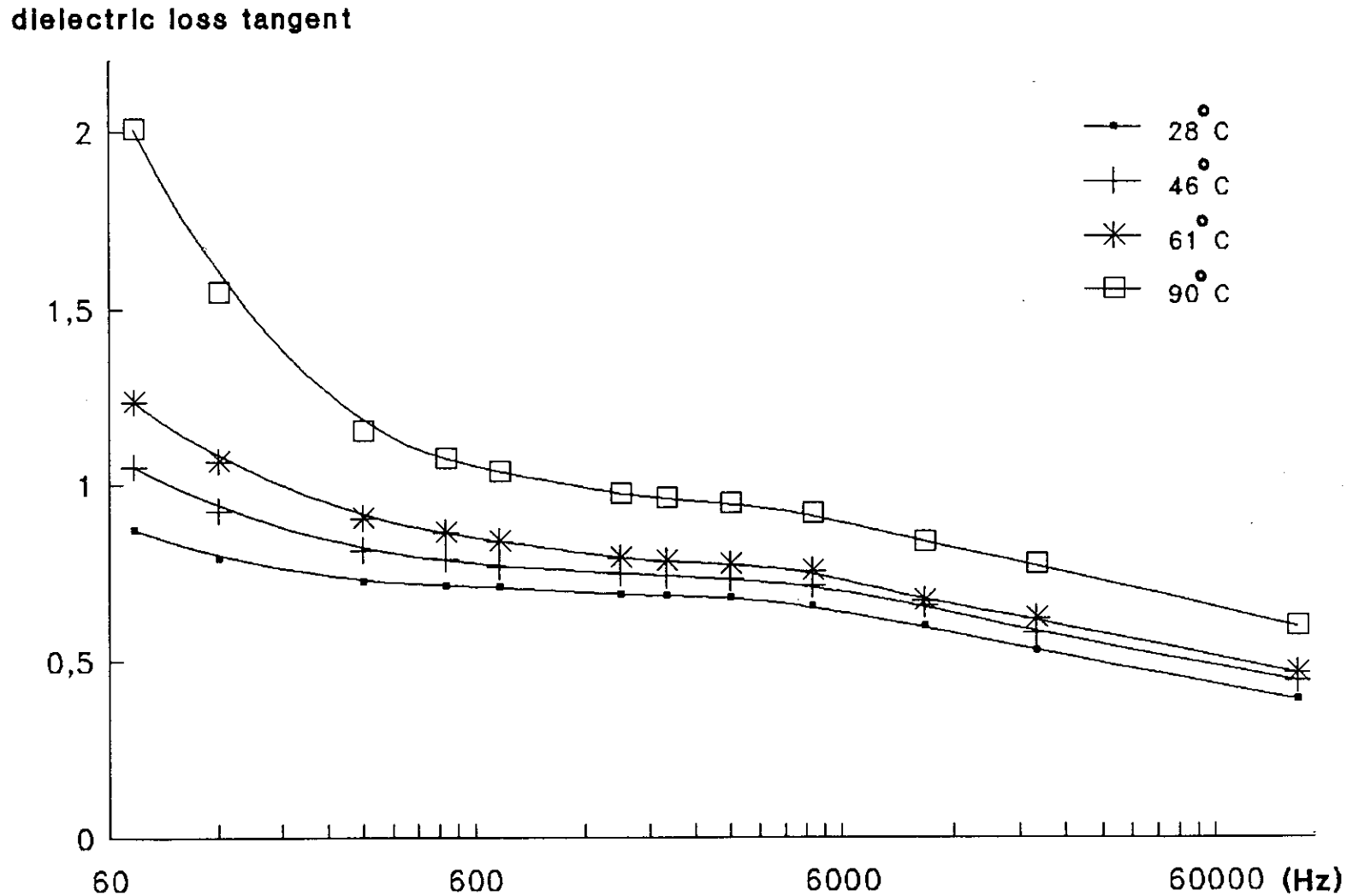

Fig.4.75. Shows the frequency dependence of tan(δ) at various constant temperatures for the sample $Se_{90}Ge_8In_2$ in the crystalline state at 120°C.

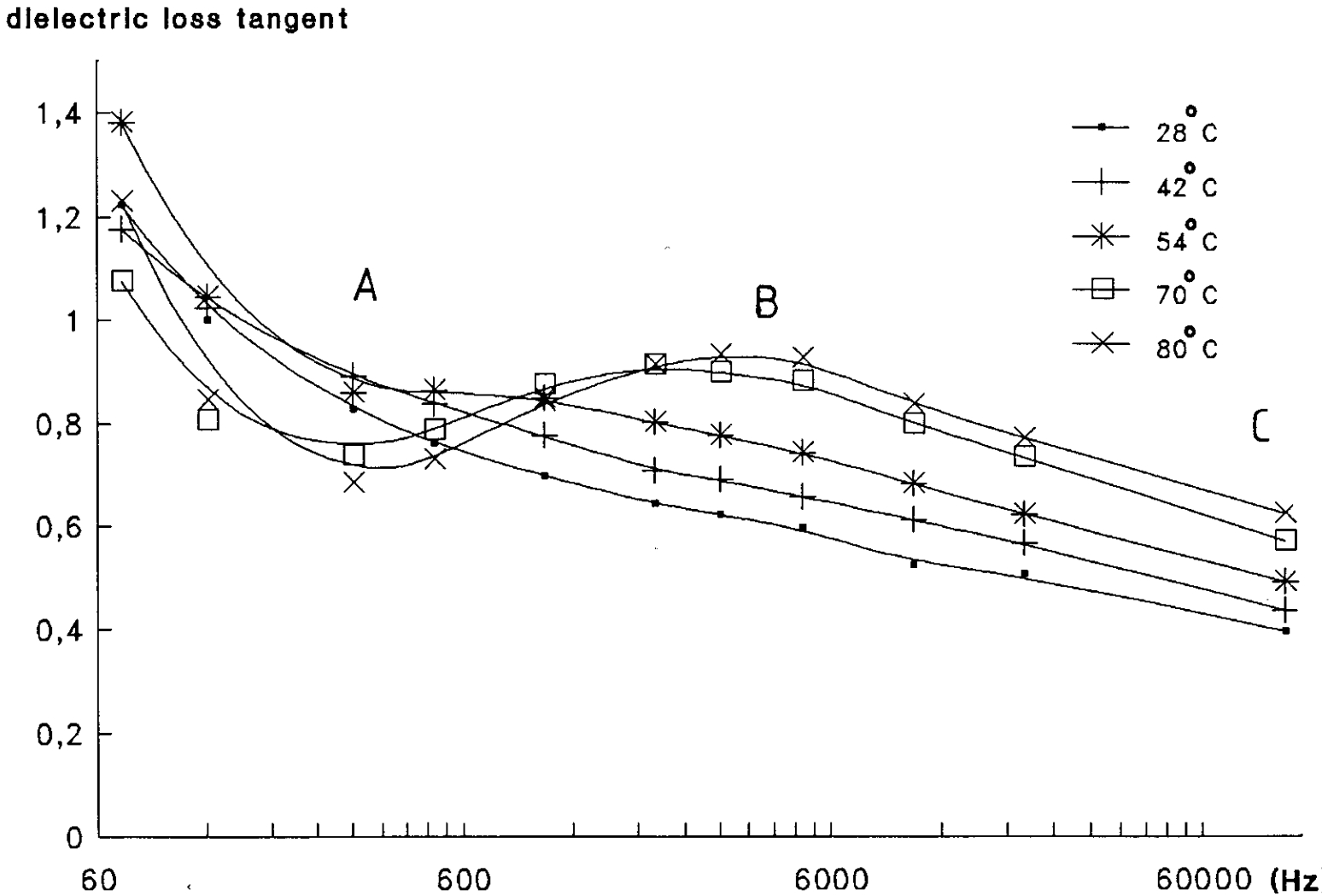

Fig 4.76: Shows the frequency dependence of tan(δ) at various constant temperatures for the sample $Se_{90}Ge_8In_2$ in the crystalline state at 130° C.

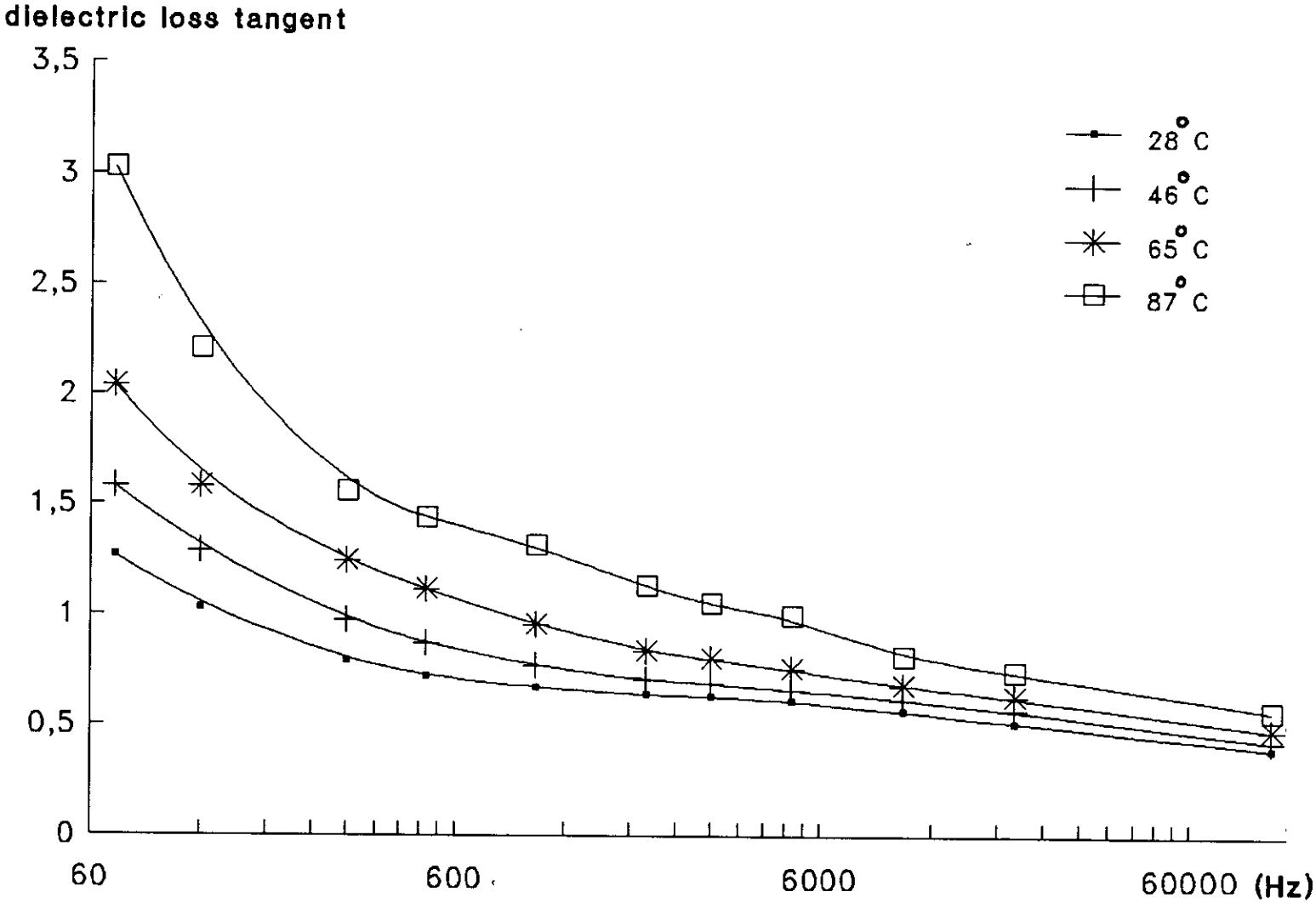

Fig.4.7: Shows the frequency dependence of tan(δ) at various constant temperatures for the sample $Se_{90}Ge_8In_2$ in the crystalline stat at 140°C.

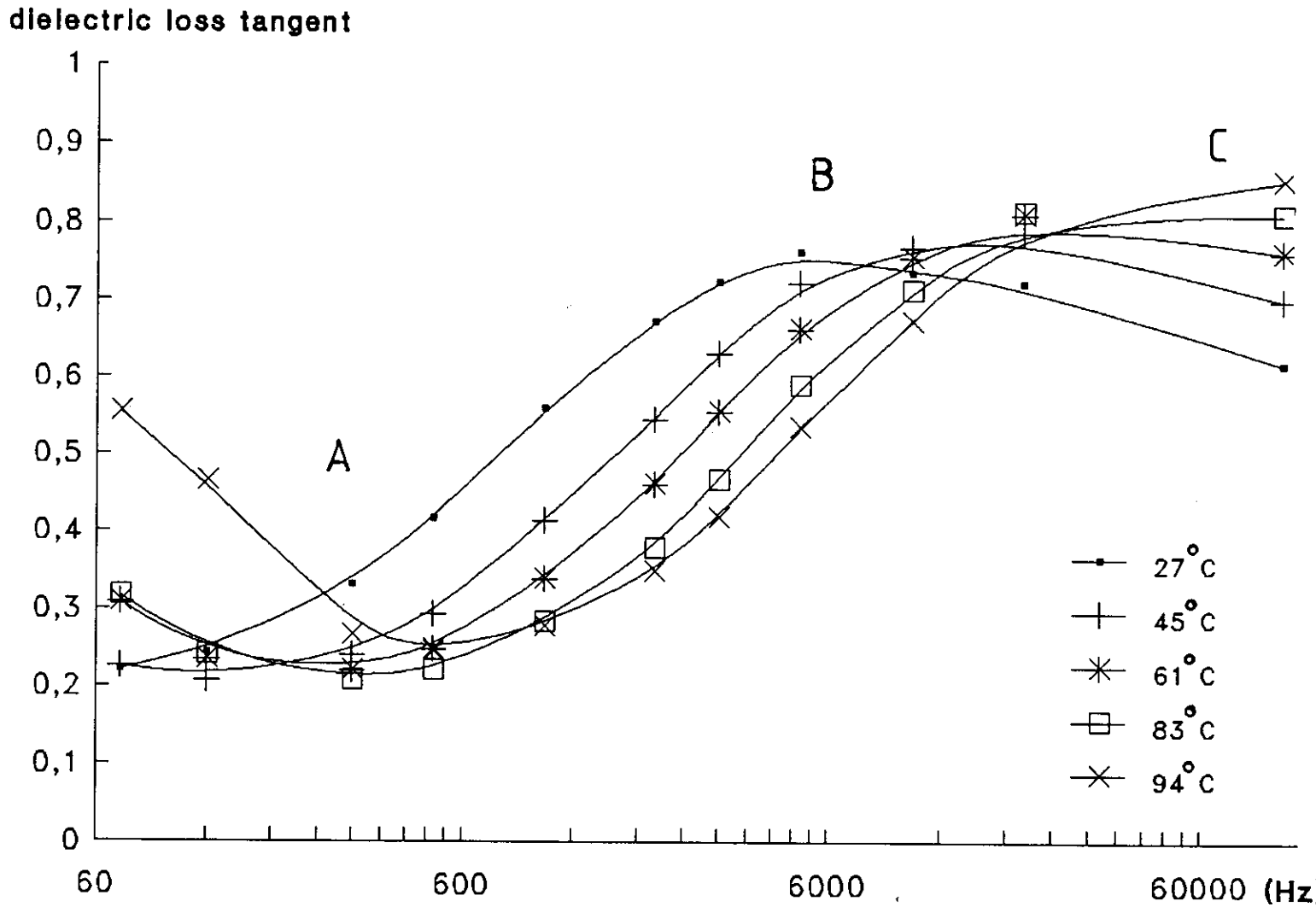

Fig.47: Shows the frequency dependence of tan(δ) at various constant temperatures for the sample $Se_{90}Ge_8In_2$ in the crystalline state at 150°C.

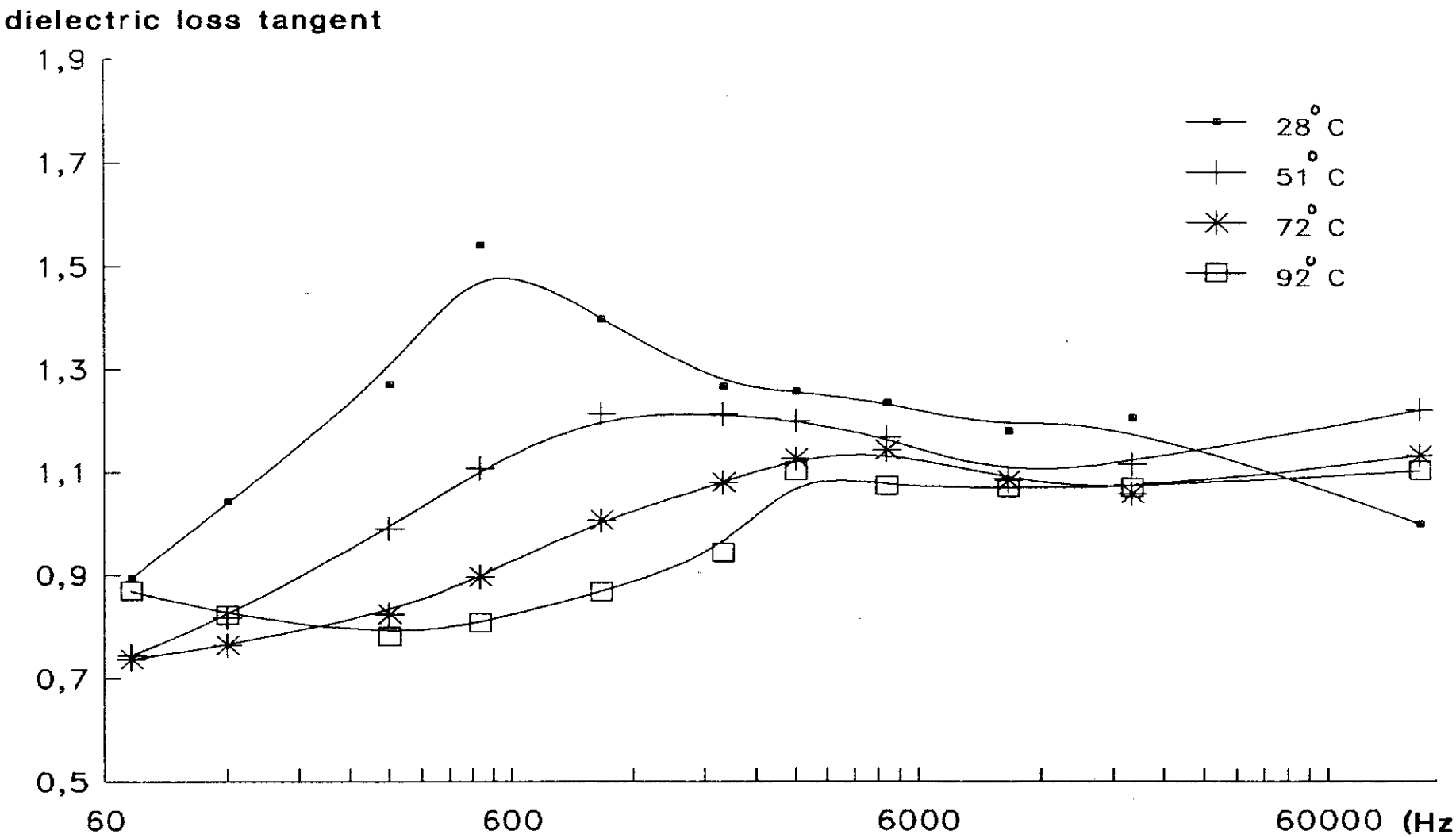

Fig.481:Shows the frequency dependence of tan(δ) at various constant temperatur for the sample $Se_{90}Ge_6In_4$ in the crystalline state at 140°C.

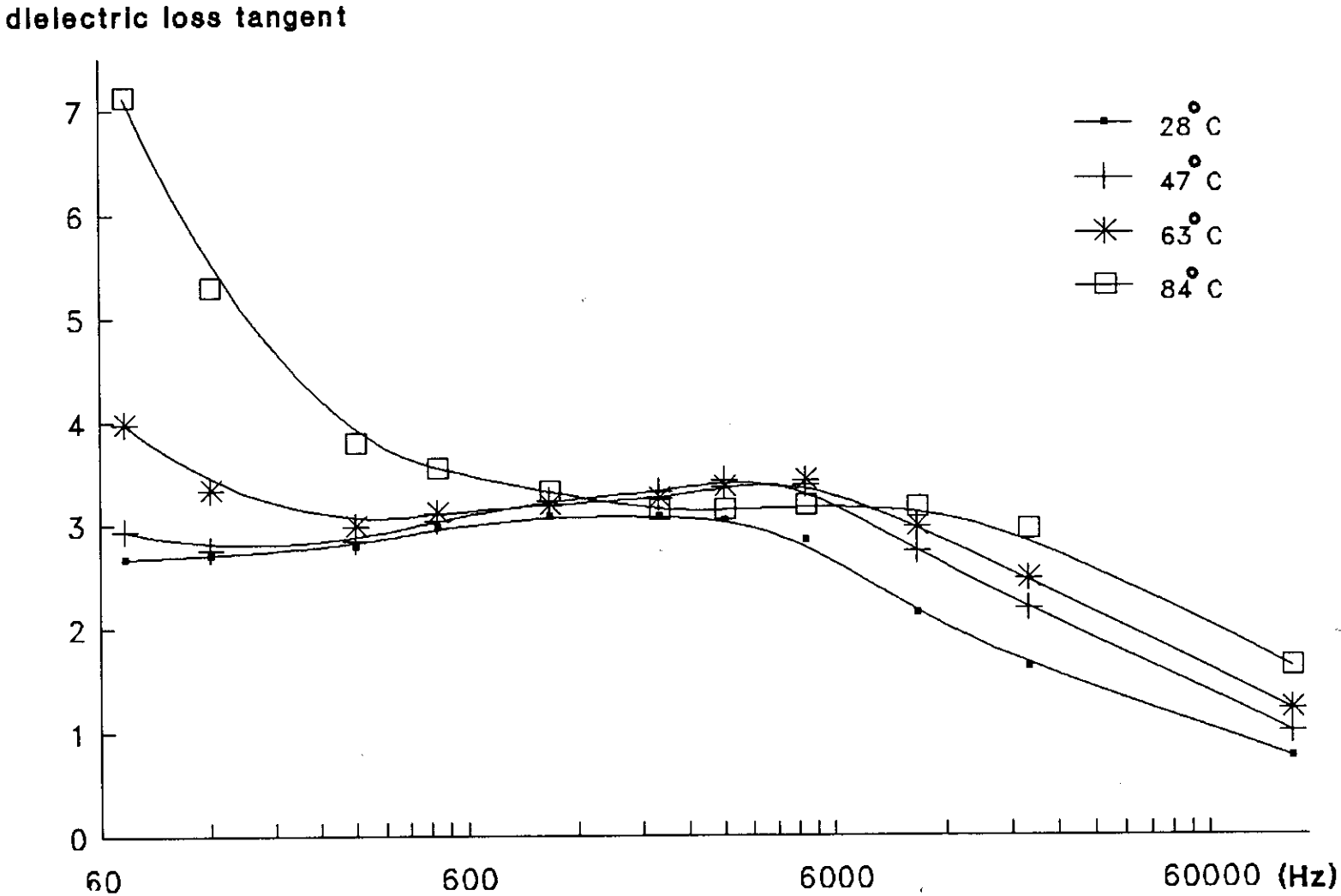

Fig 4.82 Shows the frequency dependence of tan(δ) at various constant temperatures for the sample $Se_{90}Ge_6In_4$ in the crystalline state at 150°C.

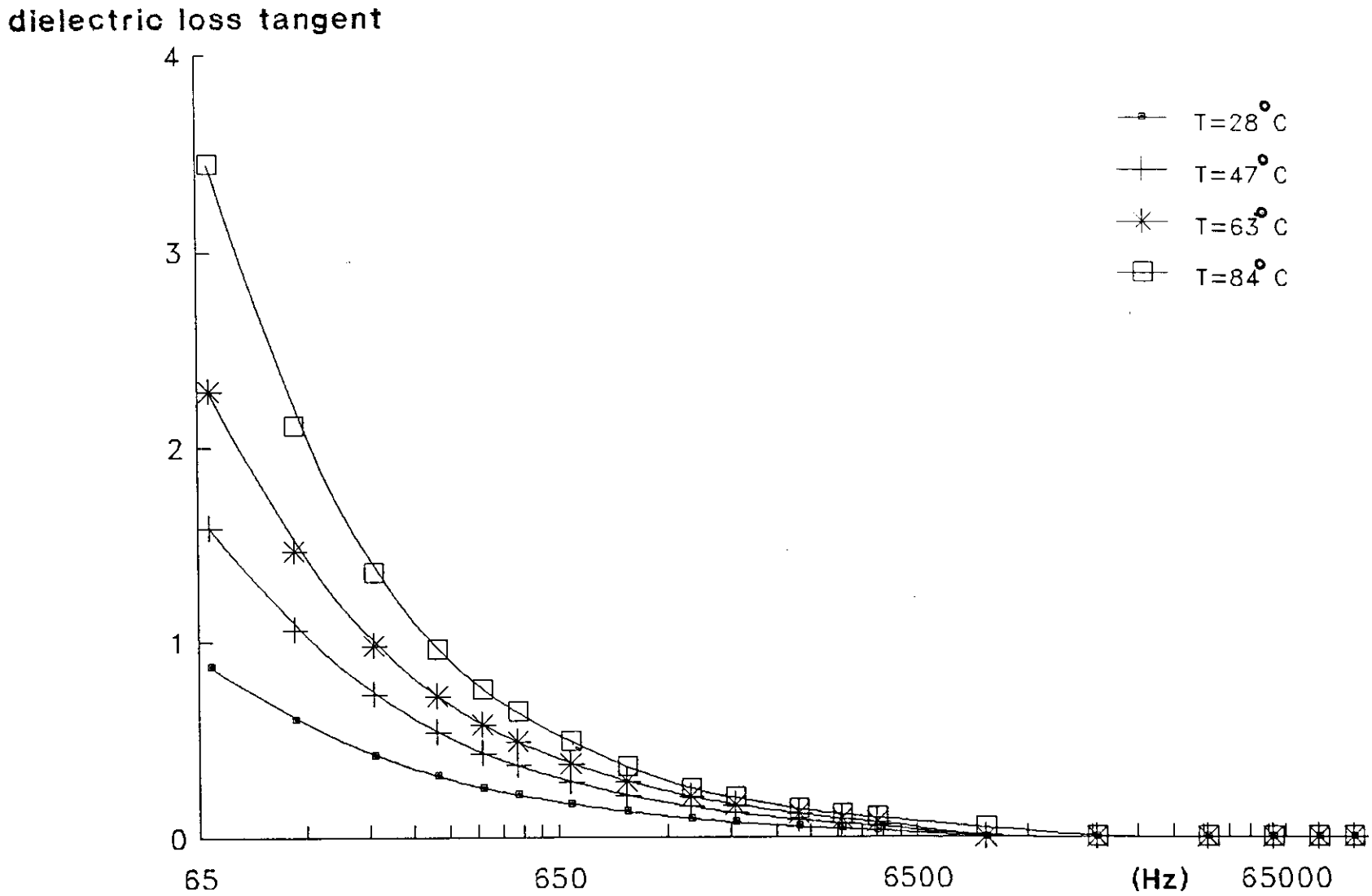

fig.4.83: The frequency dependence of tan(δ) at different ambient temperatures for $Se_{90}Ge_4In_6$ in crystalline state at 120°C.

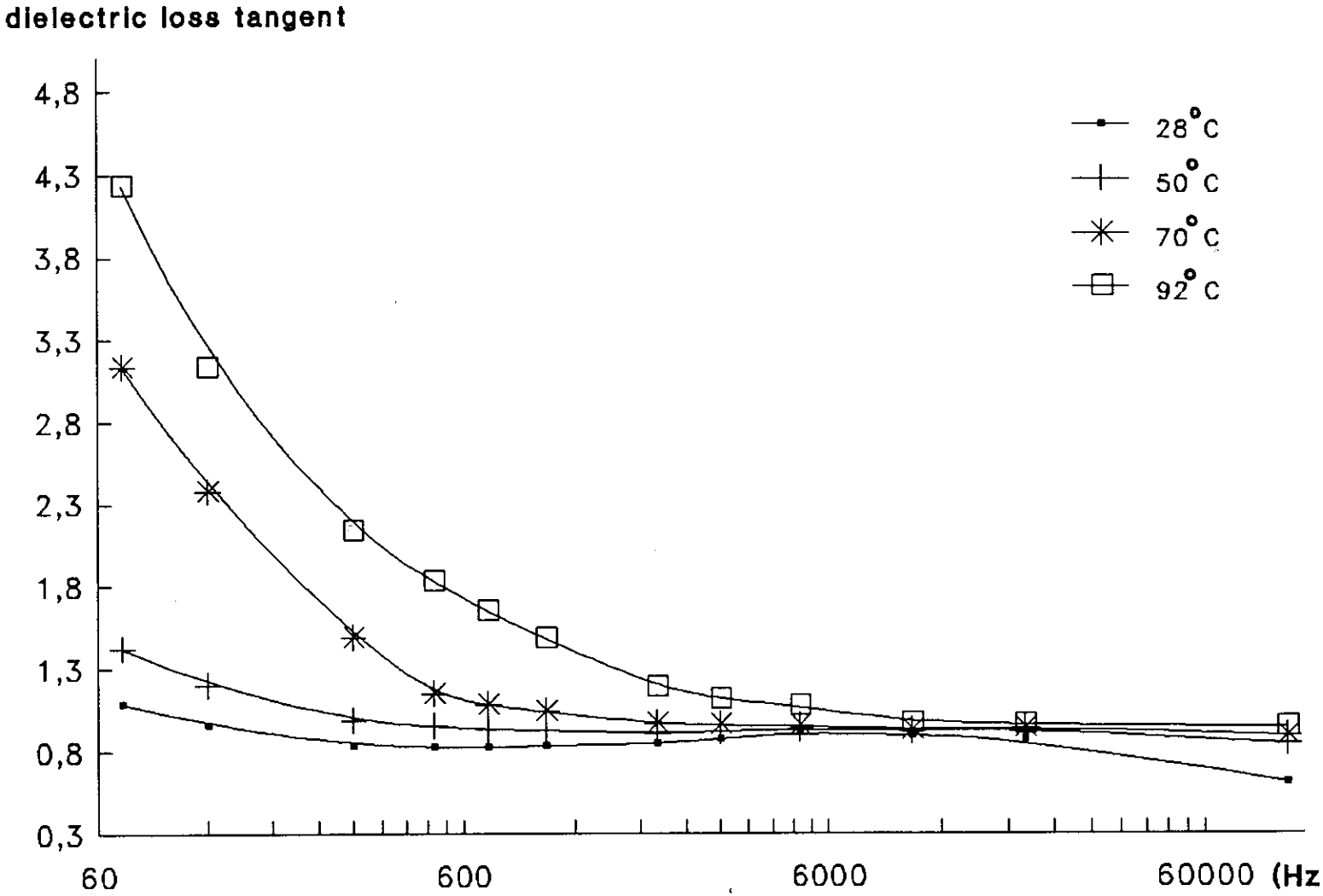

Fig 4.84 Shows the frequency dependence of tan(δ) at various constant temperatures for the sample $Se_{90}Ge_4In_6$ in the crystalline state at 130°C.

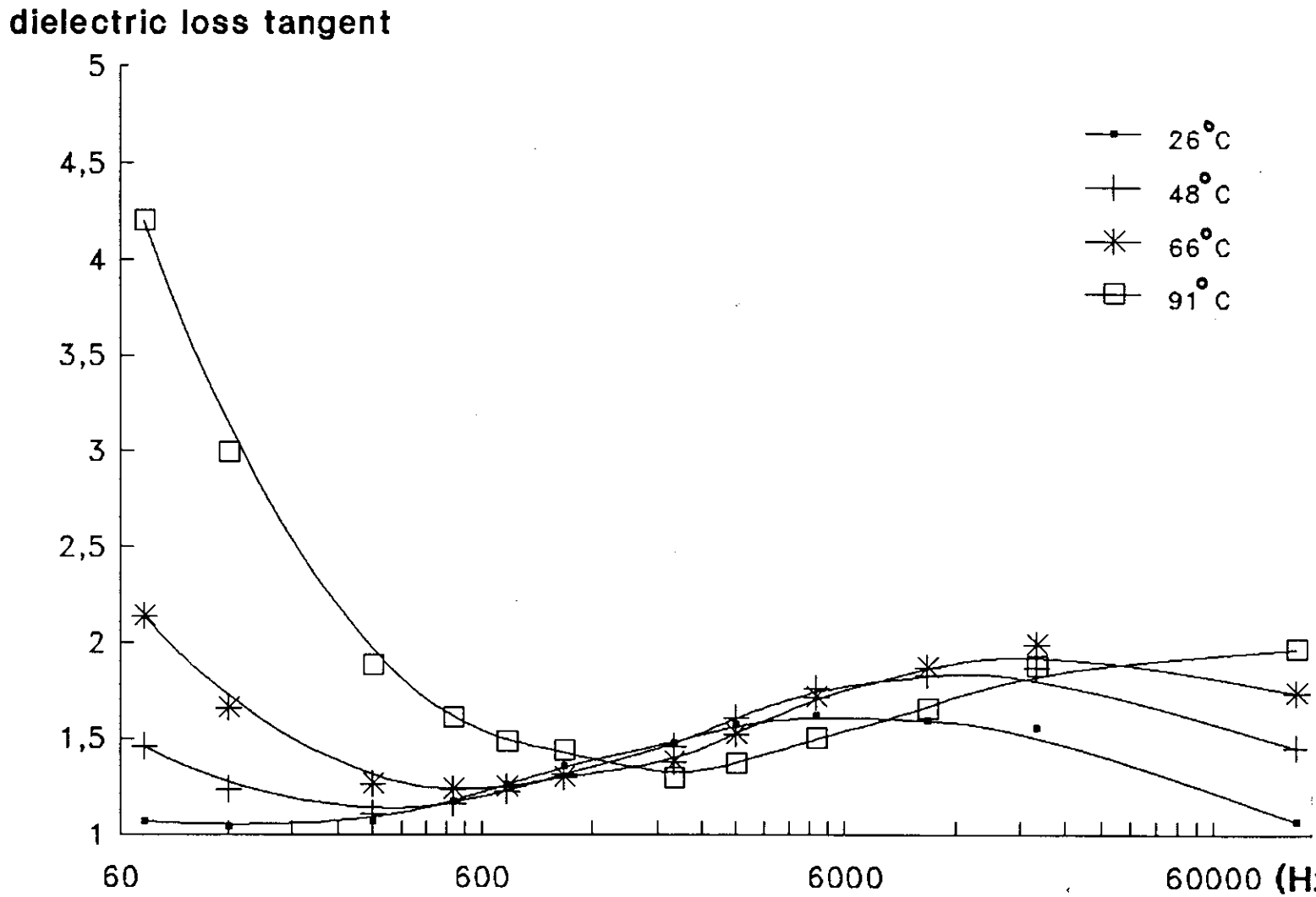

Fig 485: Shows the frequency dependence of tan(δ) at various constant temperatures for the sample $Se_{90} Ge_4 In_6$ in the crystalline state at 140° C.

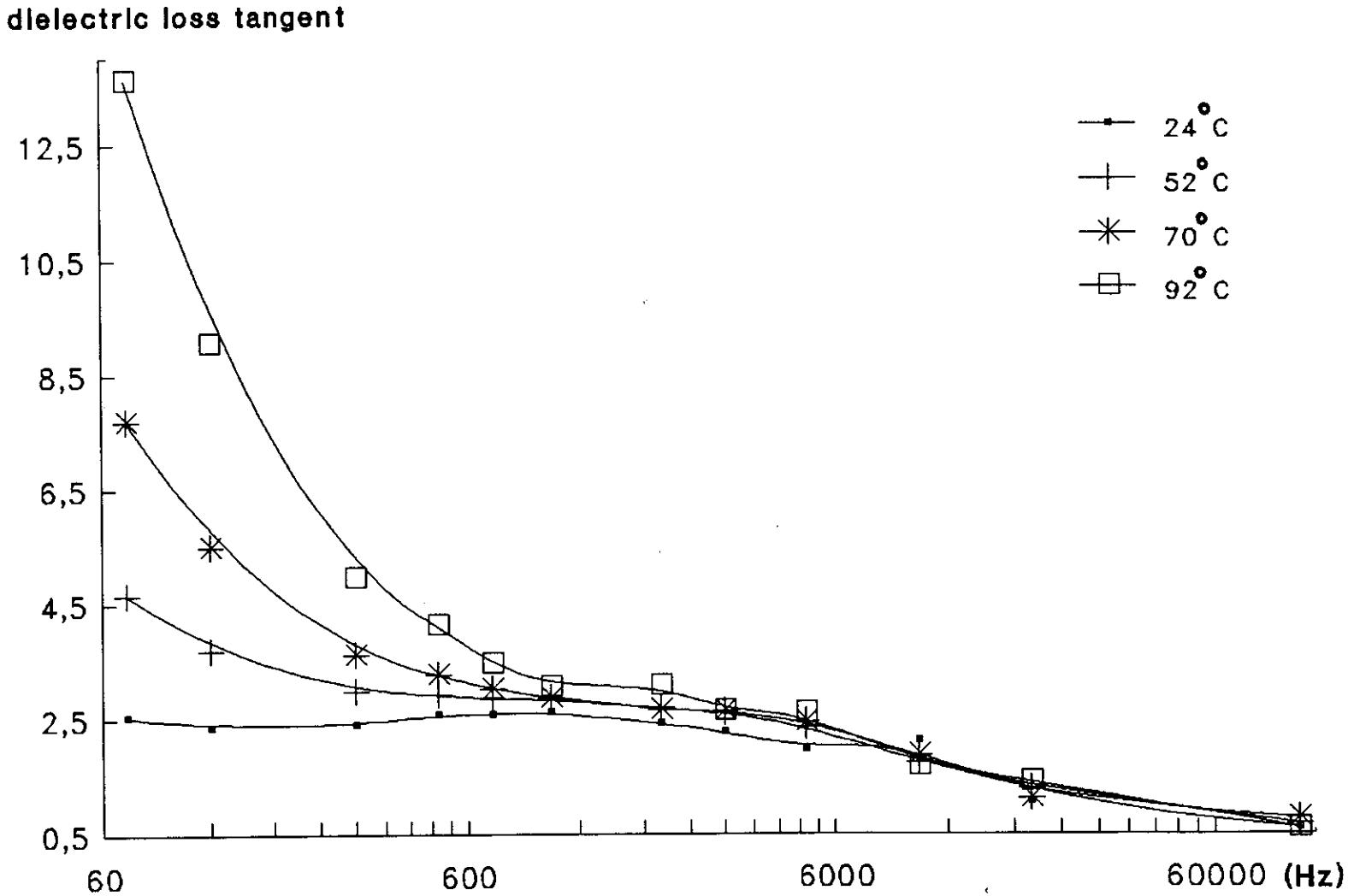

Fig. 86. Shows the frequency dependence of tan(δ)at various constant temperatures for the sample $Se_{90}Ge_4In_6$ in the crystalline state at 150°C.

followed by dielectric loss maxima. Accordingly these curves may be divided into three regions:

1-The region A,at low frequency is characterized by a trend of tan(δ)to minimize.

2-The region B,at high frequency, is characterized by a maximum loss peak and tan(δ) tends to increase to a maximum value.

3-The region C,at higher frequency, is characterized by a slowly decrease in tan δ with frequency.

The peaks associated with tan δ are common feature indicating the Deby-type dielectric relaxation process which are characterized by the relaxation frequency f_0($f_0=\omega_0/2\pi$).Since the crystals are of higher conductivity than the glass,so the more open the structure the more easily the relaxation losses can take place.

The four kinds of loss that are responsible for the loss in the

equilibrium position. Whenever the applied electric field alternates at frequency near that one of the constituent atoms, they are excited to high resonant amplitudes,accompanied by high dielectric losses.

4.2.7.THE EFFECT OF TEMPERATURE ON THE DIELECTRIC LOSS TANGENT(TAN OF Se_{90} Ge_{10-x} In_x IN THE CRYSTALLINE STATE :-

Figs.(4.87-4.90)show the temperature dependence of the dielectric loss tangent of $Se_{90}Ge_8In_2$ in the crystalline state during the temperature range(27 -100° C) at different constant values of frequency.

These curves were traced for the given sample at different crystallization temperature mainly 120,130,140 and 150° C after long period of annealing to ensure complete crystallization. From these curves it is clear that as the temperature increases the dielectric loss tangent increases. At low temperature,the tan (δ) increases with slow rate, while at high temperature range the rate of increment become more faster. These results were confirmed,since the experiment was repeated for the two samples Se_{90} Ge_6 In_4 and Se_{90} Ge_4 In_6at the same crystallization temperature as shown in figs.(4.91-4.94) and (4.95-4.98) respectively.

As a glass sample transfer through annealing,then a more open and thus more conductive structure is obtained. At low temperatures the conduction loss is the predominant while at high temperatures the vibration loss contributes with the conduction loss to the observed high dielectric loss.

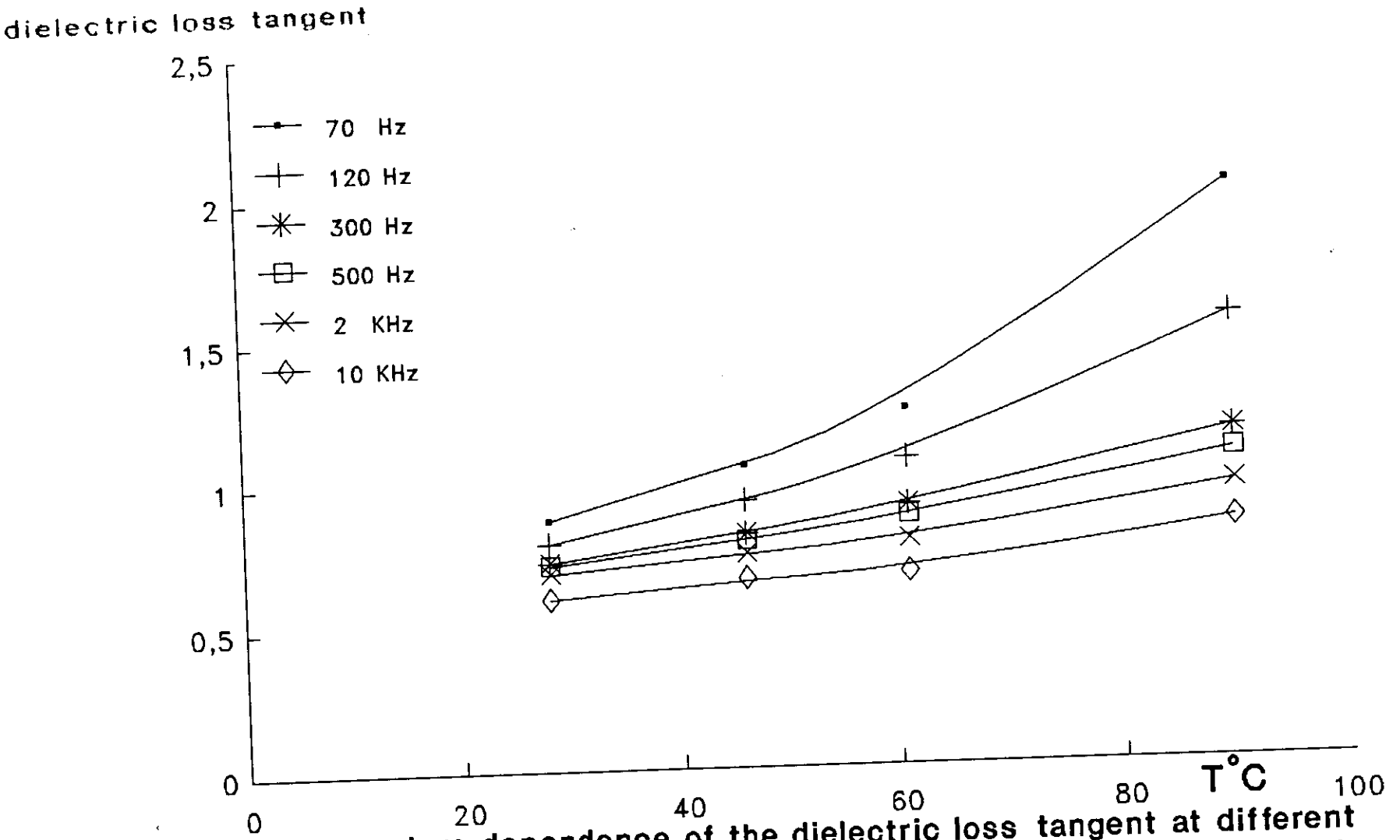

Fig 4.87 The temperature dependence of the dielectric loss tangent at different constant frequency for the sample $Se_{90}Ge_8In_2$ in the crystalline state, (120°C).

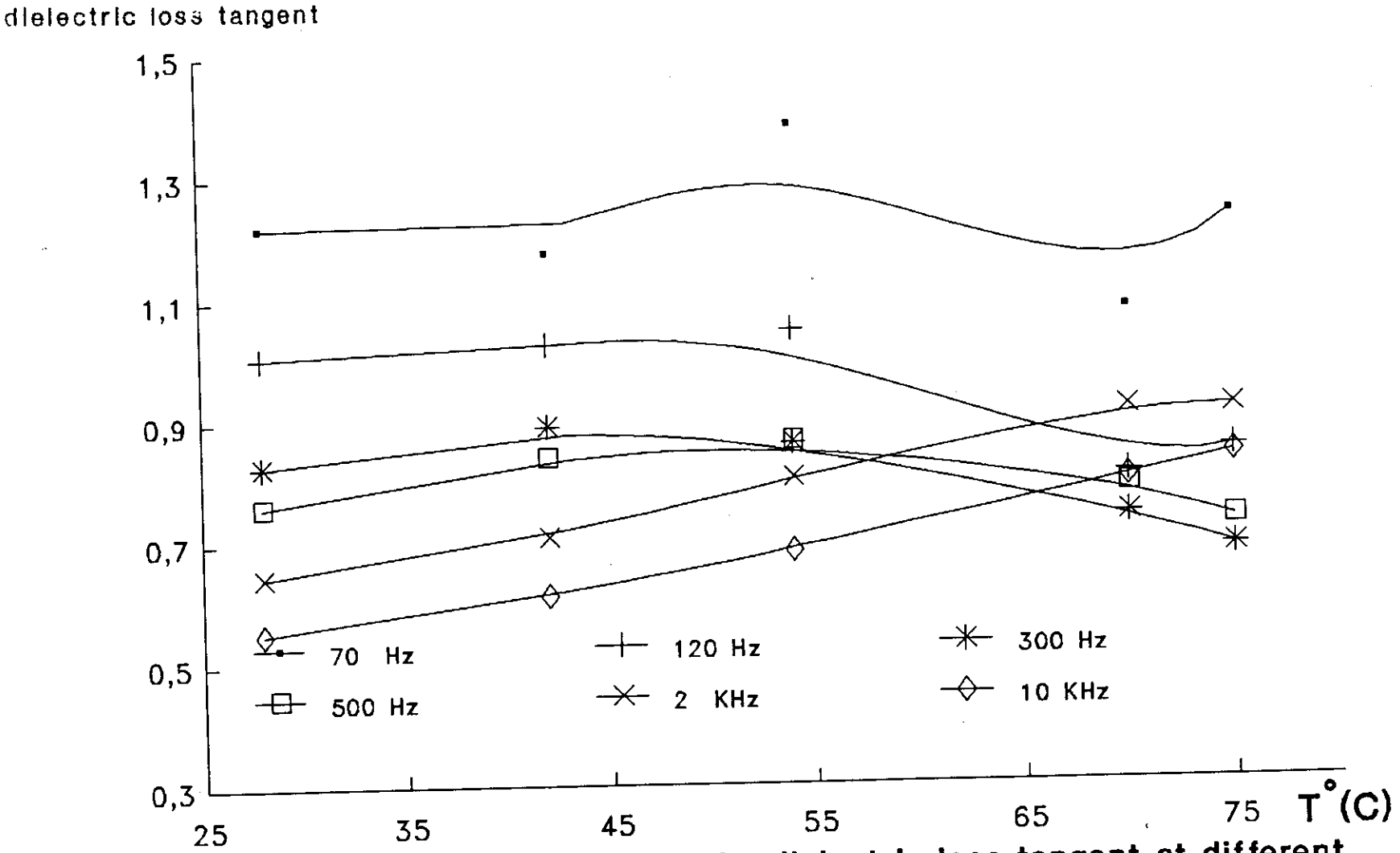

Fig.4.88: The temperature dependence of the dielectric loss tangent at different constant frequency for the sample $Se_{90}Ge_8In_2$ in the crystalline state (130°C).

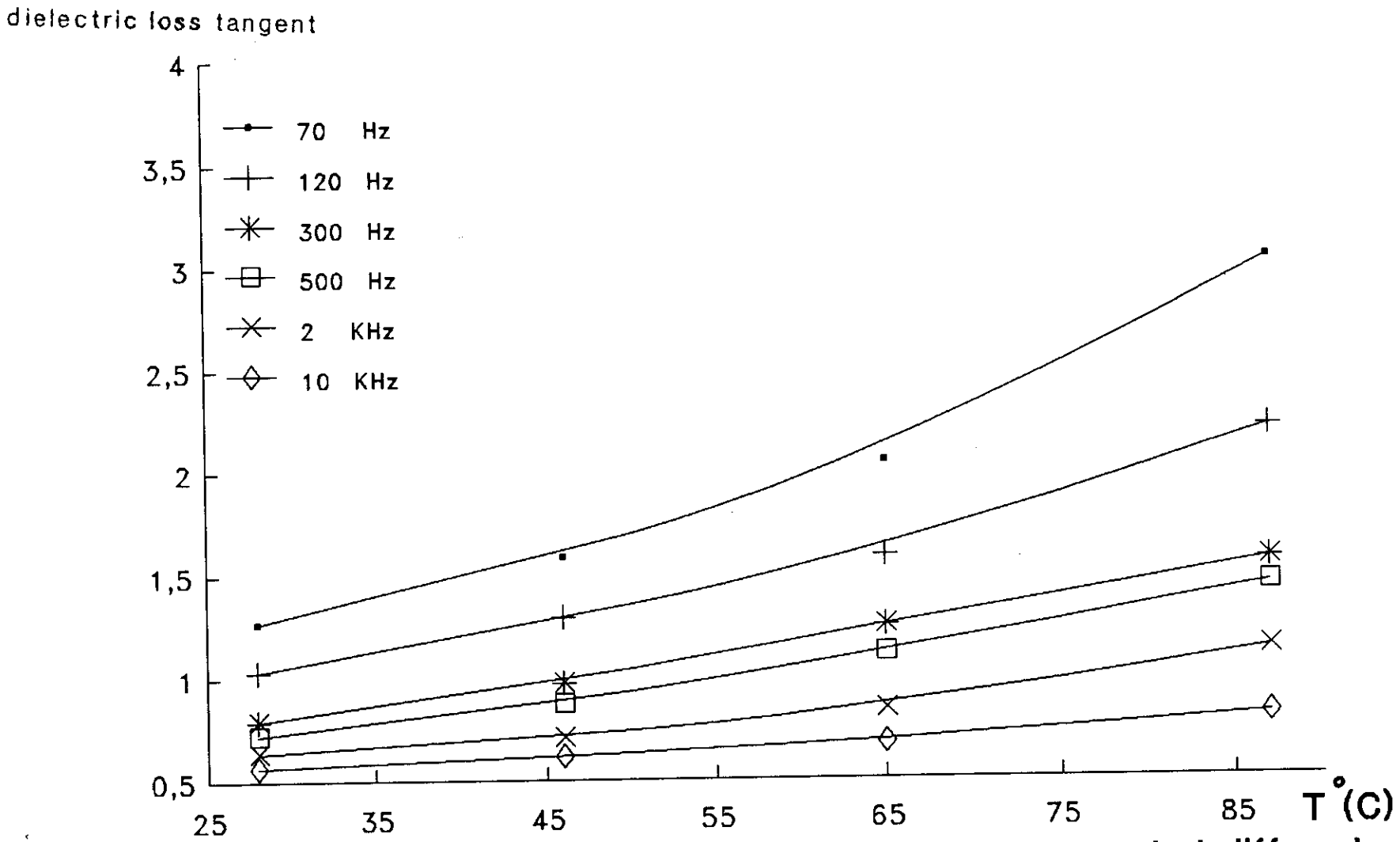

Fig.4.89: The temperature dependence of the dielectric loss tangent at different constant frequency for the sample $Se_{90}Ge_8In_2$ in the crystalline state (140°C).

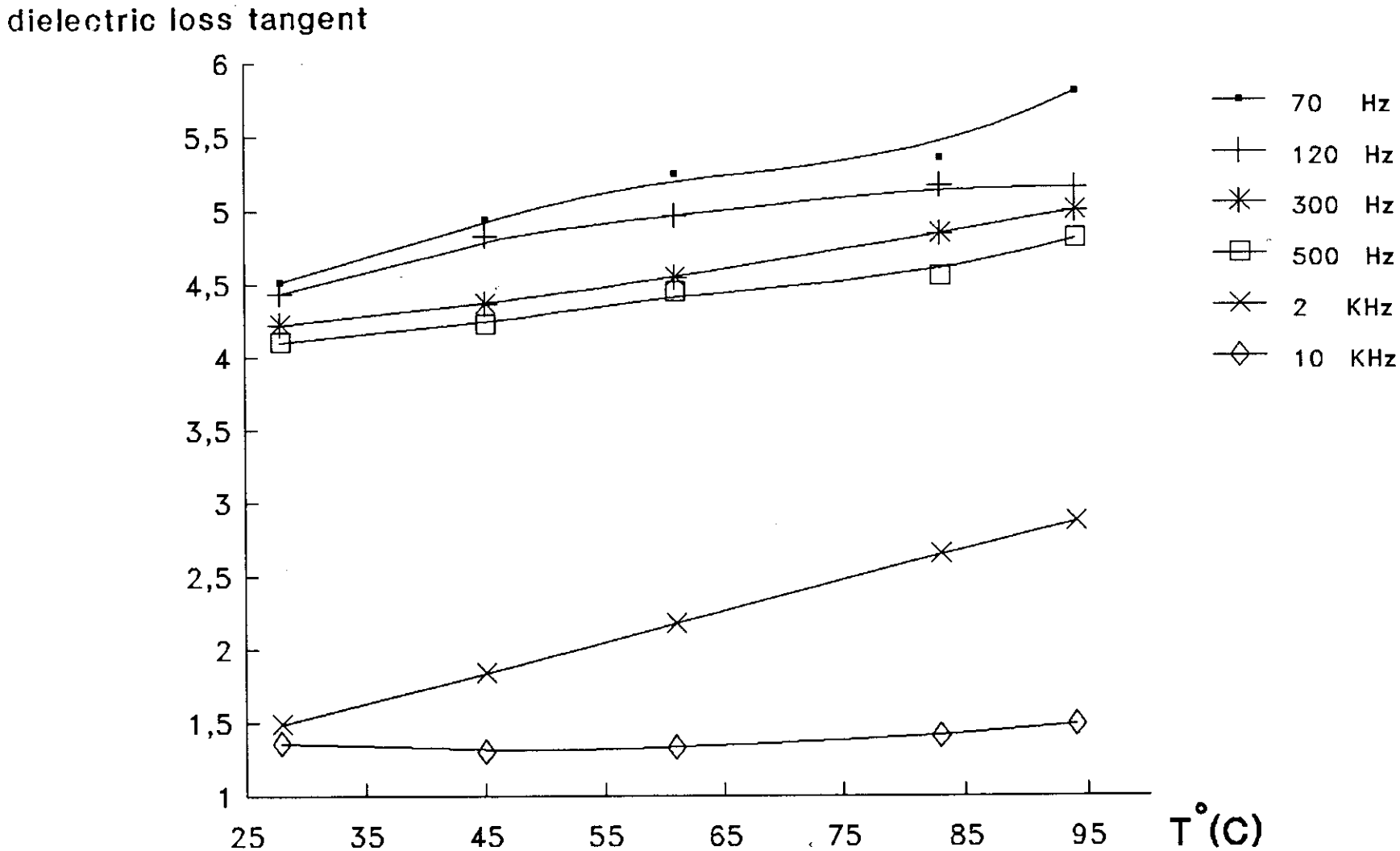

Fig.4.90 The temperature dependence of the dielectric loss at different constant frequency for the sample $Se_{90}Ge_8In_2$ in the crystalline state (150° C)

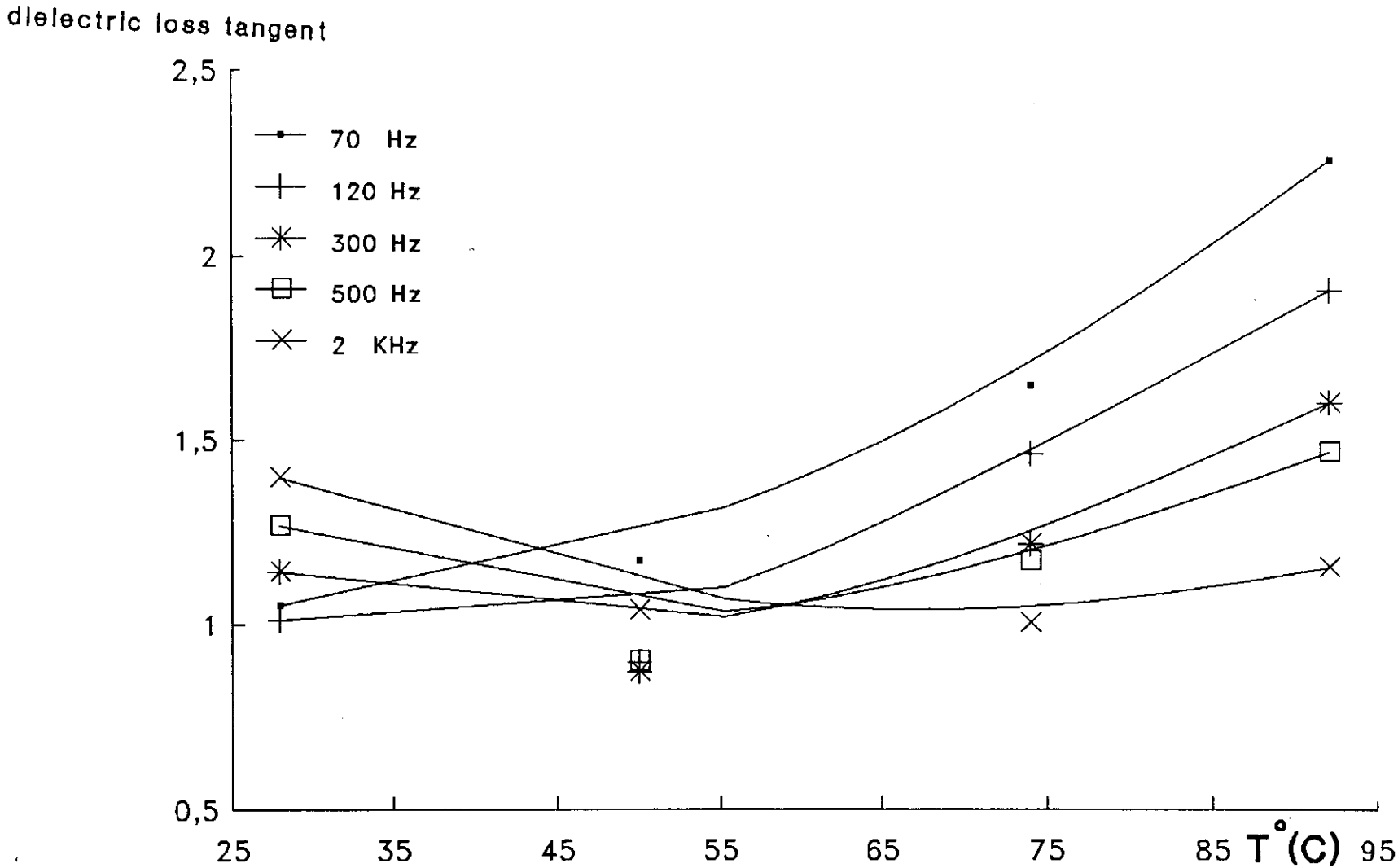

Fig.4.92: The temperature dependence of the dielectric loss tangent at different constant frequency for $Se_{90}Ge_6In_4$ in the crystalline state at 130° C.

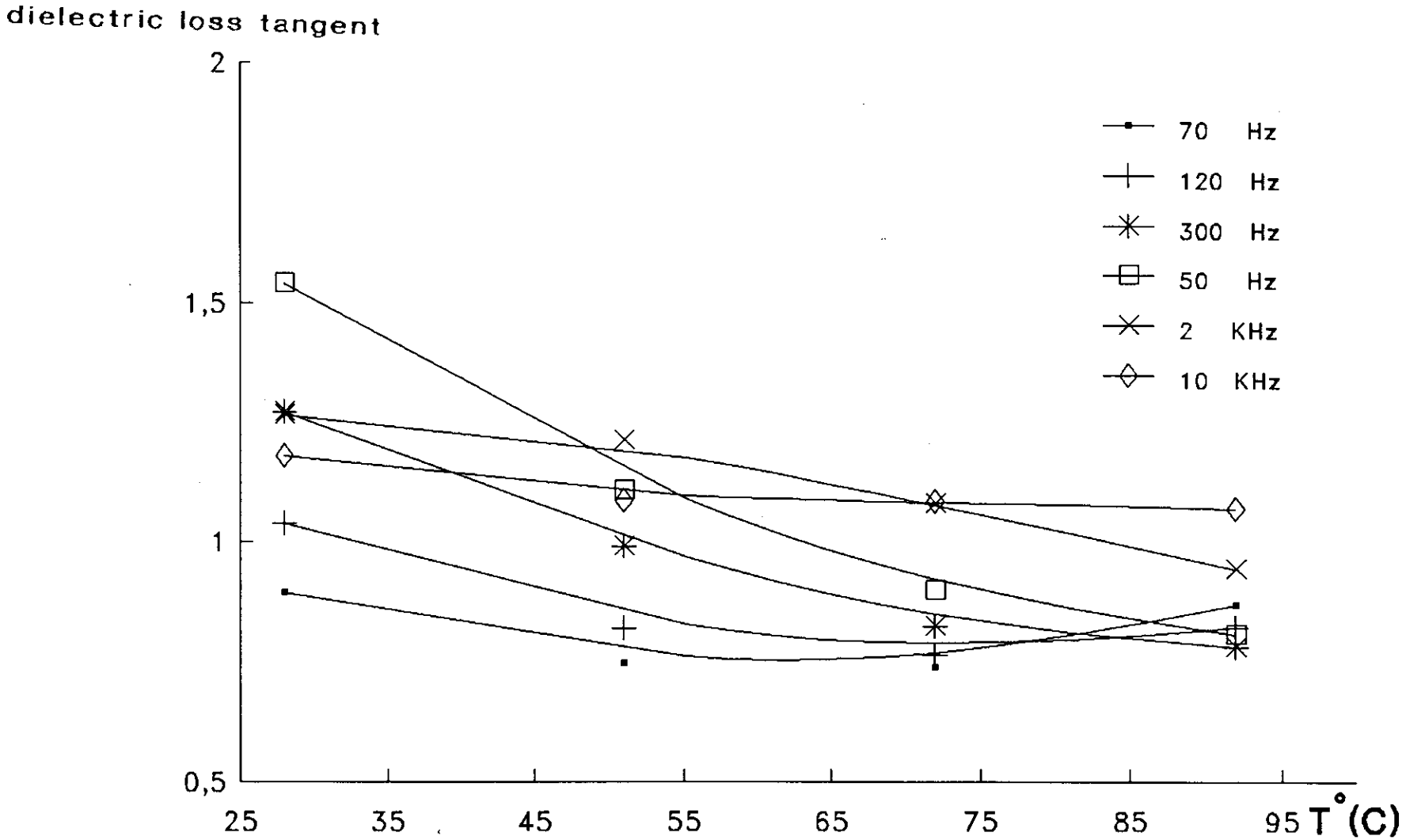

Fig4.93:The temperature dependence of the dielectric loss tangent at different constant frequency for the sample $Se_{90}Ge_6In_4$ in the crystalline state at 140° C.

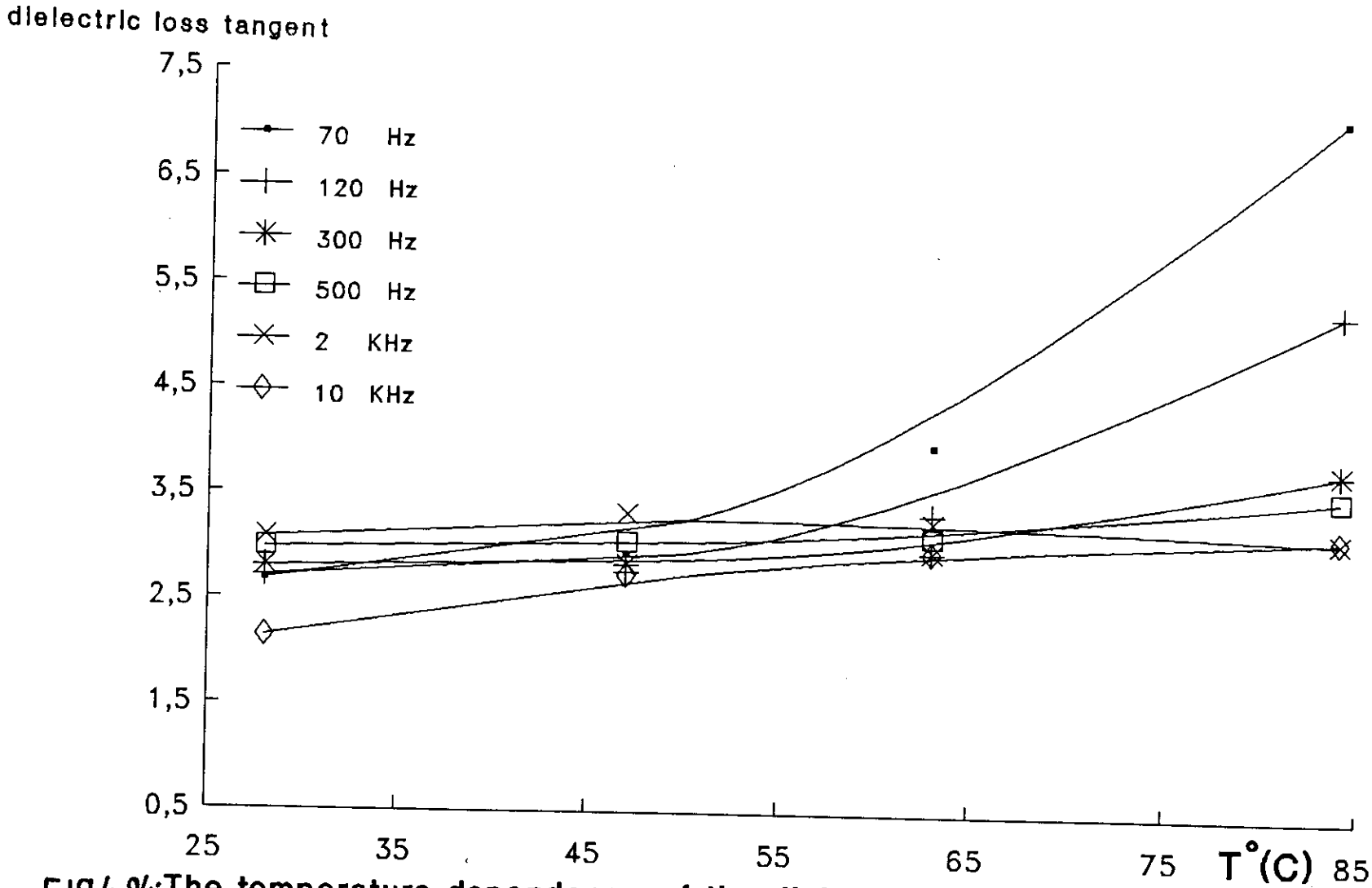

Fig.4.94: The temperature dependence of the dielectric loss tangent at different constant frequency for the sample $Se_{90}Ge_6In_4$ in the crystalline state at 150° C.

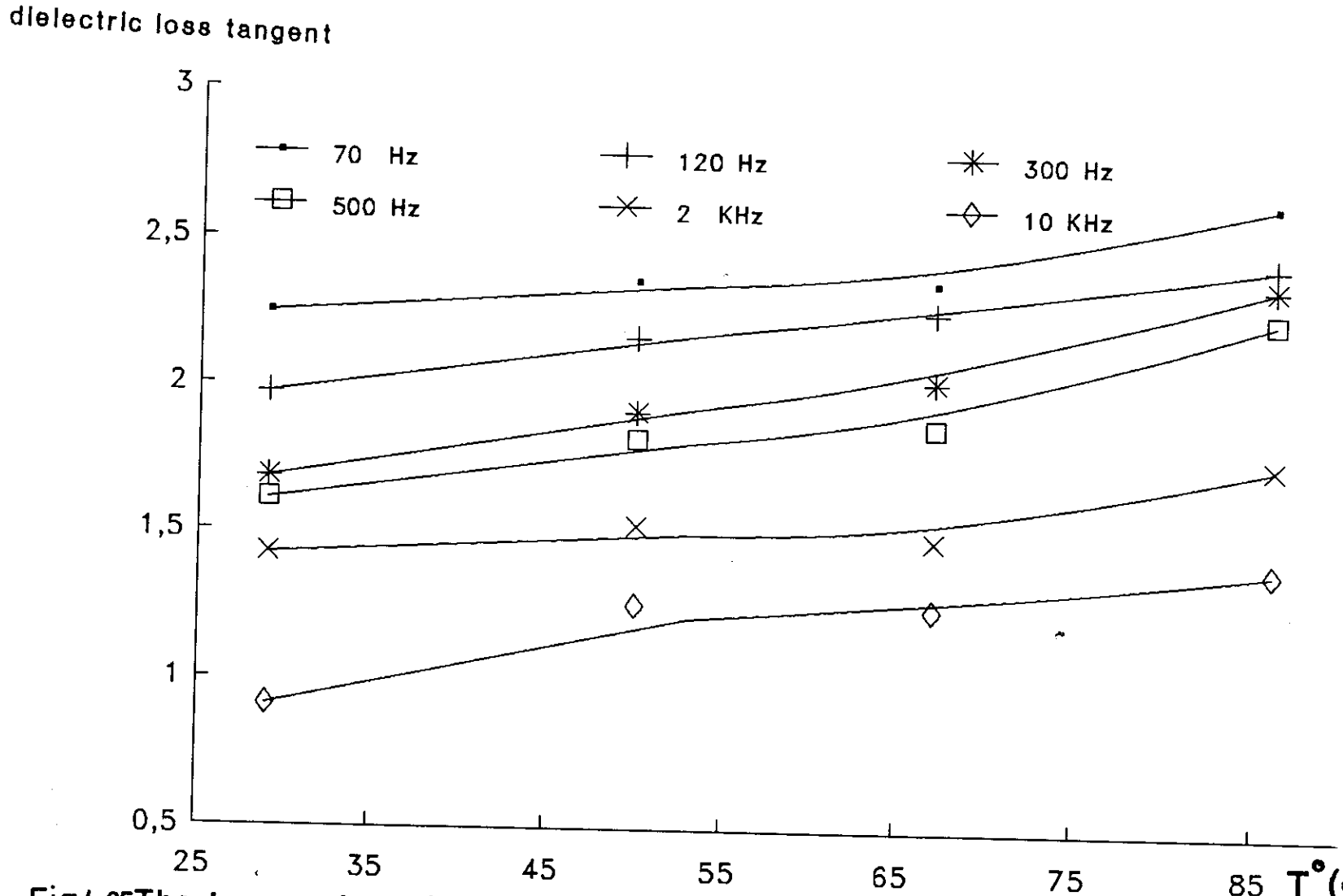

Fig4.95 The temperature depndence of the dielectric loss tangent at different constant frequency for $Se_{90}Ge_4In_6$ in the crystalline state at 120° C

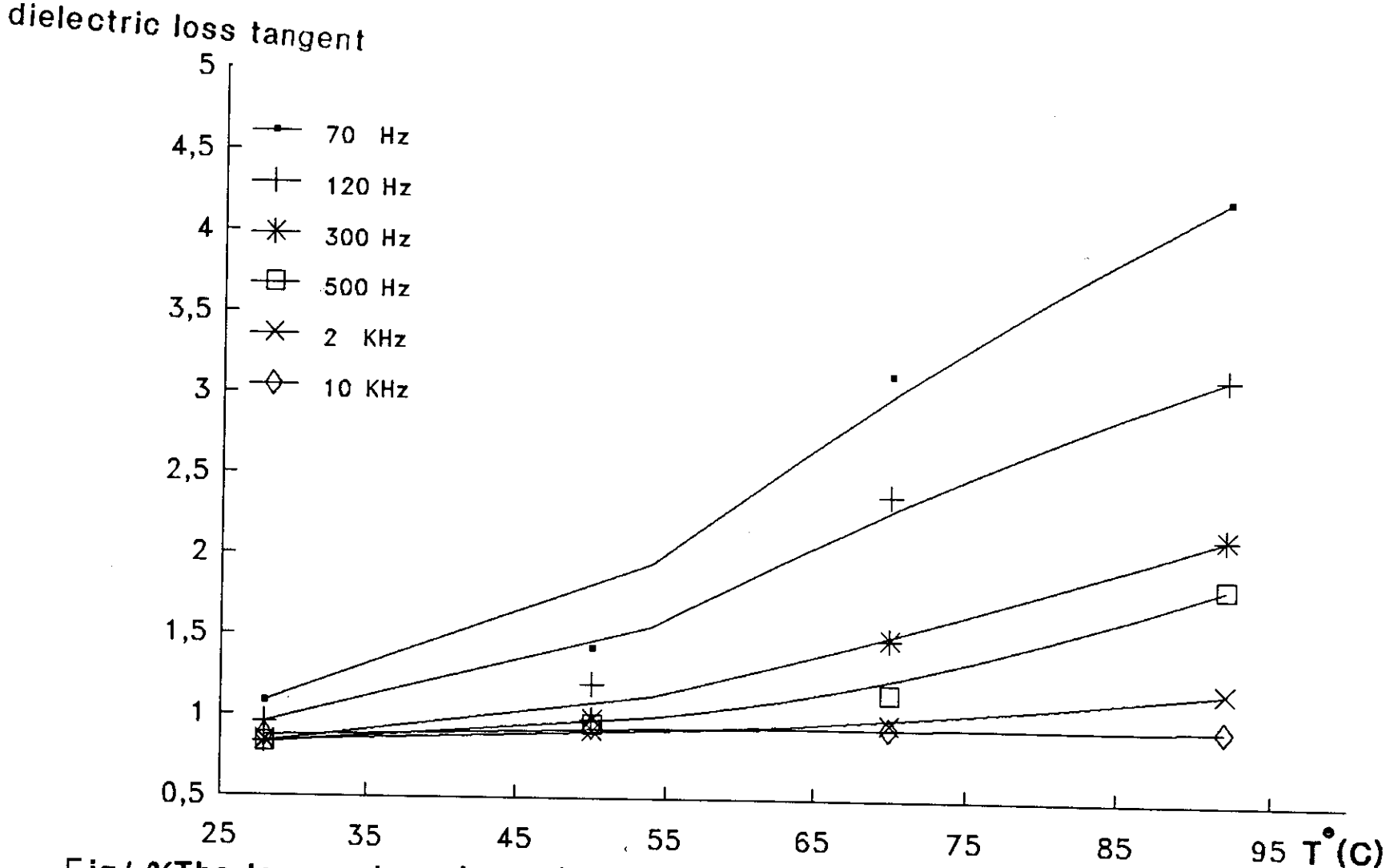

Fig.4.96: The temperature dependence of the dielectric loss tangent at different frequency for $Se_{90}Ge_4In_6$ in the crystalline state at 130°C.

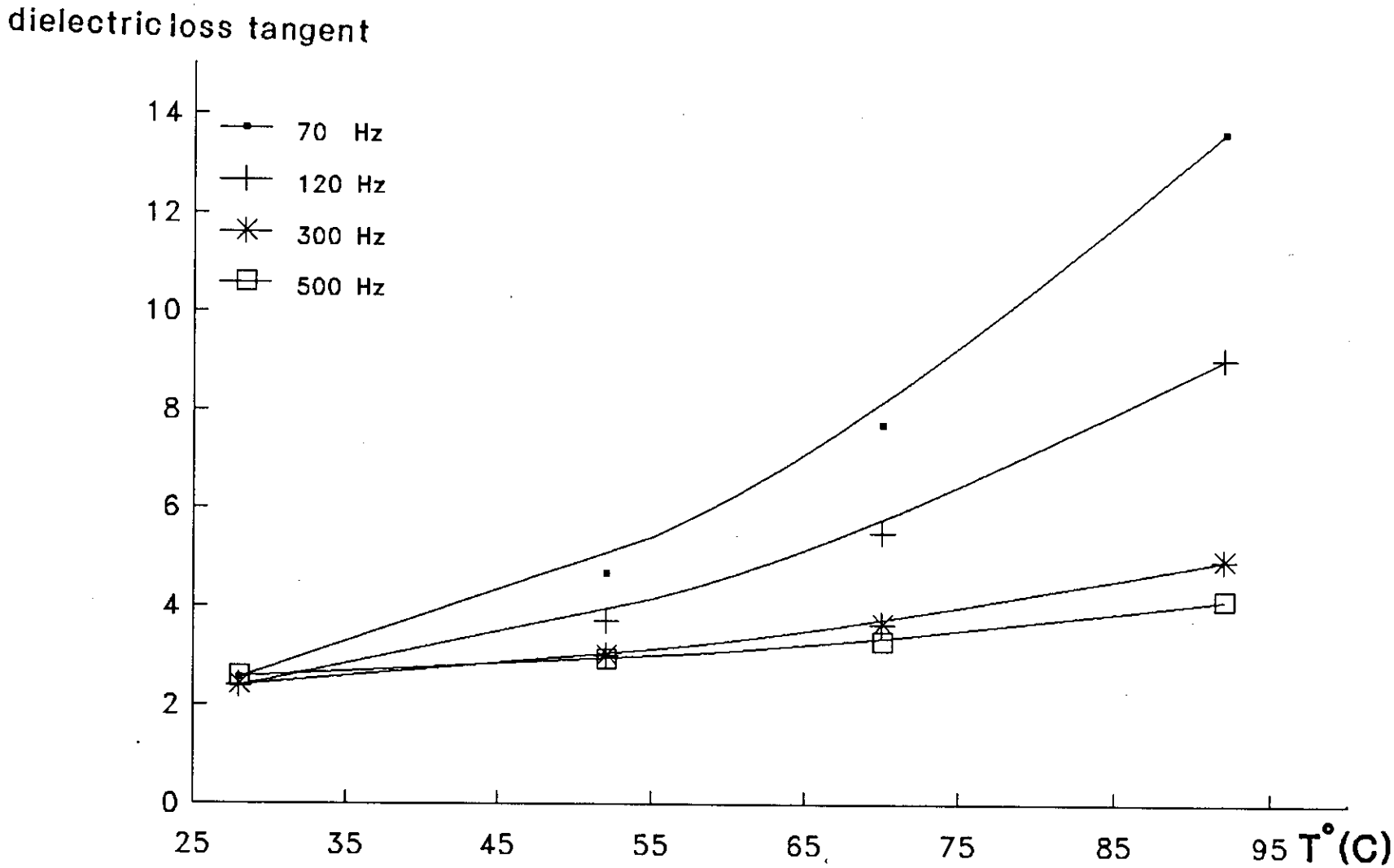

Fig.4.98: The temperature dependence of the dielectric loss tangent at different constant frequency for $Se_{90}Ge_4In_6$ in the crystalline state at 150°C.

4.3.DISORDER -ORDER TRANSFORMATION :-

Thermal energy was used to carry out the process of disorder -order transformation[113] . This process involves the nucleation and crystal growth. Nucleation is a partial ordering of the glassy structure to form small nuclei of crystalline order. This is followed by the growth of nuclei into well developed islands within the glassy matrix. The volume fraction of crystalline phase may be determined relatively by recording the change of the physical properties of the given samples as a function of time of crystallization in steps. To follow up the process of transformation, each sample of the system $Se_{90}Ge_{10-x}In_x$,where x=2,4 and 6 was divided into four parts. Each part was subjected to thermal heating in steps at one of the crystallization temperature 120,130,140 and 150°C for successive periods of time enough to verify stable amorphous-crystalline transformation.

The process of amorphous -crystalline transformation was detected by recording the change in the dielectric constant and the dielectric loss tangent as a function of time of crystallization. This was carried out for each sample at the crystallization temperature 120,130,140 and 150°C in step-wise method.

4.3.1.THE EFFECT OF ANNEALING TIME ON THE DIELECTRIC CONSTANT AND DIELECTRIC LOSS TANGENT OF $Se_{90}Ge_{10-x}In_x$:-

Figs.(4.99-4.102,4.103-4.106) show the effect of increasing the time of crystallization on both the real part of the dielectric constant and the dielectric loss tangent of the glassy sample $Se_{90}Ge_8In_2$ at different constant values of frequency.These records were traced at the crystallization temperature 120,130,140 and 150° C.

These curves show that both ε and $\tan\delta$ increases for short time of annealing and vibrate between peaks and bottoms within another period. At the maximum of the final peak the ε and tan δ start to decrease as increasing the time of annealing to reach minimum constant value. These features were detected clearly at different constant frequency below 1 KHz. Accordingly,curves of figs.(4.99-4.106) can be divided into two periods :-

I- PERIOD(A-B):-

Through which seeding process has been started as nucleation appear and disappear in meta-stable phases till reaches a critical value under a certain condition becomes stable phase.

II-PERIOD(B-C):-

This period is characterized by a decreases in ε and tan δ as increasing the time of annealing to reach constant minimum value as the sample becomes in pure stable crystalline phase.

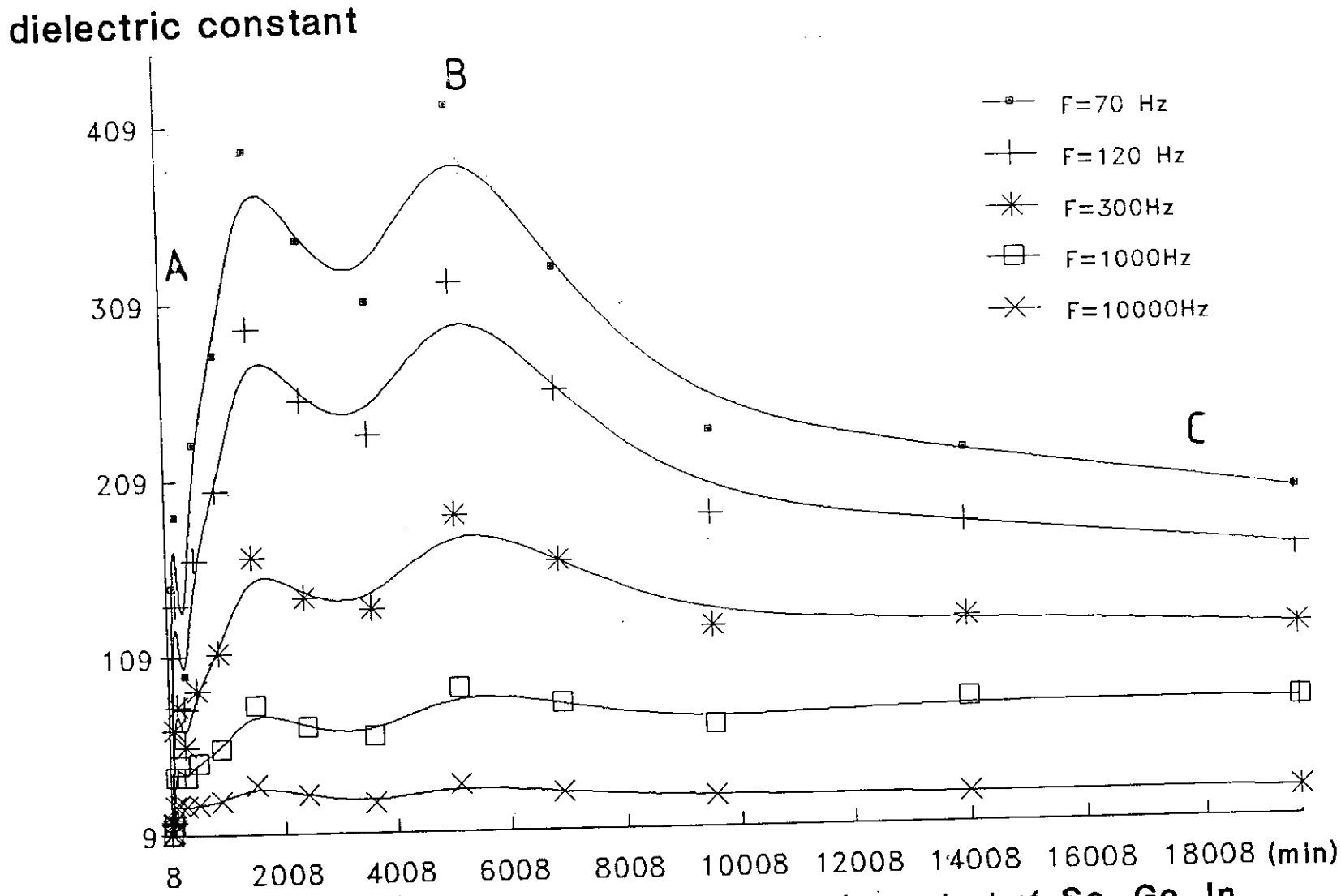

Fig.4.99 The effect of annealing time on the dielectric constant of $Se_{90}Ge_8In_2$ at annealing temperature 120°C , and at different frequencies .

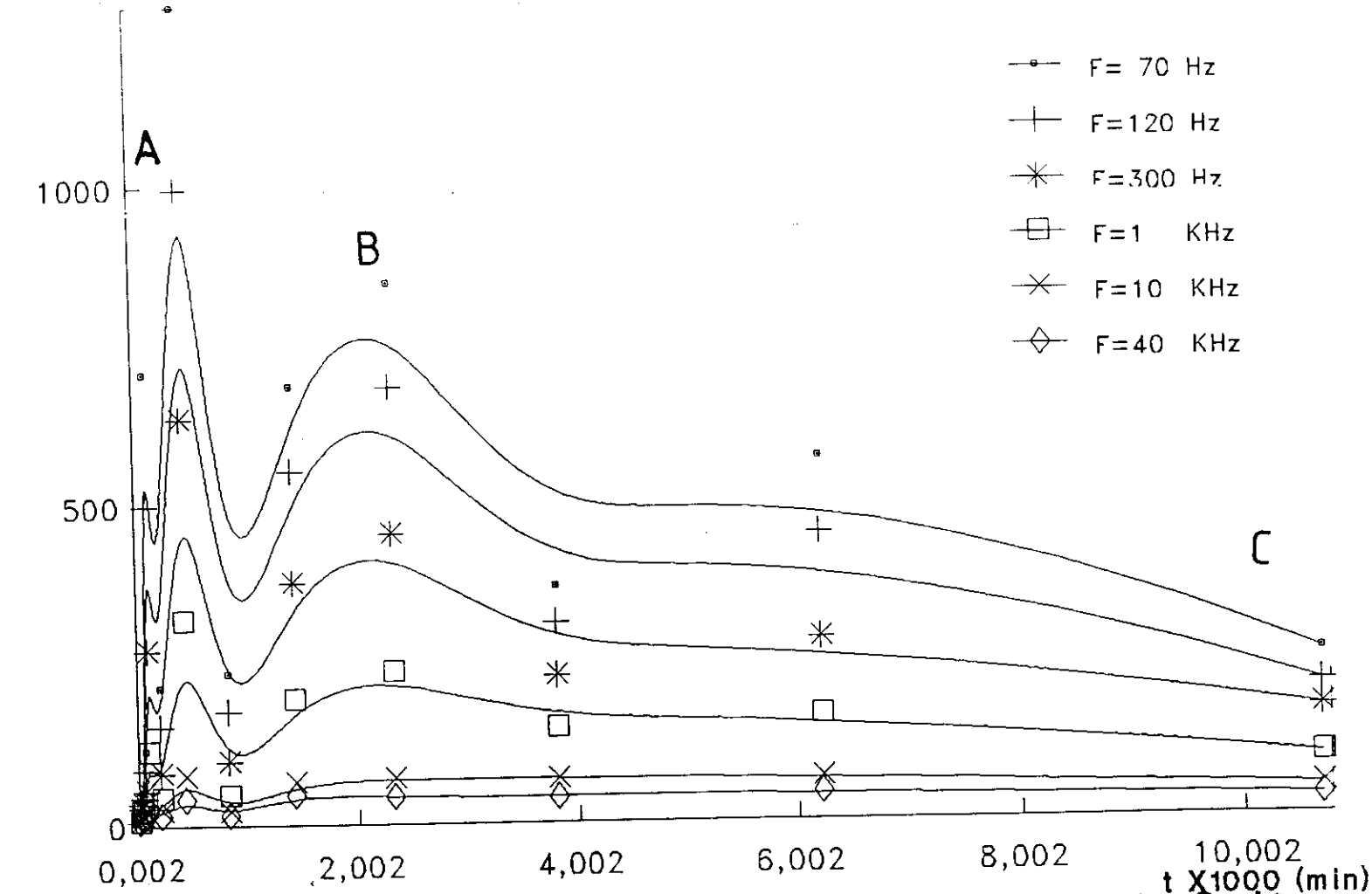

FIG.4.100: The effect of annealintg time on the dielectric constant of $Se_{90}Ge_8In_2$ bulk sample at annealing temperature 130°C, and different frequencies.

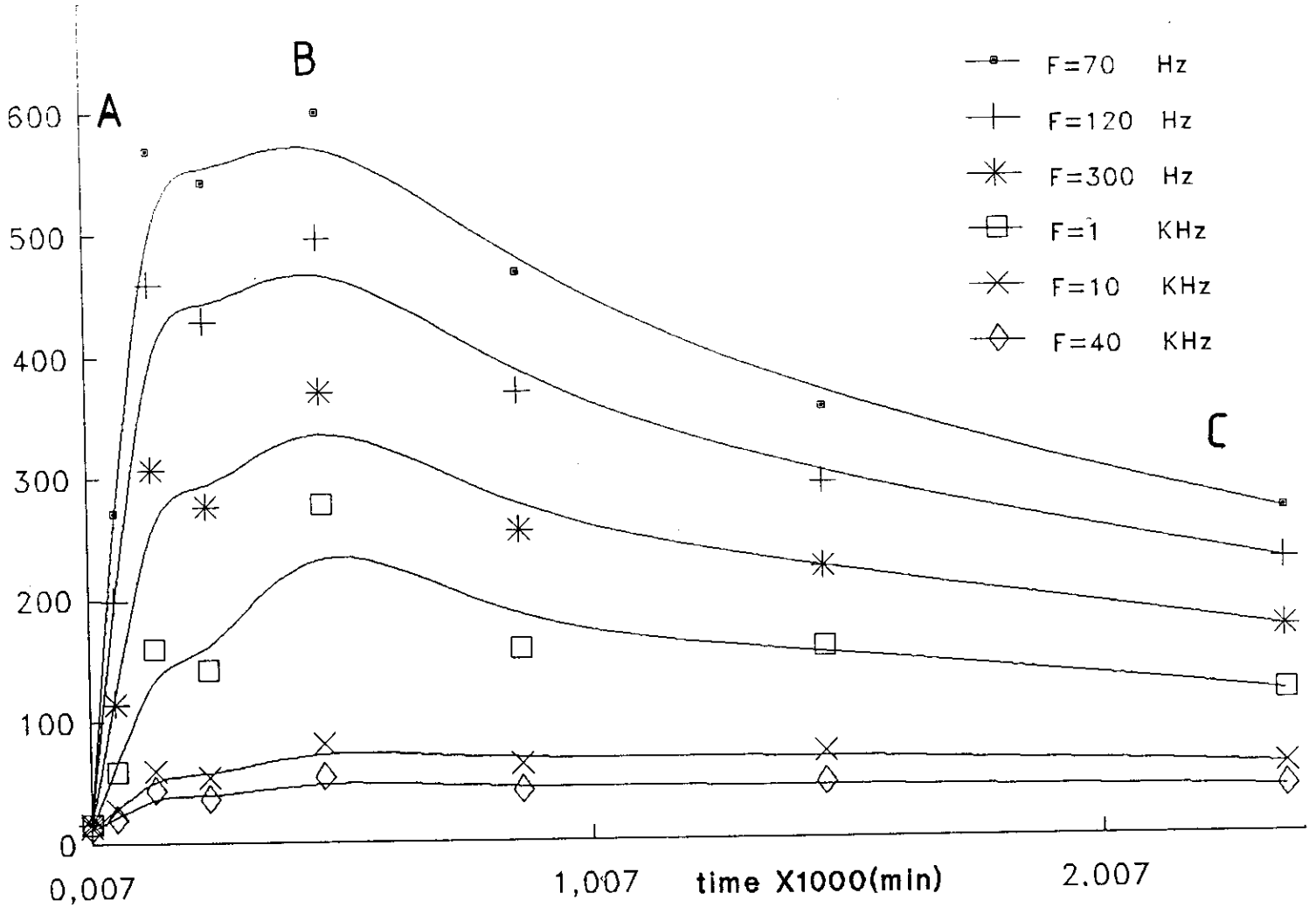

FIG.4.101: The effect of annealing time on the dielectric constant of $Se_{90}Ge_8In_2$ at annealing temperature 140°C and different frequencies .

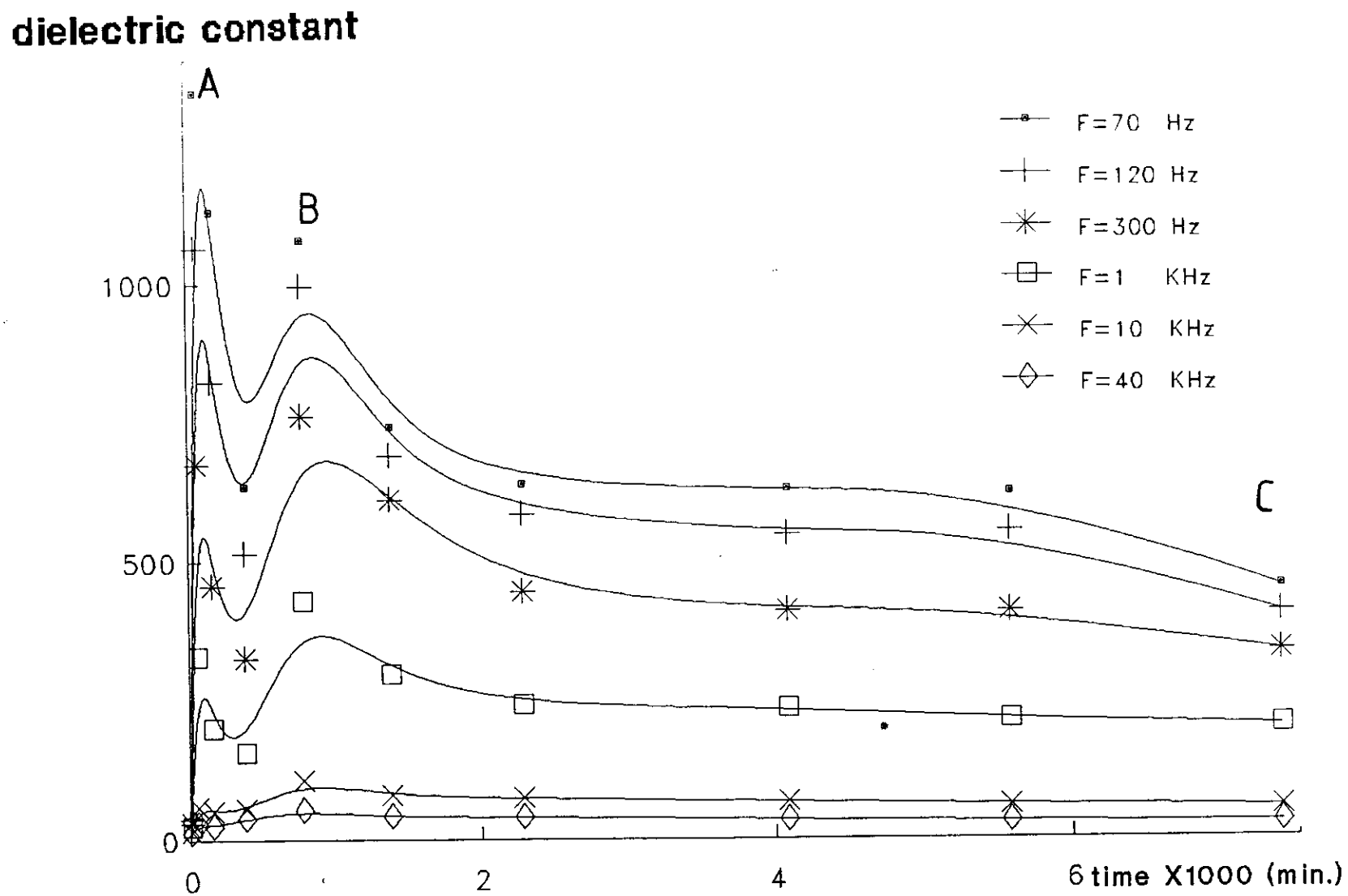

FIG4.102: The effect of annealing time on the dielectric constant of $Se_{90}Ge_8In_2$ at annealing temperature 150°C and at different frequencies .

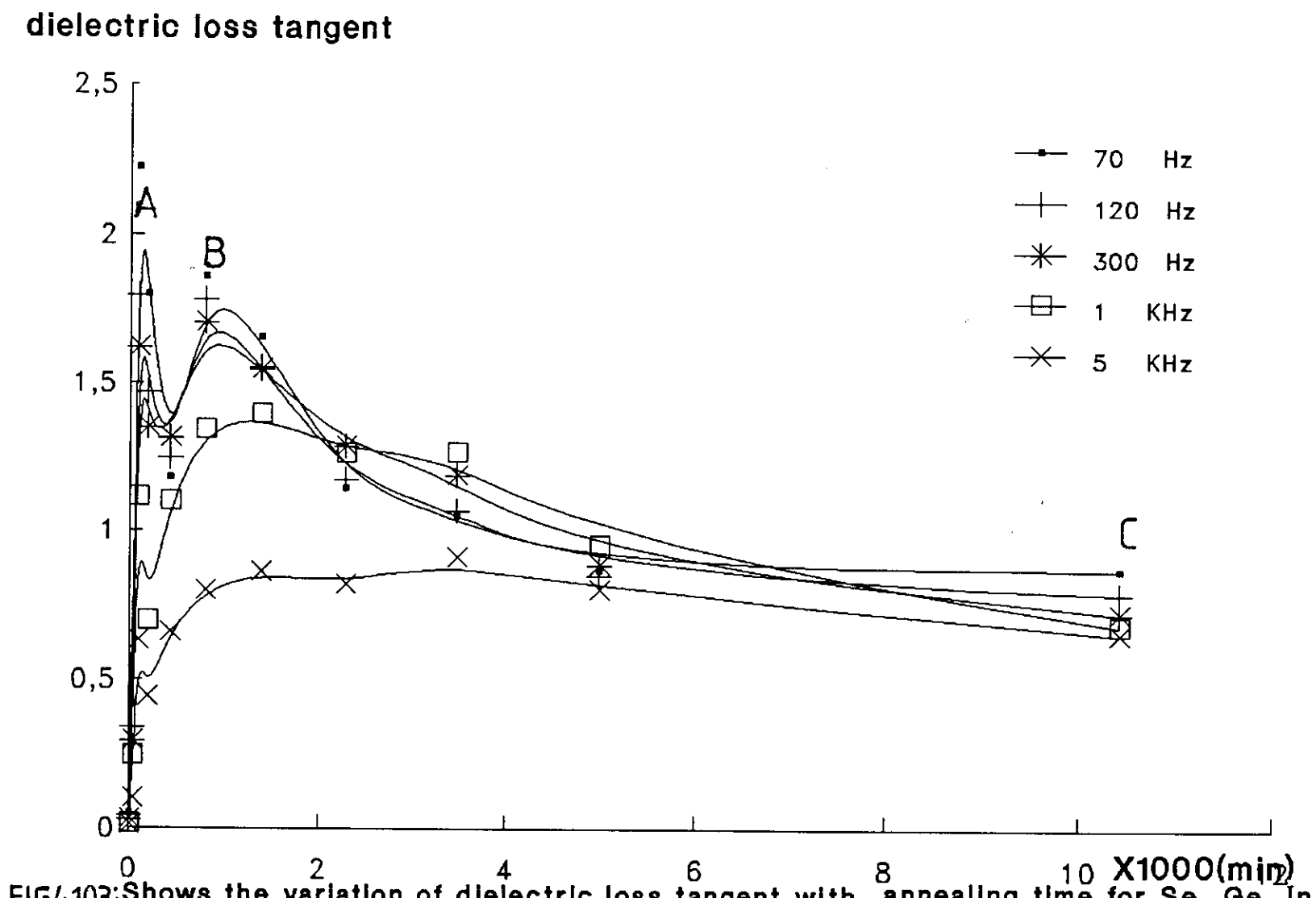

FIG4.103: Shows the variation of dielectric loss tangent with annealing time for $Se_{90}Ge_8In_2$ in the amorphous state and annealed at 120° C.

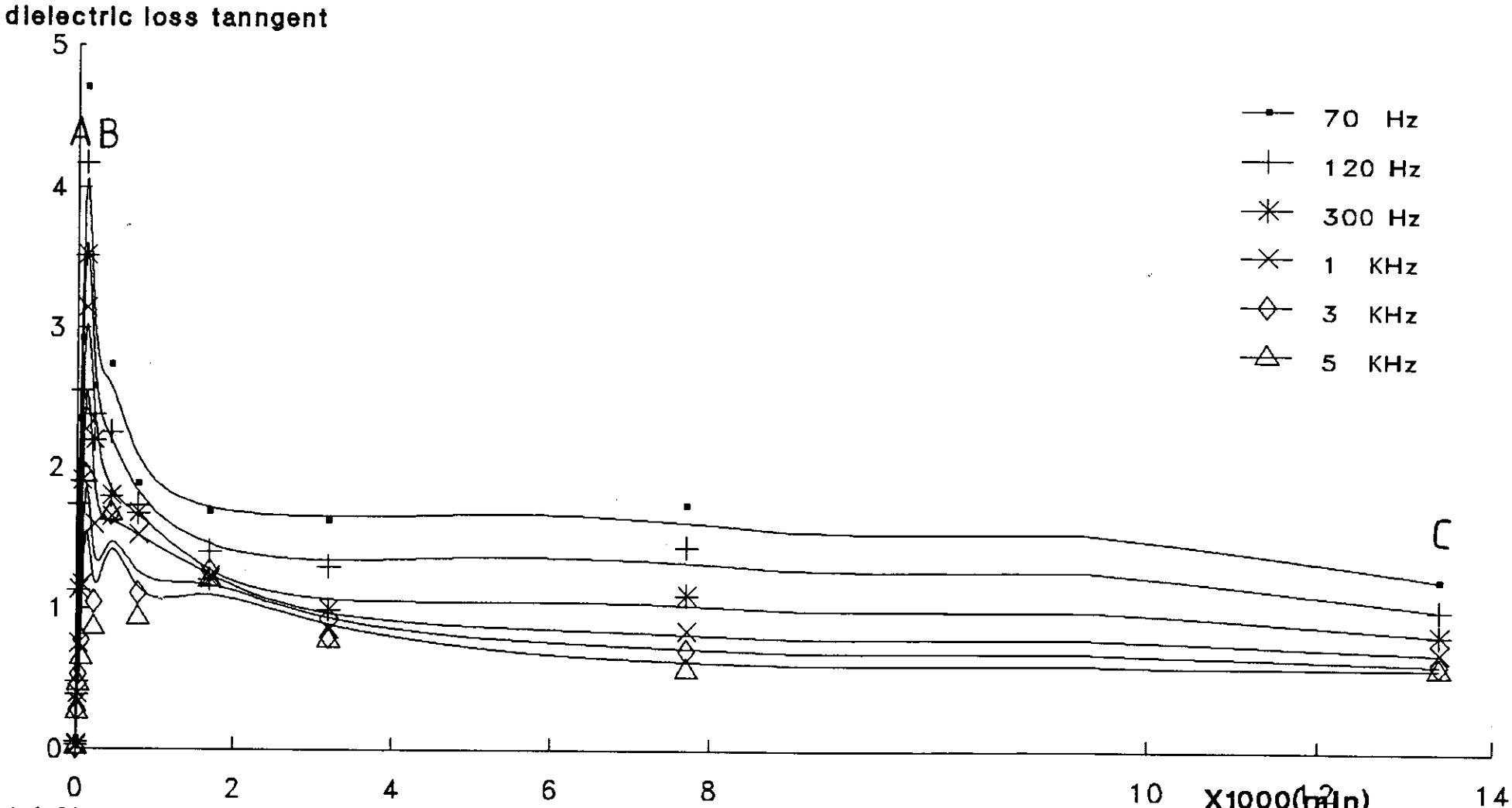

4.104: Shows the variation of dielectric loss tangent with a [redacted] nealing time for $Se_{90}Ge_8In_2$ at different constant frequencies and annealed at 13[redacted] C.

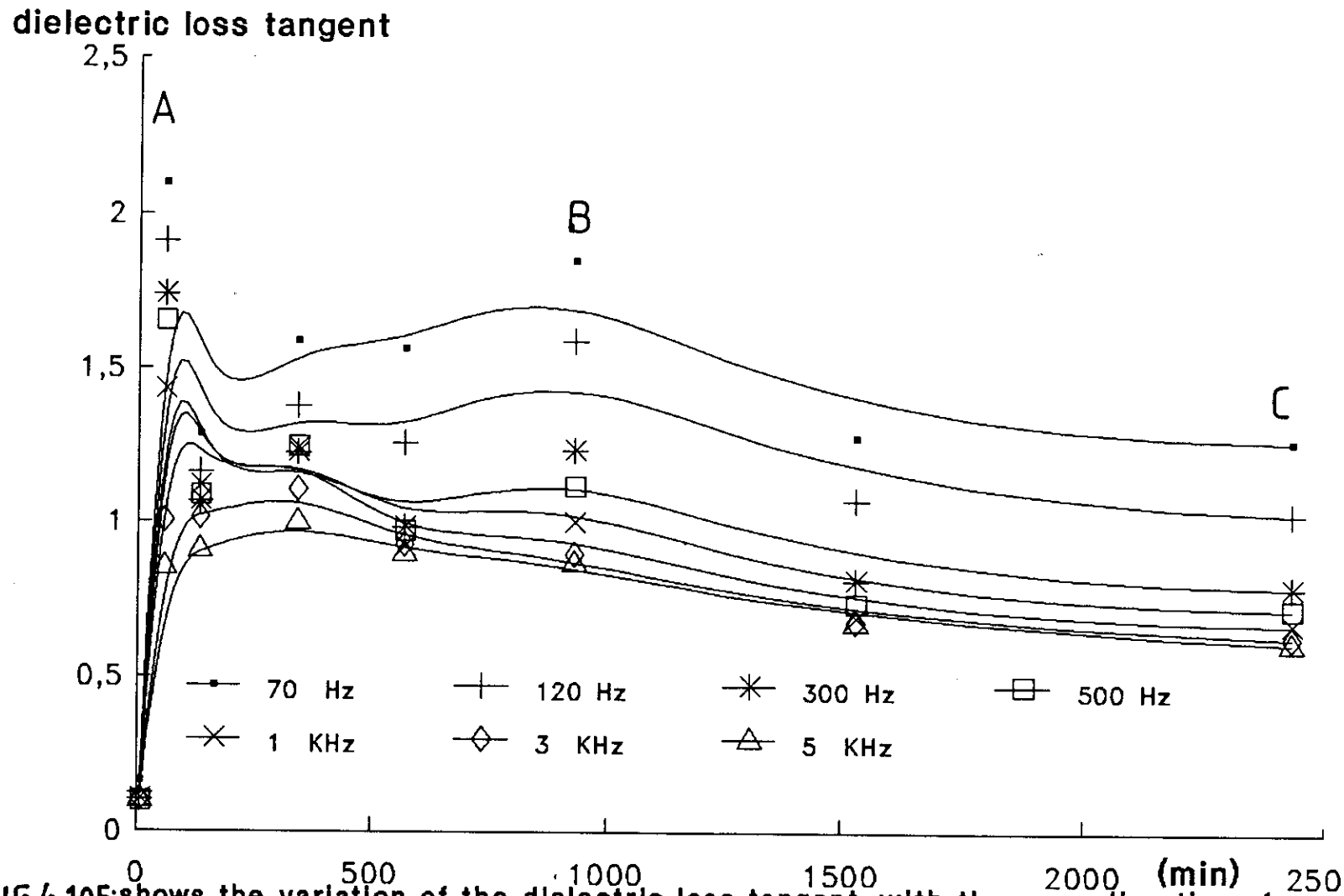

FIG.4.105: shows the variation of the dielectric loss tangent with the annealing time for $Se_{90}Ge_8In_2$ at different constant frequencies and annealed at 140°C.

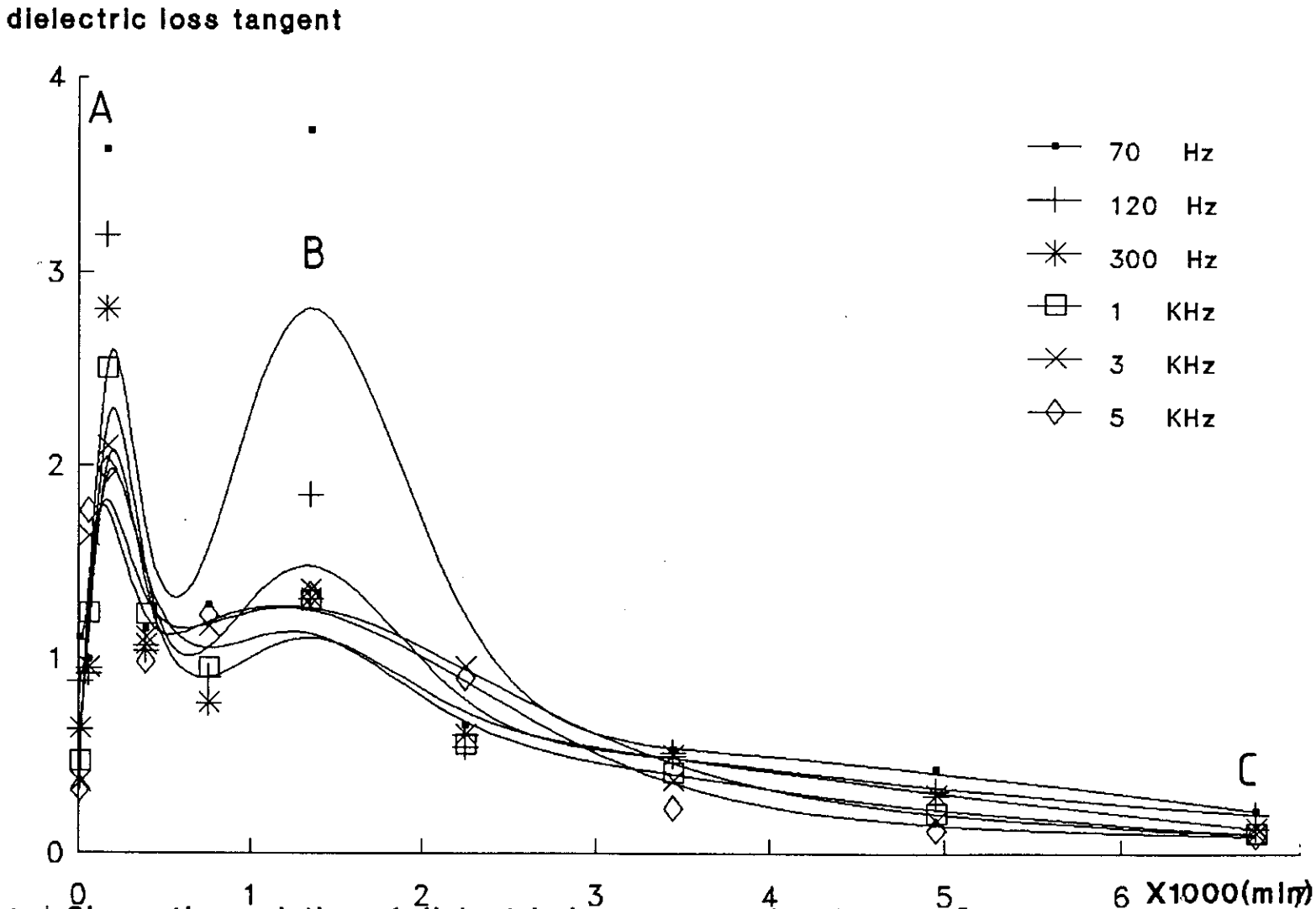

FIG.4.106: Shows the variation of dielectric loss tangent for $Se_{90}Ge_8In_2$ at different constant frequencies and annealed at 150° C.

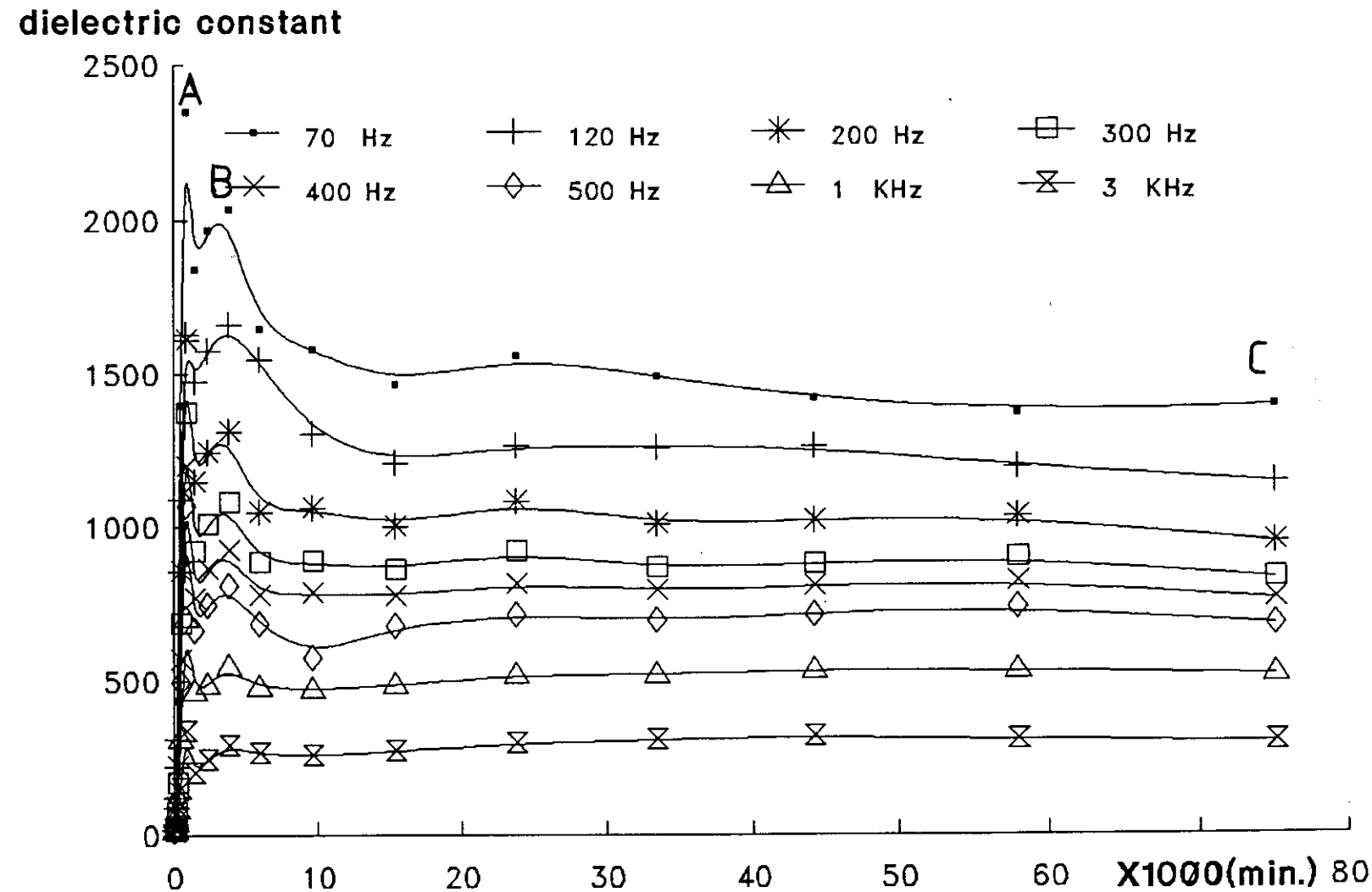

FIG.4.107: Shows the variation of the dielectric constant with the annealing time for the sample $Se_{90}Ge_6In_4$ and annealed at 120°C.

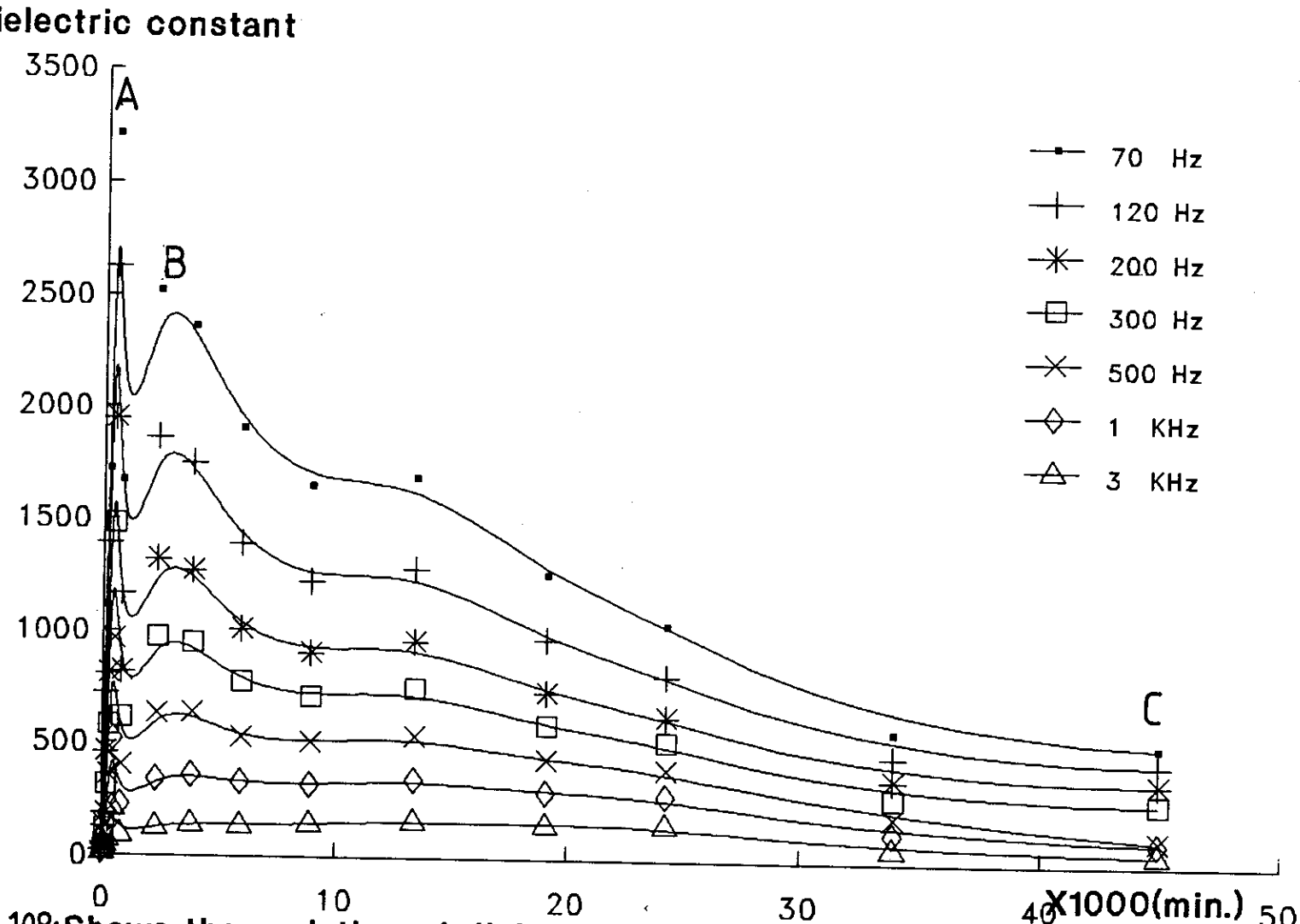

FIG.4.108: Shows the variation of dielectric constant with annealing time for $Se_{90}Ge_6In_4$ and annealed at 130°C.

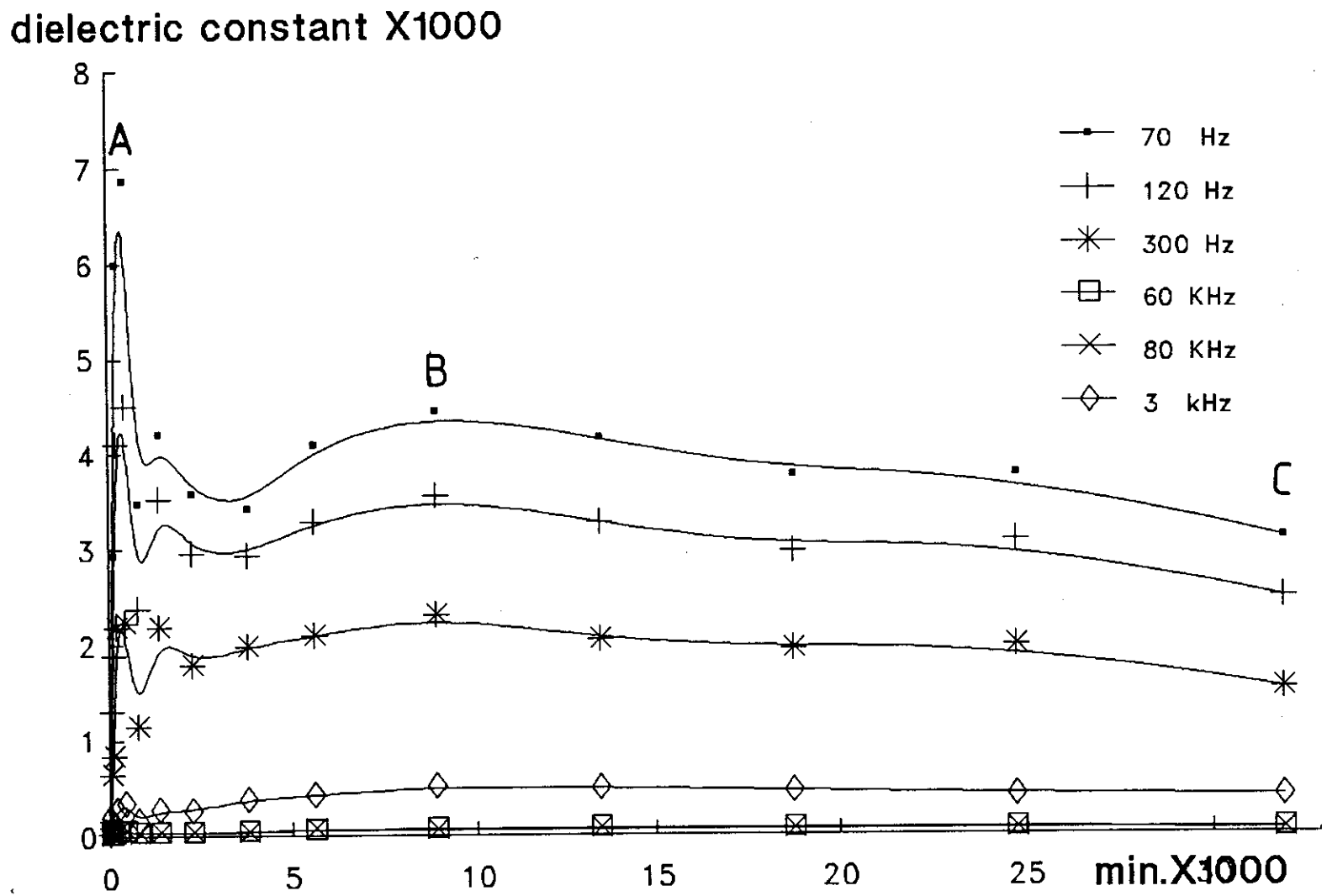

FIG.4.109: Shows the variation of dielectric constant with annealing time for $Se_{90}Ge_6In_4$ in the amorphous state and annealed at 140° C.

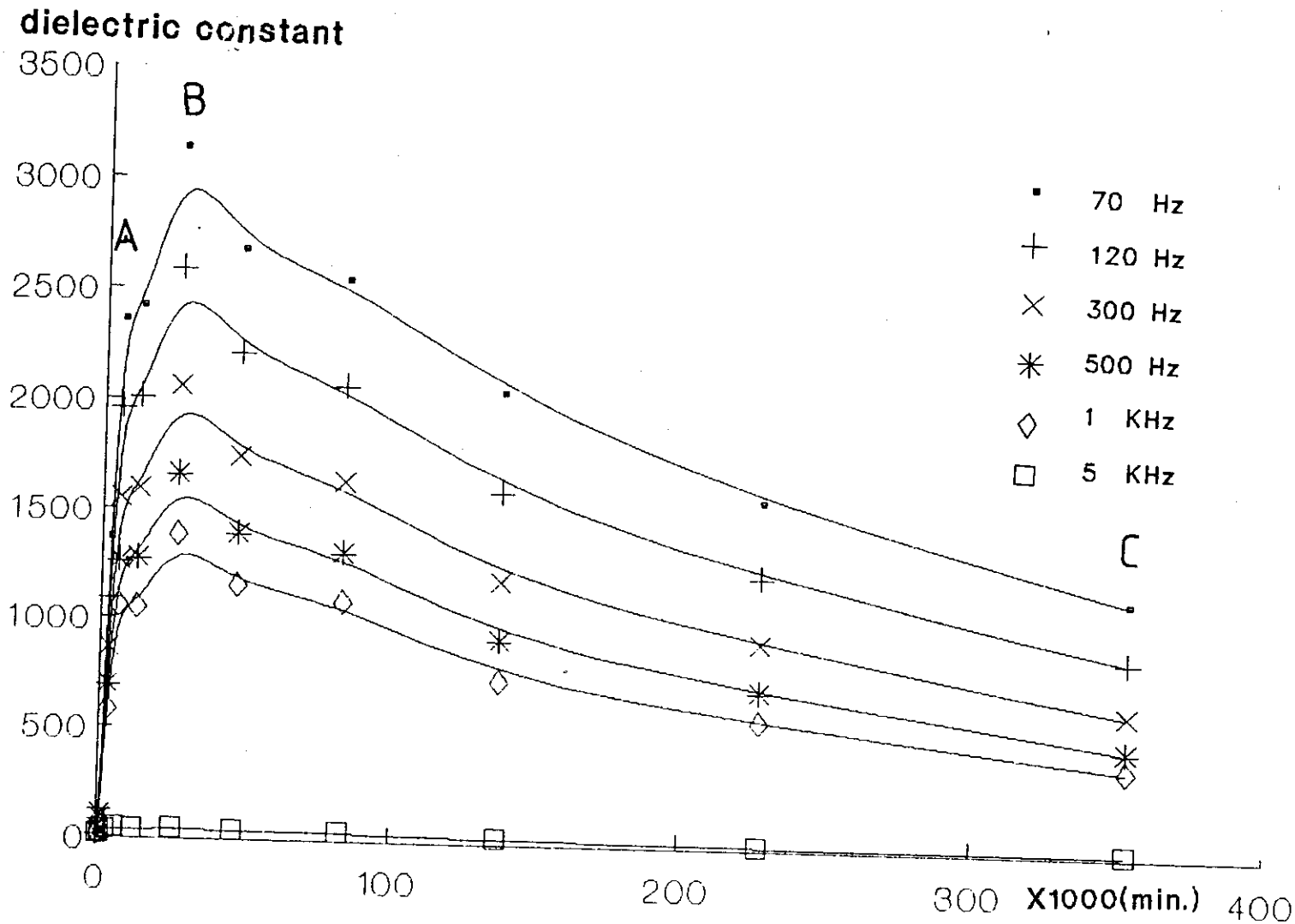

FIG.4.110: The effect of annealing time on the dielectric constant of $Se_{90}Ge_6In_4$ at annealing temperature 150°C and at different frequencies .

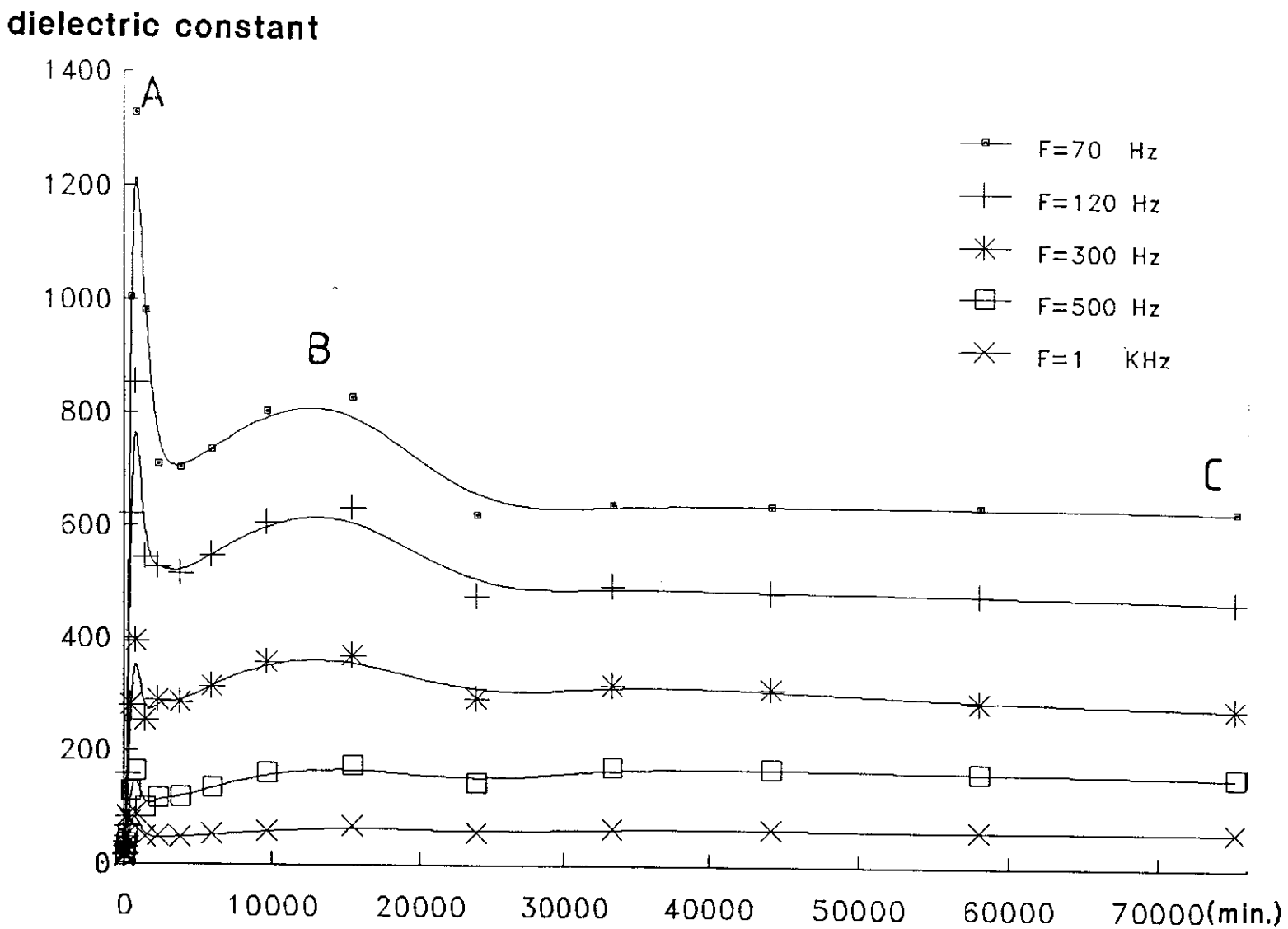

FIG.4.111: The effect of annealing time on the dielectric constant of $Se_{90}Ge_4In_6$ at annealing temperature 120° C.

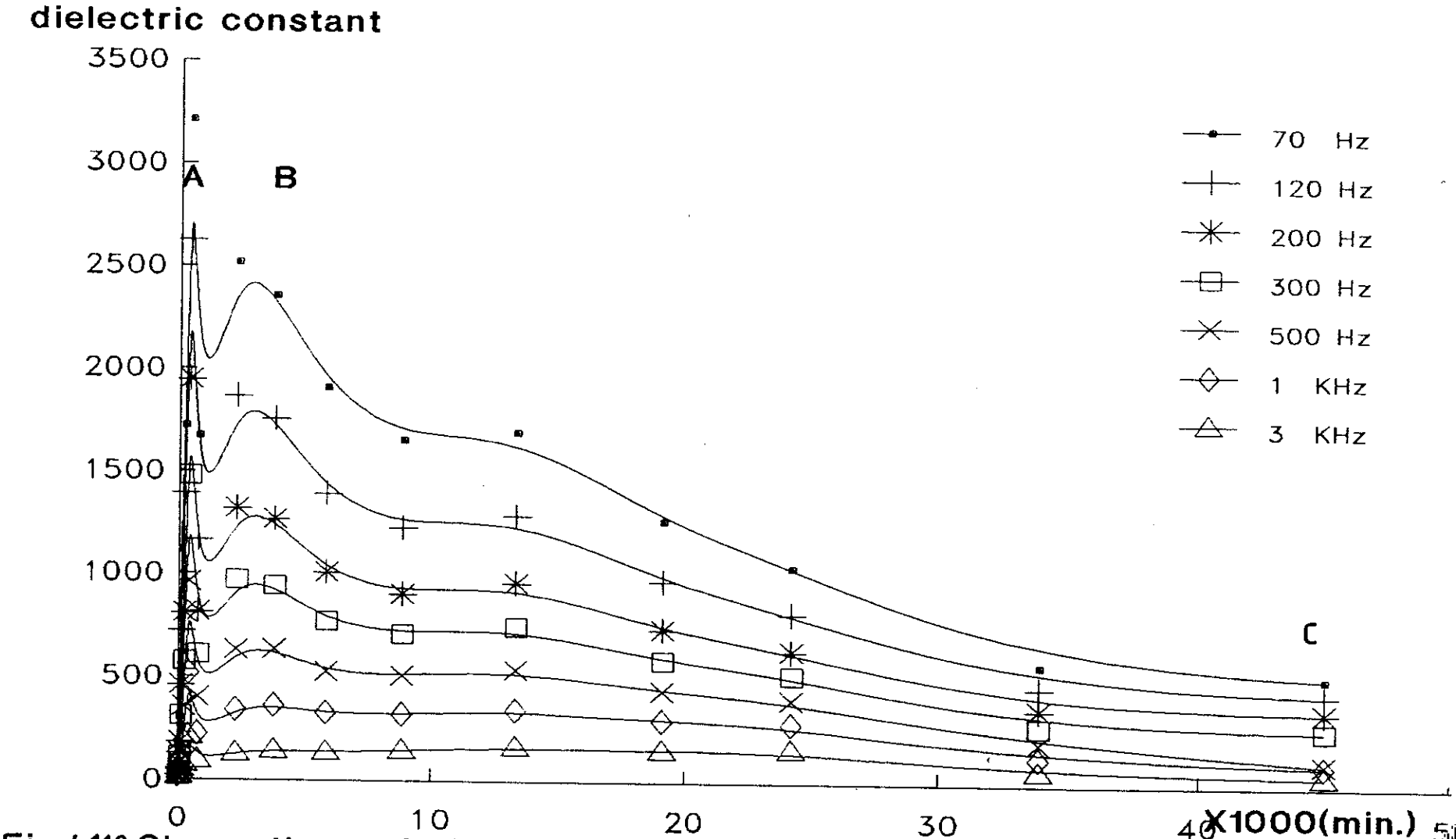

Fig.4.112: Shows the variation of dielectric constant with annealing time for $Se_{90}Ge_{4}In_{6}$ in glassy state and annealed at 130° C.

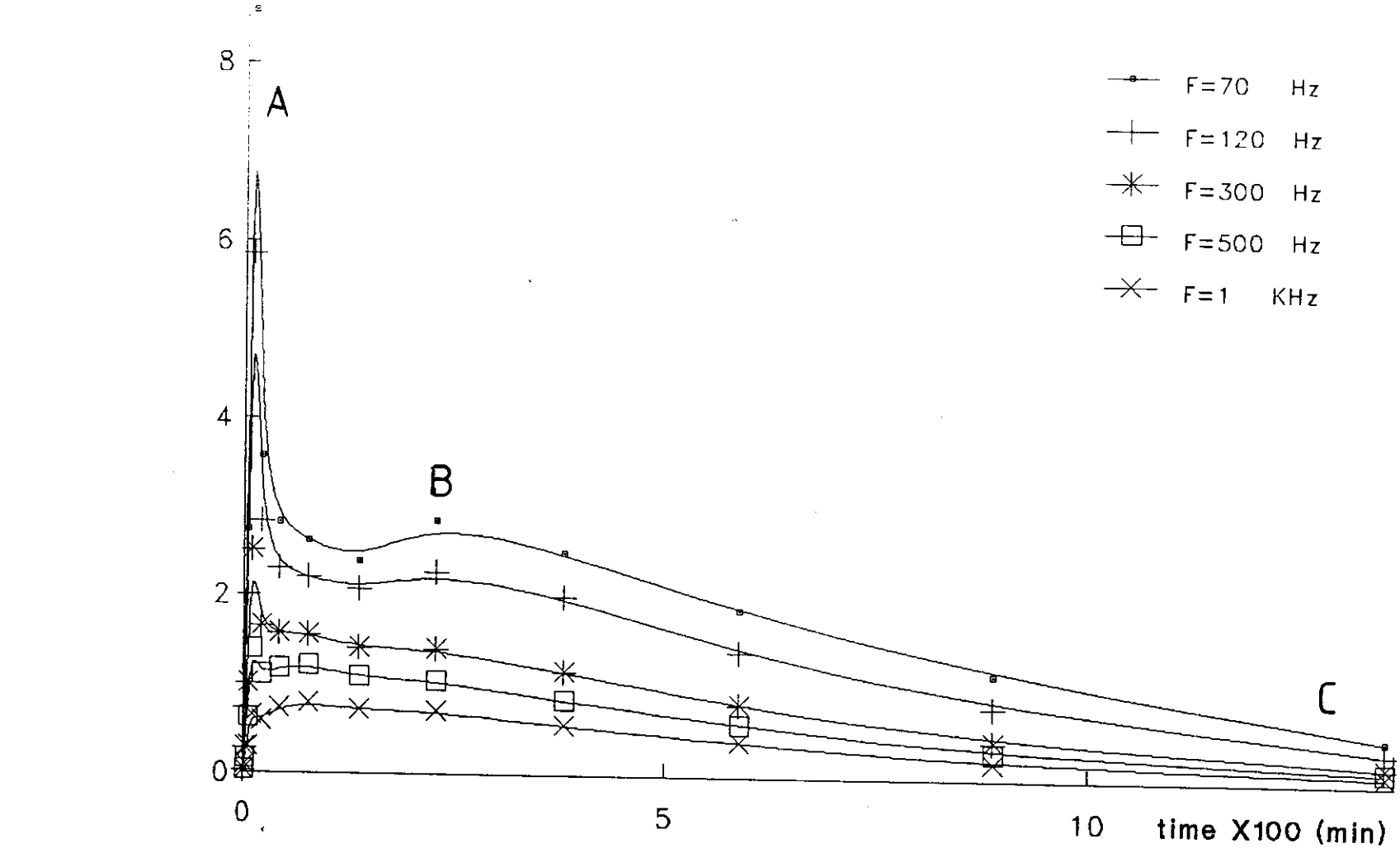

FIG. 4.13: The effect of annealing time on the dielectric constant of $Se_{90}Ge_4In_6$ bulk sample at annealing temperature 140°C .

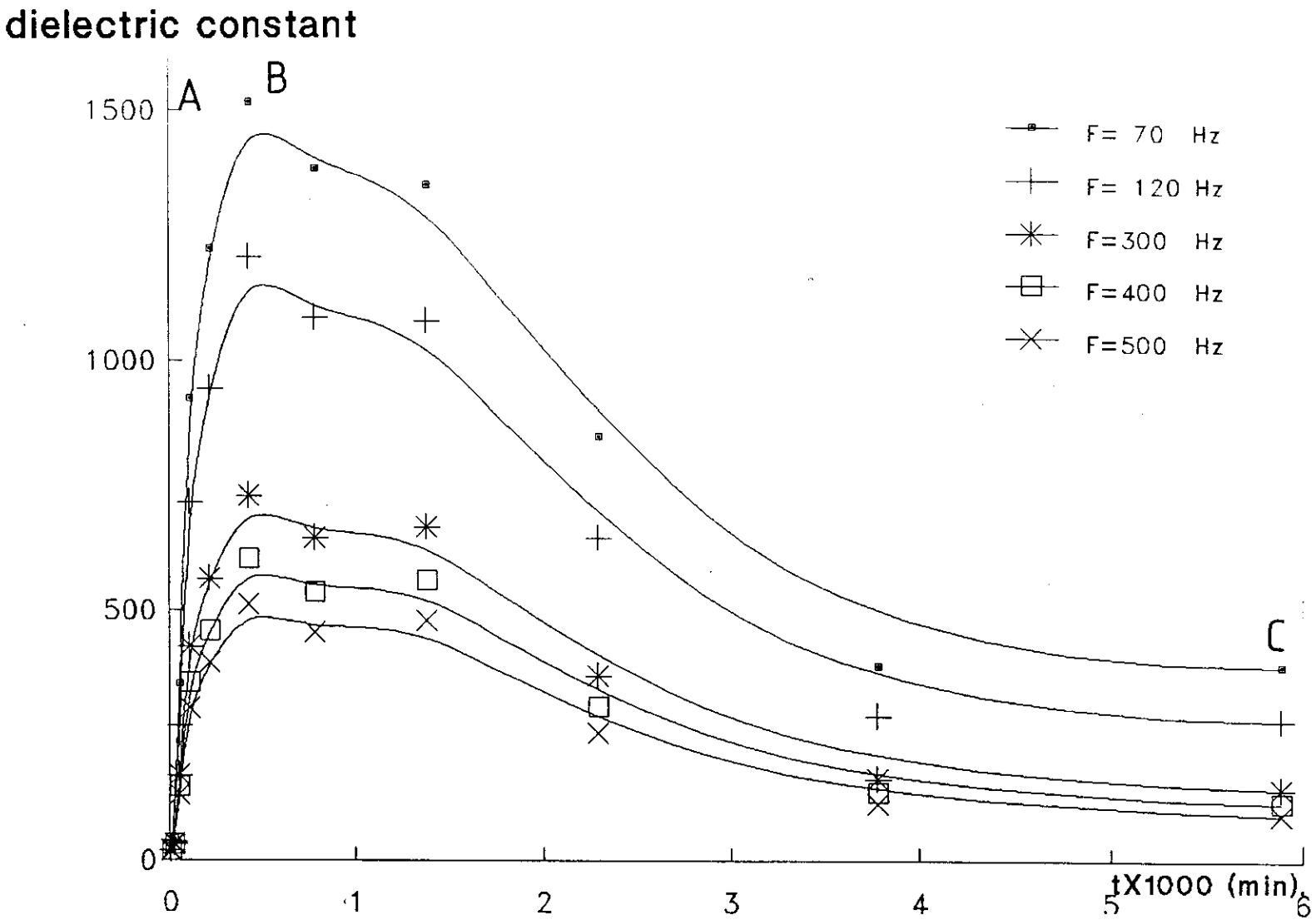

FIG.4.14: The effect of annealing time on the dielectric constant of $Se_{90}Ge_4In_6$ bulk sample annealed at 150°C.

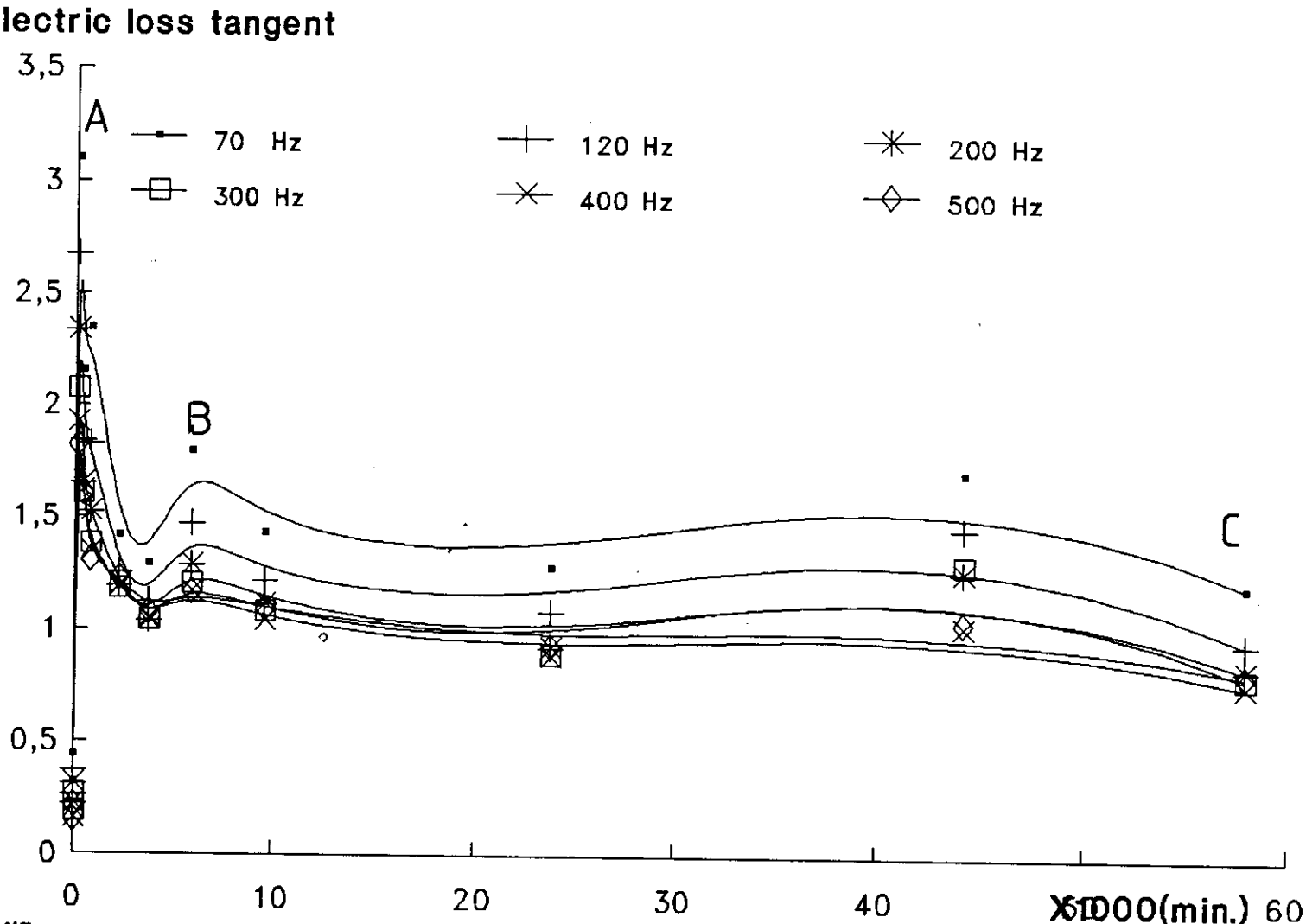

fig.4 115: Shows the variation of dielectric loss tangent with annealing time for $Se_{90}Ge_6In_4$ annealed at 120° C.

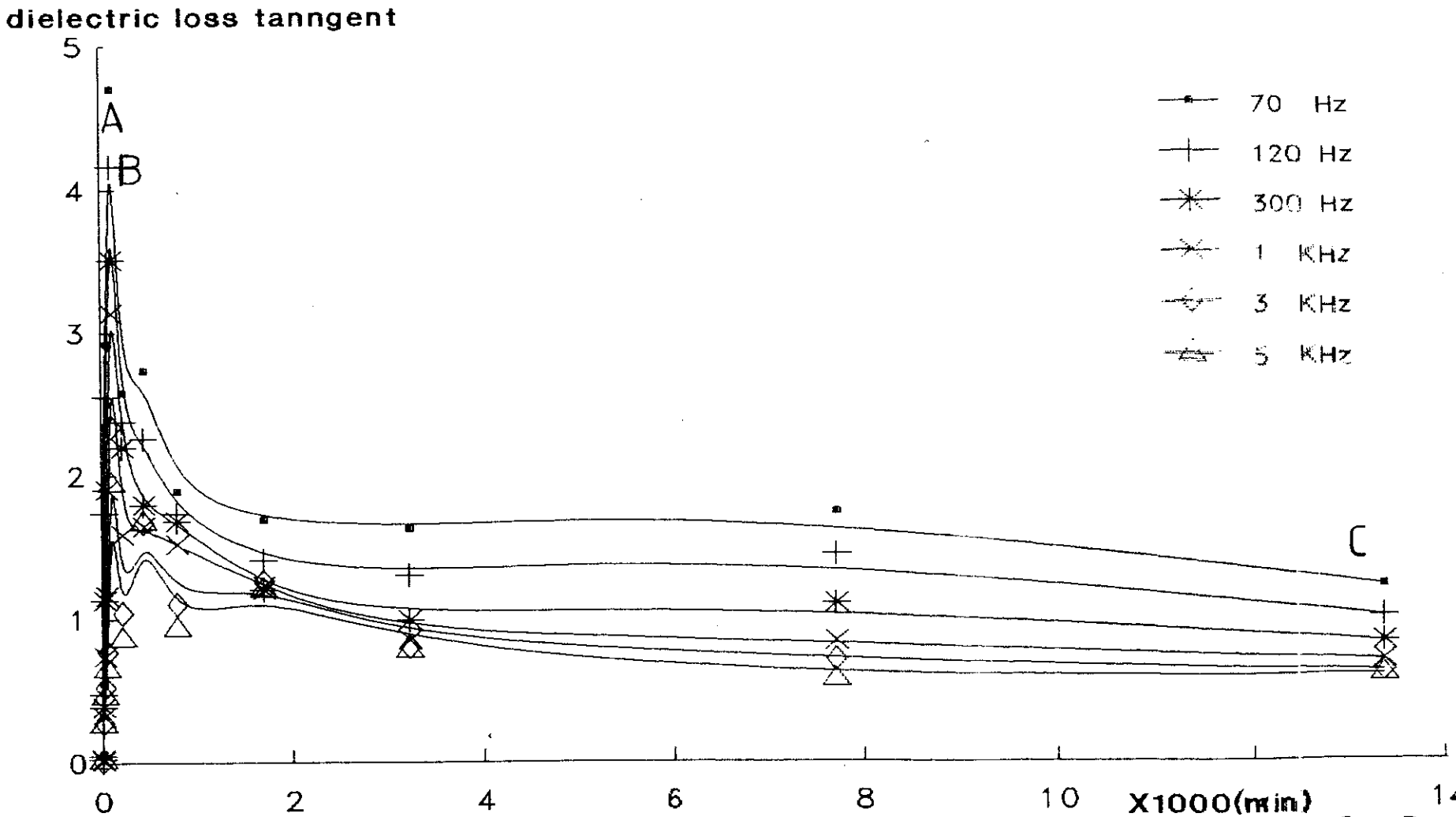

fig.4.116:Shows the variation of dielectric loss tangent with annealing time for $Se_{90}Ge_6In_4$ at different constant frequencies and annealed at 130° C.

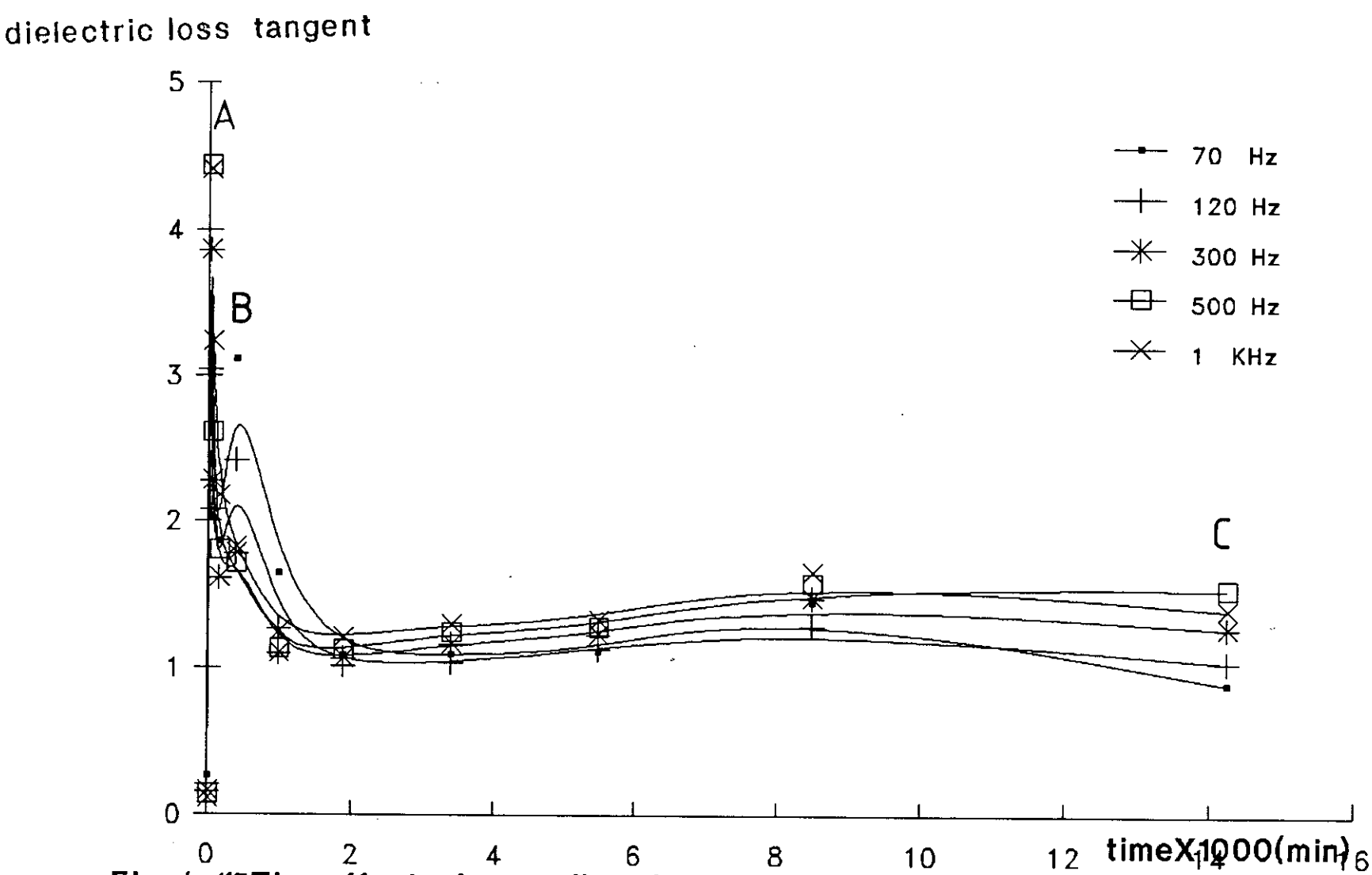

Fig. 4.117: The effect of annealing time on the dielectric loss tangent of the sample $Se_{90}Ge_6In_4$ at annealing temperature 140° C.

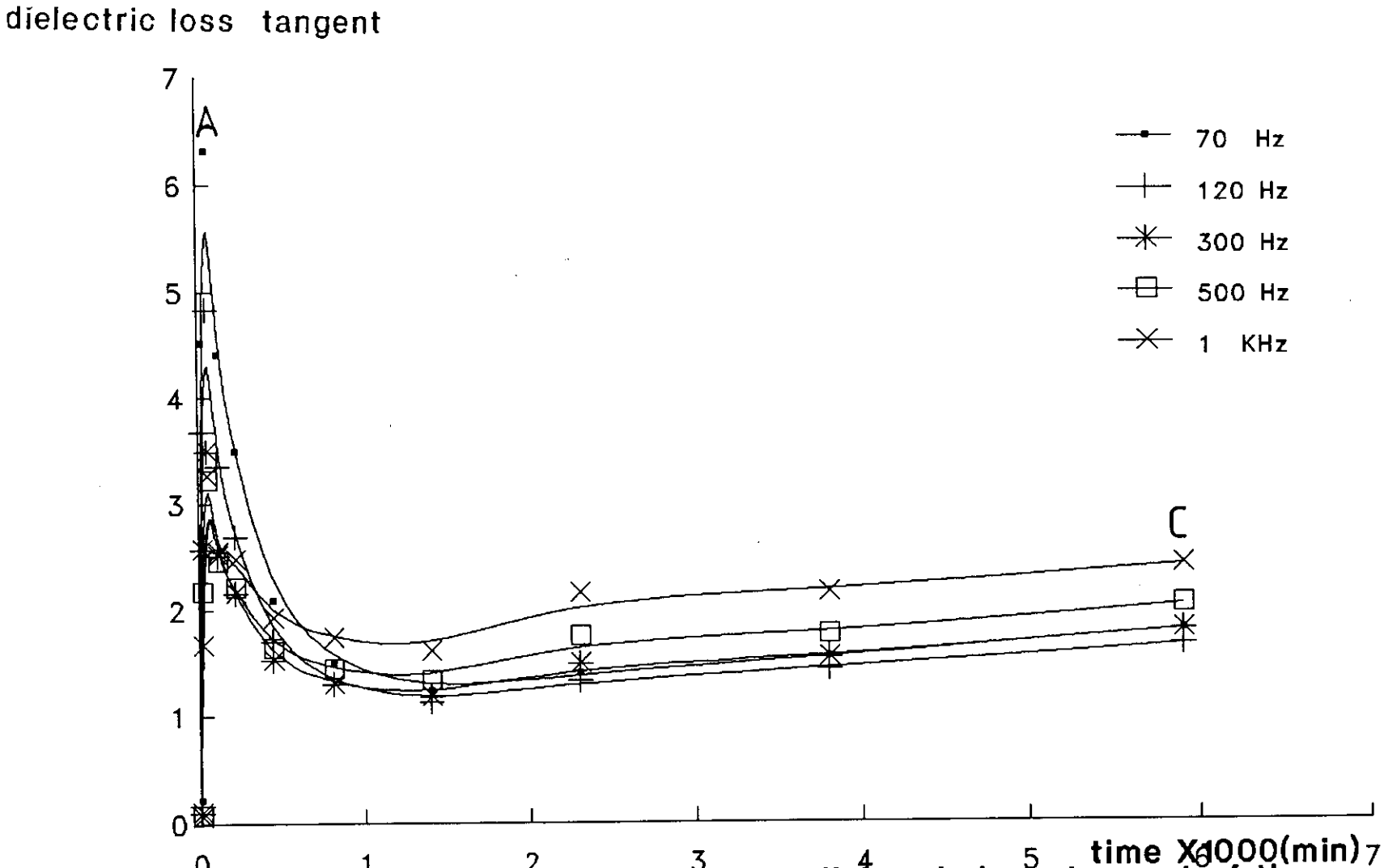

Fig.4.118: The effect of annealing time on the dielectric loss tangent of the sample $Se_{90}Ge_6In_4$ at annealing temperature 150° C.

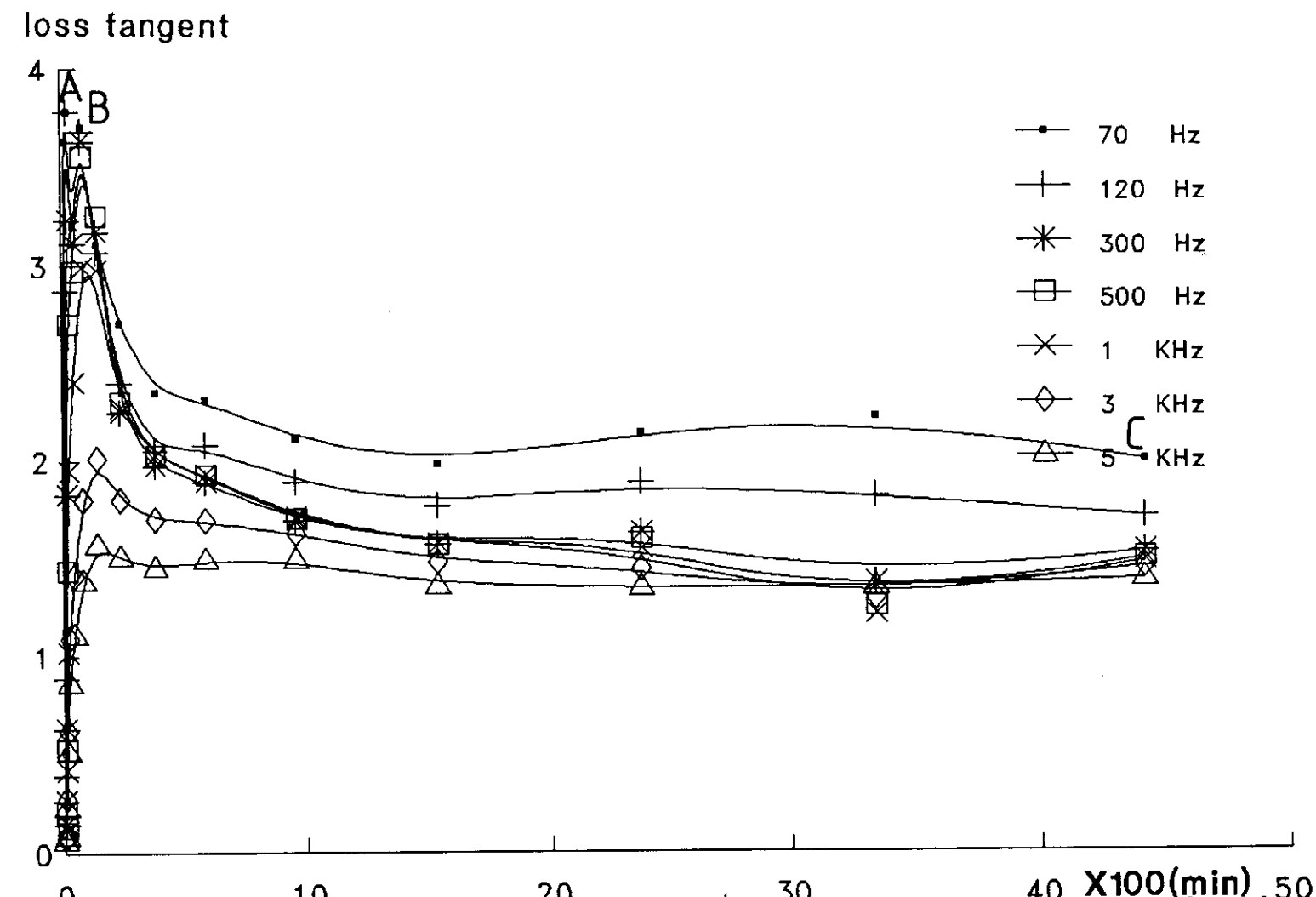

Fig 4.119: The effect of annealing time on the dielectric loss tangent for the sample $Se_{90}Ge_4In_6$ at different constant frequency and annealed at 120° C.

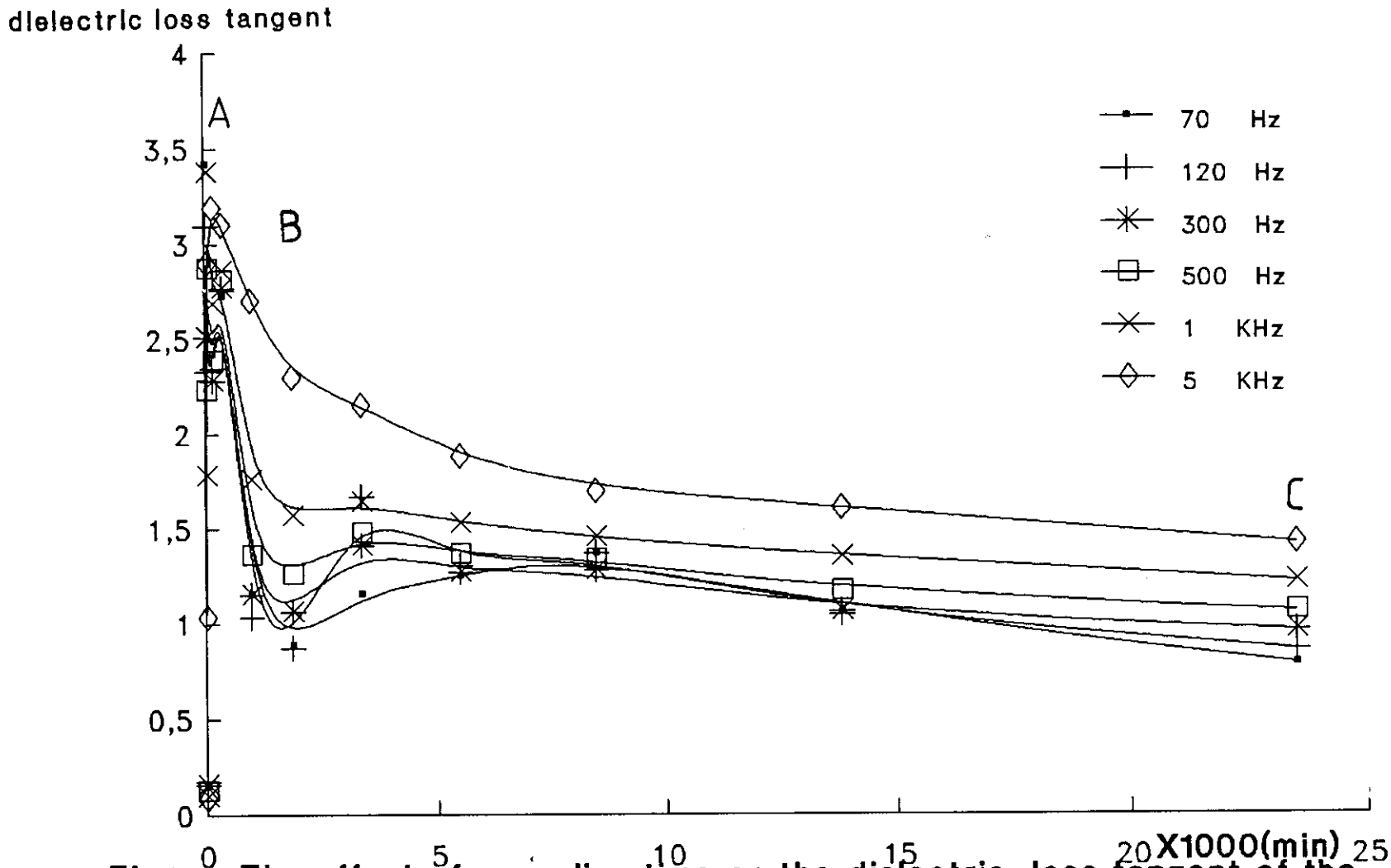

Fig.4.120:The effect of annealing time on the dielectric loss tangent of the sample $Se_{90}Ge_4In_6$ at different constant frequency and annealed at 140° C.

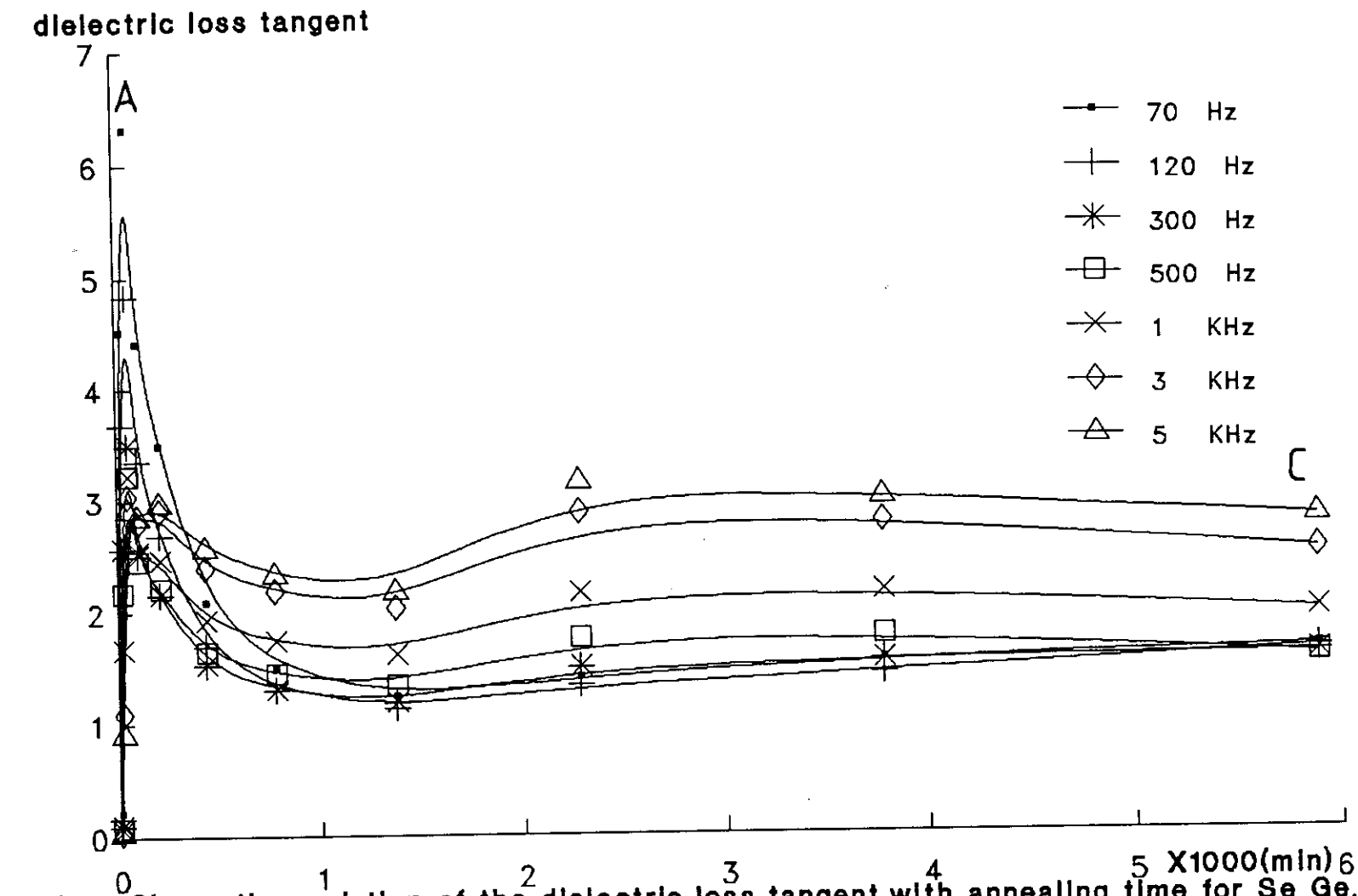

fig-4.122: Shows the variation of the dielectric loss tangent with annealing time for $Se_{90}Ge_4In_6$ at different constant frequencies and annealed at 150°C.

Figs.(4.107-4.114,4.115-4.122)show similar results for the samples $Se_{90}Ge_6In_4$ and $Se_{90}Ge_4In_6$ at the same crystallization temperatures.

4.4.1.ISOTHERMAL CRYSTALLIZATION KINETICS OF Se_{90} Ge_{10-x} In_x :

The isothermal kinetics of the system $Se_{90}Ge_{10-x}In_x$ can be expressed in terms of the transformed fraction, α, at different times. The crystallized fraction at time,t,is given by the formula:(113)

$$\alpha = P_t\text{-}P_g/P_c\text{-}P_g \qquad (4.2)$$

Where P_g and P_c are the measured physical properties at the beginning and ending of the crystallization process respectively. P_t is the physical properties at time, t, between P_c and P_g. Equation(4.2) can be applied to calculate the kinetic parameters of the amorphous-crystalline transformation during the period B-C of figs.(4.99-4.122).

4.4.2.CRYSTALLIZATION KINETICS USING THE CHANGE IN THE DIELECTRIC CONSTANT AND DIELECTRIC LOSS TANGENT:

To calculate the kinetic parameters of amorphous crystalline transformation, equation(4.2) has been applied to the curves of figs.(4.99-4.122)in the region between B and C. The analysis of the crystallization process has been carried out using Avrami equation:[97,98]

$$1-\alpha = \theta = \exp(-K\, t^{n}) \qquad (4.3)$$

Where,

θ ; is the untransformed fraction of the sample, K is the crystallization rate depending on the nucleation and growth rate,and ,n, is a constant depending on the mechanisms of nucleation and growth. The crystallization fraction, α, was computed for every sample at every crystallization temperature at different annealing times and at two different constant values of frequency for the system $Se_{90}\ Ge_{10-x}\ In_{x}$ (X=2,4 and 6). The values of n were obtained from the slope of the plot ln(-ln θ) against ln(t)[figs.4.123-4.125 for ε and 4.126-4.128 for tan(δ)],according to the equation :-

$$\ln(-\ln\theta) = \ln K + n \ln (t) \qquad (4.4)$$

The values of " n "associated with (ε)and tan(δ) are tabulated

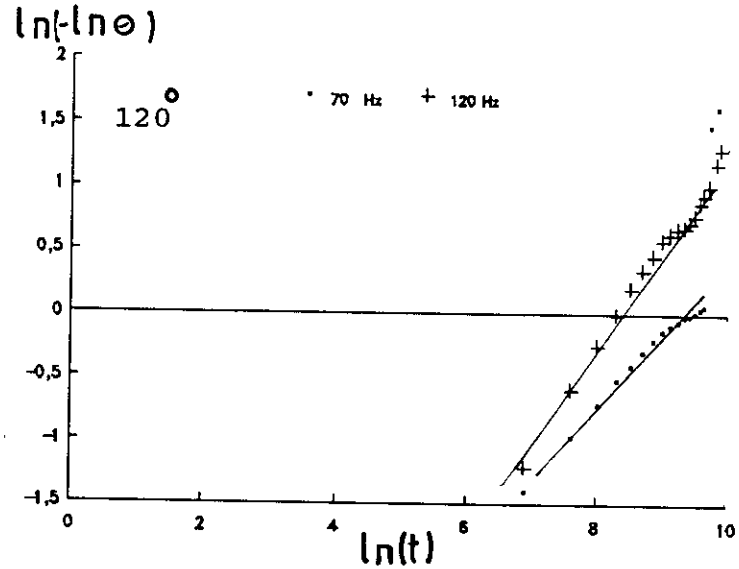

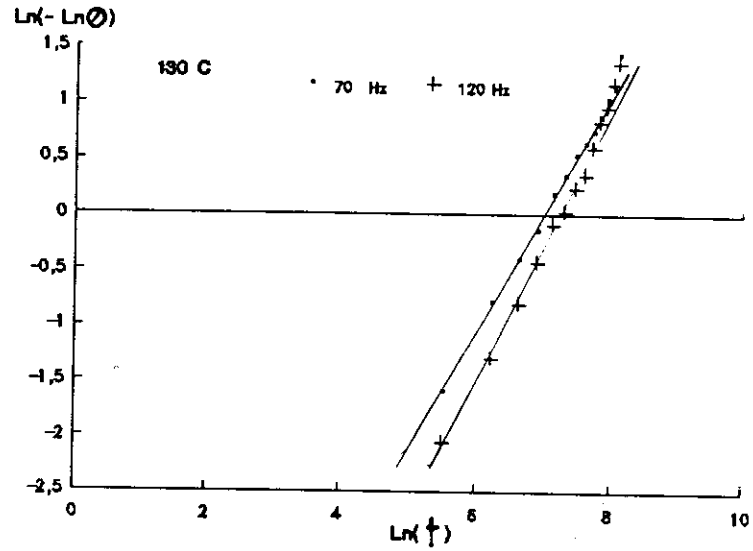

Fig.4.123:The variation of Ln(-Lnθ) with Ln(t) at different annealing temperature for the sample $Se_{90}Ge_8In_2$.

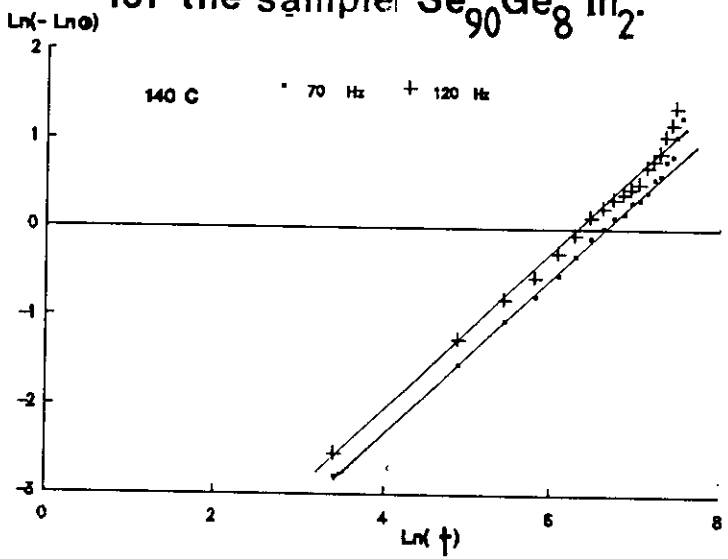

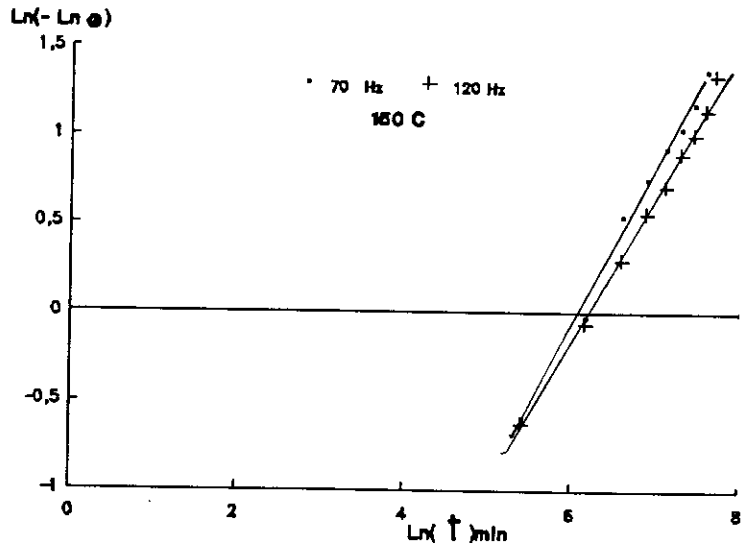

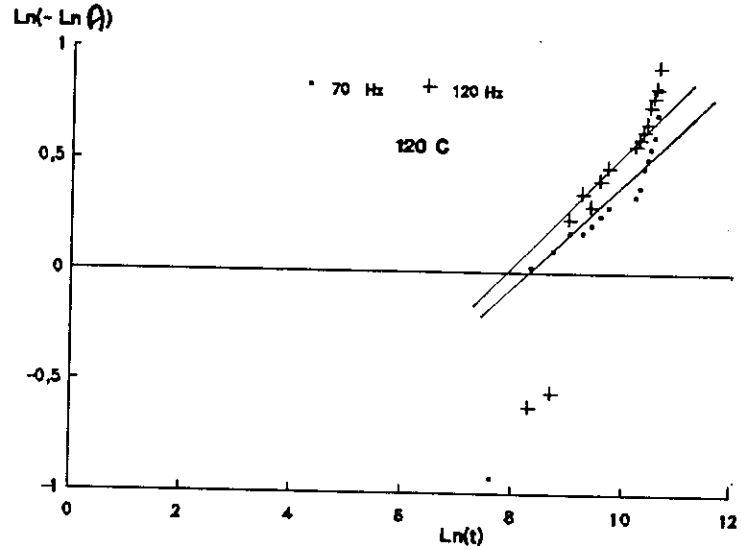

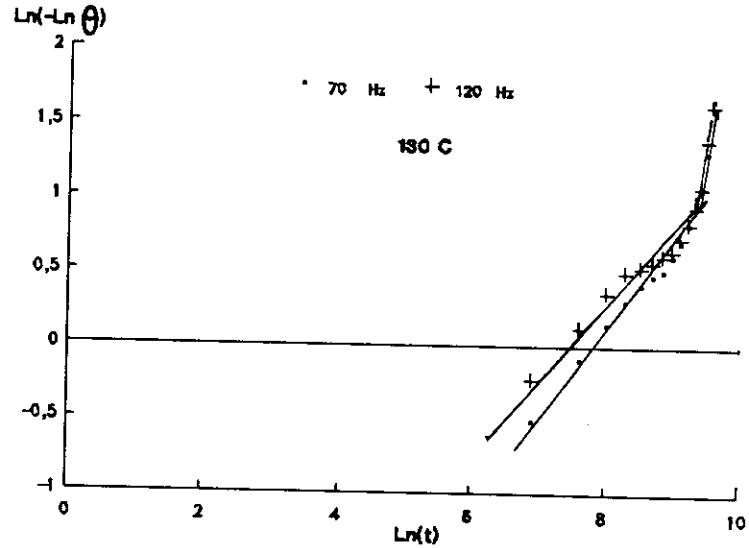

Fig.4.124:The variation of Ln(- Ln θ)with Ln(t) at different annealing temperature for the sample $Se_{90}Ge_6In_4$.

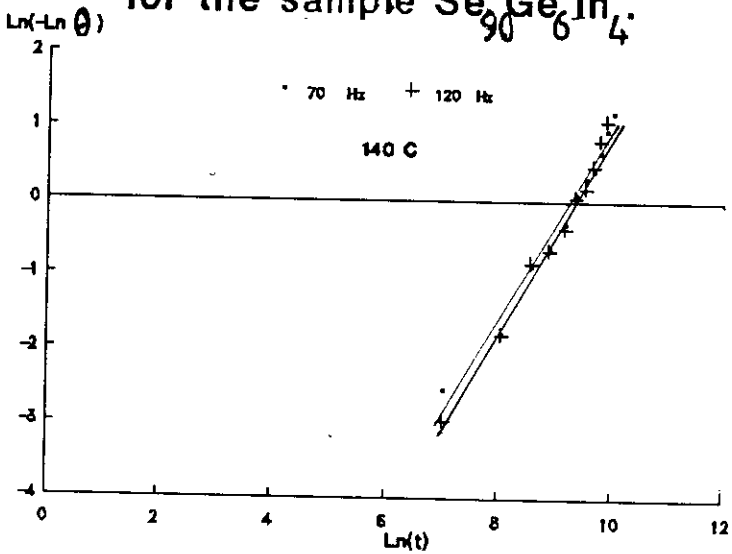

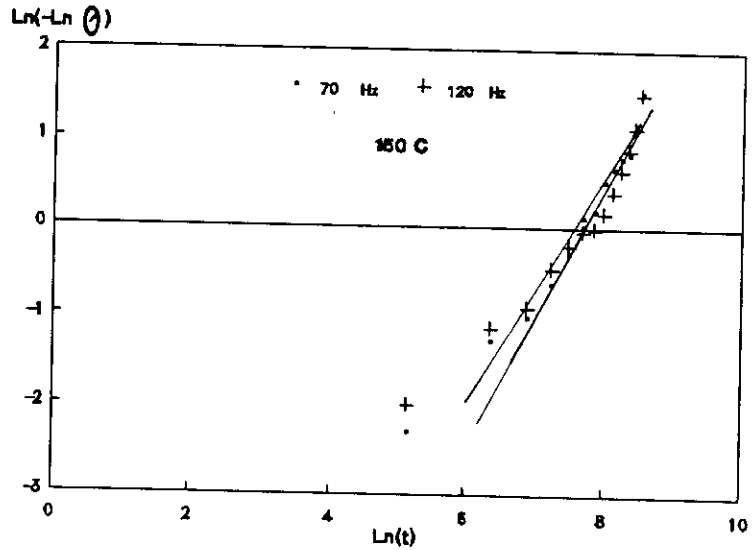

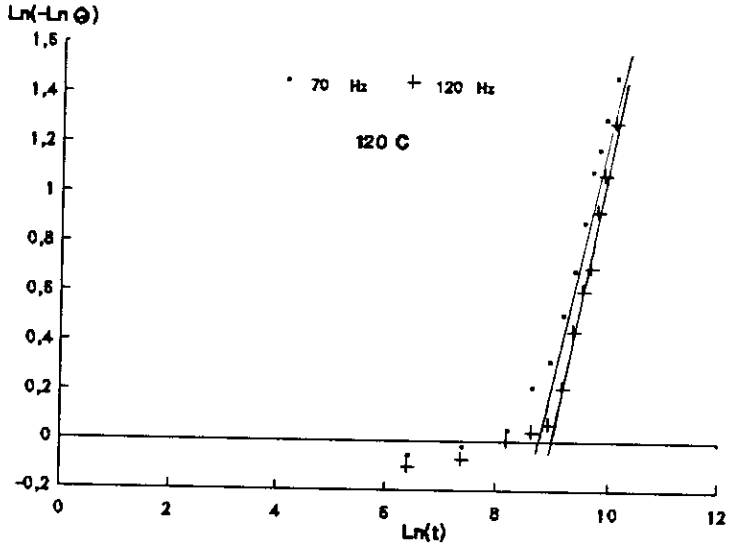

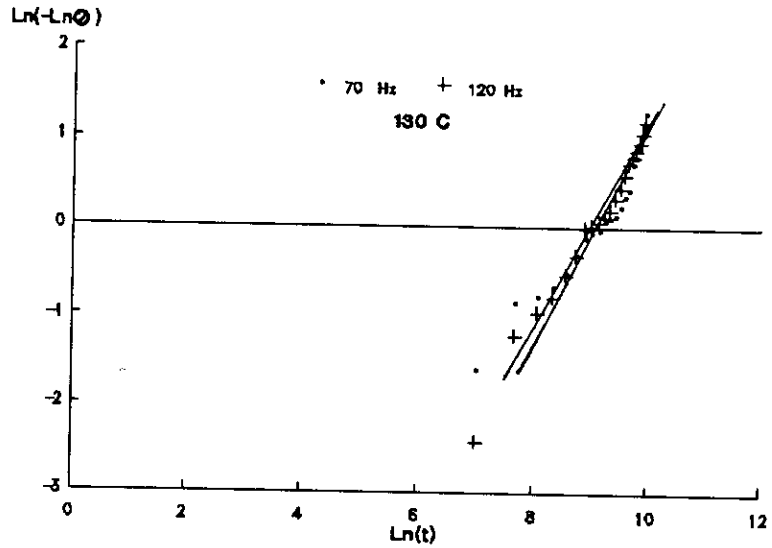

Fig.4.25: The variation of Ln(-Ln θ)with Ln(t) at different annealing temperature for the sample $Se_{90}Ge_4In_6$.

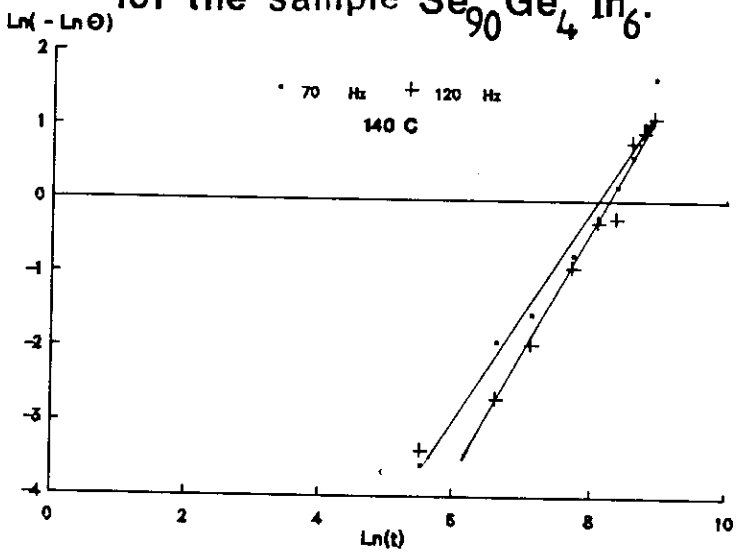

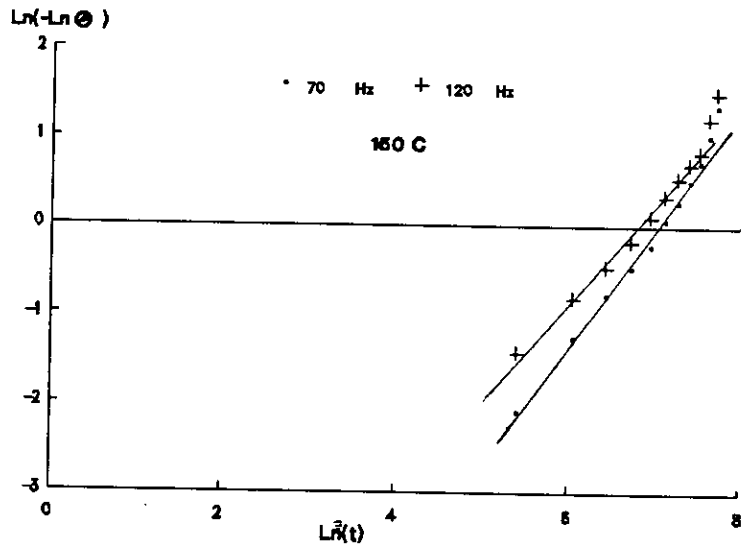

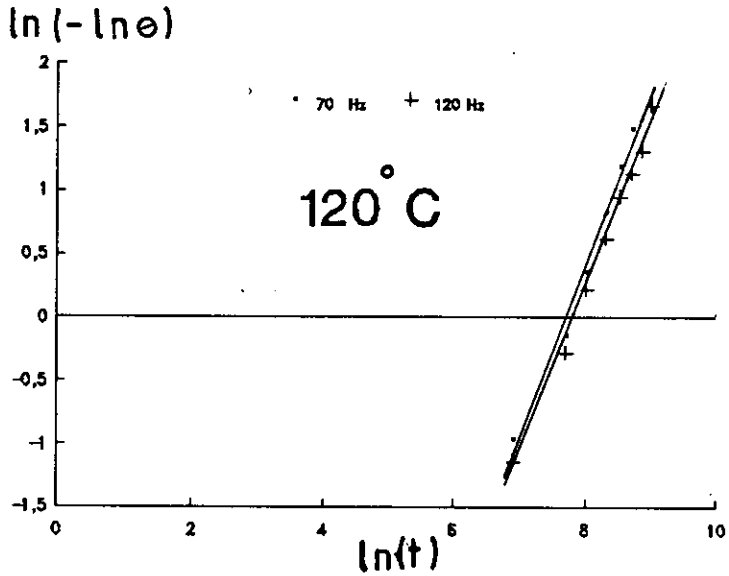

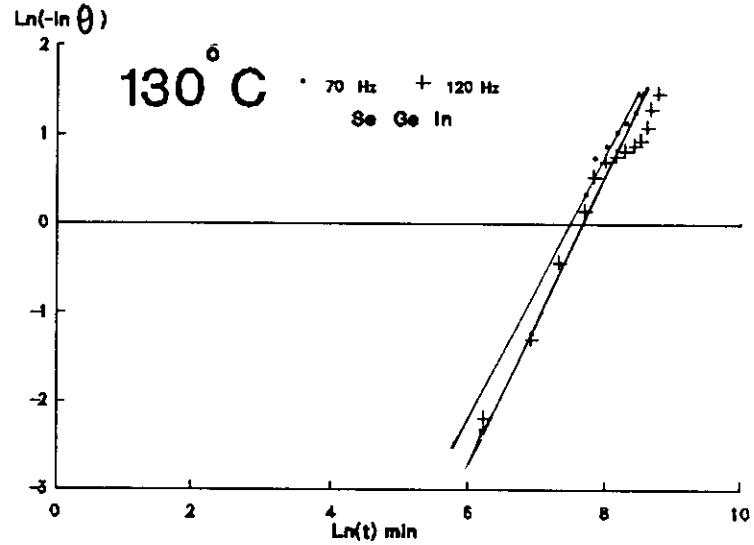

Fig4.126:The variation of Ln(-Lnθ) with Ln(t) at different annealing temperature and constant frequency for the sample $Se_{90}Ge_8In_2$.

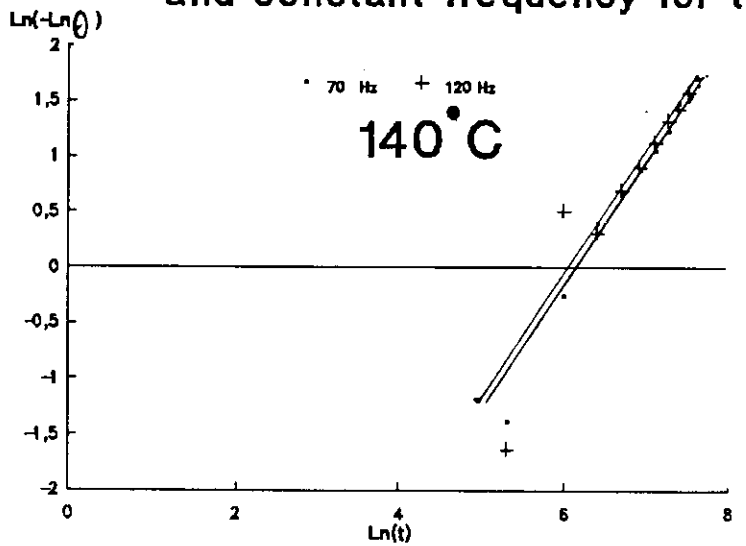

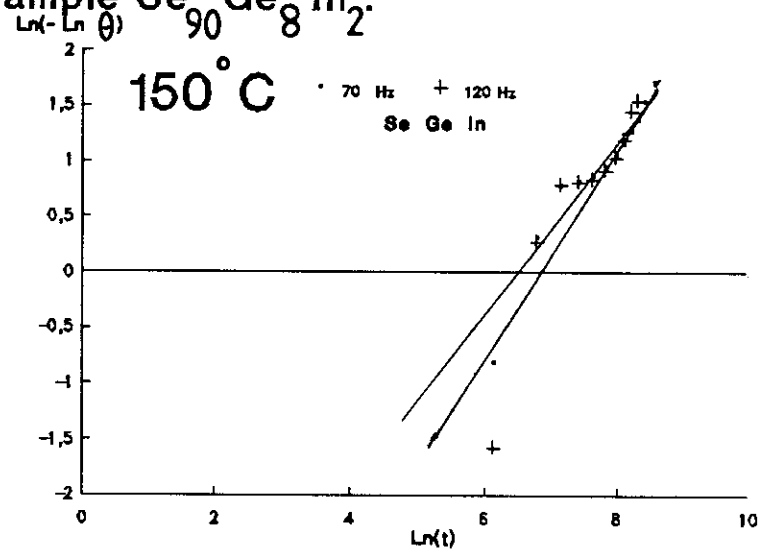

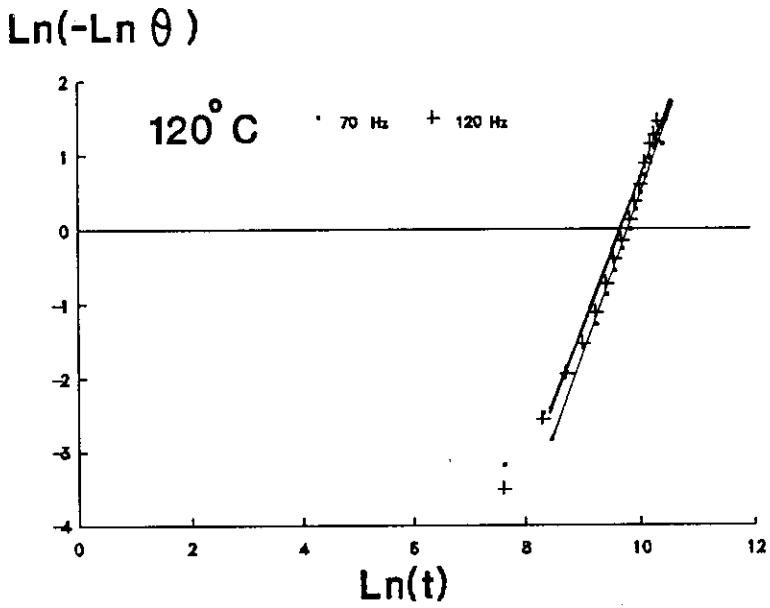

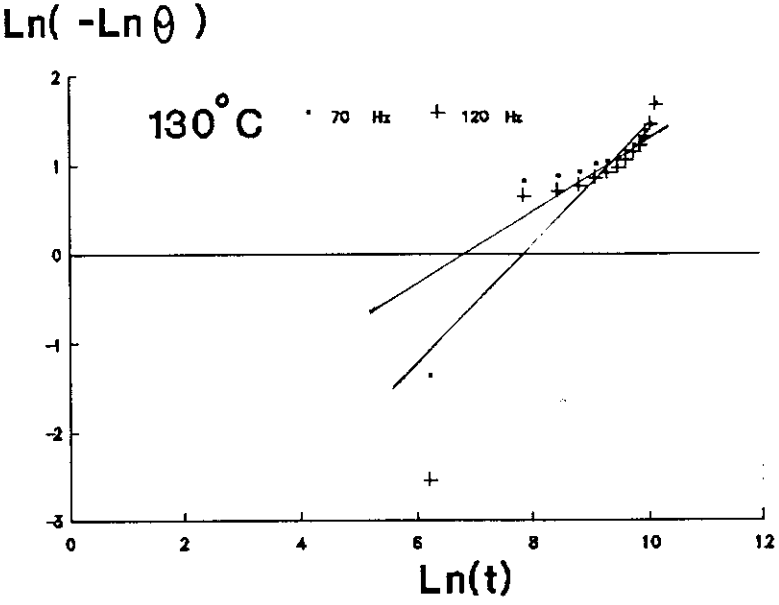

Fig 4.127: The variation of Ln(-Ln θ) with Ln(t) at different annealing temperature for the sample $Se_{90}Ge_6In_4$.

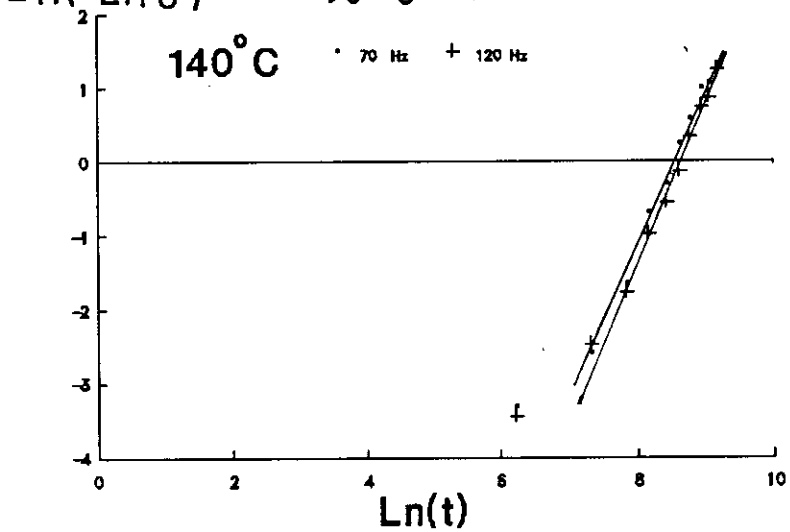

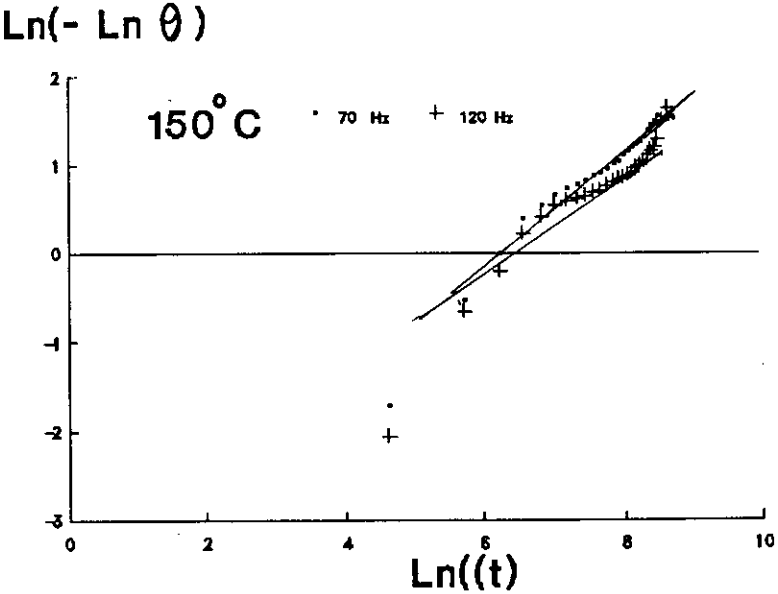

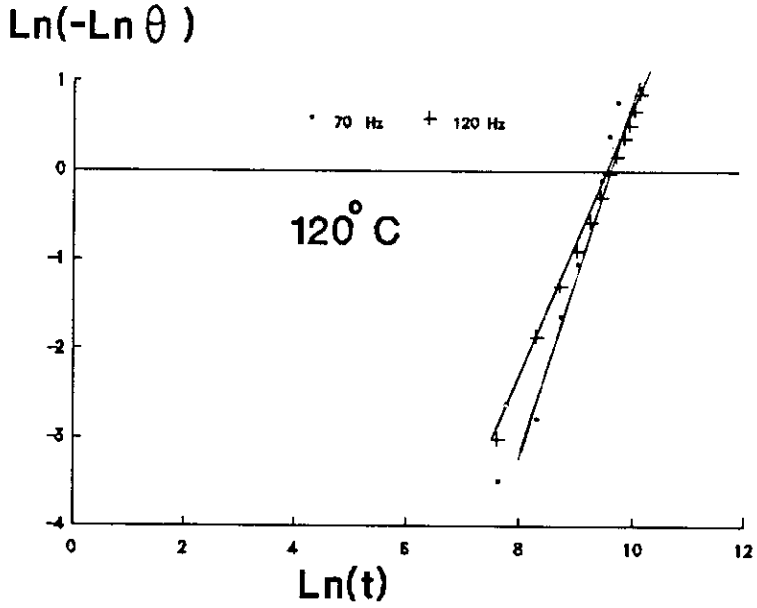

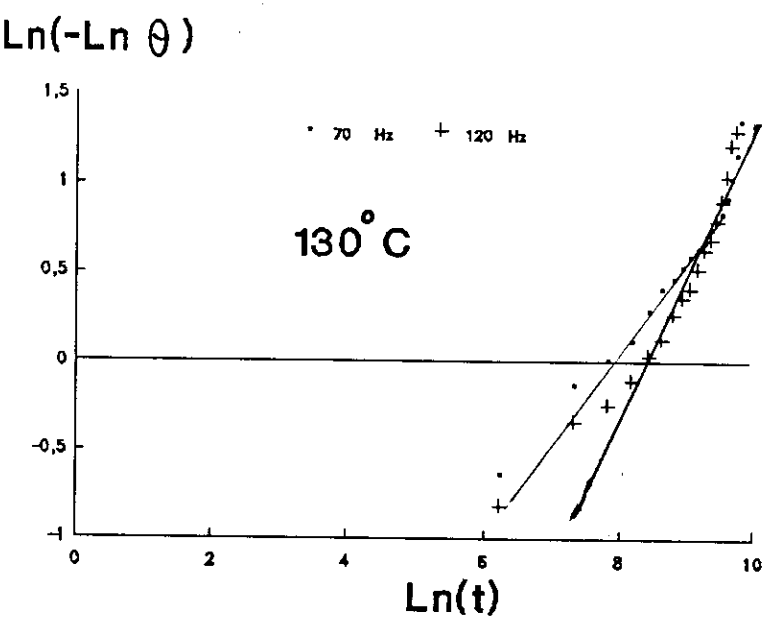

Fig.4.12: The vaelation of Ln(-Lnθ) with Ln(t) at different annealing temperature for the sample $Se_{90} Ge_4 In_6$.

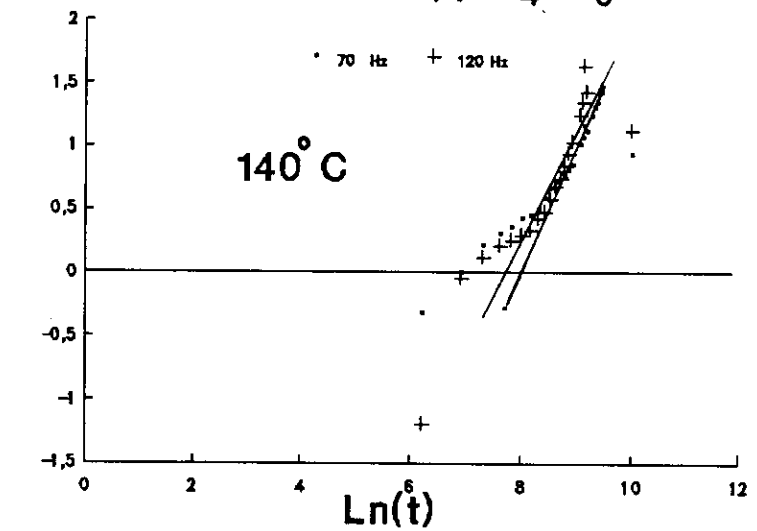

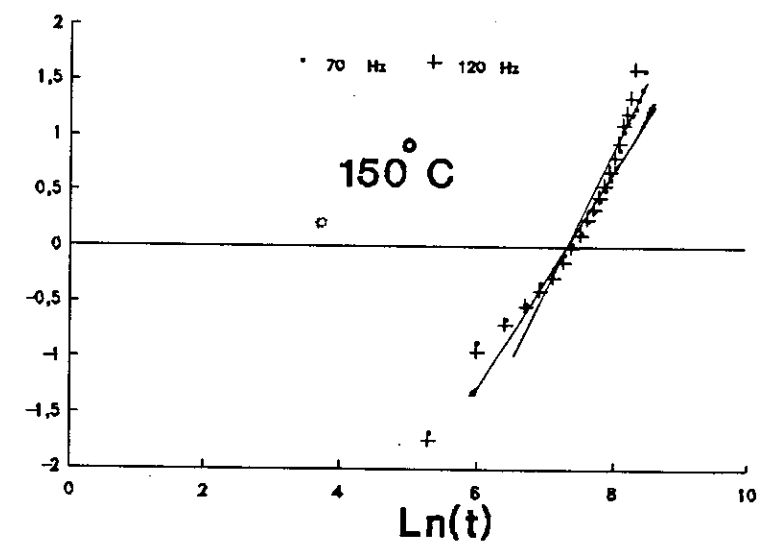

X at. %	T_c° C	n	
		70 (Hz)	120(Hz)
2	120	1,1118	1,303
	130	0,9554	0,9172
	140	0,9328	0,8298
	150	0,7664	0,8138
4	120	1,285	1,393
	130	1,1004	1,0006
	140	0,6966	0,5704
	150	0,4881	0,4868
6	120	1,448	1,487
	130	1,413	1,2105
	140	0,959	1,0494
	150	0,437	0,0622

Table(4·8)

X at.%	T_c°C	n	
		70 (Hz)	120(Hz)
2	120	1.379	1.491
	130	1.789	1.611
	140	1.343	2.064
	150	1.0297	.8
4	120	1.514	1.435
	130	1.572	0.978
	140	0.644	0.9702
	150	0.7031	0.7376
6	120	3.837	3.914
	130	1.7335	1.443
	140	1.485	1.367
	150	0.512	0.435

Table (4·9)

in tables (4·8) and (4·9) respectively. It is clear that " n " decreases as the crystallization temperature increases for each sample. This may be attributed to the deviation towards unidirectional growth as the crystallization temperature increases. However it can be noticed from tables (4.8)and (4.9) that as the Indium content in the system Se_{90} Ge_{10-x} In_x (X=2,4 and 6) increases, the fractional values of the reaction order,n,seems to increase in the temperature range below 140^0 C ,while at higher values of crystallization temperature the values of " n "appear to decrease. The increasing in " n " may be attributed to that at low temperature range, the nucleation mechanism is a temperature independent i.e.heterogeneous in nature, while as the temperature of crystallization increases the nucleation mechanism tend to be homogeneous. i.e.unidimentional mechanism. The rate of crystallization , K, at any time, at the crystallization temperature 120,130,140 and 150^0 C and at two different constant values of frequency for Se_{90} Ge_{10-x} In_x (X=2,4 and 6) was calculated from equation(4.4) and retraced as shown in figs.(4.129-4.131) and (4.132-4.134) for both ε and $\tan(\delta)$ respectively. From figs.(4.129-4.134)it is clear that the rate of crystallization , K, increases as the crystallization temperature increases. This may be attributed to the growth of the crystalline phase on the expense of the old amorphous one.

4.4.3.THE ACTIVATION ENERGY OF AMORPHOUS-CRYSTALLINE TRANSFORMATI DUE TO THE CHANGE IN ε, AND TAN(δ):-

According to Becker[102] the energy of activation necessary for the transformation of the crystalline grain, E_c ,depends on the activation energy of the transfer of the particles to the nucleus (q) and on the energy of nucleation ΔF. The dependence of K on T is given by the equation:

$$K=K_o \exp[\{-\Delta F-q\}/RT]=K_o \exp(-E_c/RT) \qquad (4.5)$$

Where T is the crystallization temperature, R is the universal gas constant, and, E_c, is assumed to be the total temperature-dependent activation energy of crystallization process.

The relation between ln(K) and (1/T) for the system, $Se_{90}Ge_{10-x}In_x$ (X=2,4 and 6) at tow different values of frequency (70,120 Hz) for both of the dielectric constant and the dielectric loss tangent are given in figs.(4.129-4.134).

The plots in case of the dielectric constant show two slopes ,each corresponds to a certain value of activation energy of crystallization, while in case of the dielectric loss the plots show one value. This indicates that the rate of crystallization is more sensitive to the crystallization temperature in case of the dielectric constant than that in case of the dielectric loss tangent.

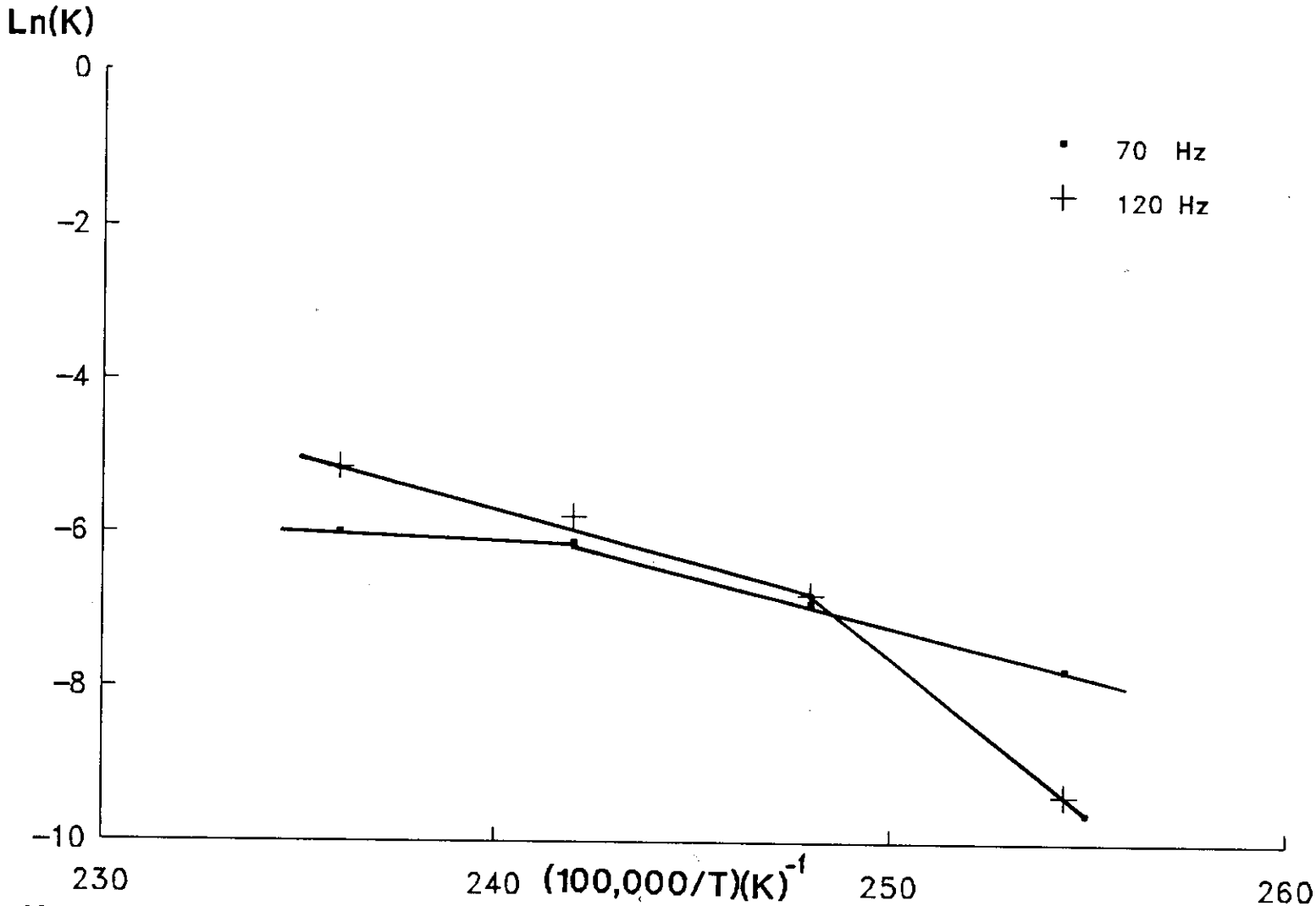

fig4.129 The effect of crystallization temperature on the rate of crystallization for the sample $Se_{90}Ge_8In_2$

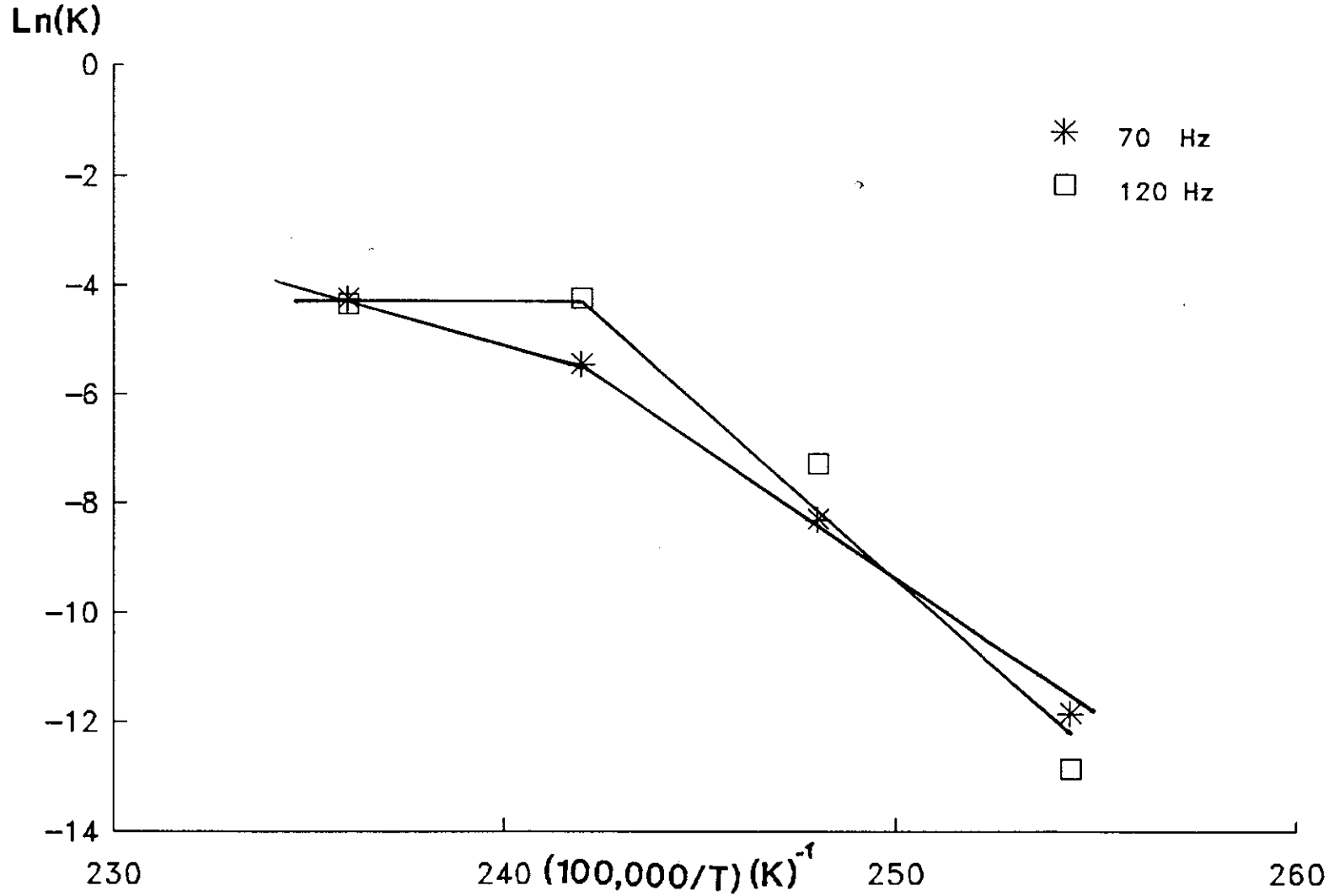

fig4.130:The effect of crystallization temperature on the rate of crystallization for the sample $Se_{90}Ge_6In_4$

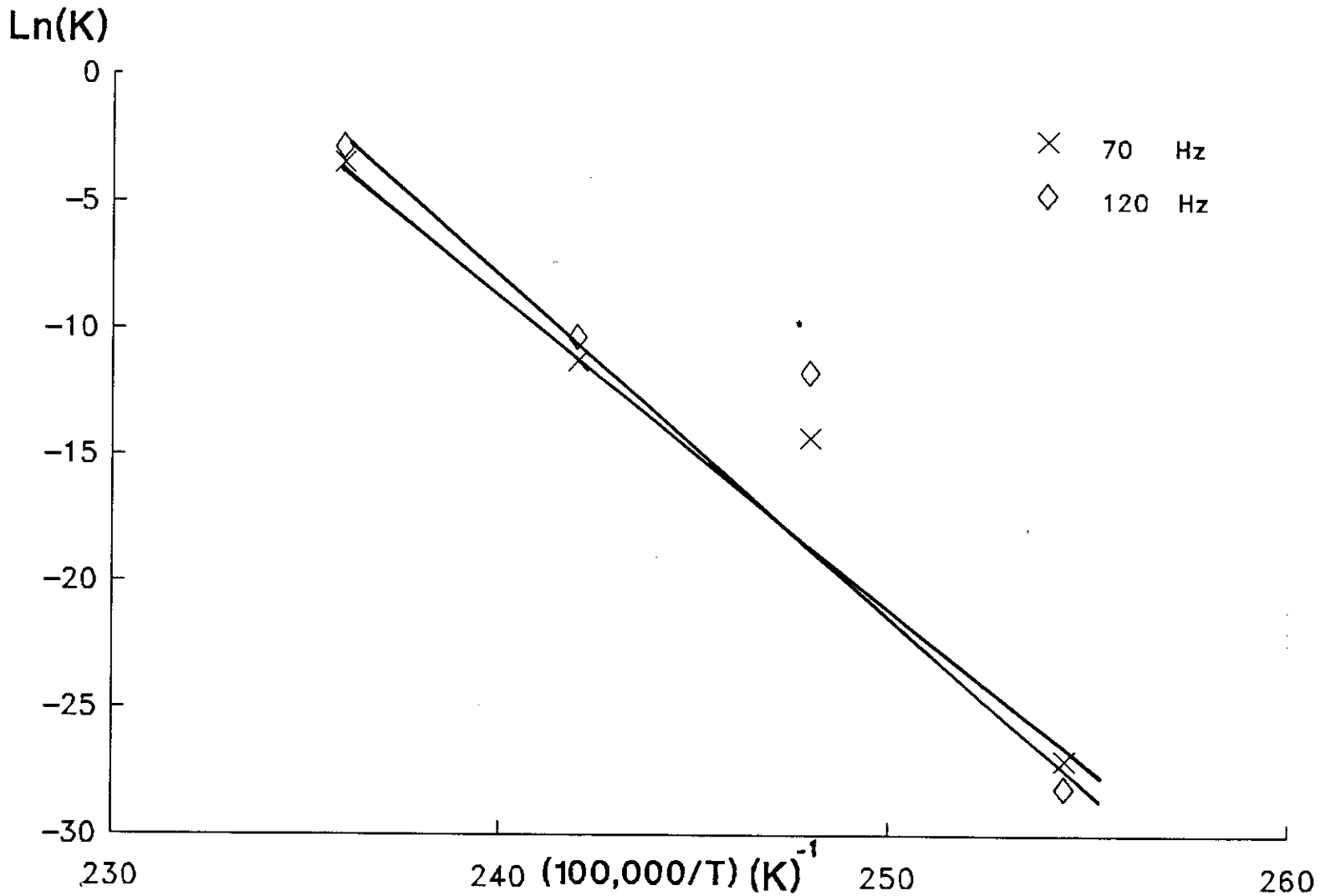

Fig.4.131 :The effect of crystallization temperature on the rate of crystallization for sample $Se_{90}Ge_4In_6$

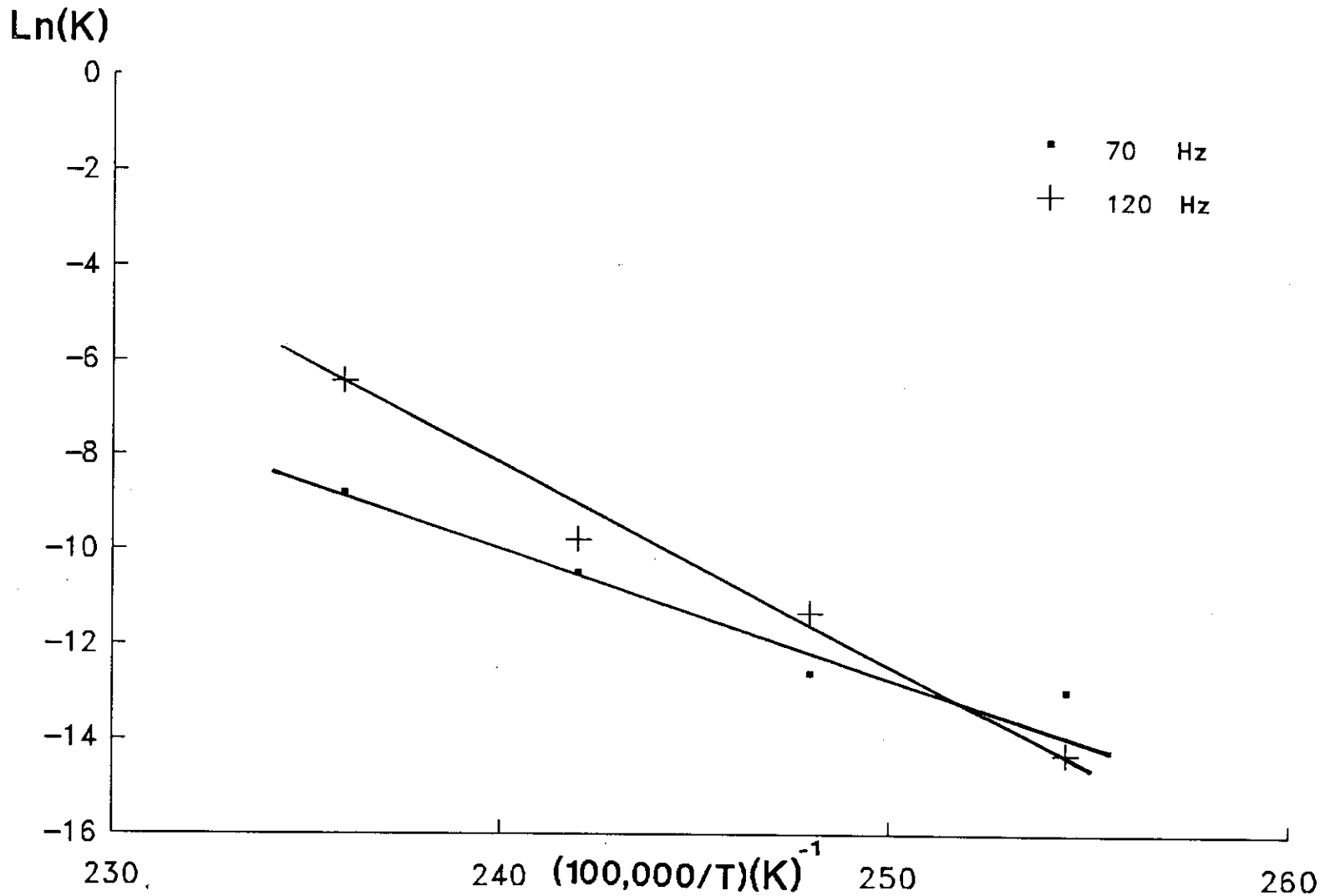

Fig.4.132 : The effect of crystallization temperature on the rate of crystallization for sample $Se_{90}Ge_8In_2$

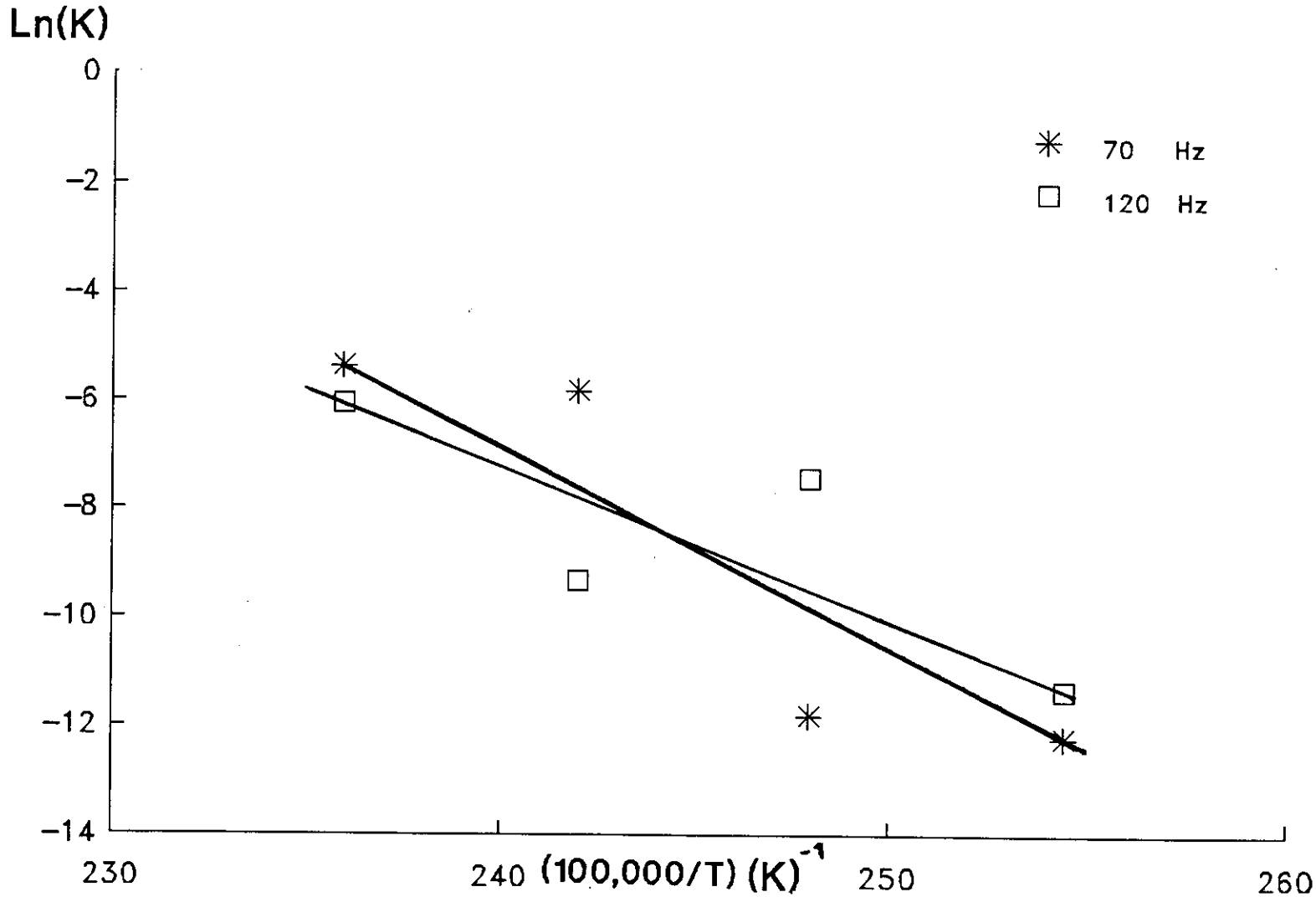

Fig.4.133 :The effect of crystallization temperature on the rate of crystallization for sample $Se_{90}Ge_6In_4$.

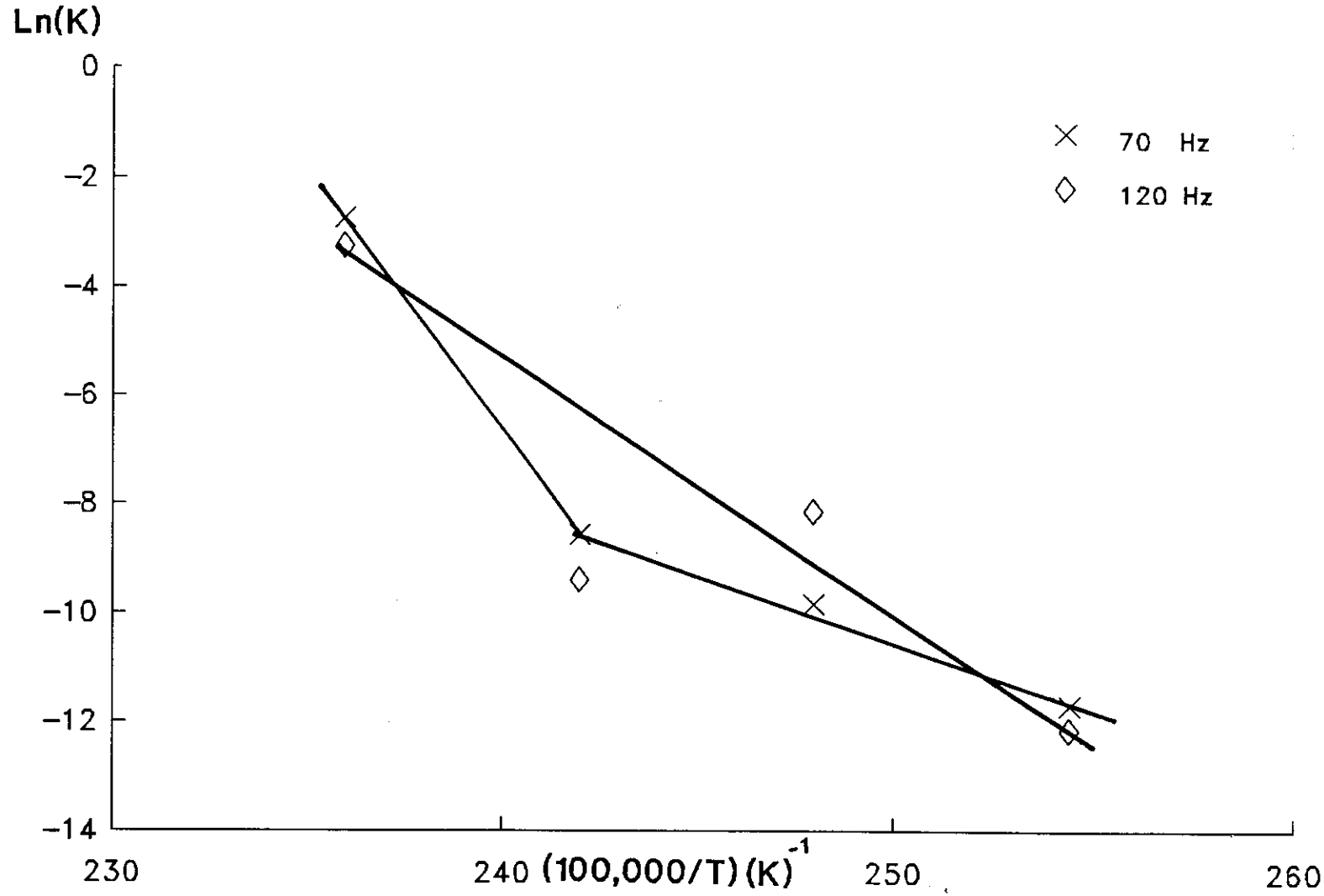

fig.4.134 The effect of crystallization temperature on the rate of crystallization for the sample $Se_{90}Ge_4In_6$.

The activation energy of crystallization of the system were calculated and tabulated in tables (4.10) and (4.11) for both ε and tan δ respectively.

From these tables it is clear that as the Indium content increases,the activation energy of crystallization increases. Such increase of E_c reflects the enhancement effect of the Indium in hindering the crystallization of Germanium and Selenium.

The increase of the apparent activation energy of crystallization as the Indium content increases may be explained once more as follows:-

As the Indium content increases in Se-Ge chains , this may leads to the attachment of the Indium atoms on Se-Ge chains. This attachment leads to an increase of the average length of Se-Ge chains. Consequently , the mobility of molecular species decreases,and much energy is required to complete the disorder-order transformation as the Indium content increases.

X at.%	ΔE (Kcal/mol)	
	70 (Hz)	120(Hz)
2	15,22	44,306
4	71,09	70,707
6	90,932	82,614

Table(4.10)

X at. %	Δ E(K cal/mol)	
	70(Hz)	120(Hz)
2	47,35	83,079
4	87,67	46,25
6	244,37	256,17

Table (4.11)

4.4.4.THE EFFECT OF CRTSTALLIZATION TEMPERATURE AND ANNEALING TIME THE DIMENSION OF CRYSTALLINE DOMAINS:-

It has been reported that the crystallites grows as a spherulite crystalline domain in the old amorphous matrix[113]. The dimension of the grow up phases may be followed by calculating the radius, r, of the may be formed crystalline domain as a function of time at different isotherms which is given by the relation[103] :

$$r^2 = 2\ K\ (t - t_n) \qquad (4.6)$$

Where "t" is the induction time. The relation between "r" and "t" for the system $Se_{90}\ Ge_{10-x}\ In_x$(X=2,4 and 6) at two different constant frequency have been plotted(figs.4.135,4.136).

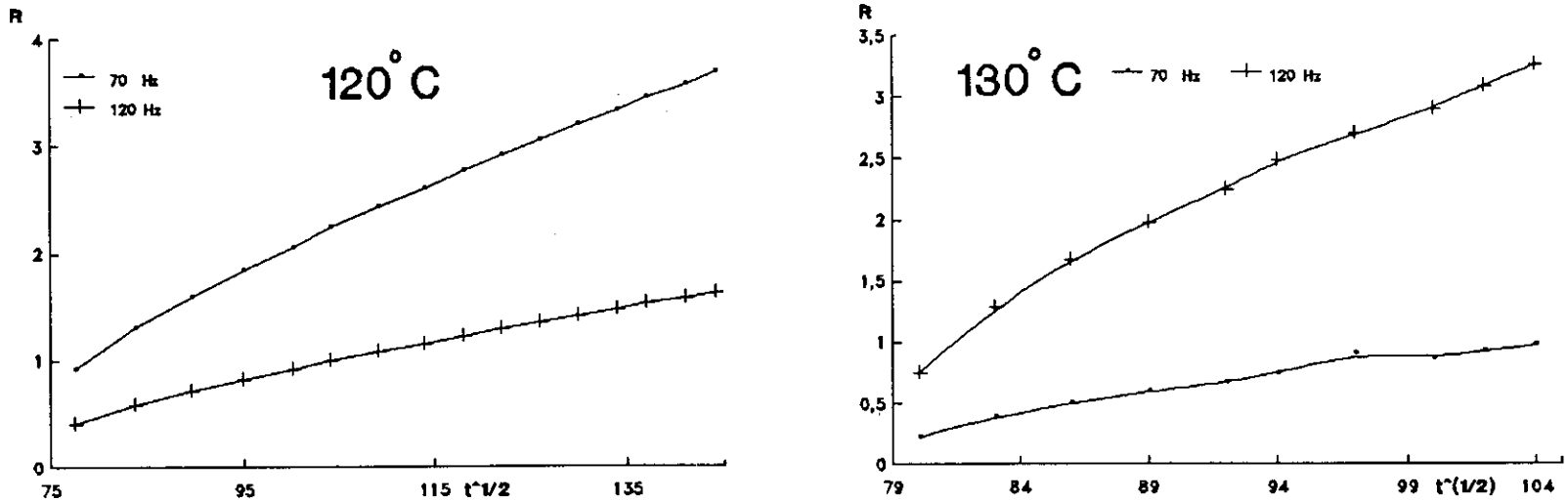

fig.4.135: The effect of crystallization time on the dimensions of the crystalline domains at two constant frequency for the sample $Se_{90}Ge_8In_2$.

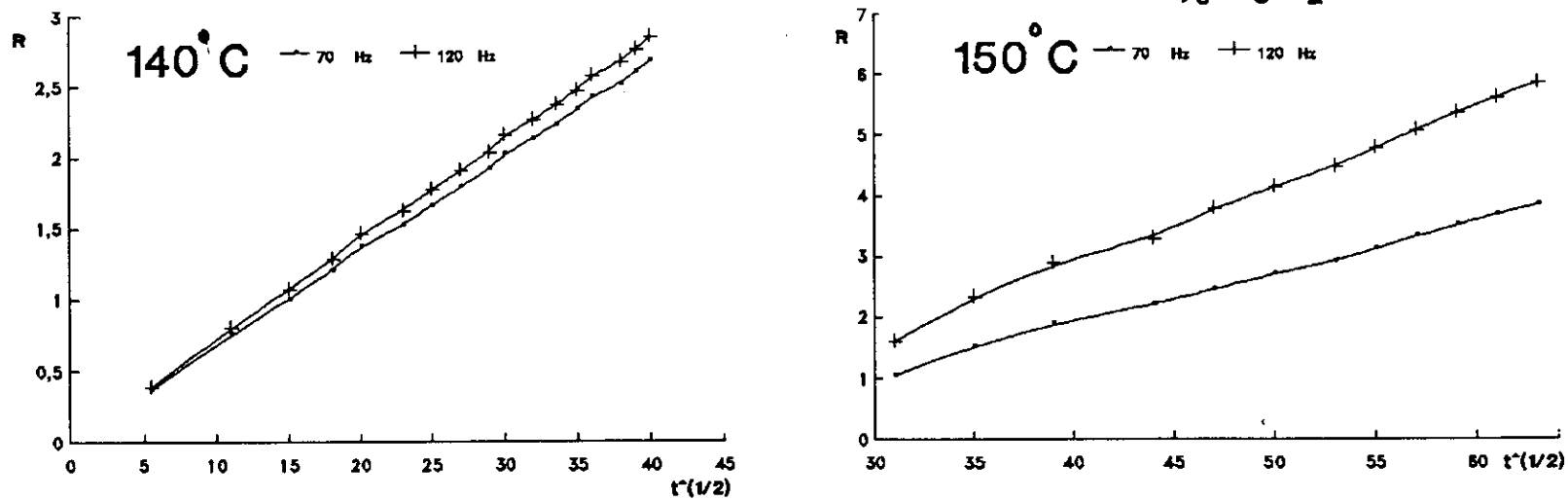

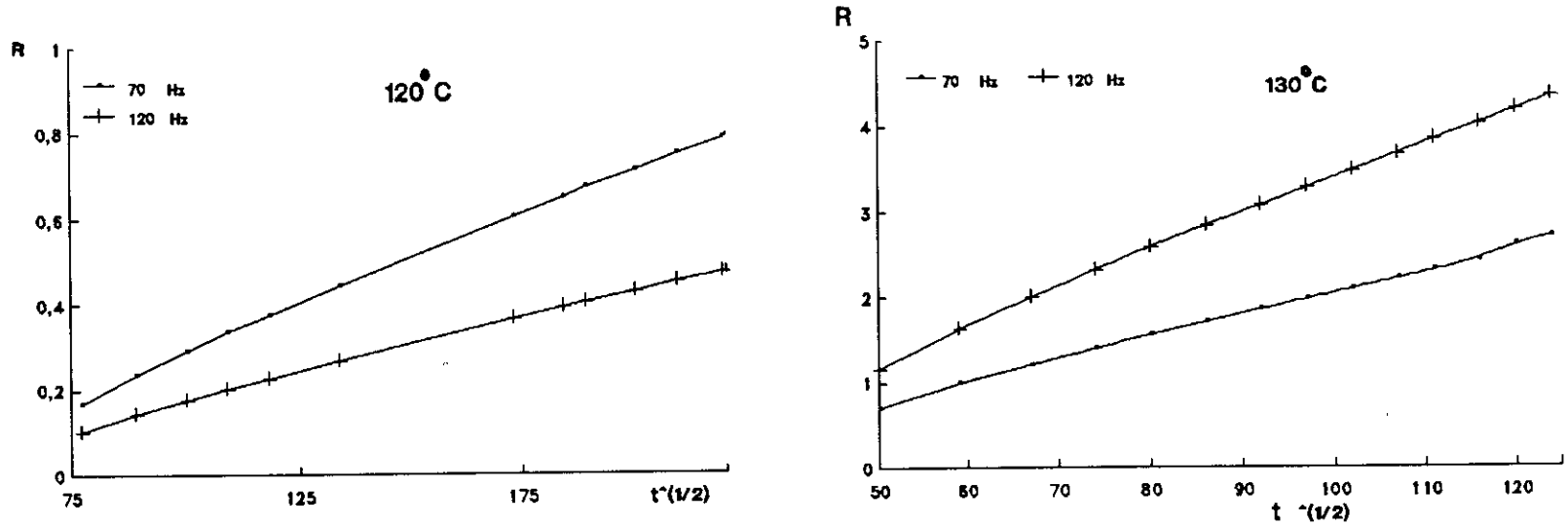

fig.4.136: The effect of crystallization time on the dimensions of the crystalline domains at two constant frequency for $Se_{90}Ge_6In_4$

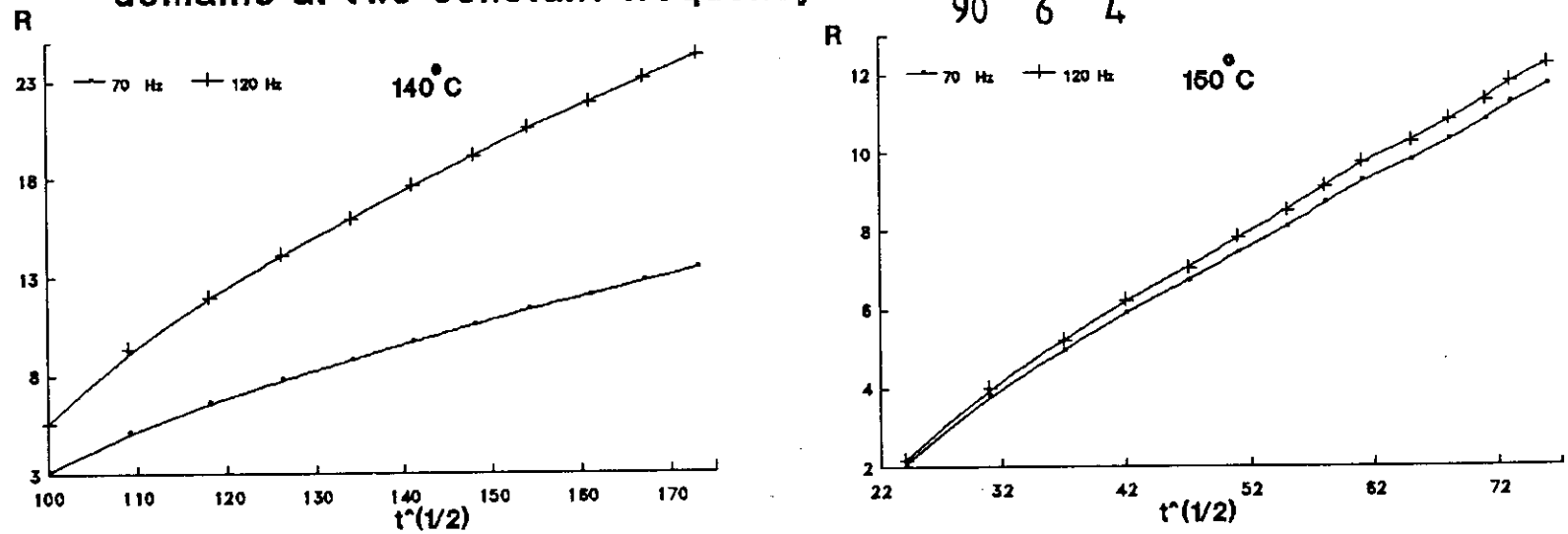

4.5.THE EFFECT OF CRYSTALLIZATION TEMPERATURE ON THE DIFFUSION COEFFICIENT :-

The growth of the crystalline domains in the old amorphous matrix has been considered as a diffusion process[103]. The diffusion coefficient (D) of such process is given by the relation:

$$D = 4.5\ K \qquad (4.7)$$

The diffusion coefficient for the system $Se_{90}\ Ge_{10-x}\ In_x$(X=2,4 and 6) for both of ε and tan (δ) at the crystallization temperature 120,130,140 and 150° C and at two different frequency(70 , 120(Hz) was calculated and tabulated in tables (4.12, 4.13)

From these tables it is clear that as the crystallization temperature increases, the diffusion coefficient increases. This mean that the crystalline phase grows and diffuse on the expense of the old amorphous matrix. This was confirmed by the increasing in the X-ray peaks.(fig.4.2).

Table(4-12)

Composition In at. %	diffusion coefficient (D)		
	T^{O}_{C}(C)	70 (Hz)	120 (Hz)
2	120	$1.028X10^{-5}$	$0,277X10^{-5}$
	130	$1,485X10^{-5}$	$5,275X10^{-5}$
	140	$12,503X10^{-5}$	$25,204X10^{-5}$
	150	$66,95X10^{-5}$	$717,5X10^{-5}$
4	120	$2,234X10^{-5}$	$5,188X10^{-5}$
	130	$3,283X10^{-5}$	$261,6X10^{-5}$
	140	0,01308	$3893X10^{-5}$
	150	0,02088	0,01023
6	120	$7,831X10^{-5}$	$6,011X10^{-13}$
	130	$0,265X10^{-5}$	$3,567X10^{-5}$
	140	$5,512X10^{-5}$	$14,48X10^{-5}$
	150	0,1367	0,25809

Table(4.13)

Copmosition In at.%	diffusion coefficient (D)		
	T_c° C	70(Hz)	120(Hz)
2	120	$1,9107X10^{-3}$	$3,771X10^{-4}$
	130	$5,0467X10^{-3}$	$50,467X10^{-4}$
	140	$9,9315X10^{-3}$	0,01387
	150	0,01122	0,02619
4	120	$3,157X10^{-5}$	$1,1484X10^{-5}$
	130	$110,7X10^{-5}$	$30,33X10^{-5}$
	140	0,01905	0,06295
	150	0,05724	0,06318
6	120	$3,645X10^{-5}$	$2,3427X10^{-5}$
	130	$23,323X10^{-5}$	$129,06X10^{-5}$
	140	$84,42X10^{-5}$	$36,77X10^{-5}$
	150	0,1723	0,2802